UNIVERSITY OF OSLO
Department of Physics

A study of night sky radiation, and heating and cooling of buildings with thermal solar collectors

Henning
Degnes-Ødemark

15th October 2009

Preface

Before I started this work, I did not know a lot about solar thermal energy, but the small Solar lab at the parking lot outside the Physics Department of the University of Oslo attracted my attention. The solar thermal collectors on the roof, seemed somehow exotic here in Norway. After checking out more about the energy group and talking to my supervisors, I was convinced. The work had a practical approach, and I have always thought it nice to combine theory and practice.

Initially my project had three parts: First, it was to measure the night sky radiation, second, to design and build a combined cooling and heating system at the lab, and third, to explore theoretically the use of a system like this in buildings. After a short time, the amount of work was found too great, and the theoretically building analysis was aborted. The practical work at the lab was carried out together with two fellow students, Øystein and Espen. The system was built, and tested. This work is reported in the master thesis of Øystein Soteland. The focus of my work changed to contain only results from the night sky radiation project, so this could be studied in more detail.

I'd really like to thank my supervisors, professor John B. Rekstad and Dr. Michaela G. Meir, for a challenging and nice master project. You where always be reachable, and always found time for questions and discussions.

A great thank to my colleagues at the office, Øystein, Espen, Svetlana and Lígia Catarina. Thank you all for the interesting discussions, and the motivation you gave me during all the hours spent at the office. I would also like to thank my cousin Hanne Ødemark, for proofreading my thesis.

And at last, but not at least, a huge thanks to my wife, Heidi. You did not help me with much the equations, but you kept faith in me and helped me through all difficult periods. Without your constant help and support I would never have been where I am today. You are the best and I love you!

Oslo, 15th October 2009

Henning Degnes-Ødemark

Abstract

Net night sky infrared radiation has been measured in Oslo, for a whole year, with a Kipp & Zonen CG1 pyrgeometer. From the infrared radiation, an equivalent sky temperature, T_{sky}, has been found through the Stefan-Boltzmann's law. The measured values have been compared to values calculated from the model of Martin and Berdahl (1984), based on a combination of self-measured values and data from the Norwegian Meteorological Institute. The model show good agreement with the measurements, especially during clear sky and overcast conditions. The highest deviations were found during changing cloud cover, but mean values show good agreement.

The sky temperature are used to find the potential for cooling through night sky radiation. A measure for the cooling potential, called cooling degree hour (CDH), has been developed. While cooling degree days (CDD) represent the cooling demand, CDH is found to represent the potential cooling through night sky radiation in Kh, with a perfect radiator. A useful transformation from CDH into possible cooling energy obtained from real systems, however, was not found, and the attempts seems to give large uncertainties.

Contents

Chapter 1

Introduction

What makes the small puddles on the ground freeze in the autumn night even though the ambient temperature never is below the freezing point? And why do we some times have to scratch ice on the car windshield but not on the side windows? The phenomenon causing these scenarios is called night sky radiation and is described in this thesis. To explain the phenomenon we have to take a look at the Earth's radiation balance, and the radiation balance between bodies.

Any body with a temperature above 0 K, will emit radiation in all directions, thus decreasing its temperature. Radiation emitted by other bodies can be received; increasing the temperature. Two bodies with different temperatures will both emit and absorb energy radiated out from the other body. The exchange of energy will in time, gibe the two bodies the same temperature. The amount of radiation is mainly defined by the body temperature. The higher the temperature, the more energy is emitted. In order to exchange energy, the two bodies need to have a clear view of each other, if not, energy will be exchange with whatever object within the field of view of the body. Horizontal objects, like puddles, have a clear view toward the sky. Windshields are tilted, but will have a larger view of the sky than the side windows, thus exchanging of energy with the sky.

During the day, solar radiation is absorbed. At night the ground surface radiates energy out toward the sky. In autumn, the temperature of the puddles can therefore decrease below the ambient temperature due to this radiation exchange, making it freeze even though the ambient temperature never gets below 0 °C.

The atmosphere is a complex collection of gases with different concentrations and different physical and chemical properties. In addition, the temperature and pressure is never constant. However, seen from the ground the radiation exchange with the atmosphere can be treated as if the atmosphere was a uniform body with a specific temperature called the sky temperature, T_{sky}. This temperature is the limit of the temperature obtained on a radiator during night sky radiation, making it more interesting than the direct radiation.

Direct measurements of the sky temperature are not available for many locations. Good models based on other meteorological data, can give estimates of the sky temperature for locations without direct measurements. In this thesis the atmospheric radiation is measured with a pyrgeometer, and the sky temperature is calculated from these measurements. The ambient temperature is also measured. The measured sky temperature is compared to a sky temperature calculated from different meteorological data, through the model of Martin and Berdahl (1984).

Energy is radiated out toward the sky, but can this be utilized as the need for cooling increases? The world's energy consumption increases, and renewable alternatives are needed. Different approaches have to be taken in order to find good renewable alternatives, and all alternatives should be investigated. Radiative cooling is interesting, and especially in combination with solar heating systems, where already operating systems can be easily modified to get an extra function.

The potential is unfortunately largest during the winter, where the normal building cooling demand is obsolete. Special industrial applications, which demands cooling during the whole year may utilize the large potential during the winter.

Chapter 2

Historical background

The study of night sky radiation and the study of the utilization of this is not a new thought. Ångström examined this phenomenon as early as in 1913, and refers to different scientists like Wilson, Wells, Six, Pouillet and Melloni, who carried out observations on the Earth's radiation to space (Ångström 1913). These scientists did their studies between $1780 - 1850$. Also mentioned is J. Maurer, who in 1885 published a paper on cooling and radiation of the atmosphere during night. Ångström also lists different papers written in the late $19th$ century and in the early $20th$ century. Ångström stated;

> "... that the influence of the density of water-vapor on the atmospheric radiation can, between certain limits, be expressed through an exponential formula."
>
> (Ångström 1913)

This made him one of the first scientists who found a model for the radiation as a function of temperature and water-vapor.

Later, more scientists have studied this phenomenon, with different approaches. Some try to replace formulas or models to express the level of radiation, as a function of different meteorological variables, to update, or to compare these models. These include Ångström (1913), Brunt (1932), Bliss (1961), Swinbank (1963), Idso and Jackson (1969), Idso (1974), Arnfield (1979), Berdahl and Fromberg (1982), Berdahl and Martin (1984), Martin and Berdahl (1984), Skartveit et al. (1996) and Iziomon et al. (2003).

A different approach has been to build different types of experimental setups to find the cooling effect obtained by radiative cooling. Scientists taking this approach includes Ali et al. (1995), Storås (1997), Al-Nimr et al. (1998), Khedari et al. (2000), Khedari et al. (2000), Meir et al. (2002), Bassindowa et al. (2007) and others.

The present work reports direct measurements of the downward atmospheric infrared radiation, and compares the measured results with the model of Martin and Berdahl (1984). The measurements where performed in Oslo, and lasted from the start of June 2008 to the start of July 2009. The measurements are interesting because similar measurements have not been previously conducted for a longer period of time in the Oslo area. The results are also challenging; both seeing how good the model fits for the direct measurements in Oslo, and finding the potential for radiative cooling with a modified solar collector system. The model from Martin and Berdahl (1984) was chosen because it takes the cloud cover into account, and therefore can be used for both clear sky and cloudy conditions. Previous measurements with a cooling system were performed by Meir et al. (2002), in which the same model was used.

There are different ways to convert and distribute/remove energy. Practical solutions used to obtain cooling in buildings are not described in this work, rather this work consentrates on the potential of radiative cooling by night sky radiation.

Cooling can also be archived with other, even solar driven, processes. Absorption, adsorption, and desiccant cooling systems all need heat to drive the process. This heat can be heated by solar collectors. Another solar driven cooling system, is based on electricity generation through solar cells, and cooling with a cooling machine. These processes, however, will not be described in this work.

Chapter 3

Theoretical background

In this section the theoretical background used in the paper will be given. The measurements and calculations in this thesis are based on different theoretical backgrounds, which includes topics within: Blackbody radiation, atmospheric absorptance, radiator physics, Fresnel's equations on reflection of light on surfaces and the model of Berdahl and Fromberg (1982)/ Berdahl and Martin (1984)/Martin and Berdahl (1984). Most of the theoretical background presented here is based on Duffie and Beckman (2006), where no other source is mentioned. The findings in Section 3.8 were developed during this thesis.

3.1 Blackbody radiation

According to the Stefan-Boltzmann's law on radiation, Equation 3.1, any object with a temperature higher than 0 K, will emit electromagnetic radiation.

$$R = \sigma \varepsilon T^4 \tag{3.1}$$

Here R is the radiated energy, σ, the Stefan-Boltzmann constant, ε the emittance of the object and T, the absolute temperature of the body. For a blackbody, the $\varepsilon = 1$, and for any real material, the emittance is in the range $0 < \varepsilon < 1$. Materials with an emittance lower than 1, are called grey bodies. All bodies emit electromagnetic radiation with a specific emission spectrum,

and the position of the maximum is described by Wien's displacement law;

$$\lambda_{\mathrm{m}} = \frac{2.90 \cdot 10^{-3}\mathrm{m} \cdot \mathrm{K}}{T}\,, \tag{3.2}$$

where λ_{m} is the wavelength of the maximum, and T is the absolute temperature of the body. A body of 298 K (25 °C), will have the maximum emittance at $\lambda_{\mathrm{m}} = 9.73\,\mu$m, directly in the atmospheric window described in Section 3.3. As seen in Figure 3.2, the maximum wavelength for radiation from the Sun lays to the left of the Earth's maximum.

3.2 Reflection from a surface

The reflection and transmission of radiation through transparent surfaces is described by Snell's law and Fresnel's laws. These laws are used in the estimation of influence of the Physics building shadowing the pyrgeometer field of view. Snell's law states the relation between two refractive indices, n_{i}, and the angles of incidence θ_{i}, and transmission θ_{t}, see Figure 3.1 and Equation 3.3.

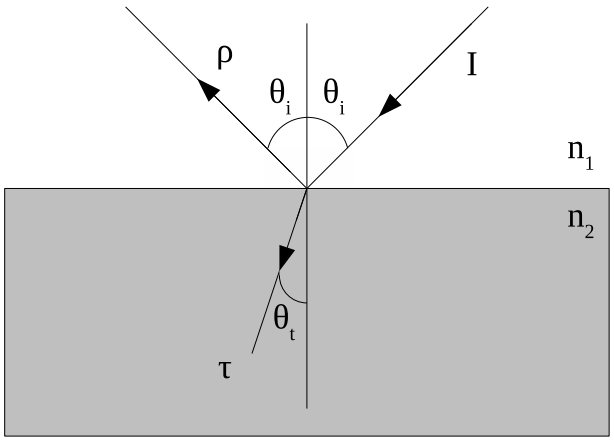

Figure 3.1: Reflectance (ρ) and transmittance (τ) of incident radiation (I) between two materials with refractive indices n_1 and n_2. Angles of incidence and transmittance indicated with θ_{i} and θ_{t} respectively.

From Snell's law, the transmittance angle, θ_{t}, can be found from the refractive indices n_{i} and the angle of incidence, θ_{i}:

$$n_1 \sin(\theta_{\mathrm{i}}) = n_2 \sin(\theta_{\mathrm{t}}) \Rightarrow \theta_{\mathrm{t}} = \arcsin\left(\frac{n_1}{n_2} sin(\theta_{\mathrm{i}})\right)\,. \tag{3.3}$$

Fresnel's laws give the reflected part of unpolarized radiation radiated toward a surface. The equations are divided in two parts: The fraction from radiation

with polarization perpendicular to the surface plane,$r_\perp$, and the fraction of radiation with the plane parallel to the surface plane, $r_\parallel$:

$$r_\perp = \frac{\sin^2(\theta_\mathrm{t} - \theta_\mathrm{i})}{\sin^2(\theta_\mathrm{t} + \theta_\mathrm{i})} \qquad r_\parallel = \frac{\tan^2(\theta_\mathrm{t} - \theta_\mathrm{i})}{\tan^2(\theta_\mathrm{t} + \theta_\mathrm{i})} \tag{3.4}$$

Unpolarized light has a random distribution of polarization, and the total reflection is then given like Equation 3.5:

$$r_\mathrm{tot} = \frac{r_\perp + r_\parallel}{2} = \rho\,. \tag{3.5}$$

In the following, ρ is used as the nomenclature for reflectance. All incoming radiation is either reflected, transmitted or absorbed, which gives the following equation:

$$1 = \rho + \tau + \alpha \Leftrightarrow \tau = 1 - \rho - \alpha\,. \tag{3.6}$$

Some of the radiation is absorbed, but in the further calculations, absorption is treated as negligible. Equation 3.8 is used in the calculation of the influence of the surrounding buildings. Any energy absorbed in the glass covering the pyrgeometer, see Figure 4.1, is in turn emitted to the sensor and to the sky. Half of the absorbed energy is then also treated as transmitted energy, so the only error in this approximation is half of the absorbed energy.

The total transmittance is dependent on the angles of incidence, θ_i, and transmittance, θ_t. The angle of transmittance is defined from the refractive indices, n_i. If we put the different equations together, the total fraction of transmittance, can be expressed as a function of the angle of incidence and refractive indices:

$$\begin{aligned}
\tau(\theta_\mathrm{i}, \theta_\mathrm{t}) &= 1 - \rho \\
&= 1 - \frac{r_\perp + r_\parallel}{2} \\
&= 1 - \frac{1}{2}\left[\frac{\sin^2(\theta_\mathrm{t} - \theta_\mathrm{i})}{\sin^2(\theta_\mathrm{t} + \theta_\mathrm{i})} + \frac{\tan^2(\theta_\mathrm{t} - \theta_\mathrm{i})}{\tan^2(\theta_\mathrm{t} + \theta_\mathrm{i})}\right]\,.
\end{aligned} \tag{3.7}$$

If we incorporate Snell's law, Equation 3.3, the total transmittance can be expressed as a function of the refractive indices, n_i, and the angle of incidence, θ_i:

$$\begin{aligned}
\tau(\theta_\mathrm{i}, n_\mathrm{i}) = 1 &- \frac{1}{2}\frac{\sin^2\left[\arcsin\left(\frac{n_1}{n_2} sin\theta_\mathrm{i}\right) - \theta_\mathrm{i}\right]}{\sin^2\left[\arcsin\left(\frac{n_1}{n_2} sin\theta_\mathrm{i}\right) + \theta_\mathrm{i}\right]} \\
&+ \frac{1}{2}\frac{\tan^2\left[\arcsin\left(\frac{n_1}{n_2} sin\theta_\mathrm{i}\right) - \theta_\mathrm{i}\right]}{\tan^2\left[\arcsin\left(\frac{n_1}{n_2} sin\theta_\mathrm{i}\right) + \theta_\mathrm{i}\right]}\,.
\end{aligned} \tag{3.8}$$

Equation 3.8 is used to estimate the influence of the Physics building to the measurements. To find the influence of the Physics building the relative area for different sections in the pyrgeometer field of view has to be known. Equation 3.9 show the area of a hemisphere, A_{h}, as a function of the elevation angle, θ_{h}, defined as $90^{\circ}(\pi/2)$ at the surface normal (unlike the angle of incidence, θ_{i}), the azimuth angle, ϕ_{h}, and the radius, r_{h}. The subscrips, h for hemisphere, is used to separate these angles from other angles in this work. Equation 3.9 is used to find the values of relative areas in Table 4.1 in Section 4.4 where the influence from the Physics building is discussed in more detail.

$$\begin{aligned} A_{\mathrm{h}}(\theta_{\mathrm{h}}, \phi_{\mathrm{h}}, r_{\mathrm{h}}) &= \int_0^{2\pi} \mathrm{d}\phi_{\mathrm{h}} \int_{\frac{\pi}{2}+\theta_{\mathrm{h}}}^{\pi} r_{\mathrm{h}}^2 \sin\theta_{\mathrm{h}} \mathrm{d}\theta_{\mathrm{h}} \\ &= 2\pi r_{\mathrm{h}}^2 \left[\cos\pi - \cos\left(\frac{\pi}{2}+\theta_{\mathrm{h}}\right)\right] \\ &= 2\pi r_{\mathrm{h}}^2 \left[-1 - \cos\left(\frac{\pi}{2}+\theta_{\mathrm{h}}\right)\right] \\ &= -2\pi r_{\mathrm{h}}^2 \left[1 + \cos\left(\frac{\pi}{2}+\theta_{\mathrm{h}}\right)\right] \end{aligned} \tag{3.9}$$

3.3 The atmosphere

The atmosphere consists of several Greenhouse gases (GHGs). Water vapor (H_2O), carbon dioxide (CO_2) and methane (CH_4) are the main contributors to the Greenhouse effect. In addition, ozone (O_3) has a peak inside the so-called atmospheric window as seen in Figure 3.2. The GHGs will absorb and re-emit some of the long-wave infrared radiation from the Earth, but not the solar radiation, which has a shorter wavelength. The total atmospheric absorptance is shown in Figure 3.2. The atmospheric window is seen between 8 μm and 13 μm. In this part of the spectrum, the atmosphere is more or less transparent to the electromagnetic radiation from the Earth, therefore the name atmospheric window. Since the temperature of the Sun and the Earth are different, the radiation spectrum from each will be shifted according to Wien's displacement law, Equation 3.2. As seen in Figure 3.2, there are several parts in the spectrum, where there is small or no absorptance from the atmosphere. However, the atmospheric window referred to earlier lays inside the part of spectrum radiated out from the Earth.

As seen in Figure 3.2, most of the energy radiated out from the Earth, are radiated out between 8 μm and 13 μm. Water vapour normally stands for

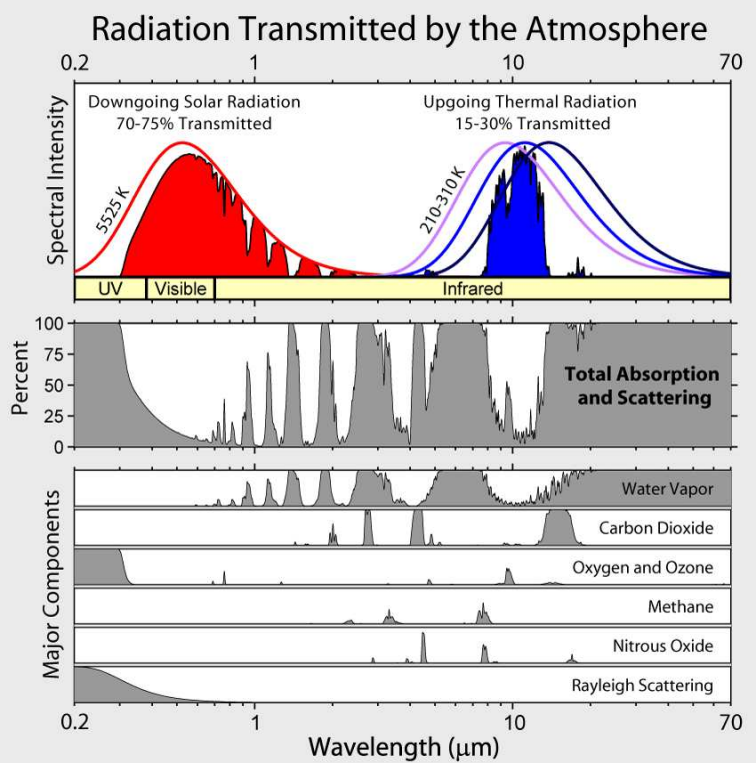

Figure 3.2: The atmospheric absorptance and the different GHGs causing the main absorptance. The figure also shows the atmospheric window between $8\ \mu$m *and* $13\ \mu$m*, where the atmosphere is more or less transparent to infrared radiation from the Earth (Source: Image created by Robert A. Rohde / Global Warming Art).*

most of the absorption outside this window. As the amount of water vapour increases, more of the radiation within this window will also be absorbed, see Figure 3.3.

The atmosphere is built up of several layers, all with different temperatures and emittance. A surface on the ground however, will only interfere with the mean of all layers. The radiation from the atmosphere can be compared to the radiation from a blackbody with a certain temperature, hence, an equivalent sky temperature, T_{sky}, can be introduced. By measuring the incoming radiation, we can use the Stefan-Boltzmann's law, Equation 3.1, to find this temperature. This process is described more in detail in Section 3.6.

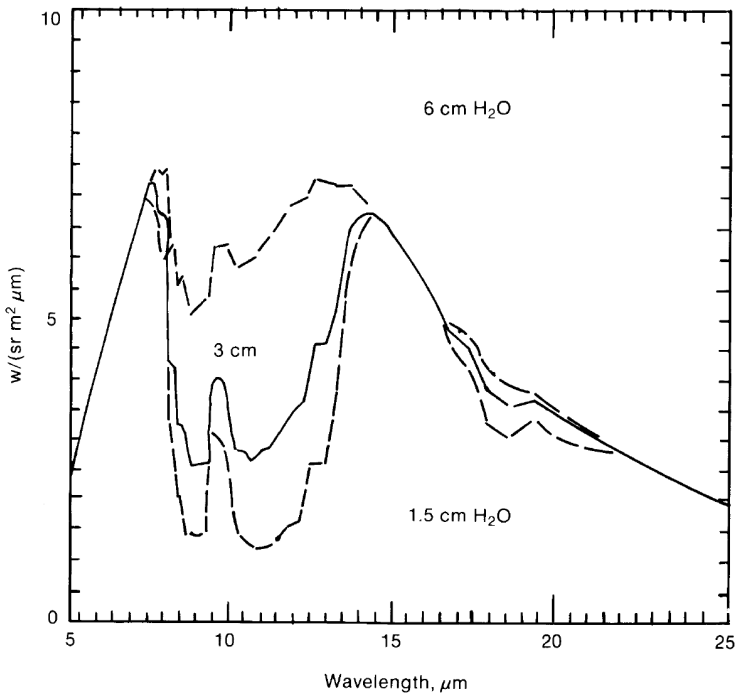

Figure 3.3: Calculated spectral radiance for a clear summer atmosphere at a midlatitude location, with different containment of water vapour. This will also mean, by Kirchhoff's law, that radiation will be absorbed. (Source: Berdahl and Martin (1978) in Martin (1989)).

3.4 Net power of a radiator

A solar collector at night will act as a radiator, as long as the amount of energy emitted by the radiator, $R_{\uparrow}$, is higher than the amount of energy absorbed, $R_{\downarrow}$, thus the net power of the radiator is defined to take positive values for gained cooling ($R_{\uparrow}>R_{\downarrow}$) (Equation 3.10). A_{rad} is the radiator area. The amount of energy radiated out from a radiator is defined by its temperature, T_{rad}, and emittance, $\varepsilon_{\mathrm{rad}}$. The amount of radiation absorbed at the radiator is given from the absorptance, α_{rad} and the equivalent sky temperature, T_{sky} (Equation 3.11).

$$\frac{P_{\mathrm{net}}}{A_{\mathrm{rad}}} = R_{\uparrow} - R_{\downarrow} \tag{3.10}$$

$$= \sigma\varepsilon_{\mathrm{rad}}T_{\mathrm{rad}}^4 - \alpha_{\mathrm{rad}}\sigma T_{\mathrm{sky}}^4 \tag{3.11}$$

$$= \sigma\varepsilon_{\mathrm{rad}}T_{\mathrm{rad}}^4 - \varepsilon_{\mathrm{rad}}\sigma T_{\mathrm{sky}}^4 \tag{3.12}$$

Following Kirchhoff's law, Equation 3.13, the radiator emittance, $\varepsilon_{\mathrm{rad}}$, can replace the radiator absorptance, α_{rad} (Equation 3.12). According to this law,

for every wavelength and for every direction of propagation of the radiation, the directional spectral emittance of a body is equal to its directional spectral absorptance:

$$\alpha_\lambda(T_{\text{rad}}, \varphi, \vartheta) = \varepsilon_\lambda(T_{\text{rad}}, \varphi, \vartheta)\,, \tag{3.13}$$

where φ and ϑ are angles defining the direction of propagation of the radiation. For any radiator one can see that for the same wavelength, λ, and absolute temperature, T_{rad}, the total absorptance, α_λ, is the same as the total emittance, ε_λ. The net energy transfer, P_{net}, can therefore be expressed as in Equation 3.14, based on the Stefan-Boltzmann's law on blackbody radiation, Equation 3.1 and Kirchhoff's law, Equation 3.13.

$$P_{\text{net}} = \sigma \varepsilon_{\text{rad}} A_{\text{rad}} (T_{\text{rad}}^4 - T_{\text{sky}}^4) \tag{3.14}$$

In Equation 3.14, both the radiator temperature, T_{rad}, and the sky temperature, T_{sky}, are measured in kelvin. The net cooling power shown in Equation 3.14, is defined so that positive values are obtained for radiator temperatures higher than sky temperatures ($T_{\text{rad}} > T_{\text{sky}}$). In other words; a positive cooling power of the radiator.

The absorptance of the radiator is often different in the visual part of the electromagnetic spectrum, than in the infrared. Nevertheless, the sky has an equivalent temperature at night near any radiator, and therefore also emit in the infrared part of the spectrum.

Radiators with major differences of absorptance for different part of the electromagnetic spectrum, are said to have selective surfaces. Two main types are made; hot and cold selective surfaces. Hot selective surfaces have high absorptance in the visual part of the spectrum and low absorptance in the infrared part. Following Kirchhoff's law, this will also give a low emittance in the infrared part of the spectrum. These surfaces will act as good solar absorbers, but will be useless in radiative cooling due to the low emittance in the infrared area. The other type of surfaces is called cold selective and has the opposite properties, with low absorptance in the visual and high absorptance (and emittance) in the infrared part of the spectrum. These surfaces can be good radiators, even at daytime but could not be used as solar absorbers (Holter et al. 1998). This work concentrates at combined heating and cooling systems, and selective surfaces will therefore not be part of this study.

3.5 Solar collectors used as radiators

A solar collector absorbs solar radiation, converts it into heat and transport the heat to either an instantaneous use or to a storage for later use. There are mainly two types of solar collectors; flat plate collectors and vacuum tube collectors. Flat plate collectors can either be made of metal or of special high temperature resistant polymers. Due to different thermal conductivity, the metal and polymer collectors have different designs. Polymer collectors have a larger contact area for the absorber and the energy transfer fluid than the metal absorbers. Metal absorbers are mainly made of copper or aluminum. There are several reasons why much research is made to find polymers as alternatives to metal absorbers, for example the price and accessibility of raw materials. To cover a relatively small fraction of the world energy need with copper collectors, a large amount of all copper mined had to be used for collectors. To cover the same fraction of energy with polymer collectors, almost a negligible fraction of the total crude oil production would be needed. Polymer collectors also have the potential for lighter weight, more energy efficient life cycle and more.

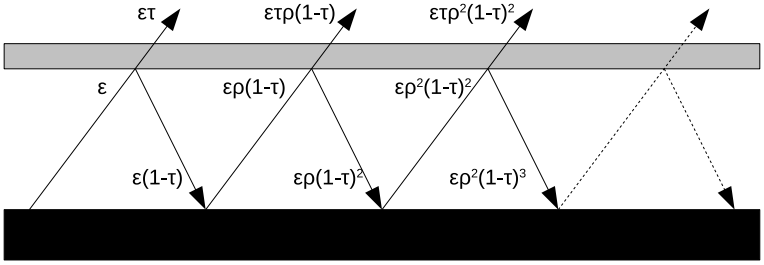

Figure 3.4: Sketch of radiation paths in a solar collector, with a single-wall cover sheet, used as radiator. The black bar at the bottom represents the solar absorber used as a radiator and the gray bar at the top represents the cover sheet. $\varepsilon = \varepsilon_{\text{rad}}$*,* $\rho = \rho_{\text{rad}}$*,* $\tau_{\text{rad}} = 0$*,* $\alpha_{\text{cs}} = 0$*,* $\tau = \tau_{\text{cs}}$ *and* $\rho_{\text{cs}} = (1 - \tau)$.

Most solar collectors have a so-called cover sheet, in order to avoid heat loss and have a higher efficiency. These cover sheets will be mostly transparent to solar radiation, which is in the visual part of the spectrum and less transparent in the infrared part of the spectrum. Used in radiative cooling, cover sheets leads to a substantial reduction in the system emittance. Figure 3.4 shows the radiation path for a solar collector with a single-walled cover sheet. In such a system, a first approximation to the total system emittance is the product between the radiator's emittance and the transparency of the cover sheet: $\varepsilon_{\text{sys}} = \varepsilon_{\text{rad}}\tau_{\text{cs}}$. In this approximation, all energy not transmitted through the cover sheet, is reflected and absorbed in the absorber.

A better approximation is to encounter reflectance in the cover sheet and the absorber. Two small assumptions are still made: First, the absorber plate has no transmittance of radiation, and second, the cover sheet has no absorptance. This means that all radiation reflected from the cover sheet, hits the absorber plate and will either be absorbed or reflected. Radiation reflected at from the absorber plate vwillin turn either be transmitted through the cover sheet of reflected back again. The small amount of energy absorbed in the cover sheet, is in turn radiate out in both directions according to the temperature of the cover sheet, thus the error of this approximation will be very small. Transmittance in the absorber can also be treated as negligible.

These assumptions leads to the following equations for the absorber/radiator and the cover sheet:

$$\varepsilon_{\text{rad}} + \rho_{\text{rad}} = 1 \tag{3.15}$$

$$\rho_{\text{cs}} + \tau_{\text{cs}} = 1 \Rightarrow \rho_{\text{cs}} = (1 - \tau_{\text{cs}}) \tag{3.16}$$

where ε_{rad} is the radiator emittance, ρ_{rad} and ρ_{cs} reflection for the radiator and cover sheet respectively, and τ_{cs} the transmittance of the cover sheet.

Figure 3.4 shows the radiation path for several reflections both in the cover sheet and in the absorber. Here, the following parameters are used: $\varepsilon = \varepsilon_{\text{rad}}$, $\tau = \tau_{\text{cs}}$, $(1-\tau) = \rho_{\text{cs}}$ and $\rho = \rho_{\text{rad}}$. For each time the ray is reflected, less energy is left. The eequationsin Figure 3.4 show the coefficients at different places in the path. In sum, the emittance for the total system will be like shown in Equation 3.17[1]:

$$\varepsilon_{sys} = \sum_{n=0}^{\infty} \varepsilon\tau\rho^n(1-\tau)^n = \varepsilon\tau \sum_{n=0}^{\infty} \rho^n(1-\tau)^n = \frac{\varepsilon\tau}{1-(1-\tau)\rho}\,. \tag{3.17}$$

As seen from Equation 3.17 and Figure 3.4, the total system emittance when reflection is encountered, is higher than the $\varepsilon_{\text{rad}}\tau_{\text{cs}}$ product, since
$0 \; < \; (\; 1 \; - \; \tau \;) \; \rho \; < \; 1.$

The emittance of any real radiator, ε_{rad}, is less than 1. The amount $(1- \varepsilon_{\text{rad}})$ is lost because the radiator is not a perfect blackbody. This can not be totally eliminated, but higher emittance values can be reached.

The system developed at the University of Oslo, consists of solar collectors with polymer absorbers, and a twin wall polycarbonate coversheet. In 2008,

[1]The transition in the equation follows by the rule for a geometric series:
$\sum_{i=0}^{n} X^i = \frac{1-X^n}{1-X}$

Fernandes da Silva, measured the emissivity for the new absorber materials to be between 70.7% ±0.1% and 73.3% ±0.1%, in the range from 8 μm to 14 μm wavelength. The report of Bijma et al. (1997), finds the transmittance of IR radiation through the coversheet material, used in the solar heating system developed at the University of Oslo, for different thickness. The transmittance is a function of thickness of the cover sheet, and decreases rapidly between $10 - 1000$ μm. The transmittance for a 0.5 μm cover sheet is found to be approximately 30%. A twin-wall coversheet, with a wall thickness of 0.5 μm for each wall, can be approximated with the equation of the system emittance found for single wall cover sheets. The transmittance of the twin wall coversheet is then set to $\tau = 0.3 \cdot 0.3 = 0.09$. The total system emittance, ε_{sys} is found in Section 3.5:

$$\varepsilon_{\text{sys}} = \frac{\varepsilon_{\text{rad}}\tau}{1-(1-\tau)\rho} = \frac{0.7 \cdot 0.09}{1-(1-0.09)0.3} = 0.087\,. \tag{3.18}$$

Here, an absorber emittance of 0.7, is used. As seen, only about 9% is radiated out from the solar collector. This is of course just the amount of radiated energy. In addition, convection and conduction will also transfer energy. Tappel (2007) studied forced convection of solar collectors in order to prevent overheating of polymer collectors. Forced ventilation could be used in order to cool down water at night, but then the ambient temperature will be the limit of cooling. Radiator surfaces with main purpose for cooling could be made in addition to covered solar collectors used for heating.

The difference between collectors with and without polycarbonate cover sheets is large, and reveals that cooling through night sky radiation with solar collectors, must be done without cover sheets.

3.6 Model for calculation of T_{sky} from meteorological data

There are several different formulas for the description of the sky temperature from surface meteorological measurements, as mentioned in Chapter 2. The atmosphere is often treated as a blackbody following the Stefan-Boltzmann's law in Equation 3.1. The radiation measured, R_{atm}, then refers to an equivalent sky temperature, T_{sky}, see Equation 3.19. Because the sky temperature is not easily measured, efforts have been made to link the sky temperature to the

ambient temperature by introducing the emittance, ε_{sky}. In total, the set of equations is:

$$R_{\text{atm}} = \sigma T_{\text{sky}}^4 = \sigma \varepsilon_{\text{sky}} T_{\text{A}}^4 \tag{3.19}$$

R_{atm} is the measured long wave radiation from the atmosphere given in W/m^2, T_{sky} and T_{A}, the equivalent sky temperature and ambient temperature in kelvin. Berdahl and Fromberg (1982) found an ε_{sky}, to relate the sky temperature to the ambient temperature for clear sky conditions. This clear sky emittance, ε_0, were adjusted by Berdahl and Martin (1984), and Martin and Berdahl (1984) found a sky emittance, which also included cloud cover, thus made it possible describe the sky temperature for different cloud cover conditions. In the present work, the references will therefore be to the paper of Martin and Berdahl (1984), but with the knowledge of the previous work of Berdahl and Fromberg (1982) and Berdahl and Martin (1984). Marlo Martin is also mentioned in the acknowledgments, as one of the main contributors to the first paper.

Skartveit et al. (1996) compared different formulas both with measurements and with MODTRAN[2] simulations. They found that the formulas from Berdahl and Fromberg (1982) and Frank and Püntener (1986) gave the best results. The measurements in Skartveit et al. (1996), were conducted at 15 different stations in Europe and North America[3]. One of the stations was at the University of Bergen in Norway. In addition to the findings from Skartveit et al. (1996), the modification of Martin and Berdahl (1984) to also estimate the radiation during non-clear sky conditions, makes it one of the most interesting formulas to study.

The empirical model from Martin and Berdahl (1984), is based on measurements at six different locations in the southern United States. The formula is split into two different cases, clear sky and cloudy conditions. For clear sky conditions, Equation 3.20 is used.

$$\varepsilon_0 = 0.711 + 0.0056 T_{\text{dp}} + 0.000073 T_{\text{dp}} + 0.013 \cos\left(\frac{2\pi t_{\text{m}}}{24}\right) \tag{3.20}$$

T_{dp} is the dew-point temperature in $^\circ C$ and t_{m} hours from midnight in solar

[2]MODTRAN (From: MODerate resolution atmospheric TRANsmission), is an atmospheric radiative transfer model. The simulation software model atmospheric propagation of electromagnetic radiation (Spectral Sciences 2009).

[3]Different locations at; $42^\circ N - 65^\circ N; 113^\circ W - 22^\circ E$ and $17 - 990$ meters above sea level (Skartveit et al. 1996).

time (see Equation 3.23). This formula for ε_0 should be valid within a dew-point temperature range of -20 °C to 30 °C. There are different equations used to estimate this temperature. In this work, Equation 3.21 and 3.22 (Duffie and Beckman 2006) are used. The formula for the dew point temperature is based on relative humidity, RH, and the dry bulb temperature T_{dry}.

$$T_{\text{dp}} = C_3 \cdot \frac{[ln(RH) + C_1]}{C_2 - [ln(RH) + C_1]} \tag{3.21}$$

$$C_1 = \frac{C_2 \cdot T_{\text{dry}}}{C_3 + T_{\text{dry}}} \tag{3.22}$$

Relative humidity, $0 \leq RH \leq 1$, is downloaded in hourly values from the Norwegian Meteorological Institute's website, `www.eklima.no`. $C_2 = 17.08085$ and $C_3 = 234.175$. In the present experiments, the ambient temperature is used instead of the dry bulb temperature, $T_{\text{dry}} = T_{\text{A}}$ in $^{\circ}C$, as in the experiments of Meir et al. (2002).

The solar time, t_{solar}, differs from standard time, t_{loc}, according Equation 3.23.

$$t_{\text{solar}} = t_{\text{st}} + 4(L_{\text{st}} - L_{\text{loc}}) + E \tag{3.23}$$

Here, L_{st} is the standard meridian for the local timezone (345° for Oslo), L_{loc}, the longitude of the location (10.41° for Oslo) and E is defined as:

$$\begin{aligned} E = 229.2(&0.000075 + 0.001868\cos B - 0.032077\sin B \\ &-0.014615\cos 2B - 0.04089\sin 2B)\,, \end{aligned} \tag{3.24}$$

where $B = (d-1)\frac{360}{365}$, and d is the day of the year.

Under cloudy conditions, Equation 3.20 is adjusted to Equation 3.25, which takes care of the amount of clouds. As seen, Equation 3.25 is valid in both clear sky and overcast conditions, because the fractional cloud cover, $n = 0$ in clear sky conditions.

$$\varepsilon_{\text{sky}} = \varepsilon_0 + (1 - \varepsilon_0)\varepsilon_{\text{c}} n e^{-\frac{z_{\text{c}}}{z_*}} \tag{3.25}$$

In Equation 3.25, the fractional cloud cover $0 \leq n \leq 1$, the base cloud height z_{c} is measured in km, $z_* = 8.2$ km, and the hemispherical cloud emittance,

$\varepsilon_c \approx 1$, for low altitude clouds, but varies with cloud base height. For cirrus clouds with 4 km $< z_c <$ 11 km, $\varepsilon_c = 0.74 - 0.084(z_c - 4)$ and when $z_c >$ 11 km, $\varepsilon_c = 0.15$. In all measurements made during this year, the cloud altitude was never reported to be higher than 2.5 km.

3.7 Cloud cover

The cloud cover is measured in Oslo at the Norwegian Meteorological Institute every third hour. The measurements are carried out by visual observations made by trained staff members at the Institute. Both the altitude and cloud cover are estimated by visual observations. To estimate the altitude of clouds, z_c, nearby hills with known heights are used for low altitude clouds. Clouds at higher altitudes are estimated mostly by looking at cloud types. Different types of clouds are formed at different altitudes, thus giving a quite good estimate of height. The altitude of all clouds are taken at the base of the cloud, and there is always the lowest cloud present, which sets the value (Norwegian Meteorological Institute 2009). The cloud cover is divided into two different values: Lower cloud cover, NH, and cloud cover, NN. In this work, the mean value of the two observations, NX, are used together with the cloud base height, z_c, even though the altitude is based on the lowest cloud present. Both NH and NN is given as a number from 0 to 8. The cloud cove fraction, n in Equation 3.25, however, takes values from 0 to 1, hence $n = NX/8$.

In Equation 3.25, the altitude has an exponential dependency, normalized by the constant, $z_* = 8.2$ km. One problem with the cloud cover estimation, is that the location of the clouds in the sky is not specified. Clouds in the horizon do not influence the pyrgeometer measurements in the same manner as clouds zenith to the pyrgeometer. This was found to be the main reason for uncertainty in Equation 3.25.

3.8 Cooling degree hours

It might be a challenge to convert the measured infrared radiation from the atmosphere into more useful information, regarding the cooling potential. The term cooling degree hour (CDH) is an attempt to make this information more easily available. First of all, it is an attempt to say something about the

potential for utilization of radiative cooling, similar to what the cooling degree day (CDD) say something about the demand for cooling. The definition of CDH is shown in Equation 3.26, which shows the CDH for one night, CDH_{n}.

$$CDH_{\mathrm{n}} = \int_{sunset}^{sunrise} (T_{\mathrm{rad}} - T_{\mathrm{sky}})\,\mathrm{dt} = \int_{\mathrm{sunset}}^{\mathrm{sunrise}} \Delta \mathrm{T}_{\mathrm{rad-sky}}\mathrm{dt} \tag{3.26}$$

Both the radiator temperature and the sky temperature can be given in kelvin or in degree Celsius. Since the CDH_{n} is based on a temperature difference, $CDH_{\mathrm{n/m}}$ will be given in Kh. In this work, the radiator temperature, T_{rad}, is set to 298 K (25 °C). The choice of radiator temperature is based on some assumptions about a cooling system. A cooling system based on radiative cooling needs some kind of heat store, since the cooling demand in buildings is highest during the day, while energy is radiated out toward the sky during the night. During a day with cooling of the building, the temperature in the heat store will increase. Temperatures above 25 °C can rarely be utilized to cooling, at least in Norway. In other parts of the world, different radiator temperatures might be more useful. During a night with radiation, the temperature in the heat store will decrease when energy is radiated out towards the night sky, thus lowering the radiator temperature. The rate of temperature change is system dependent, and therefore a constant temperature has been set. Comparison of the cooling potential can also easily be made with a constant radiator temperature.

The definition of CDH for each night is not as useful as the sum of CDH for longer periods of time. In places like Norway, with short summers and cold winters, the total CDH for a year is a large number. This, however, is of little relevance when the cooling demand normally only is present during the summer. Monthly sums for CDH are therefore more interesting:

$$CDH_{\mathrm{m}} = \frac{n_{\mathrm{m}}}{N_{\mathrm{m}}} \sum_{i=1}^{N_{\mathrm{m}}} CDH_{\mathrm{n,i}}\,, \tag{3.27}$$

where, n_{m} is the number of nights and N_{m} the number of nights with measurements in a given month m. This normalization will take care of nights missing/without measurements.

3.8.1 Getting a measure of energy back from cooling degree hours

An effort was made to try to use the cooling degree hours to get back to the possible energy radiated out from a specific system. To find the energy from CDH, different re-arrangements and approximations was made. First,

$$\overline{CDH_{\mathrm{m}}} \approx \overline{\Delta T_{\mathrm{rad-sky}}} \cdot \overline{NL}_{\mathrm{m}} \cdot n_{\mathrm{m}} \,, \tag{3.28}$$

where $\overline{NL}_{\mathrm{m}}$ is the mean length of nights in month m, and n_{m} is the number of nights in month m. This is equivalent with:

$$\overline{T_{\mathrm{rad}} - T_{\mathrm{sky}}} = \frac{\overline{CDH_{\mathrm{m}}}}{\overline{NL}_{\mathrm{m}} \cdot n_{\mathrm{m}}} \,. \tag{3.29}$$

A modification of the equation for net power reveals:

$$P = \sigma \varepsilon_{\mathrm{rad}} A_{\mathrm{rad}} (T_{\mathrm{rad}}^4 - T_{\mathrm{sky}}^4) = \sigma \varepsilon_{\mathrm{rad}} A_{\mathrm{rad}} [T_{\mathrm{rad}}^4 - (T_{\mathrm{rad}} - (T_{\mathrm{rad}} - T_{\mathrm{sky}}))^4] \,, \tag{3.30}$$

which is approximately:

$$P \approx \sigma \varepsilon_{\mathrm{rad}} A_{\mathrm{rad}} \left[T_{\mathrm{rad}}^4 - (T_{\mathrm{rad}} - (\overline{T_{\mathrm{rad}} - T_{\mathrm{sky}}}))^4 \right] \,. \tag{3.31}$$

If Equation 3.31 is combined with Equation 3.29, the following approximation for the mean net power is made:

$$\overline{P_{\mathrm{net,m}}} \approx \sigma \varepsilon_{\mathrm{rad}} A_{\mathrm{rad}} \left[T_{\mathrm{rad}}^4 - \left(T_{\mathrm{rad}} - \left(\frac{\overline{CDH_{\mathrm{m}}}}{\overline{NL}_{\mathrm{m}} \cdot n_{\mathrm{m}}} \right) \right)^4 \right] \,. \tag{3.32}$$

When CDH_{m} is known, the mean net cooling power for any system in month, m, given the mean night length, $\overline{NL}_{\mathrm{m}}$, and the number of nights in month m. Several attempts was tried to get this to give reasonable values for the power or the energy. Unfortunately this was not achieved, and it seems that the uncertainties from this calculations also would have been high.

3.8.2 Cooling degree days

The cooling degree hours may look similar to the formula for heating/cooling degree days (HDD/CDD). The degree days, however, are a measure for the heating and cooling demand, and are based on the temperature difference between a chosen indoor temperature and the ambient temperature. The

cooling degree days multiplied with the UA value for a certain house, gives an estimate of the energy needed for cooling. In Oslo, $\overline{CDD} = 9\,^{\circ}\mathrm{C} \cdot \mathrm{days}$ for the period $1960 - 1991$. The value varies between $-11\,^{\circ}\mathrm{C} \cdot \mathrm{days}$ and $29\,^{\circ}\mathrm{C} \cdot \mathrm{days}$, which gives the mean of $9\,^{\circ}\mathrm{C} \cdot \mathrm{days}$ (Benestad 2008). The definition of CDD used is:

$$CDD = \overline{T}_{\mathrm{A}} - 22\,, \tag{3.33}$$

where, $\overline{T}_{\mathrm{A}}$, is the mean ambient day temperature in $^{\circ}C$. The equation is only defined for $\overline{T}_{\mathrm{A}} > 22$, and is defined as 0 for every $\overline{T}_{\mathrm{A}} \leq 22$, which does not explain the negative values obtained and reported by Benestad (2008).

One can argue about the definition in areas with large daily fluctuations in ambient temperature. Large fluctuations in temperature between day and night, may lead to cooling demands during daytime even with the daily mean ambient temperature below 22 °C.

Benestad (2008) also states that the CDD in Oslo, is likely to increase as a consequence of increasing ambient temperature due to global warming. An increasing ambient temperature is likely to increase the cooling demand and also decreasing the heating demand.

Chapter 4

Experimental set-up

In this section, the experimental set-up for the measurements of the infrared night sky radiation is presented in detail. The pyrgeometer used for radiation measurements, and the ambient temperature sensor are described. Section 4.3 explains the data acquisition with the different parts in the chain of data-acquisition. The placement of the experiment is treated in Section 4.1.1, followed by the detailed study of the shadowing from the surrounding buildings. Also an error analysis of the setup is derived. As part of the error analysis, data from the calibration of the ambient temperature sensor are presented.

4.1 The pyrgeometer

Net atmospheric night sky radiation has been measured with a Kipp & Zonen CG1 net pyrgeometer, see Figure 4.1. The main parts of the instrument are the 64-thermocouple thermophile, which act as a thermal detector. A PT-100 temperature sensor at the edge of this thermal detector, at the cold junctions, which measures the pyrgeometer temperature. A 12 V heater and a drying cartridge, keeps the temperature and humidity at certain levels. Radiant energy is absorbed and converted to heat by a disc painted with "carbon black", a paint with high absorptance. The heat flows through a thermal resistance, to the pyrgeometer body acting as a heat sink. The temperature difference across the thermal resistance of the detector is converted to a voltage by the thermophile. Above the thermal detector, a coated silicon window keep the detector shielded from wind and rain. The coating allows only long wave radiation to pass through the window, see Figure 4.2. The flat window makes

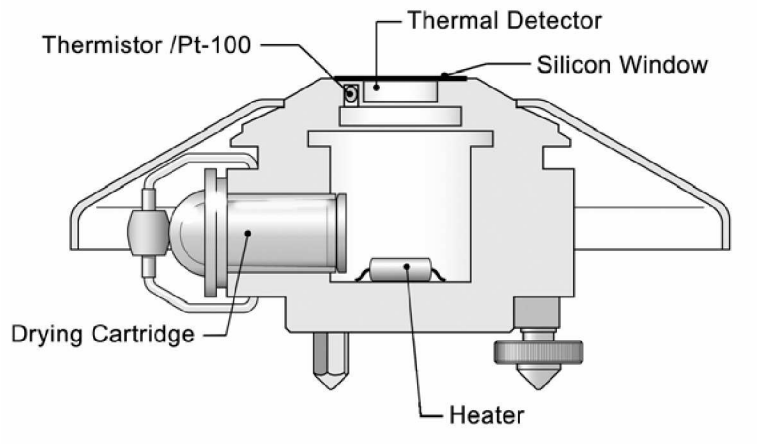

Figure 4.1: Sketch of Kipp & Zonen CG1 net pyrgeometer, with the most important components. (Source: Kipp & Zonen (2009))

the field of view only 150°, but the measured values are quite representative because the pyrgeometer is normally calibrated against a Kipp & Zonen CG 4, with a 180° field of view. A 12 V external power supply was connected to the heater inside the pyrgeometer. When the measurements started, the instrument used was about one year old, and according to the user manual, calibration should be conducted every second year. We decided that no new calibration was required at the present stage (Kipp & Zonen 2009).

The net radiation, R_{net}, is proportional to the output voltage from the pyrgeometer, U_{emf}, measured in μV, with the sensitivity $S = 1.102 \cdot 10^{-5} \frac{\mu V}{W/m^2}$:

$$R_{net} = \frac{U_{emf}}{S} \, . \tag{4.1}$$

The downward atmospheric radiation, R_{atm}, is found by substraction of the pyrgeometer radiation from the net radiation:

$$R_{atm} = R_{net} - \sigma T_p^4 \, . \tag{4.2}$$

The temperature of the pyrgeometer, T_{p} was measured in kelvin.

The transmission of the silicon glass window of the pyrgeometer is shown in Figure 4.2. It transmits more than 50% of the incoming radiation between 4.5 μm to 40 μm. For a body with a temperature of 0 °C, 92.8% of the energy is within this part of the spectrum.

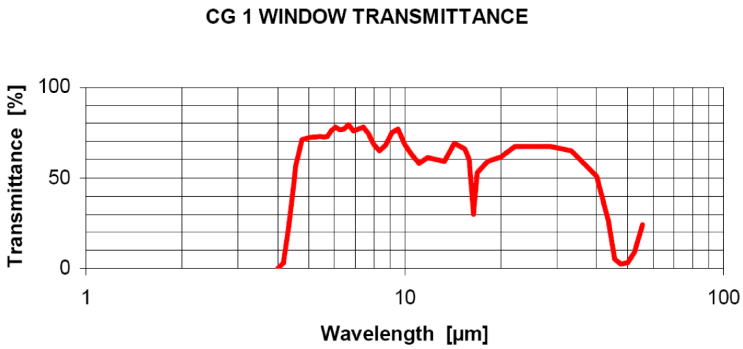

Figure 4.2: The transmittance of radiation through the pyrgeometer glass. Note the logarithmic scale on the x-axis.(Source: Kipp & Zonen (2009))

4.1.1 Pyrgeometer field of view

The experiments were performed in the Solar lab, a small stand-alone building on the parking lot outside the Physics Department building at the University of Oslo. The pyrgeometer was mounted at the roof of the small lab, in a horizontal position. A built-in spirit level on the pyrgeometer was used to keep the pyrgeometer horizontal. It was checked several times during the experiment and only minor deviations were found and corrected. A sketch of the experimental setup, with the relevant parameters, is shown in Figure 4.3. The surface temperature, or the pyrgeometer temperature in this case, T_{P}, the ambient temperature, T_{A}, and atmospheric radiation, R_{atm}, are measured. The equivalent sky temperature can then be found.

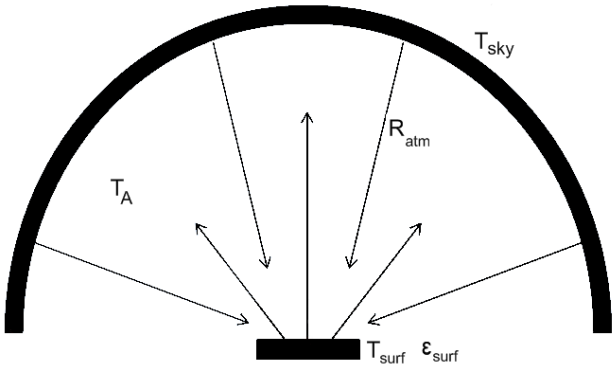

Figure 4.3: The experimental setup for measuring the night sky radiation. The atmospheric radiation R_{atm} and the pyrgeometer temperature T_{surf} are measured with the pyrgeometer. The ambient temperature T_{A} is measured with a thermocouple.

The so-called field of view or optical angle of the pyrgeometer is 150°, and the

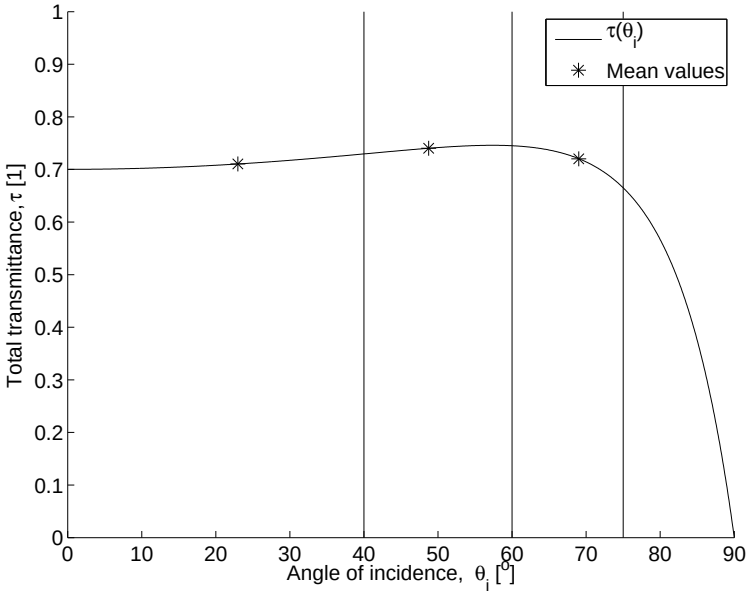

Figure 4.4: The total transmittance as a function of angle of incidence. The $*$ symbols mark the mean values for the transmittance between the lines.

Table 4.1: Mean values for different total transmittance $\bar{\tau}$ between certain angle of incidence θ_{i}. The area is relative tot the total field of view to the pyrgeometer, A_{rel}.

θ_{i} [°]	$\bar{\tau}$	A_{rel}
$0-40$	0.7104	0.18
$40-60$	0.7403	0.30
$60-75$	0.7202	0.52

placement of the pyrgeometer relative to the Physics Department, is shown in Figure 4.8. As described in Section 3.2, reflectance of radiation at a surface is given by the angle of incidence and the refractive index of the surface. The refractive index for the pyrgeometer window is 3.42. The high refractive index lower the total transmittance, but keeps the transmittance at a more constant rate at higher angles of incidence (Van Wely 2009). The total transmittance in the pyrgeometer window as a function of the angle of incidence, is shown in Figure 4.4. The angle is measured from the surface normal. Some angles are indicated with lines; 40°, 60° and 75°. In between the lines, $*$ mark the mean value for the total transmittance between the lines.

The relative areas are found through Equation 3.9, and shown in Table 4.1, together with the mean transmittance in different ranges in the angle of incidence.

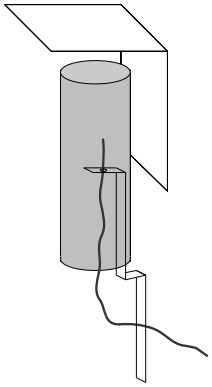

Figure 4.5: The ambient temperature sensor inside a steel tube (grey) with a mounted shield to prevent the sensor to be cooled by radiative cooling during night.

4.2 The ambient temperature sensor

The ambient temperature was measured with a thermocouple, type T from Labfacility Ltd. (UK), (WT-032-D). The temperature sensor was placed inside a metal tube with 27 mm outer diameter, with a shield to prevent from cooling due to night sky radiation, see Figure 4.5. The ambient temperature sensor was placed close to the pyrgeometer on the roof of the Solar lab.

Between 02:54 and 13:04 the 28.04.2009, the ambient temperature sensor measured temperatures below -40 °C. The reason was not found, and the measurements were deleted. The sensor measured apparently correct values both prior and past this period, so no further actions were taken.

4.3 Data handling

Both the pyrgeometer and the thermocouple were connected to a personal computer (PC) through a National Instruments terminal block (type:TBX-68T). A cable connects the terminal block to an internal, PCI data acquisition card (DAQ) in the computer. The input signals are sampled and digitalized by the DAQ card. All data acquisition was made in a self-written LabVIEW[1] program shown in Appendix A.1.1. The program is a so-called virtual in-

[1]LabVIEW (short for Laboratory Virtual Instrumentation Engineering Workbench) is a platform and development environment for a visual programming language from National Instruments (National Instruments 2009).

strument (VI), which process the incoming signals. The VI consists of two parts, the block diagram, which shows the signal paths and calculations, and the front panel, which shows graphs and controllers in real-time. The main purpose for this program was the data-logging, but some graphs are shown at the Front panel to be able to check the results in realtime. All data were collected with 30 seconds interval and the different data collected are shown in Table 4.2. The voltage signals collected in the raw data are not used in the calculation programs made in MATLAB[2]. Both the temperatures and the radiation measured are based on these voltages, but were calculated directly in the data acquisition program. The recorded voltage signals could be used to reproduce the calculated temperatures and radiation in case errors in the VI were found.

The data acquisition setup is shown in Figure 4.6. The sensors, connected to the terminal block, produce a voltage which is measured in the PCI DAQ card, and transferred into the computer and the logging software, LabVIEW.

Raw data files have different length, due to different start and stop times of the logging program. To ease the processing of the data, a Java program, see Appendix A.1.2, was made to combine all raw data files, and to convert them into CSV format[3].Another Java program combined and converted the downloaded meteorological data files into CSV format, and the sunrise/sunset data were manually converted to CSV file in the text-editor Emacs. Figure 4.7 shows how raw data from different sources were converted to CSV files, imported into the MATLAB program, before calculations and the convertion to H5 file format were performed.

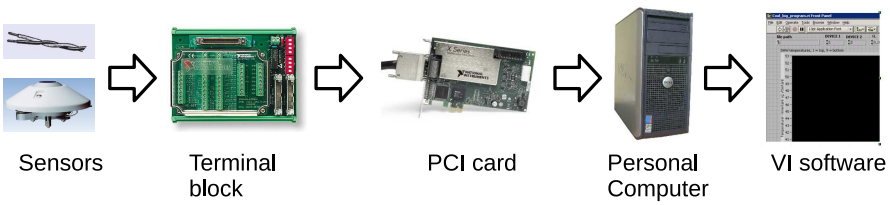

Figure 4.6: The data acquisition setup. A pyrgeometer and a thermocouple were connected to the terminal block. The terminal block were linked to a PCI card in the computer, and data logged by the LabVIEW software.

[2]MATLAB® (from MATrix LABoratory) a MathWorks™ software and a high-level technical computing language and interactive environment for algorithm development, data visualization, data analysis, and numeric computation (MathWorks 2009).

[3]Comma Separated Value, all values are separated by a ';'.

Table 4.2: Example of data collected from the pyrgeometer measurements; T = Temperature, V = Voltage, R = Radiation. The first six columns are shown at the top, and the next ten columns under the first six.

Year ($YYYY$)	Month (MM)	Day (DD)	Hour (hh)	Minute (mm)	Second (ss)
2008	06	02	17	18	07
2008	06	02	17	18	14
2008	06	02	17	18	44
⋮	⋮	⋮	⋮	⋮	⋮

V_{T0} [mV]	V_{TA} [V]	V_{TP} [mV]	V_{P} [mV]	T_0 [°C]	T_{A} [°C]	T_{P} [K]	R_{atm} [W/m^2]	R_{net} [W/m^2]	$T_{\mathrm{sky,pyr}}$ [°C]
0,092397	0,000022	0,112079	-0,001496	32,031769	32,557553	304,200930	349,790223	-135,749995	7,106795
0,092394	0,000022	0,112084	-0,001496	32,032421	32,554602	304,214976	349,839338	-135,790560	7,116633
0,092392	0,000062	0,112101	-0,001499	32,033051	33,515728	304,259041	349,843573	-136,067760	7,117481
⋮	⋮	⋮	⋮	⋮	⋮	⋮	⋮	⋮	⋮

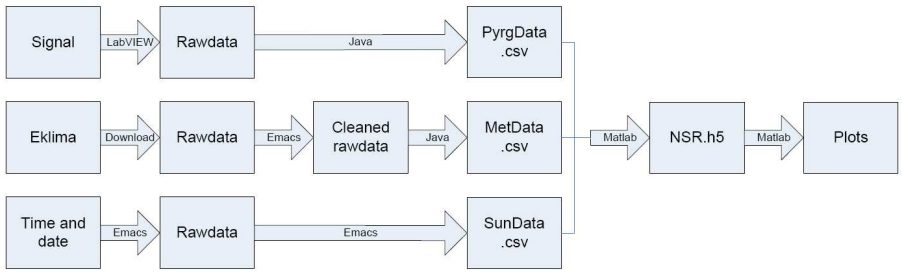

Figure 4.7: Raw data from different sources are converted into CSV files, imported into the MATLAB program 'NSR.m', where calculation and convertion to H5 format takes place. The H5 data can then be imported by another MATLAB program, to make plots.

Data were acquired from the start of June 2008 to the end of October 2009. Some days have missing data for different reasons: The most common being that the automatic update of Microsoft Windows restarted the computer without warning. However, due to security reasons, the computer staff of the University did not allow us to turn off the automatic update function. Unfortunately, sometimes the restart of the computer was not detected for several days, leading to missing data. Another reason for missing data was power failures. All measurements are listed in Table A.1, with an indication of missing data. The automatic update problems could have been avoided by using an offline computer, but with an on-line computer the measurements could be started, restarted and monitored from any other on-line computer through remote desktop connections. Another reason to choose the on-line computer, is the ability to backup the data at a server, physically separated from the Solar lab and the computer.

Timetables for sunrise and sunset in Oslo were downloaded from Time-And-

Date[4]. The sunset/sunrise times was given in local time, and the data logger uses the internal clock to time-stamp the measurements. Therefore, raw data text files and sunset/sunrise times are dated with Norwegian summer time during the summer. The night where summertime is introduced, a gap in the measurements would occur when the clock is adjusted one hour ahead. When the clock is turned one hour back in autumn, two different measurements get the same time-stamp. To avoid these problems, all graphs are represented in normal time, GMT+1. This made it easier, since all data from the Norwegian Meteorological Institute are in the time-format GMT+1. The time conversion were done when data are imported into the MATLAB program 'NSR.m', when data were imported and converted to HDF5 (H5) file format (more details below)[5].

The raw data CSV files were imported into MATLAB with the program 'NSR.m'. This program consists of several functions, which perform different steps of the data-handling. The entire program is shown in Appendix A.1.3. In this program, different raw data are imported, combined and converted to a H5 file. The H5 file format is a format which stores the data binary. In practical terms this greatly reduced the time for reading data from file. The HDF5 file system has a hierarchic data format, which makes it possible to store different kinds of data in different parts of the file. The structure of the file is shown in Figure A.3. As seen, the file is divided into three main groups. Group 1 contains data measured from the pyrgeometer. Group 2 contains meteorological data downloaded from `www.eklima.no`, and data for sunset/sunrise downloaded from `www.timeanddate.com`. Group 3 contains different sets of calculated data. All datasets have their own smaller dataset with the header of the file. Separating out the header makes the importing of the datasets into matrices more efficient. The large amount of data collected, made calculations time consuming and therefore, storing pre-calculated data saved a lot of calculation time. Since many graphs were produced with different combinations of calculated data, storage of pre-calculated data could be imported directly. Some of the calculations had to be done in loops, and MATLAB works in general slow with loops. On the contrary, matrix operations are very fast, and the well-developed plot functions made me choose MATLAB for the data handling.

[4] `www.timeanddate.com`

[5] More information about the HDF5 file format is found in `www.hdfgroup.org`

4.4 Shadowing of the surrounding buildings

Ideally, the pyrgeometer should be placed in an site with no obstructions inside the instrument's field of view (Kipp & Zonen 2009). Since the experiments had to be performed at the Solar lab, this was not possible to achieve. Due to the location of the Solar lab, close to the Physics Department building, parts of the surrounding building fall inside, within the field of view of the pyrgeometer. Since the building blocks some of the view of the pyrgeometer, we say that the building creates a "shadow", seen in Figure 4.8

This will have an effect on the measurements, because the building most likely will have a temperature higher than the sky. A higher temperature will give a higher measured radiation level. To find the size of the shadow, the surrounding of the experimental setup was drawn in the 3D drawing program Google SketchUp[6]. The placement of the experimental setup was measured with a measuring tape. For simplicity, the Solar lab is not drawn in Figure 4.8.

The 3D drawing allowed a visualization of the so-called shadowing area, the area where the surrounding buildings obstruct the pyrgeometer field of view. shown in Figure 4.8. The area was found by drawing lines from the pyrgeometer to the top of the building, where the building is inside the pyrgeometer's field of view. Then all lines where made with equal length, and the area at the end of lines where closed to get the area of the shadow. The shadowing area was then compared to the area of the total pyrgeometer view at same distance from the instrument, and was found to be about 15.4% of the total field of view. This percentage, however, can not be used directly to find the total building influence of the measurements, because the measured radiation level has an angular dependence according to Fresnel's laws, see Section 3.2. Of the total area, about 60% is between 60 ° and 75 °, 40% is between 40 ° and 60 °. This was estimated from the 3D drawings in Google SketchUp. The offset error caused by the surrounding buildings is described in Section 4.5.

Another implication of the shadowing of the pyrgeometer is the time for sunset and sunrise. Timetables for sunset/sunrise were found for Oslo, but these do not consider shadowing of buildings. As shown above, the location of the pyrgeometer, according to the surrounding buildings, was drawn in a 3D model. This model was located on to the satellite image in Google Earth[7].

[6]Google SketchUp is a 3D drawing program, which can be downloaded for free at `http://sketchup.google.com`.

[7]Google Earth is Googles world map/satellite photo program, available for free download

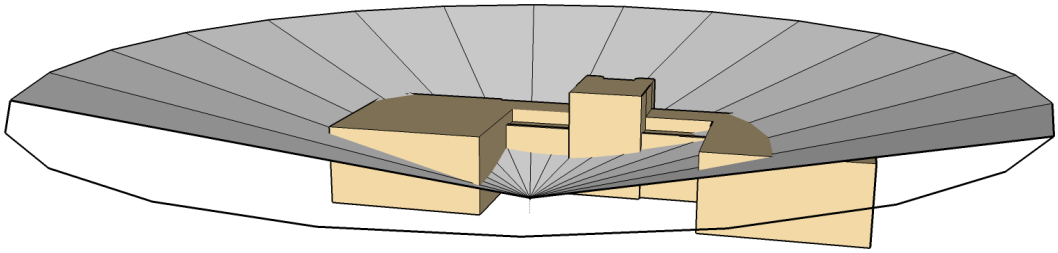

(a)

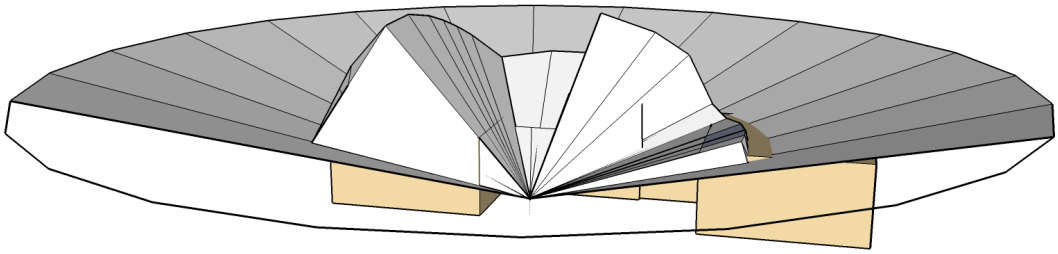

(b)

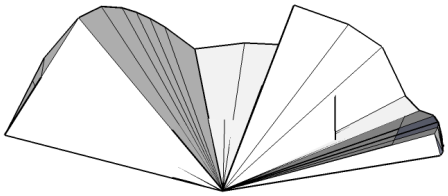

(c)

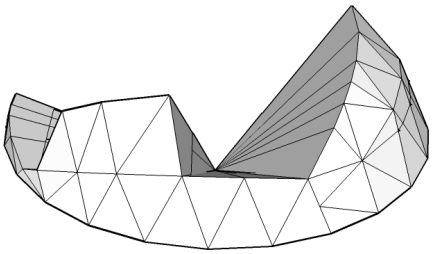

(d)

Figure 4.8: (a) A 3D sketch of the Physics Department building, with the placement of the experimental setup. A cone, visualizing the pyrgeometer field of view of 150° *is outlined. (b) The area of the shadow is made, by drawing lines on top of the building. (c) Removal of the building, leaves only the shadowing area left. (d) The shadowing area seen from the other side.*

The shadowing function in the Google SketchUp can be set to real sunlight when the exact location is found. This analysis showed that sunlight would hit the pyrgeometer and the ambient temperature sensor exactly at the time when we see the rise and start of the fluctuation in T_A (See Figure 5.1). This was also confirmed by visual observation.

As discussed above, the times used for sunset/sunrise are not the accurate times when the sun hits the pyrgeometer or not. However, all data analysis was made according to the sunset/sunrise tables downloaded and plotted into the graphs, to make the results more interesting to other locations with different surrounding buildings. Surrounding buildings may prevent solar radiation from reaching the radiator, leading to a longer period for radiative cooling. On the other hand, the surrounding buildings most probably have a higher temperature than the sky, leading to higher values of radiation. If, however, experiments with solar collectors used as radiators are conducted at the Solar lab this must be taken into consideration.

4.5 Uncertainty analysis of the measurements

The uncertainty of the measurements are a combination of statistical and systematic errors. Statistical errors are shown in the ripple of continuing measurements, while systematic errors produce an offset value. In this section the error analysis of both the pyrgeometer and the ambient temperature sensor is shown. Most of the theory from error analysis is found in Taylor (1997). There are several terms to keep in mind when dealing with uncertainty analysis. It is important to know that true values can not be obtained. Instead of true values, the term accepted value are often used, since we can not know true values. The term accuracy can be defined as how close the measurements are to the accepted value. A higher accuracy means that the measurements is closer to the accepted value (i.e. a smaller value). During calibration the precision is found by analyzing the ripple. Precision is measured in standard deviations, σ.

at `www.earth.google.com`

The pyrgeometer

The pyrgeometer manual states an accuracy of ±10% for daily totals, and the solar radiation is mentioned as the main source of error. However, this is not a problem during night-time measurements, and therefore, higher accuracy (i.e. $< \pm 10\%$) can be expected. The manual also states that the estimated inaccuracy of measurements is less than ±20 W/m^2. If 20 W/m^2 is the inaccuracy of the net radiation, R_{atm}, the error in sky temperature will be between ±3.32 K and ±6.61 K, in the measured interval of atmospheric radiation, see Figure 4.10.

One can work out something about the statistic precision by looking at the ripple in the measurements. If there is a steady cloud cover or if there is a totally clear sky, and there are no other effects influencing the measurements, the ripple can be read out. Figure 4.9 shows the ripple from a period of time with no/minimal amount of clouds. It is seen from this example that the ripple is of about ±1 W/m^2, which is quite accurate. This would correspond to an uncertainty in T_{sky} in the interval of ±0.17 K and ±0.33 K. This however, does not say anything about the offset errors.

There is reason to believe that the uncertainty is somewhere between the two examples described above. Figure 4.10 shows the uncertainty in the sky temperature for different uncertainties in the atmospheric radiation, between ±1 W/m^2 and ±20 W/m^2. The errors are calculated as shown in Equation 4.3:

$$\delta T_{\text{sky}} = \frac{T^{+}_{\text{sky}} - T^{-}_{\text{sky}}}{2}\,, \tag{4.3}$$

where T^{+}_{sky} and T^{-}_{sky} are defined as:

$$T^{+}_{\text{sky}} = \left(\frac{R_{\text{atm}} + \delta R_{\text{atm}}}{\sigma}\right)^{1/4} \qquad T^{-}_{\text{sky}} = \left(\frac{R_{\text{atm}} - \delta R_{\text{atm}}}{\sigma}\right)^{1/4}\,. \tag{4.4}$$

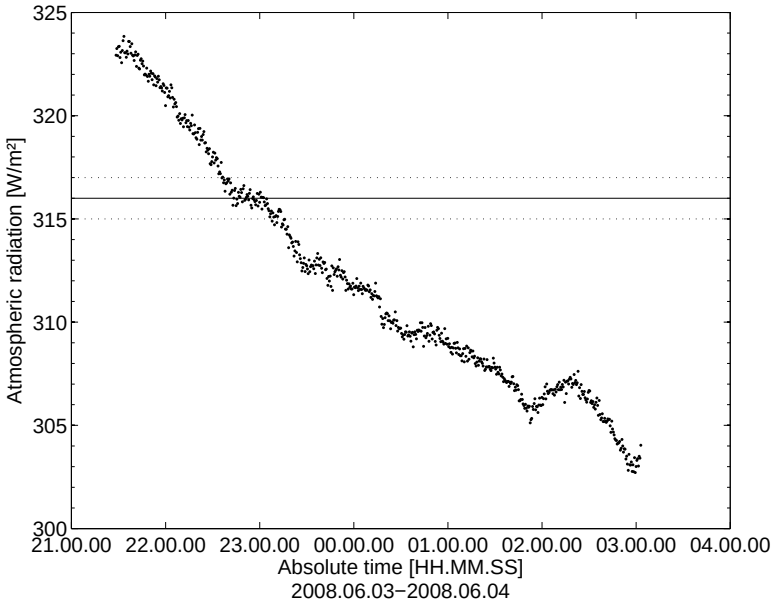

Figure 4.9: The ripple from measurements of the atmospheric radiation. Solid line inserted at 316 $\mathrm{W/m^2}$*, and broken lines at* 315 $\mathrm{W/m^2}$ *and* 317 $\mathrm{W/m^2}$*. This indicates that the ripple of the atmospheric radiation lays well below* ± 1 $\mathrm{W/m^2}$ *during this night.*

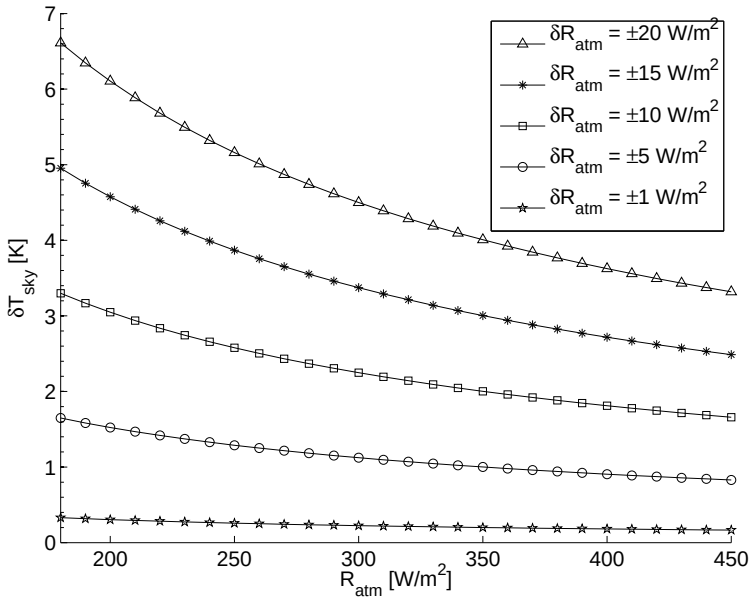

Figure 4.10: Uncertainty in T_{sky}*, for different uncertainty in* R_{atm}*. The range of* R_{atm} *is taken within the range of measurements.*

Since the total accuracy should be within 10% for daily totals, and the ripple on a clear night show about ± 1 $\mathrm{W/m^2}$, a total uncertainty of ± 10 $\mathrm{W/m^2}$ will not be to underestimate the uncertainty. This uncertainty leads, according

to Figure 4.10, to an uncertainty in the sky temperature in the range from ± 1.6 K to ± 3.3 K.

In addition to the uncertainty in the measurements, both due to statistical errors shown in the ripple and the stated inaccuracy of the manual, we have the offset error caused by the Physics building, found in Section 4.4. This shift/offset is also dependent on the different temperatures both on the Physics building and in the sky. In this calculation, a refractive index of 1.0 and 3.42 was used for air and the coated pyrgeometer silica window respectively. In Section 3.2 the relative areas and mean total transmittance were found, and the total radiation reaching the pyrgeometer is then given in Equation 4.5.

$$\begin{aligned} R_{\text{actual}} = &\left[(0.18 \cdot 0.71) + (0.3 \cdot 0.74 \cdot 0.938) + (0.52 \cdot 0.72 \cdot 0.908)\right] \sigma T_{\text{sky}}^4 \\ &+ \left[(0.3 \cdot 0.74 \cdot 0.062) + (0.52 \cdot 0.72 \cdot 0.092)\right] \sigma T_{\text{Pb}}^4 \end{aligned} \tag{4.5}$$

In Equation 4.5, the fraction of the total relative areas is multiplied with the mean transmittance within the span and the relative fraction of area from the sky and the Physics building. All data is found in Table 4.3. R_{actual} is the actual radiation absorbed at the pyrgeometer (R_{net}).

The atmospheric radiation absorbed by the pyrgeometer if there where no surrounding buildings would be:

$$R_{\text{sky}} = \left[(0.18 \cdot 0.71) + (0.3 \cdot 0.74) + (0.52 \cdot 0.72)\right] \sigma T_{\text{sky}}^4 \, . \tag{4.6}$$

The offset error in the radiation measurements, is therefore:

$$\delta R_{\text{rad,offset}} = \left(\frac{R_{\text{actual}}}{R_{\text{sky}}} - 1 \right) \cdot 100\% \, , \tag{4.7}$$

shown for different temperatures in Figure 4.11.

The offset error in the measurements of the night sky radiation caused by the surrounding building is dependent on the different temperatures involved, since the radiation measured at the pyrgeometer will be a sum of the atmospheric radiation R_{atm} and radiation from the surrounding buildings R_{PB}. Both the sky temperature and the temperature of the building surface, must therefor be taken into account. The offset error for different sky temperatures, and for different temperature differences, $\Delta\ T_{\text{PB}-\text{sky}} = T_{\text{PB}} - T_{\text{sky}}$, is shown in Figure 4.11.

Table 4.3: All fraction of areas within different spans of angle of incidence, θ_i, together with the mean of total transmittance, $\overline{\tau(\theta_i)}$. A_{tot} is the fraction of the total area within the current span of angle of incidence. A_{Pb} is the fraction of the area covered by the Physics building and A_{sky} is the remaining fraction covered by the sky

θ_i [°]	$\overline{\tau(\theta_i)}$	A_{tot}	A_{Pb}	A_{sky}
$0 - 40$	0.71	0.18	0.0	1.0
$40 - 60$	0.74	0.30	0.062	0.938
$60 - 75$	0.72	0.52	0.092	0.908

From the analysis it is seen that the error caused by the Physics building, is highest when the difference in temperature between the building and the sky temperature, ΔT_{PB-sky}, is large, and at low sky temperatures. At most, the error is about 6%, at $T_{sky} = -40$ °C, and with a building temperature, $T_{PB} = 0$ °C. All measurements, however, show that the sky temperature lays at most 26.6 K below the ambient temperature, thus the building temperature would be at least 13.4 K above the ambient temperature in the top line in Figure 4.11.

A normal summer night with clear sky, has a sky temperature around 0 °C, and an ambient temperature of about +18 °C. Suppose that the building temperature is +25 °C, the plot in Figure 4.11 then shows that the error would be about 3%. Corresponding to an offset error in the sky temperature of 1.74 K.

On the other end, a building temperature of about +10 °C, and a sky temperature −25 °C will give an error of about 4.6%, corresponding to an error in the sky temperature of 2.6 K. An extreme case would be a sky temperature of −40 °C and a building temperature of +25 °C. This will lead to a measured sky temperature 5.76 K higher than the actual sky temperature. If the building temperature is the same as the sky temperature, there would be no error in the measurements, and therefore the lower part of this uncertainty becomes 0 K. The other side of the range is set to about 3 K, which is obtained from $T_{sky} = -25$ °C and $T_{PB} = +15$ °C. The extreme case with 65 K difference between the sky temperature and the building temperature is very unlikely.

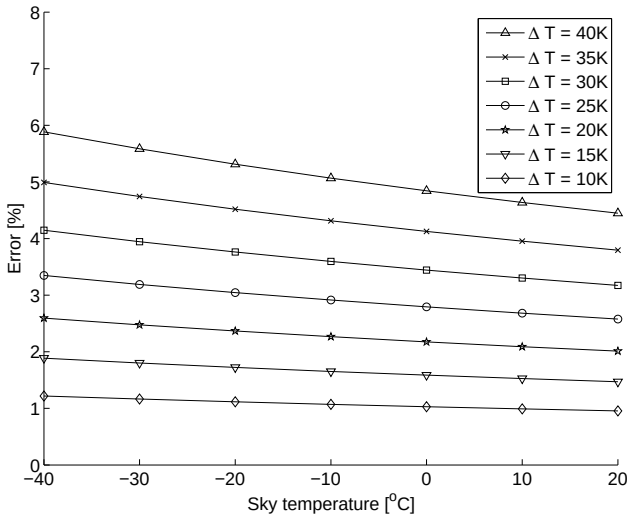

Figure 4.11: The error in the measurements, caused by the surrounding buildings, for different $\Delta T = T_{\mathrm{PB}} - T_{\mathrm{sky}}$ as a function of T_{sky}.

The ambient temperature sensor

Error and uncertainties in measurements of ambient temperature can be treated in another way, since the sensor was calibrated before the experiment started. Calibration cancels out offset errors and can be used to find the uncertainty of the temperature measurements.

The precision of the thermocouple can be shown from the calibration when the thermocouple is kept in the ice-water mixture. Figure 4.12 shows an outlier at about 0.8 °C, which is circled in the plot. The ice-water mixture should hold a temperature of 0 °C, but we observe a ripple of about ±0.2 °C, see Table 4.4 and Figure 4.13. LabView records the data with 7 significant numbers. All significant numbers are kept in the calculations.

Grubb's law, shown in Equation 4.8, makes a test for when suspicious data-points can be deleted.

$$G = \frac{|x - \bar{x}|}{\sigma} \tag{4.8}$$

When a value x, has a $G > G_{\mathrm{Critical}}$, it can be deleted. Here $\bar{x}$ is the mean

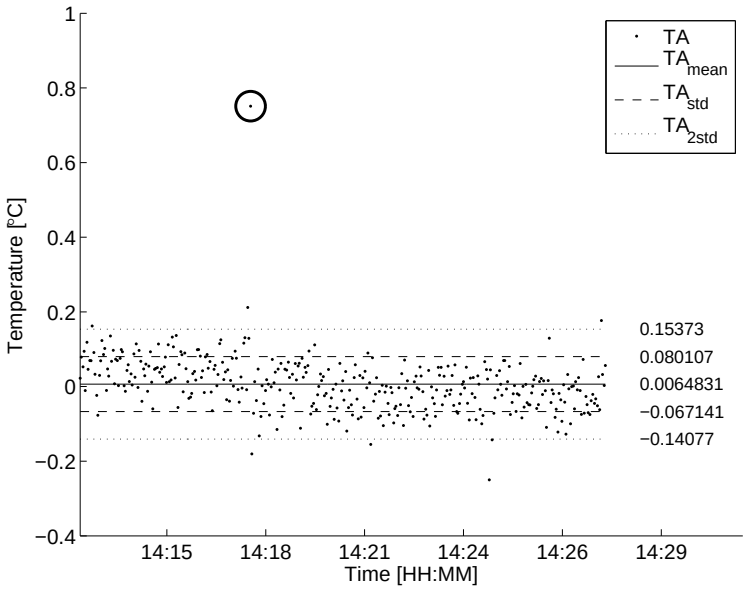

Figure 4.12: Error analysis of T_{A} sensor in ice-water mixture. Included in the graph is the mean value, solid line, the standard deviation, dashed lines, and two times the standard deviation, dotted lines. Also shown is a circled outlier.

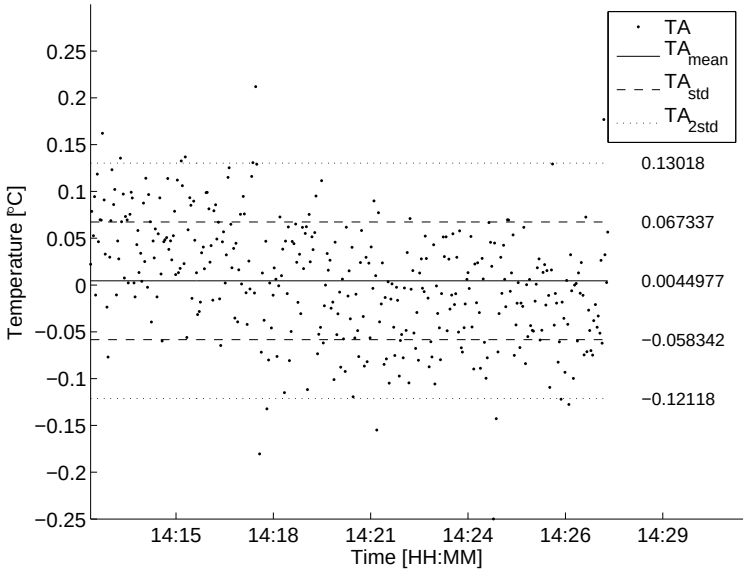

Figure 4.13: Same as Figure 4.12, but with the outlier removed.

value for all measurements. G_{Critical} can be chosen in each case. Figure 4.14 shows all G values for the dataset, and we see that a G_{Critical}-value of 4 will be enough to remove the data-point circled in Figure 4.14 and Figure 4.12, which lays unnatural high.

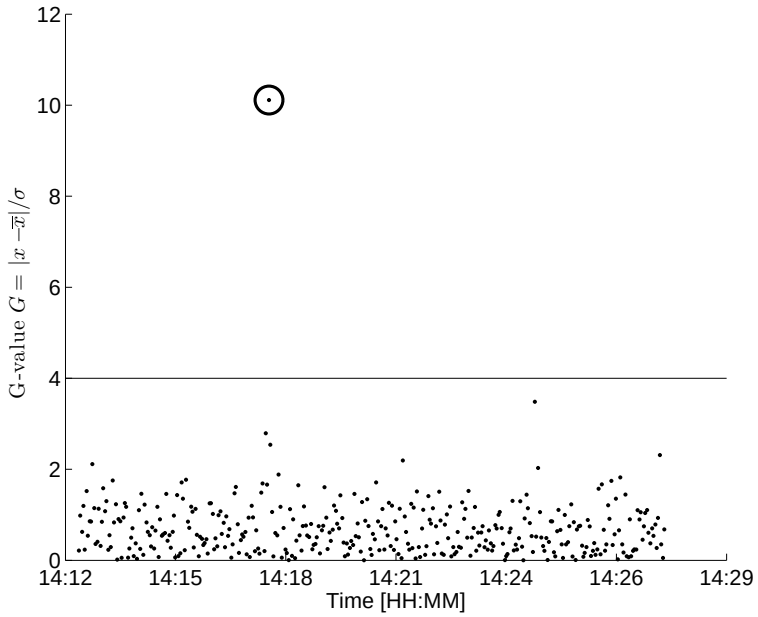

Figure 4.14: G-values for all data-points in the calibration experiment. The circled point can be deleted from the dataset with a good margin.

Removal of the statistical outlier gives the values shown in Table 4.4.

Table 4.4: Analysis data from T_A-sensor in ice-water mixture, with the removal of one statistical outlier.

Statistical data	Temperature [°C]
$T_{A,mean}$	0.0045
$T_{A,median}$	0.0049
$T_{A,std}$	0.063
$T_{A,max}$	0.21
$T_{A,min}$	-0.25

When calibrated against the alcohol thermometer, the only uncertainty will be the ripple effect, and as shown above, the ripple lays within ±0.2 K. Two times the standard deviation will give a value of ±0.13 K. In addition there will be an uncertainty in the alcohol thermometer and in the manual read-out from this. The scale of this thermometer gives a readout error of ±0.05 K. The alcohol thermometer is not calibrated to any other thermometer in this setup, but showed 0.0 °C when held into the ice-water mixture.

At other temperatures, the thermocouple shows a similar ripple effect and the calibration carried out at different temperatures from 15 °C to 80 °C, at 5 K steps gives ripple in the same order. The difference between the maximum

and the minimum value, $T_{\mathrm{A,max}} - T_{\mathrm{A,min}}$, measured for all temperatures in the calibration process is between 0.48 K and 0.96 K. And the 2σ is in the range of ± 0.17 K and ± 0.35 K for all temperatures. Since the calibration of the temperature sensor gave several series of measurements, the standard deviation from these measurements could have been used for singular measurements of temperature later in the experiment. When the ambient temperature is used in calculations of the sky temperature, a mean value over some temperature measurement will be used. Thus equal out some of this uncertainty. All in all, the uncertainty of the T_{A}-sensor will be ± 0.4 K for the whole temperature range measured.

The Berdahl Fromberg formula

The uncertainty in the formula of Berdahl and Martin (1984) can be quite big due to propagation of errors. If we start out with finding the uncertainty in ε_0, we only have uncertainty in the dew point temperature, T_{dp}. For different uncertainties in T_{dp}, we get different uncertainties in ε_0, as seen in Figure 4.15. For instance will a precision in T_{dp} of ± 1 K, give an uncertainty in ε_0 in the range from ± 0.0012 to 0.0085.

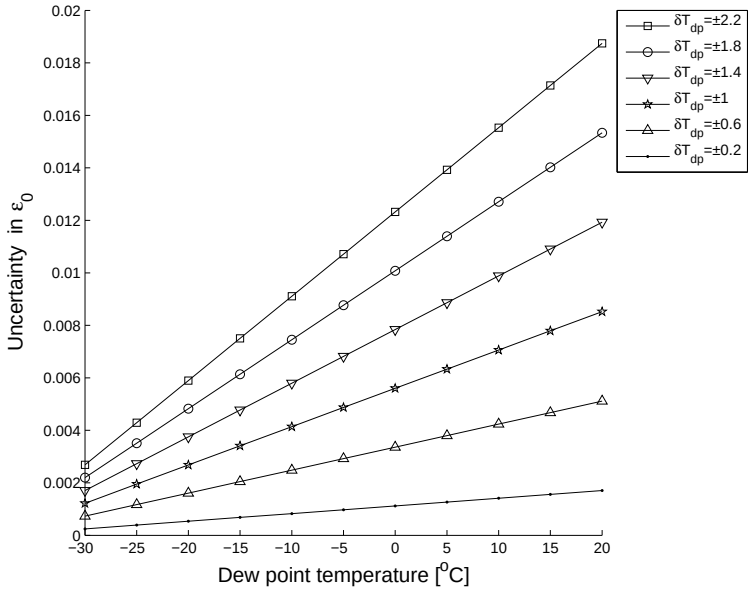

Figure 4.15: Different uncertainties in ε_0, for different uncertainties in T_{dp}.

In the formula of ε there are several parts, all with differnet uncertainties, thus

the total uncertainty based on propagation of error is:

$$\frac{\delta\varepsilon}{\varepsilon} = \sqrt{\left(\frac{\delta\varepsilon_0}{\varepsilon_0}\right)^2 + \left(\frac{\delta\varepsilon_0}{\varepsilon_0}\right)^2 + \left(\frac{\delta\ n}{n}\right)^2 + \left(\frac{\delta\ e^{-\frac{z_c}{z_*}}}{e^{-\frac{z_c}{z_*}}}\right)^2} \tag{4.9}$$

Uncertainty in the cloud base height taken to be somewhere between ±100 m and 250 m, leads to an uncertainty in the exponential part between ±0.012 and ±0.031. Since the cloud-cover NX is given as a number between 0 and 8, the uncertainty can be set to ±0.5, giving an uncertainty in n, of $\pm\ 0.5/8\ =\ \pm 0.0625$. The hemispherical cloud emittance, ε_c, is said to be known exact, with no uncertainty. The uncertainties are all relative, and will therefore be given in ranges. (Ranges are here indicated with $[a, b]$, meaning from a to b):

$$\frac{\delta\varepsilon_0}{\varepsilon_0} = \pm\frac{[0.0012, 0.0085]}{[0.4, 1]} = \pm[0.0012, 0.02125]\,. \tag{4.10}$$

$$\frac{\delta n}{n} = \pm\frac{0.0625}{[0.125, 1]} = \pm[0.06, 0.50] \tag{4.11}$$

$$\frac{\delta\ e^{-\frac{z_c}{z_*}}}{e^{-\frac{z_c}{z_*}}} = \frac{\delta z_c}{z_*} = \pm\frac{[0.1, 0.250]\text{km}}{8.2\text{km}} = \pm[0.0122, 0.0305] \tag{4.12}$$

$$\frac{\delta\varepsilon}{\varepsilon} = \pm[0.06, 0.50] \tag{4.13}$$

As seen from the equations above, the uncertainty in the emissivity has a great range. There are, however, very unlikely that all the uncertainty in the uncorrelated parts of the equations will be added at the same time. Uncertainty in ε will give an uncertainty in the sky temperature as shown in Equation 4.18.

$$T_{\text{sky,met}} = \varepsilon^{1/4} T_A \tag{4.14}$$

$$\frac{\delta T_{\text{sky,met}}}{T_{\text{sky,met}}} = \pm\sqrt{\left(\frac{\delta\varepsilon^{1/4}}{\varepsilon^{1/4}}\right)^2 + \left(\frac{\delta T_A}{T_A}\right)^2} \tag{4.15}$$

$$\frac{\delta\varepsilon^{1/4}}{\varepsilon^{1/4}} = \frac{1}{4}\frac{\delta\varepsilon}{\varepsilon} = \frac{[0.06, 0.50]}{4[0.63, 1]} = [0.015, 0.125] \tag{4.16}$$

$$\frac{\delta T_A}{T_A} = \frac{0.4}{[257, 300]\text{ K}} = [0.0013, 0.0016] \tag{4.17}$$

$$\frac{\delta T_{\text{sky,met}}}{T_{\text{sky,met}}} = \pm[0.015, 0.125] \tag{4.18}$$

The highest possible uncertainty in $T_{\text{sky,met}}$ is $\pm 12.5\%$, but it is not likely that the error in any calculation will be this high. The range of $T_{\text{sky,met}}$ is measured to be between 231.0 K and 291.3 K, leading to errors in the range from ± 28.9 K to ± 36.5 K, if the high end of the uncertainty is used. Using the lower end of the uncertainty, and the same range of temperatures, however, gives error in $T_{\text{sky,met}}$ in the range from ± 3.5 K to ± 4.4 K.

The major source of error is the cloud cover. Under clear sky and fully clouded conditions, the errors in these measurements are as good as zero. This is because the cloud cover shifts from 0 to 1 when the first cloud is present, even though this cloud covers less than 1/8 of the sky. The same is present when the sky has a full cloud cover. If one spot of clear sky is seen, the cloud cover is shifted to 7. The biggest deviations between measured and calculated values are observed during changing cloud cover. These deviations are caused by positioning of clouds in the sky, which is not recorded. Mean values will cancel out this error, so we should expect a higher accuracy when finding mean values for longer periods of time. In Section 5.3, the highest observed standard deviation in the difference of $T_{\text{sky,pyr}}$ and $T_{\text{sky,met}}$ is 5.9 K, which leads to $2\sigma = \pm 11.8$ K. The smallest standard deviation is ± 2.67 K $\Rightarrow$ $2\sigma = \pm 5.34$ K. This may be used as an estimate of the uncertainty of $T_{\text{sky,met}}$. Table 4.5 summarizes the uncertainties for the measured values.

Table 4.5: Table of uncertainties for the measured and calculated values (ranges shown with [a, b]*).*

Temperature	Uncertainty [K]
T_{A}	± 0.4
$T_{\text{sky,pyr}}$	$\pm[1.6, 3.3]$
$T_{\text{sky,pyr}}$ (offset)	$+[0, 3]$
$T_{\text{sky,met}}$	$\pm[5.34, 11.8]$

Chapter 5

Results

In this section a selection of results will be described. Measurements of the sky temperature were made with 30 sec intervals. This leads to a large amount of data, which is most reasonable to represent as one graph per night. All raw data can be found as graphs in Appendix A.2.2. In addition, a list of all the measurements is found in Appendix A.2.1. Three nights representing typical examples of different cloud cover are described in detail. The same graphs are shown in Appendix A.2.2, for all nights. In some cases, presumptions had to be made and the background for these, are all discussed more in detail in the next section, Section 6. All sky temperature measurements are presented as a function of different variables. Section 5.3 compares measured values to values found from the model of Martin and Berdahl (1984). Cooling power is found based on a radiator temperature of 25 °C.

5.1 Typical graphs

Measurements have been taken from 02.06.2008, and until 30.09.2009, but in the data analysis, no measurements after the night 6-7.07.2009 are included. All raw data graphs in Appendix A.2.2 have the same axis, and legend as shown here, but in order to save space, all legends have been removed from the appendix graphs. Most nights can be divided into three main categories, based on cloud conditions. Typical graphs for different cloud conditions are shown in Figures 5.1 - 5.3. The three main categories are clear sky, completely overcast and changing cloud cover. Changing cloud cover is here represented with a night where clouds move in during the night. All graphs have the same

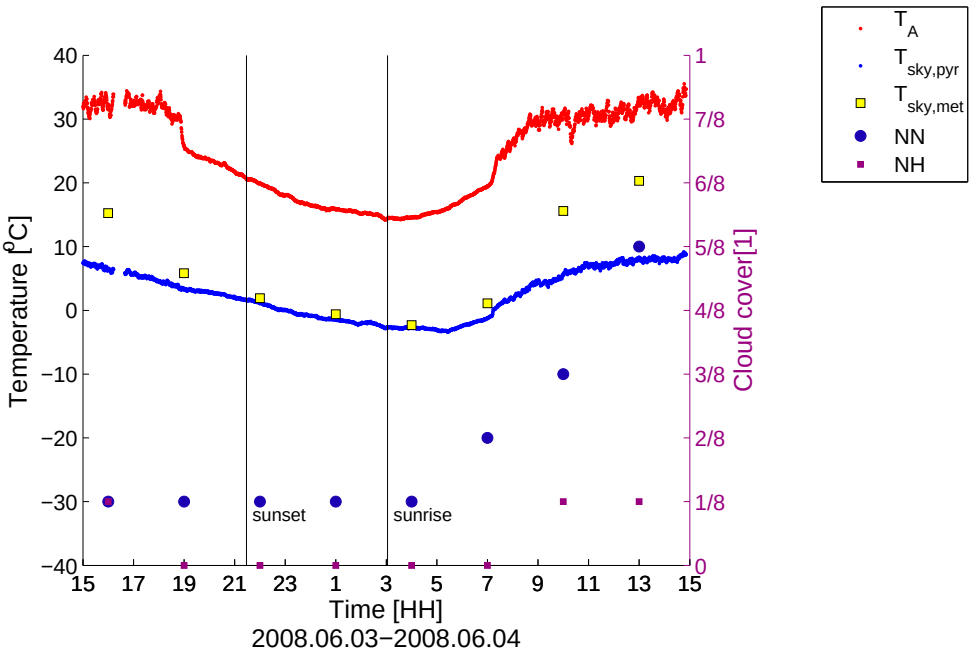

Figure 5.1: Typical graph of a clear sky night showing measurements compared to calculated values. The sky temperature is well below the ambient temperature.

axis, where the x-axis represents the absolute time in hours from 15:00 day one to 15:00 day two, in Norwegian normal time, GMT+1. The left y-axis shows temperatures in $^{\circ}C$, and the right y-axis shows the cloud cover represented in eights. The reason for the representation in eights, is because the values from the Meteorological Institute are given as a number between 0 and 8 and the formula from Martin and Berdahl (1984) takes values of cloud cover in a fraction of one. The small red colored dots are measurements of the ambient temperature, T_{A}, while the small blue dots represent the sky temperature, $T_{\mathrm{sky,pyr}}$, indirectly measured with the pyrgeometer. The yellow boxes show the sky temperature, $T_{\mathrm{sky,met}}$, calculated from the formula of Martin and Berdahl (1984). Cloud cover is represented by large blue circles and purple squares for cloud cover, NN, and lower cloud cover, NH, respectively. The times for sunset and sunrise are shown as vertical black lines.

In Figure 5.1, the lower cloud cover, NH, is zero while the cloud cover, NN, is 1/8 during the night. The sky temperature is about 20 K below the ambient temperature. The calculated sky temperature, $T_{\mathrm{sky,met}}$ lays less than 0.5 K above $T_{\mathrm{sky,pyr}}$ during the night. At daytime, the calculated values is several degrees higher, compared to the measured values. The reason for this is discussed in Section 6.2. It can be seen that the ambient temperature sensor fluctuates more at daytime, when it is exposed to direct sunlight. All data

analysis were therefore only made with values obtained during nighttime.

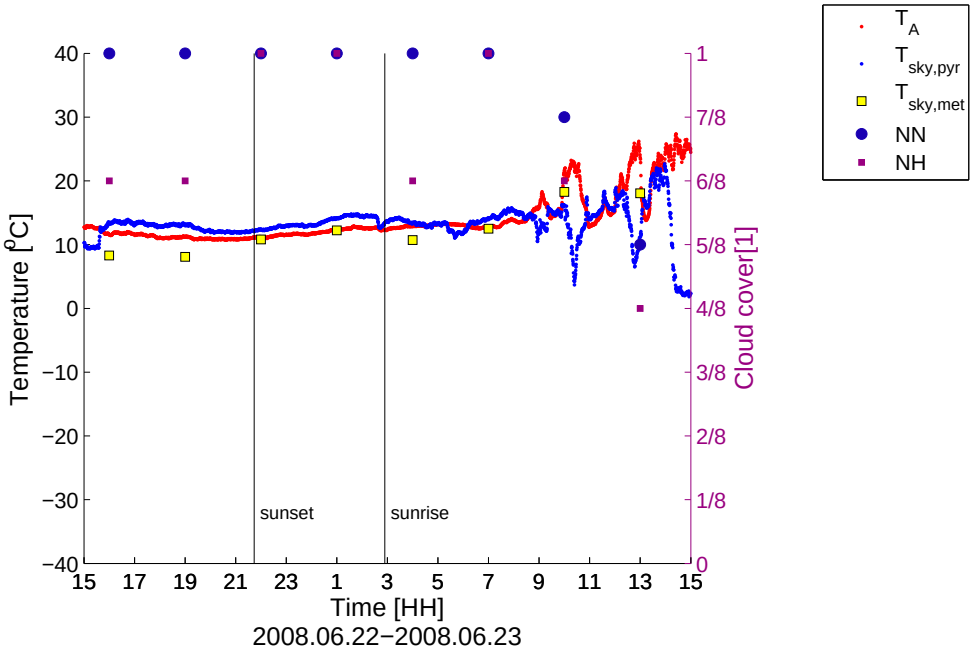

Figure 5.2: Typical graph showing one overcast night of measurements compared to calculated values. The sky temperature is close to and higher than the ambient temperature.

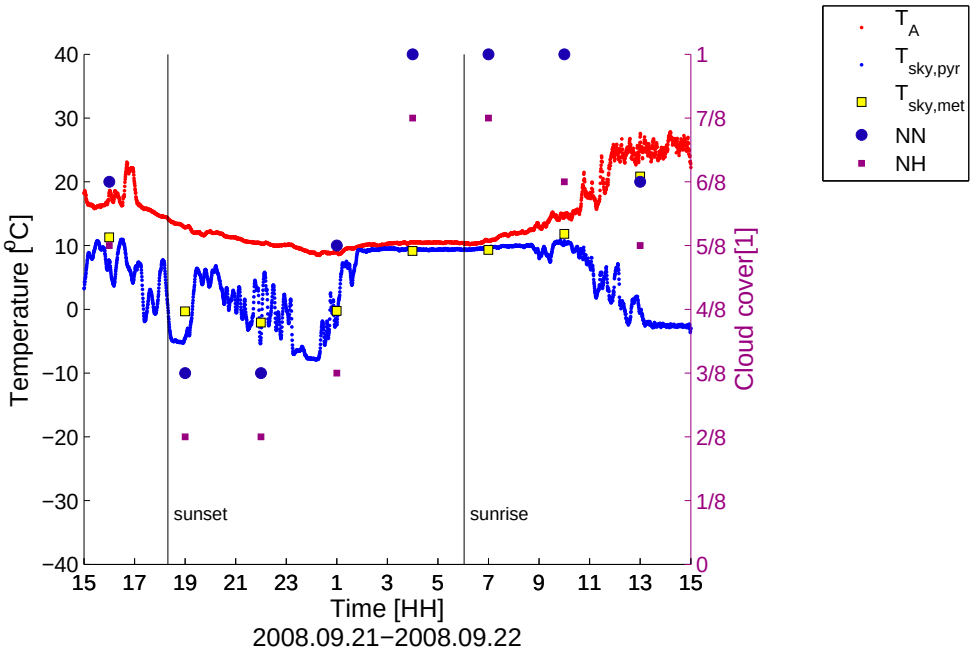

Figure 5.3: Typical graph showing a rise in cloud cover during the night, representing changing cloud cover.

Figure 5.2 shows a night with overcast sky, NH and NN are 8/8. The measured sky temperature, $T_{\mathrm{sky,pyr}}$, is here between 1 K and 2 K higher than the ambient temperature, while $T_{\mathrm{sky,met}}$ lays less than 0.4 K below T_{A}. The fact that the sky temperature is measured higher than the ambient temperature, is discussed in Section 6.1.

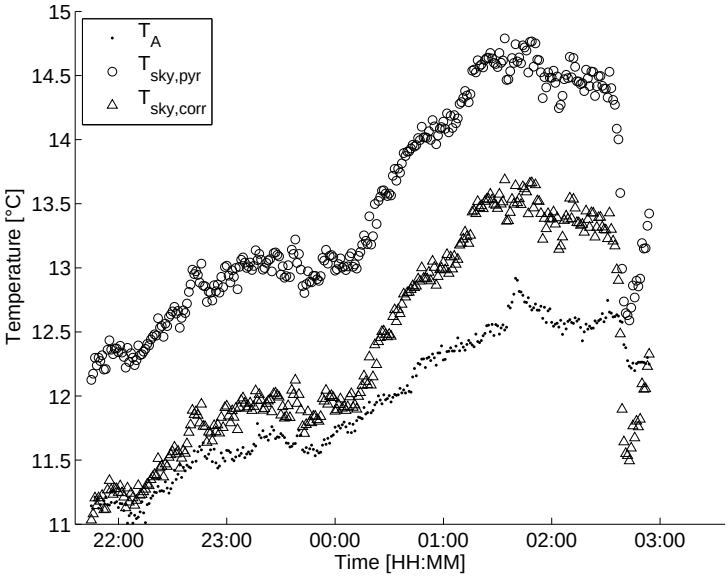

Figure 5.4: T_A, $T_{sky,m}$ and the sky temperature, $T_{\mathrm{sky,corr}}$, corrected for the influence of the surrounding building on the measurement. The correction factor was set to 0.985.

Section 4.4 discusses the radiation influence of the surrounding building. The estimated offset-error in R_{atm}, can in this example be set to +1.5%, see Section 6.1. Figure 5.4 shows how the measured sky temperature is closer to the ambient temperature when the measured radiation is corrected with a factor of 0.985. As seen from Figure 5.4, the correction factor leads to a sky temperature about 1 K below the measured sky temperature, but still above the ambient temperature. Figure 5.5 shows the correction in R_{atm}, needed to obtain $T_{\mathrm{sky}} = T_{\mathrm{A}}$. For this night, the correction is between -0.5% and -3%, corresponding to a building temperature of about 20 °C.

The third category is shown in Figure 5.3, representing changing cloud cover. The cloud cover is rising during the night, making the sky temperature increase. The calculated values of the sky temperature also increases. A larger fluctuation in the measured sky temperature, is observed until the sky is overcast and clouds are covering the whole sky. One can see that the calculated sky temperature at 19 o'clock, is overestimating the sky temperature, but we also see a rise in the measured sky temperature immediately after. $T_{\mathrm{sky,met}}$

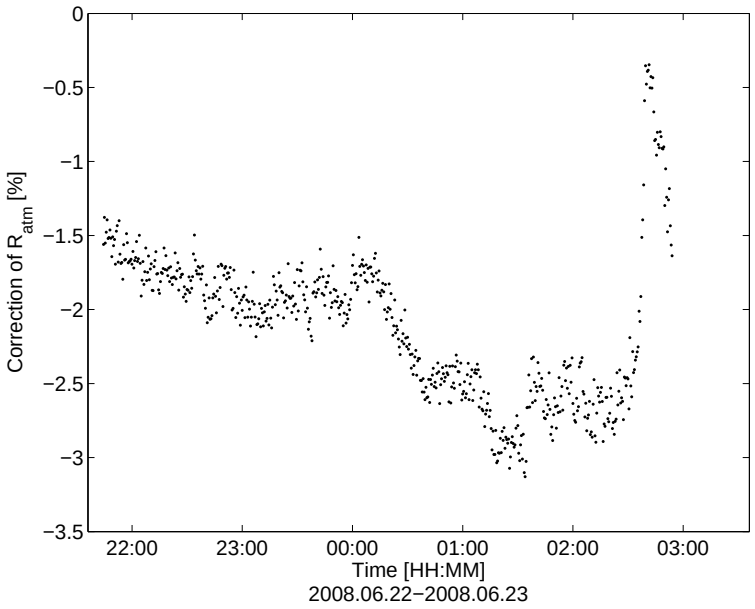

Figure 5.5: Correction of R_{atm} in order to obtain $T_{\mathrm{sky,met}} = T_{\mathrm{sky,pyr}}$.

shows here a deviation from $T_{\mathrm{sky,pyr}}$ of 4.2 K. This was found when $T_{\mathrm{sky,met}}$ was compared to the mean value of $T_{\mathrm{sky,pyr}}$ for ± 5 measurement points, equal to the mean value over about 5 min. The two next values for $T_{\mathrm{sky,met}}$ lays within 1.9 K from the $T_{\mathrm{sky,pyr}}$, and the last is 0.2 K above the measured value.

5.2 Sky temperature

The indirectly measured sky temperature can be presented in different ways. All calculations used in this thesis are based on measurements made during night-time.

5.2.1 All measurements

Figure 5.6 shows both measured values, blue dots, and values calculated with the formula of Martin and Berdahl (1984), red dots. Every measurements made during night-time are shown. As seen from the figure, the calculated values, $T_{\mathrm{sky,met}}$, lay mostly within the measured sky temperatures, $T_{\mathrm{sky,pyr}}$. The variation in the sky temperature is not evenly distributed. Both the measured and the calculated values, show a broader band during the winter. For the first months, from June to September, the sky temperature vary from about

+10 °C to −10 °C. In August the measurements show a higher sky temperature with variation from about 0 °C to 15 °C. From October to February the over all sky temperature decreases, and the difference between highest and lowest sky temperature increases. In February, the sky temperature varies from −30 °C (−40 °C for $T_{\mathrm{sky,met}}$) to 0 °C. From March to June 2009 the sky temperature increases, and again the difference between the maximum and minimum measured values are smaller.

5.2.2 Every night measured

Another, similar presentation is used in Figure 5.7, to show the the sky temperature for each night. The length of the bars is $T_{sky,max} - T_{sky,min}$ for each night. To make it more clear, the direct measurements are shown in the top part of the figure, blue bars, and calculated values can be observed in the lower part of the figure, red bars. Even though every measured night is represented, the most important is to see the trends during the year. Two trends are shown. First the over all temperature is lower during the winter. Secondly, the difference of maximum and minimum values, i.e the length of the bars, for each night is higher in the winter. The gaps result from nights with missing data.

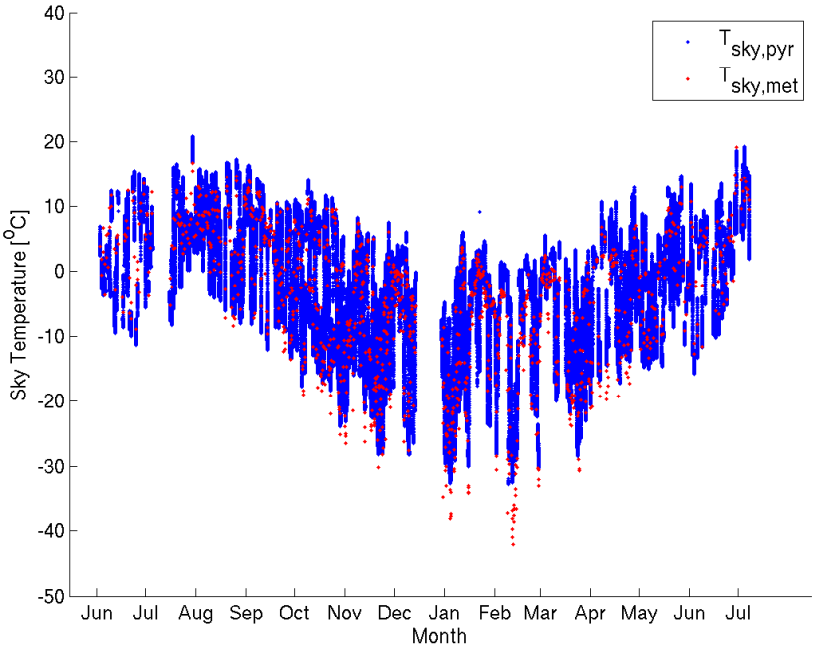

Figure 5.6: Sky temperature for all measurements made at night. The blue dots show the measured values, and the red dots show values calculated from meteorological data.

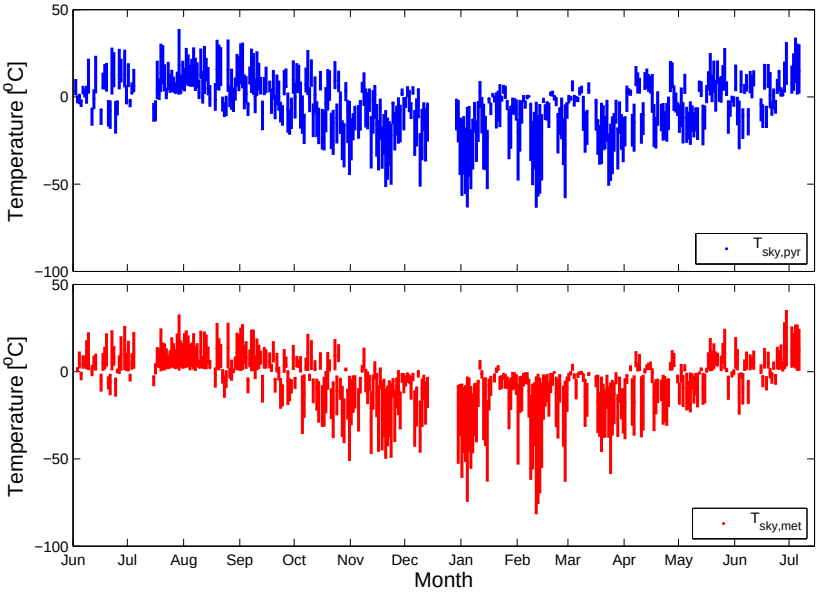

Figure 5.7: Mean night sky temperature for all months. The bars represent the maximum and minimum values measured for each particular night. Measured night sky temperatures are shown at the top, blue bars. Values based on meteorological data are shown at the bottom, red bars.

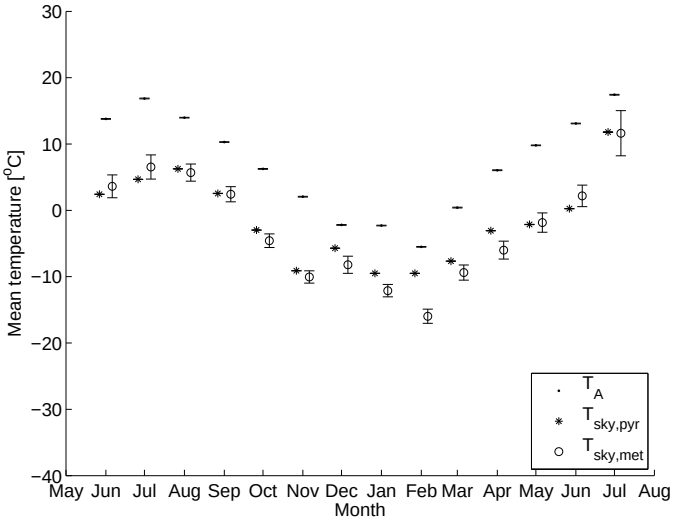

Figure 5.8: Mean night sky and ambient temperatures for each month. Notice the large errorbar for July 2009, which arise from few measurements.

5.2.3 Monthly mean values

In Figure 5.8, the mean temperatures for each month are plotted. Both the measured and calculated sky temperature is shown, together with the mean ambient temperature. Here the mean values are only taken over those days in each month with measurements.

The plot in Figure 5.8 also reveals the trend the of lower sky temperature during the winter, with the actual difference between $T_{\text{sky,pyr}}$, and $T_{\text{sky,met}}$ shown more exactly in Table 5.1. The highest deviation is found in February 2009, with 6.47 K.The possible reasons for the high deviation, are discussed in Section 6.3. The smallest deviation is in September 2008 with 0.12 K. The mean of all deviations is 1.78 °C, and the standard deviation of all deviations, is 2.22 K.

$\Delta\overline{T_{\text{sky}}} > 0$ when $T_{\text{sky,pyr}}$ is higher than $T_{\text{sky,met}}$. In most cases the mean values of $T_{\text{sky,pyr}}$ is higher than $T_{\text{sky,met}}$. It is important to know that the values for July 2009 is not for the whole month, but from 01.07 to 08.07. This makes the uncertainty of the sky temperature measurements higher. The error bars in Figure 5.8 are based on two times the standard deviation for each measurement, listed in Table 5.2. The standard deviation for the mean value can be lowered by the amount of measurements taken, because the standard deviation is the same for every temperature in this temperature range, and is calculated as

Table 5.1: Mean values for sky and ambient temperature for each month with measurements, from June 2008 to July 2009. $\Delta\, T_{\,\mathrm{sky}} = T_{\mathrm{sky,pyr}} - T_{\mathrm{sky,met}}$.

Month	$\overline{T_{\mathrm{sky,pyr}}}$ [°C]	$\overline{T_{\mathrm{sky,met}}}$ [°C]	$\overline{T_{\mathrm{A}}}$ [°C]	$\Delta\overline{T_{\mathrm{sky}}}$ [K]	$\Delta T_{\mathrm{pyr-A}}$ [K]	$\Delta T_{\mathrm{met-A}}$ [K]
June	2.43	3.63	13.79	-1.20	-11.36	-10.16
July	4.68	6.53	16.86	-1.85	-12.19	-10.33
August	6.25	5.69	13.98	0.56	-7.73	-8.28
September	2.55	2.43	10.30	0.12	-7.74	-7.87
October	-2.97	-4.58	6.25	1.61	-9.22	-10.83
November	-9.11	-10.04	2.06	0.94	-11.16	-12.10
December	-5.71	-8.20	-2.20	2.49	-3.51	-6.00
January	-9.50	-12.11	-2.29	2.61	-7.21	-9.82
February	-9.50	-15.97	-5.51	6.47	-3.99	-10.46
March	-7.67	-9.38	0.41	1.71	-8.08	-9.79
April	-3.07	-6.00	6.05	2.93	-9.12	-12.04
May	-2.13	-1.84	9.80	-0.29	-11.93	-11.64
June	0.25	2.18	13.10	-1.93	-12.85	-10.92
July	11.80	11.62	17.43	0.17	-5.63	-5.81

$\sigma_{\mathrm{mean}} = \frac{2\sigma_{\mathrm{meas.}}}{\sqrt{N}}$ (Taylor 1997).

Table 5.2: Standard deviations used in the error bars in Figure 5.8. Since mean values are found, the length of the error bars are divided by $\sqrt{N}$*, where* N *is the number of measurements.*

Standard deviation	Degree [K]
$2\sigma_{\mathrm{T_A}}$	$\pm$0.4
$2\sigma_{\mathrm{T_{sky,pyr}}}$	$\pm$3.3
$2\sigma_{\mathrm{T_{sky,met}}}$	$\pm$11.8

The mean ambient temperature for each month lays at most from 12 K to 13 K higher than the sky temperatures, dependent on which value is used for T_{sky}. The difference between the ambient and sky temperature is smallest in February for $T_{\mathrm{sky,pyr}}$, but as mentioned, this is the month with the highest deviation between $T_{\mathrm{sky,pyr}}$ and $T_{\mathrm{sky,met}}$, and $T_{\mathrm{sky,met}}$ shows a lower value.

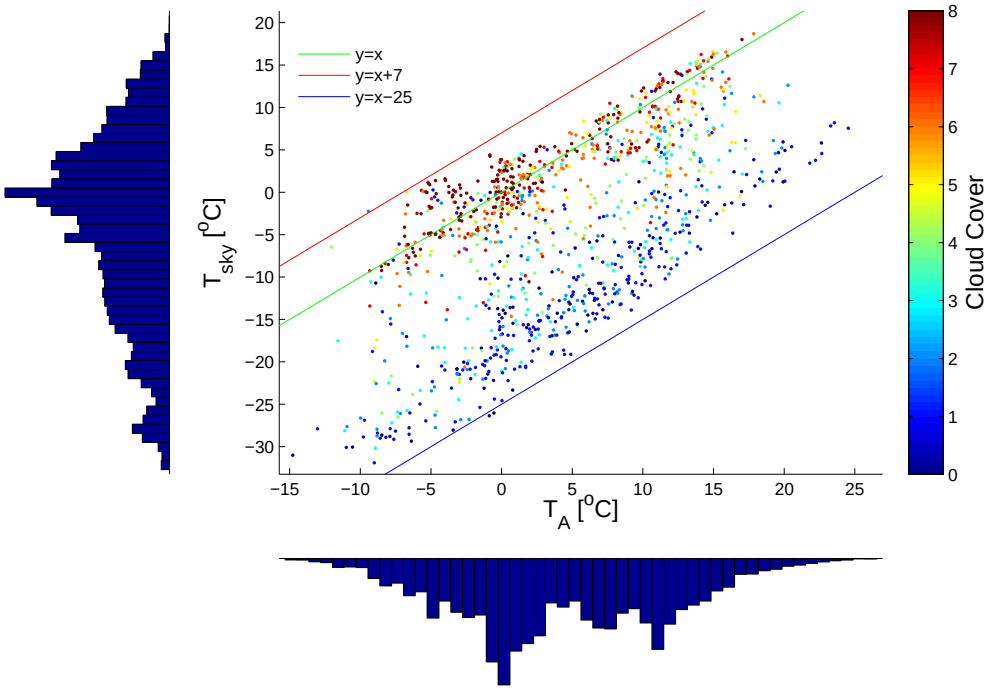

Figure 5.9: Night sky temperature as a function of the ambient temperature, with cloud cover represented in colors. The red and blue lines are inserted to indicate the upper and lower boundaries of the measurements. The green line shows the line where $T_{\mathrm{sky}} = T_{\mathrm{A}}$. The histograms outside the plot shows the distribution of points.

5.2.4 $T_{\mathrm{sky,pyr}}$ as a function of cloud cover

As seen in Section 3.6, the cloud cover has most influence on the sky temperature. A fully overcast sky will give a sky temperature similar to the ambient temperature. Figure 5.9 shows the sky temperature as a function of the ambient temperature, with the mean cloud cover, NX, represented in different colors. Clear sky is represented with dark blue dots and fully overcast sky with red dots.

Figure 5.9 is a graph with a lot of information. The measured sky temperature, $T_{\mathrm{sky,pyr}}$, is plotted as a function of the ambient temperature. The green line is drawn where $T_{\mathrm{sky,pyr}} = T_{\mathrm{A}}$. From the theory in Section 3.6, we see that the emissivity, $\varepsilon_{\mathrm{sky}}$, become higher and close to one in fully overcast sky. This imply that the sky temperature should be the same as the ambient temperature. Two

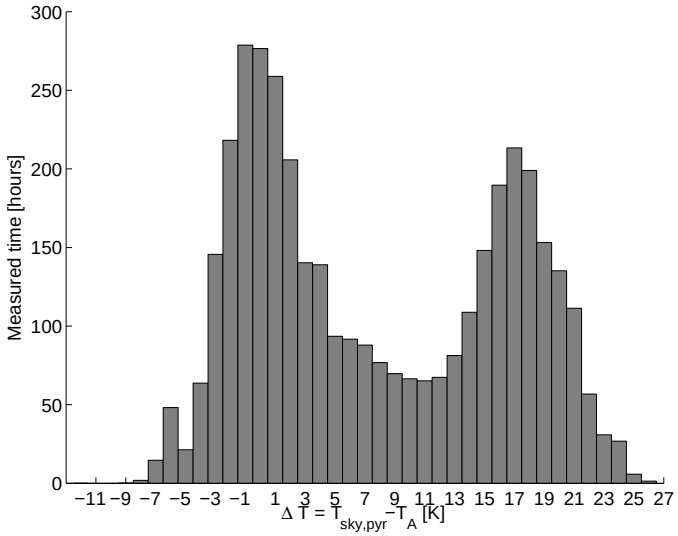

Figure 5.10: The distribution of $\Delta T_{\mathrm{A-sky}} = T_{\mathrm{A}} - T_{\mathrm{sky}}$, with the height of the bars showing the number of seconds with measurements for a given temperature difference.

other lines are also drawn, the red line $T_{\mathrm{sky,pyr}}$ =T_{A} +7 °C, and the blue line $T_{\mathrm{sky,pyr}}$ =T_{A} −25 °C. All measurements fall within the upper red and the lower blue lines. This means that at most, the measured sky temperature is 25 K lower than the ambient temperature, and 7 K above the ambient temperature.

It is seen that the sky temperature is closer to the ambient temperature at higher cloud cover values. Some data points even lie above the ambient temperature. The histograms at the left and bottom part of Figure 5.9 show the distribution of data points on each axis. A different shape of the distributions are seen. The distribution of observed sky temperature has one peak at aboute 0 °C, while the distribution of sky temperature at different ambient temperatures has a bimodal shape (i.e. the distribution has two peaks with a local minimum), with peaks at $T_{\mathrm{A}} = 0$ °C and 11 °C.

The graph also indicates an non-equal distribution of measurements. There are more measurements around the green line, indicating $T_{\mathrm{sky,pyr}} = T_{\mathrm{A}}$, and there is a higher density of measurements for $T_{\mathrm{sky,pyr}} = T_{\mathrm{A}}$ −20 K.

Perpendicular to the lines drawn into the figure, is the distribution of temperature depression; $\Delta T_{\mathrm{A-sky}} = T_{\mathrm{A}} - T_{\mathrm{sky}}$, which is shown in Figure 5.10. The histogram in this figure show the number of hours for a given measured $\Delta T_{\mathrm{A-sky}}$. This is a more general number than the distribution of measurements, which can be read out from Figure 5.9.

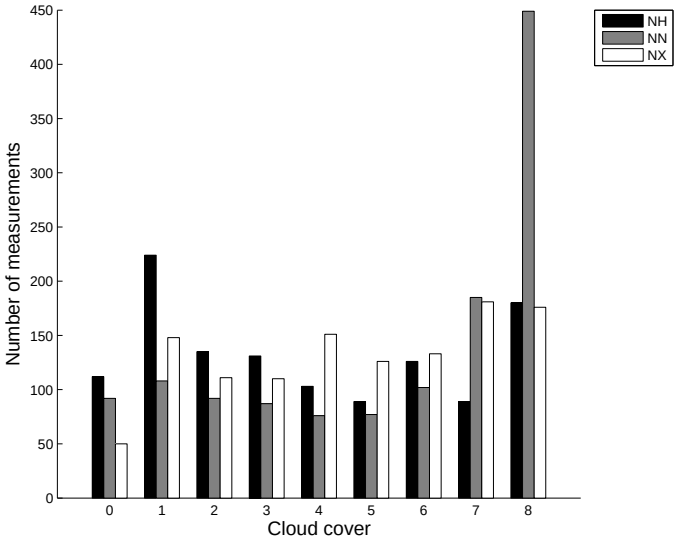

Figure 5.11: The distribution of the cloud cover for the whole period of measurements for NH, NN, and for the mean of the two observed values, NX, which is used in the calculations.

The difference between the sky temperature and the ambient temperature, shown in Figure 5.10, reveals a clearly bimodal distribution, indicating that there are more measurements taken where $\Delta T_{\mathrm{A-sky}} = T_{\mathrm{sky,pyr}} - T_{\mathrm{A}}$ is close to 0 K, or where it is close to 17 K. The local minimum is at 11 K.

In comparison, Figure 5.11 shows the distribution of cloud cover for the same period of measurements. Also here, a weak bimodal shape can be seen. Cloud cover is the variable with the most influence, so this distribution should show the same shape.

5.3 Calculated values versus measured values

As seen from the typical graphs in Figures 5.1-5.3, the calculated value from the model of Martin and Berdahl (1984) gives values within 0.5 K for clear skies, 2 K at cloud covered sky and larger deviation under changing cloud cover. To visualize the difference between the measured and calculated values, Figure 5.12 shows the graph of $T_{\mathrm{sky,met}}$, as a function of $T_{\mathrm{sky,pyr}}$. If no difference were observed, the plot would show a straight line; the longer distance from this line, the larger the deviation. As seen from the broken lines in Figure 5.12, most of the points lay within ± 10 K.

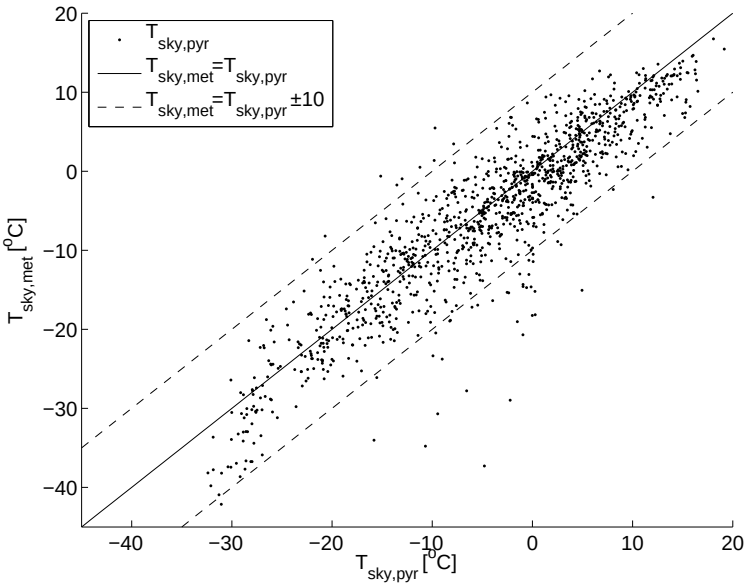

Figure 5.12: $T_{\mathrm{sky,met}}$ as a fumction of $T_{\mathrm{sky,pyr}}$. Solid line indicates $T_{\mathrm{sky,met}}$ = $T_{\mathrm{sky,pyr}}$. The broken lines are drawn where $T_{\mathrm{sky,met}}$ = $T_{\mathrm{sky,pyr}}$ ±10.

The difference between $T_{\mathrm{sky,met}}$ and $T_{\mathrm{sky,pyr}}$ can also be seen in Figure 5.13 and Table 5.3. The negative mean value reveales that over all, the measured values are higher than the calculated values. The standard deviation, $\sigma_{\Delta \mathrm{T_{sky}}}$ =±4.61 K, and two times the standard deviation is ±9.22 K, which means that 95% of all measurements lays within ±9.22 K. Figure 5.13 is a function of time and reveals that during the winter the highest deviations occur. Some of the values in Figure 5.13 are very low, and Table 5.3 reveals that the most negative value is −32.46 °C. The large deviations are discussed in Section 6.4. Since the deviation can be both negative and postitive, it is useful to take a look at the absolute value of ΔT_{sky}. This shows that the smallest deviation is 0.01 K.

Table 5.3: Statistic values for ΔT_{sky} =$T_{\mathrm{sky,met}}$ - $T_{\mathrm{sky,pyr}}$, and the absolute value of the difference, $|\Delta T_{\mathrm{sky}}|$.

	ΔT_{sky} [K]	$\lvert\Delta T_{\mathrm{sky}}\rvert$ [K]
Min	-32.45	0.01
Max	16.39	32.45
Mean	-1.24	3.49
Median	-1.20	2.74
Std	±4.61	±3.31

Figure 5.14 show the distributions of ΔT_{sky} for each month, and the statistical

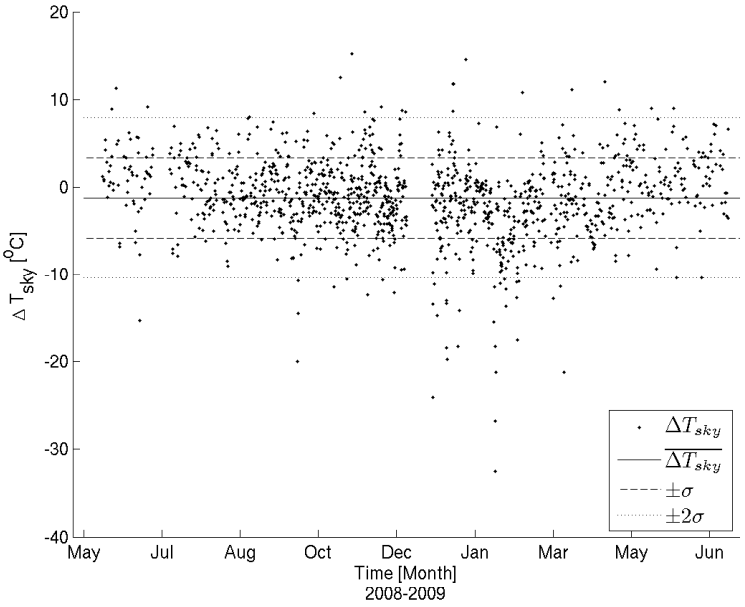

Figure 5.13: ΔT_{sky} =$T_{\text{sky,met}}$ - $T_{\text{sky,pyr}}$ *as a function of time.*

data for each distribution are shown in Table 5.4. The mean values reveals small mean deviation for each month, but the standard deviations show some variation throughout the year.

To get a deeper analysis of the difference between the measured and calculated sky temperature, it is useful to check when the highest deviations are found. Figure 5.13 revealed the highest deviations during the winter. Figure 5.15 shows the distribution of Δ T_{sky} for different cloud cover, NX. Negative values means that the measured values are higher than the calculated values. Table 5.5 reveals that most of the mean values are negative, and the most negative mean value is when $NX = 0$. This might be just due to outliers, but the median for clear sky also indicates the most negative value.

For clear sky and near clear sky the distributions show a peak, with a tail at the left side. The trend is that the distribution is more flat for cloud covers, NX from 4 to 5, and the peaks reappear at NX in the range from 6 to 8, this time with a tail on the right hand side. The highest, most distinct peak is observed at fully overcast sky. Tails at the left hand side will appear when $T_{\text{sky,pyr}} > T_{\text{sky,met}}$. The model is here underestimating the measured values. Tails at the right hand side will on the contrary, mean that the calculated values overestimate the measurements.

As seen in Section 5.1, $T_{\text{sky,met}}$ will miss the exact values of measurements during changing cloud covers. This is also seen here in the more evenly dis-

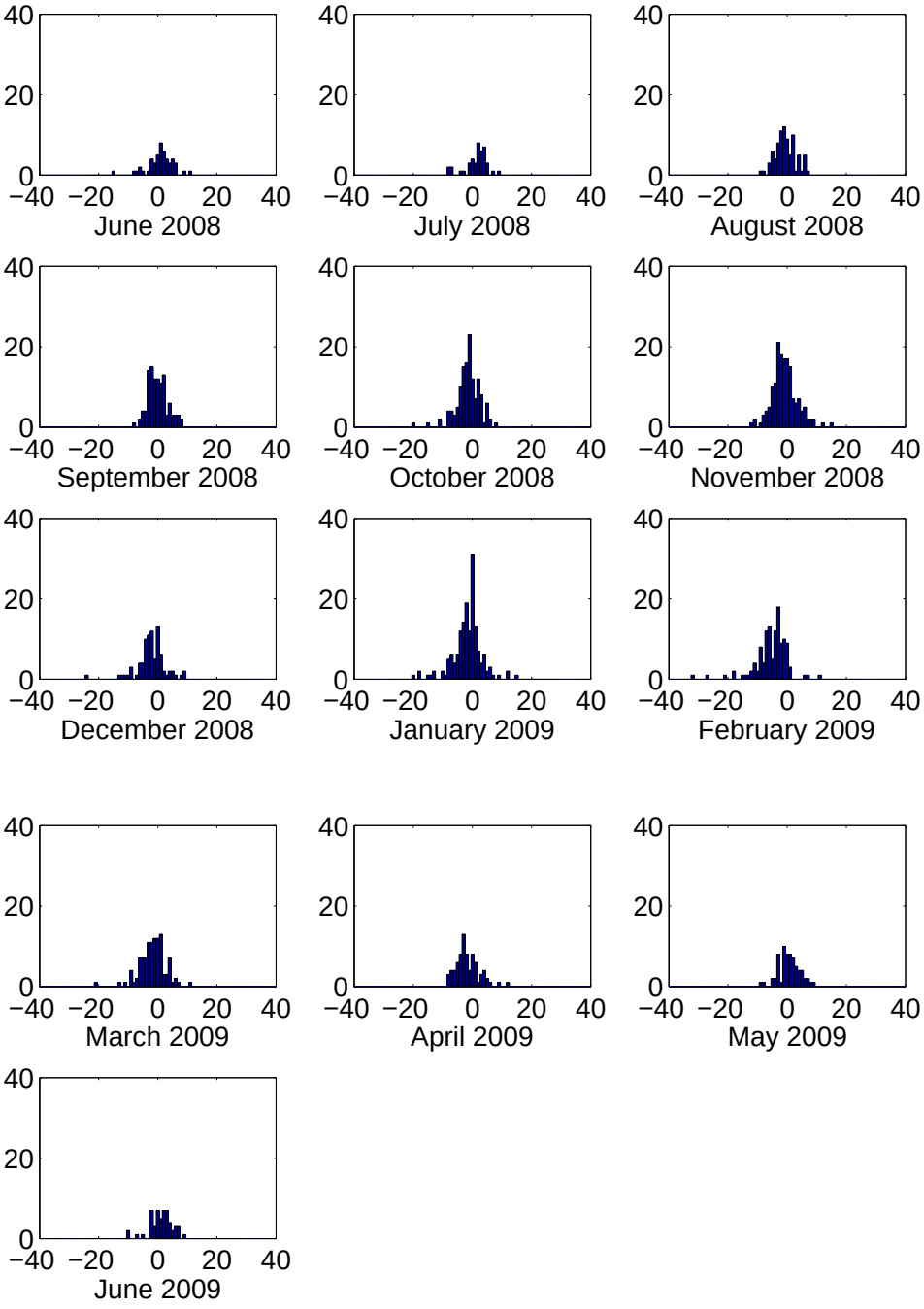

Figure 5.14: The distribution of ΔT_{sky} for each month with measurements except July 2009 with only a few measurements.

Table 5.4: Minimum, maximun, mean, median and the standard deviation of the distribution of ΔT_{sky} for each month shown in Figure 5.14.

Month [MM]	Min [°C]	Max [°C]	Mean [°C]	Median [°C]	Std [K]
6	-15.3	11.3	0.879	1.18	±4.52
7	-7.9	9.14	1.34	2.09	±3.72
8	-9.02	6.74	-0.61	-1.24	±3.42
9	-8.28	8.03	-0.028	-0.439	±3.28
10	-20.0	8.38	-1.4	-1.24	±3.98
11	-12.4	15.2	-0.852	-1.1	±4.24
12	-24.1	8.78	-2.24	-2.03	±4.77
1	-19.8	14.5	-1.68	-1.29	±4.99
2	-32.5	10.8	-5.22	-4.07	±5.56
3	-21.2	11.2	-1.73	-1.47	±4.35
4	-8.42	12.1	-1.66	-2.45	±3.91
5	-9.37	9.0	0.701	0.522	±3.57
6	-10.4	9.01	1.27	1.77	±3.91

tributions under cloud covers between 4 and 6. The distribution here is also more evenly distributed around zero. The smallest standard deviations are observed at $NX = 1$ and at fully cloud covered sky, $NX = 8$.

5.4 Cooling power and energy

The cooling power for a radiator with a temperature of 25 °C can be calculated with Equation 3.14. A night with clear sky conditions during the summer will give a net radiative power like the one shown in Figure 5.16. As seen, the power at this night is between 125 W/m^2 and 145 W/m^2. This is based on a constant radiator temperature of 25 °C.

The radiator temperature is in this calculation set to a constant 25 °C, and the emittance is set to one. The area is also excluded, from Equation 3.14. Energy radiated out each night is calculated by using Equation 5.1:

$$E_{\text{net}} = \int_{\text{sunset}}^{\text{sunrise}} \sigma \left(T_{\text{rad}}^4 - T_{\text{sky}}^4\right) \text{dt} = \int_{\text{sunset}}^{\text{sunrise}} \sigma \Delta \text{Tdt} \, . \tag{5.1}$$

The integration is made in MATLAB, and are based on the timestep between

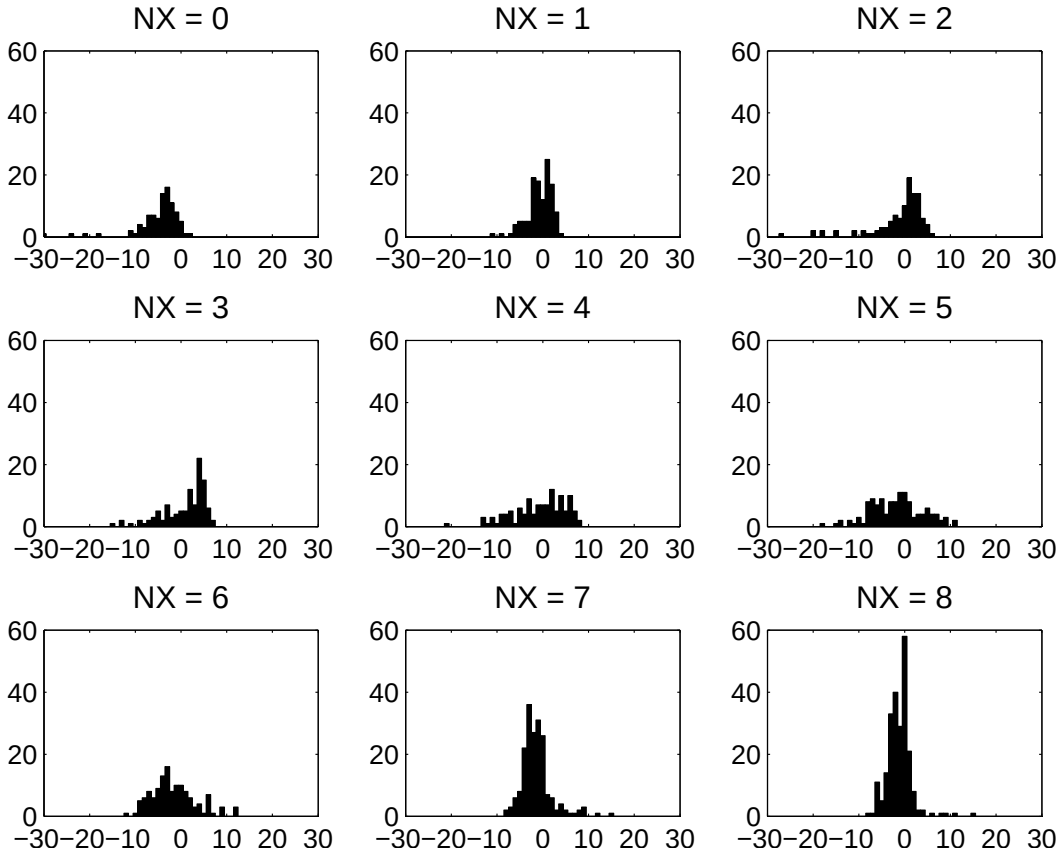

Figure 5.15: Histograms showing the distribution of the difference in $\Delta\, T_{\mathrm{sky}} = T_{\mathrm{sky,met}} - T_{\mathrm{sky,pyr}}$ *, for different cloud covers,* $NX = \frac{NH+NN}{2}$.

two measurements, usually 30 sec. Figure 5.17 show the net energy radiated out per area by a perfect blackbody radiator each night.

It is seen that each night between 0.5 kWh/m^2 and 4.5 kWh/m^2 is potentially radiated out toward the sky. The sum for all measured nights in that month, one gives the results shown as E_{pyr} in Figure 5.18. Because of some missing measurements, the average of the measured nights is multiplied with the number of nights in each month, shown as $E_{\mathrm{pyr,mean}}$ in Figure 5.18. The figure also shows the energy based on the modelled values of $T_{\mathrm{sky,met}}$, E_{met} and $E_{\mathrm{met,mean}}$. Since the cloud data is only measured every third hour, a linear interpolated value is made for $T_{\mathrm{sky,met}}$.

Figure 5.18 shows the potential energy radiated out from a 1 m^2 radiator at 25 °C. The formula uses an emissivity, $\varepsilon_{\mathrm{rad}} = 1$, so the total energy shown is the maximum potential of energy radiated out for this period. The energy lays between 15 kWh/m^2 and 65 kWh/m^2 per month.

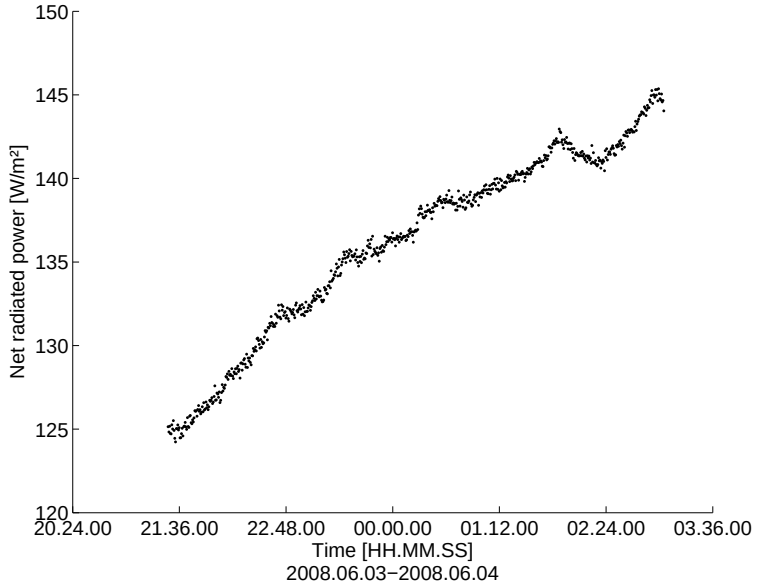

Figure 5.16: Instantaneous net cooling power for a perfect radiator at 25 °C *during a clear sky summer night.*

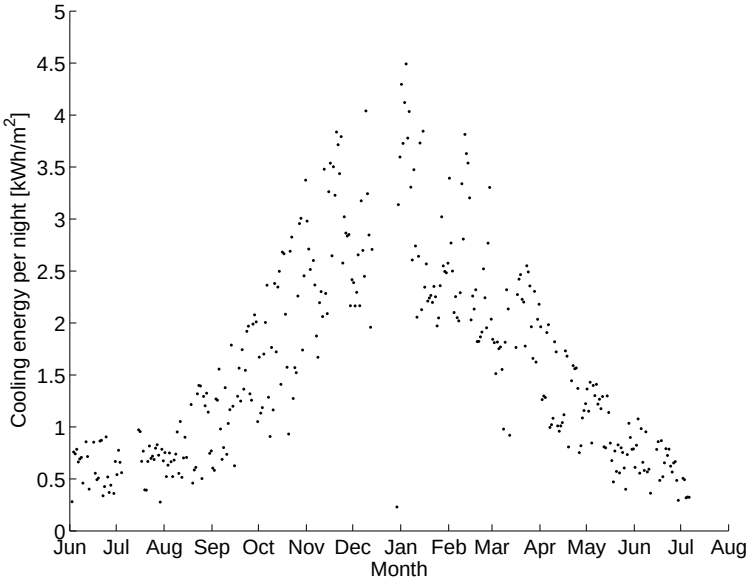

Figure 5.17: Net cooling energy radiated out by a perfect radiator at 25 °C *during each night with measuremets.*

Table 5.5: Minimum, maximun, mean, median and the standard deviation of ΔT_{sky} for each cloud cover, NX.

NX [1]	Min [°C]	Max [°C]	Mean [°C]	Median [°C]	Std [K]
0	-32.5	2.34	-4.87	-3.89	±5.08
1	-10.8	4.32	-0.626	-0.345	±2.67
2	-26.8	6.41	-1.09	0.585	±5.9
3	-14.8	7.15	0.837	2.41	±4.8
4	-21.2	7.79	-0.783	0.338	±5.74
5	-18.2	11.3	-1.82	-1.7	±5.78
6	-11.5	12.5	-1.67	-2.65	±4.88
7	-8.43	14.5	-1.38	-1.66	±3.33
8	-7.89	15.2	-1.2	-1.11	±2.69

Since the measurements were only conducted for one year, one will experience different results for other years. For a more accurate estimation; mean values for measurements and calculations made for several years has to be conducted.

Table 5.6 also lists the difference in energy based on $T_{\text{sky,pyr}}$ and $T_{\text{sky,met}}$. As seen, the difference within the measured period is less than 5%.

5.4.1 Cooling degree hours

As explained in Section 3.8, cooling degree hours (CDH) represent a measure on the cooling potential, while cooling degree days (CDD) represent the cooling demand. The cooling demand found for Oslo is, according to Benestad (2008), about 9 °C · days. Using the same formula, Equation 3.33, and meteorological data for 2008 in Oslo, 8.7 °C · days is obtained. There were only six days with a mean temperature above 22 °C, in June and July. For 2009, the CDD were 17.6 °C · days with ten days in the end of June and in the beginning of July. Table 5.4.1 shows the CDD for 2008 and 2009 with different temperature definitions in the CDD.

The potential for cooling in each month represented in the form of cooling degree hours, are shown in Figure 5.19. CDH based on measurements and values calculated from Martin and Berdahl (1984) show only minor deviations. The larges deviation between the cooling degree hours based on measurements and meteorological values is in February. The deviation is here 16%. The

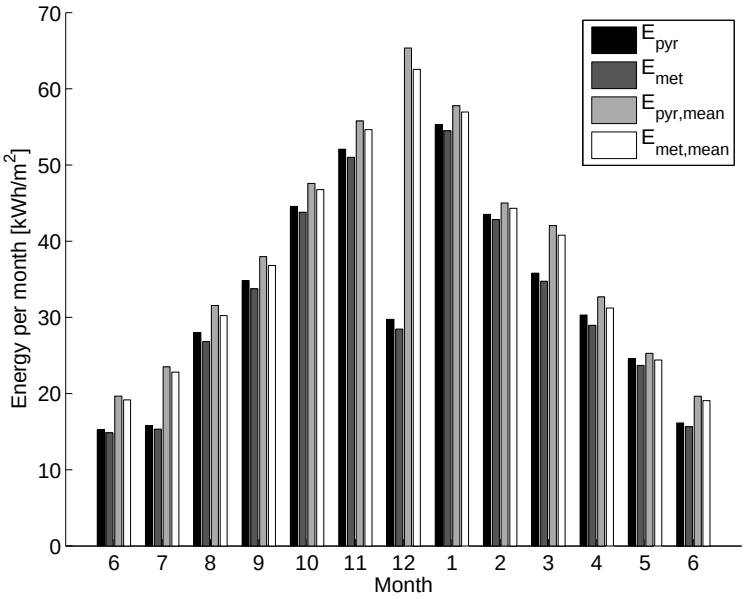

Figure 5.18: The potential energy radiated out with a constant radiator temperature of 25 °C. E_{pyr} *is calculated from* $T_{\text{sky,pyr}}$ *, while* E_{met} *is based on* $T_{\text{sky,met}}$*. The mean values are corrected for days without measurements.*

Table 5.6: Difference in calculated potential energy radiated out from a radiator at 25 °C. *E with bar represent mean values.*

Month (mm)	E_{pyr} [kWh]	E_{met} [kWh]	ΔE [kWh]	$\bar{E}_{\text{pyr}}$ [kWh]	$\bar{E}_{\text{met}}$ [kWh]	$\Delta \bar{E}$ [kWh]	ΔE [%]
6	15.2	14.8	0.385	19.7	19.2	0.498	2.53
7	15.8	15.3	0.472	23.5	22.8	0.701	2.98
8	28.0	26.8	1.18	31.6	30.2	1.33	4.22
9	34.8	33.7	1.06	38.0	36.8	1.16	3.05
10	44.6	43.8	0.763	47.6	46.8	0.814	1.71
11	52.1	51.0	1.06	55.8	54.6	1.14	2.04
12	29.7	28.5	1.28	65.4	62.6	2.81	4.29
1	55.3	54.5	0.782	57.8	57.0	0.818	1.41
2	43.5	42.8	0.681	45.0	44.3	0.704	1.56
3	35.8	34.7	1.07	42.0	40.8	1.25	2.98
4	30.3	29.0	1.35	32.7	31.2	1.45	4.45
5	24.6	23.7	0.858	25.3	24.4	0.884	3.5
6	16.1	15.7	0.482	19.7	19.1	0.587	2.98

Table 5.7: Different cooling degree days for Oslo for different temperature definition in the formula.

Mean Temperature [°C]	CDD for 2008 [°C · days]	CDD for 2009 [°C · days]
20.5	25.8	33.0
21.0	18.9	27.6
21.5	13.7	22.6
22.0	8.7	17.6

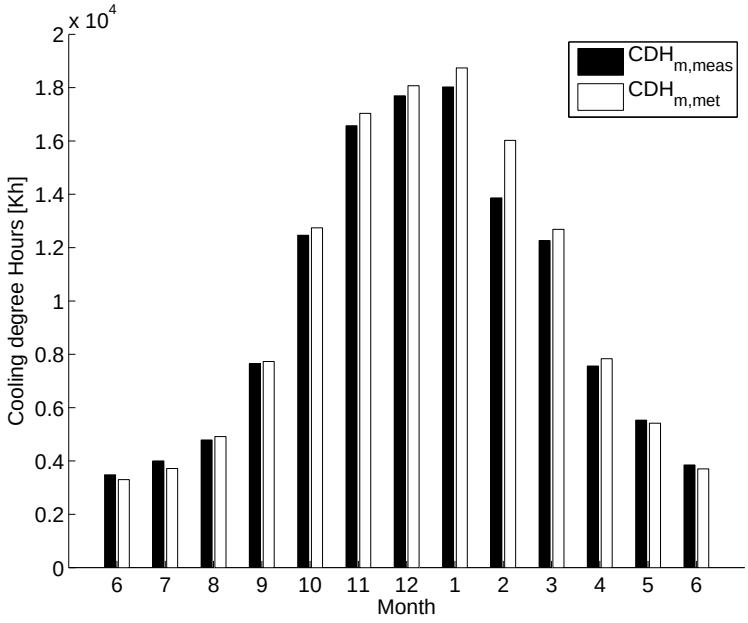

Figure 5.19: Cooling degree hours for each month, calculated for both measurements and meteorological data.

deviation in February is also seen in other representations of the calculated sky temperature, and are discussed in Section 6.3.

Chapter 6

Discussion

In this section, the results from Chapter 5 are reviewed in the same order as they appear in the previous section. Whenever the results are based on presumptions, these will be discussed and the background for the assumptions will also be explained. After the evaluations of typical measurements, Section 6.1, daytime values and the shadowing of the pyrgeometer will be investigated, Section 6.2 - 6.2. Then the sky temperature measurements and the different representations will be explained and compared in Section 6.4.

6.1 The typical measurements

From the results shown in Section 5.1, we see that the sky temperature is well below the ambient temperature under clear sky conditions. As expected, we observe a higher sky temperature with more clouds present. Under fully cloudy conditions, the sky temperature becomes more or less similar to the ambient temperature. This is also expected because clouds will absorb most of the radiation from the ground and radiate back to the Earth, see Section 3.3. A sky temperature similar to the ambient temperature means that a radiation equilibrium has been achieved. Lower clouds have a temperature more similar to the ambient air, and an equilibrium is established more easily. High altitude clouds will normally have a lower temperature and an equilibrium with the ground may not be established at all. Therefore, the lower cloud cover, NH, will be more important to the measurements than the higher cloud cover, NN. This is also taken into account in the formula from Martin and Berdahl (1984). The base cloud height is used in the exponential part of Equation 3.25. The

higher the clouds, the smaller the exponential part gets, and the smaller the sky emissivity becomes. A smaller sky emissivity will again lead to lower sky temperatures.

Some of the measurements even show a sky temperature higher than the ambient temperature, as seen in Figure 5.2. There can be different explanations for this. First, the sky temperature may actually be higher than the ambient temperature, this is called inversion layers. Inversion layers can, however, not explain all the measurements where $T_{\mathrm{sky,pyr}} > T_{\mathrm{A}}$. Secondly, rain or snow covering the pyrgeometer may influence the measurements. Third, and most likely, the surrounding building emits heat towards the sensor. As discussed in Section 4.1.1 and Section 4.4, the influence of the building gives an offset error of less than 6% within the chosen temperature limits. This offset may cause the measured sky temperature to be higher than the ambient temperature.

The correction for building radiation is shown in Figure 5.4. A correction factor of 0.985 was chosen, corresponding to 1.5%. As seen in Figure 4.11, this corresponds to a sky temperature of about 10 °C, as measured, and a building temperature of about 25 °C. This should be a good estimate for a brick building in the summer with an ambient temperature of about 12 °C, taken into consideration that the building has been heated during the day.

The last night shown in Section 5.1 is a night with changing cloud cover. The cloud cover increases during the night and therefore, as explained above, the sky temperature also rises. The larger fluctuation of the measured sky temperature is caused by the partly cloud-covered sky. Clouds that pass directly above the instrument cause a higher influence on the sky temperature than clouds at the horizon. The fluctuations in the measured sky temperature can be caused by passing clouds, with clear sky in between. The observed cloud cover is a mean of the whole hemisphere, without information about the location of clouds. The calculated sky temperature will therefore often not coinside with the measurements under changing cloud cover and partly cloud-covered sky.

6.2 Daytime values

As explained in Section 4.4, a model of the Physics Department building was made in Google SketchUp and placed in an accurate position on a map/satellite image in Google Earth. The shadowing function in the program was set to real

sunlight, and this shows that sunlight hits the pyrgeometer and the ambient temperature sensor exactly at the time when we see the start of the fluctuation in the ambient temperature, as seen in Figure 5.1 in Section 5.1. This was also confirmed by visual observation. The placement of the temperature sensor was chosen to be as close to the pyrgeometer as possible. The pyrgeometer had to be placed in an open place and was therefore, also exposed to direct sunlight during the day. Direct sunlight will heat up the pyrgeometer window, causing a window heating offset of 25 W/m^2 at 1000 W/m^2 normal incidence of solar radiation (Kipp & Zonen 2009). Data of the sky temperature/radiative balance obtained during the day are interesting in studies of solar collector performance. Data obtained during daytime must be corrected for absorbed solar radiation causing a window heating offset, if they are to be used in other studies. In daytime measurements, the irradiation should be measured, so the correction of the infrared radiation can be more correct. For daytime measurements, a extra sun-screen can be mounted to shadow the pyrgeometer window for direct solar radiation.

In this work, the nighttime measurements were most important since radiative cooling with thermal, non-selective solar collectors used as radiators can only be utilized during the night. Since the experimental setup was placed where parts of the surrounding buildings were shadowing the view, the sunlight does not strike the setup exactly at the time of sunrise, shown in Figure 5.1. By convenience, the sunset/sunrise timetables downloaded were used instead of finding the actual sunset/sunrise times for the experiments.

6.3 Sky temperature

The sky temperature measurements have been presented in different ways in Section 5.2. All in all, the agreement between the measured values and the values calculated from meteorological data through the theory of Martin and Berdahl (1984), seems to be quite good. Figure 5.6 shows that the calculated values, most of the time are in good agreement with the measured values. In January and February we see that some of the calculated values is lower than the measurements. This is most probably because of the weather in this period, with snow covering the pyrgeometer. The experimental setup was not monitored each day and sometimes, a thick layer of snow covered the pyrgeometer, and the instrument was completely buried under the snow. In lighter snow falls, the snow melted on top of the pyrgeometer and made a

water film which covered the detector glass. How rain and snow influenced the measurements were not observed. Radiators used for cooling would, however, experience the same conditions as the pyrgeometer.

Figure 5.7, which shows the max/min sky temperature represented as bars, also indicates the good agreement between the measurements and the calculated values. The same trend is shown, and both parts of the figure look similar. As expected, the sky temperature is lowest during the winter. The sky temperature is also higher during the autumn than in spring. The span between the maximum and minimum sky temperature is also highest during the winter season.

The measured mean sky temperature for February, is higher than the calculated sky temperature. This is observed in Figure 5.8, where the mean values for both the measured and calculated sky temperature are plotted together with the ambient temperature. All months indicate that the calculated and the measured values of the sky temperature lie well below the ambient temperature. Some months illustrate a very good agreement between the measured and calculated values; especially August and September in 2008 and May and June in 2009.

An interesting observation about the sky temperature is shown indirectly in Figure 5.9 and in Figure 5.10. The distribution of the measured $\Delta\ T$, is also an indicator of the distribution of cloud cover. Based on the theory of Martin and Berdahl (1984), the cloud cover has a large influence on ε, which connects the sky temperature to the ambient temperature. The distribution shows that for all time measured, most of the time there has been a high cloud cover. This is shown in the distribution where the highest peaks of the distribution are where $\Delta\ T\ \approx 0$ °C and $\Delta\ T\ \approx -20$ °C.

6.4 Calculated values versus measured values

An interesting analysis of the precision of the model of Martin and Berdahl (1984) is made in Section 5.3. The nine histograms in Figure 5.15 illustrate that there are variations in the distribution of the difference between the calculated and measured values for different cloud covers.

The figure proves that the distribution for overcast sky has the most significant peak. Table 5.5 show that the standard deviation is smallest at cloud covers

of 1 and 8. The mean value at $NX = 1$ is also closest to 0.

Cloud covers between $3 - 5$ gives a more even distribution around zero, indicating that the calculated values are equally often overestimated as underestimated. Most of the values of ΔT_{sky} are within ± 10 K.

Another interesting point is that the tails of the distribution changes from pointing forward to backward as the cloud cover rises. In practical terms this means that for clear skies, the sky temperature calculated with the model is more often underestimated ($T_{\text{sky,met}} < T_{\text{sky,pyr}}$). For more cloudy skies, the modeled temperature is more often overestimated ($T_{\text{sky,met}} > T_{\text{sky,pyr}}$), and we get more negative ΔT. As seen from Figure 5.15, the distribution around zero for partly covered sky is more flat, and does not have any distinct peaks. The reason for this can be found when we take a closer look at Figure 5.3, which shows an example of a night where the cloud cover increase during the night. When the cloud cover is around 3, the measurements fluctuate more, indicating passing clouds. The cloud cover does not say anything about the location of the clouds. Clouds at the horizon will not affect the pyrgeometer measurements as much as clouds directly above the pyrgeometer, but this information is not present in the observed cloud cover, NH or NN. The probability of overestimation or underestimation is therefore greater at cloud covers between 3 and 5. At the same time, the over- and underestimation have about the same probability, seen from flat-shaped distribution at these cloud covers. High deviation was also found in Figure 5.3, where the deviations was explained from uncertainty in the position of clouds.

6.5 Cooling power and energy

To find the cooling effect and energy gained from radiative cooling, some assumptions must be made. Both geographical differences and the great dependency of the system involved are important variables to take into account. It is therefore more useful to find the potential for radiative cooling with as few predefined parameters as possible.

In this report, the radiator is set to a constant temperature of 25 °C and is treated as a perfect blackbody with an emissivity, $\varepsilon_{rad} = 1$. This makes it possible to get an idea of the total possible amount of energy that can be radiated out in a perfect system. In addition, both convection and conduction will contribute to cooling, but since these factors are mainly dependent on

system design, they were not be encountered in this work. In Section 3.8 the choice of radiator temperature is discussed.

Most solar collectors are not mounted in a horizontal position, especially not in Norway. To have the highest efficiency for heat collection, the solar absorbers should be in a position perpendicular to the incident solar radiation. Due to the low path of the sun during the Norwegian winter, with the highest heating demand, solar collectors are often mounted in a vertical position. All measurements in this work was made with the pyrgeometer in a horizontal position, in order to obtain the highest area of sky within the pyrgeometer's field of view. No analysis was made for solar collectors at different tilt angles, but a simplified model is used in the work of Meir et al. (2002).

The energy calculated from $T_{\text{sky,pyr}}$ and $T_{\text{sky,met}}$ also reveals a very good match between modeled and measured values. All in all, the deviation between the two is at all time lower than 5%. This proves that the formula can be useful for monthly mean sums, even though it might produce larger errors in specific nights. The values based on $T_{\text{sky,met}}$ are all lower than the one based on $T_{\text{sky,pyr}}$. This means that in sum, $T_{\text{sky,pyr}}$ is lower than $T_{\text{sky,met}}$. $T_{\text{sky,met}}$ is here based on linear interpolated values.

6.6 Cooling degree days and cooling degree hours

The cooling degree days (CDD) are calculated to find the need for energy used for cooling buildings. The cooling demand in Norway and Oslo is limited for most buildings. Benestad (2008), however, claims that the cooling degree days will increase in Oslo and most other cities as a result of global warming. The heating degree days will decrease, so in total, we are likely to see a shift in the amount of energy used, from heating toward cooling. The negative values obtained by Benestad (2008) has not yet been investigated.

Cooling degree hours found in Section 5.4.1 show that it can be found from meteorological values through the model of Martin and Berdahl (1984), with only minor deviations. Further calculations on the cooling degree number was attempted, with no good results. CDH works as a general number of the difference between a radiator and the sky temperature. Incorporated into the number are the length of nights, which also is easily available information. This may make the cooling degree number useful in comparison for different places, even though mean power or energy was achieved obtained with the

method developed in Section 3.8.

6.7 Challenges in this work, and future perspectives

During the long period of measuring, some complications have been encountered, and a lot of things could have been done different.

The missing measurements due to power failure and computer restarts, could have been minimized by turning off automatic updates, or by using a battery driven data logger. In addition different sources of error, like rain or snow should be analyzed, and logged during the measurements. A more regular and frequent monitoring and cleaning of the pyrgeometer, could reveal more uncertainties, and make different errors be discovered at an earlier stage. Data analysis should be executed after shorter periods of time, and compared to a log of other external factors, like heavy snow, rain, cleaning etc. Data analysis done after long periods of time made it harder to find reasons for large deviations. In this work, only very large, non-natural deviations have been removed.

The challenges encountered during this work, however, has lead to great knowledge.

Chapter 7

Conclusion

The main goal for this work was to measure the infrared night sky radiation during one year in the Oslo area. The infrared night sky radiation is important to the Earth's energy balance. Cooling systems based on radiative cooling is an exciting idea and the potential is not well known. In addition, the radiative cooling is important in agriculture. Plants may freeze even with an ambient temperature above 0 °C, and a better understanding and prediction of this may be useful. Radiation from the atmosphere can be compared to a blackbody with a certain temperature. This temperature is called the sky temperature, T_{sky}. After more than one year of measurements, a large amount of data has been collected. For the year of measurements, the sky temperature was measured in the range from −32.7 °C to 20.9 °C. More interesting is the sky temperature depression, $\Delta T_{\text{A}-\text{sky}}$ which is measured in the range from 26.6 K to −11.3 K, meaning a sky temperature higher than the ambient temperature was measured. The distribution of the depression has a bimodal shape with peaks at 0 K and 18 K. The bimodal shape indicates that the temperature depression is more often around 0 K and 18 K than 12 K, where the local minimum is.

Direct measurements of the atmospheric radiation have been compared to the model of Martin and Berdahl (1984). The Cloud cover is found to be the most important factor for deviation between measured and calculated values, both from measurements and from the error analysis. The model fits well for clear and fully overcast sky. Most problems occur during partly cloud-covered sky and changing cloud cover. Larger deviation between measured and calculated values is mainly caused by the uncertainty in the clouds position. Mean sums over longer periods of time, like months, reveal a good match

between the measured and calculated values. Deviations between the measured and calculated monthly mean sky temperatures are in the range from 0.12 K to 6.47 K, with standard deviations for the distributions of each month in the range from ±3.28 K to ±5.56 K. The highest deviations between the model and the measured values were found to be 32.5 K, in February, probably caused by snow covering the pyrgeometer.

The amount of energy possible to radiate out from a blackbody radiator at 25 °C each month is found and varies from 15 kWh/m^2 per month in the summer to 65 kWh/m^2 per month in winter. A measure for the cooling potential through night sky radiation, cooling degree hours (CDH) has been developed. CDH is found to give the potential for radiative cooling, but attempts to get power or energy back from the CDH was not succeeded.

References

Al-Nimr, M. A., Z. Kodah, and B. Nassar (1998, 08). A theoretical and experimental investigation of a radiative cooling system. *Solar Energy 63*(6), 367–373.

Ali, A. H. H., I. M. S. Taha, and I. M. Ismail (1995). Cooling of water flowing through a night sky radiator. *Solar Energy 55*(4), 235 – 253.

Ångström, A. (1913, 06). Studies of the nocturnal radiation to space. *The Astrophysical Journal 37*, 305–321. Provided by the SAO/NASA Astrophysics Data System.

Arnfield, A. J. (1979). Evaluation of empirical expressions for the estimation of hourly and daily totals of atmospheric longwave emission under all sky conditions. *Quarterly Journal of the Royal Meteorological Society 105*(446), 1041–1052.

Bassindowa, H., S. Al-Faidi, M. Bahafzallah, M. Al-Edini, A. Al-Ayiashi, O. Al-Rabghi, and M. Akyurt (2007, 12). An experimental investigation on night radiative cooling. *Saudi Engineering Conference 7th*, 99–110.

Benestad, R. E. (2008). Heating degree days, cooling degree days and precipitation in europe. Technical Report 4/2008, Meteorological Institute, Oslo.

Berdahl, P. and R. Fromberg (1982). The thermal radiance of clear skies. *Solar Energy 9*(4), 299 – 314.

Berdahl, P. and M. Martin (1984). Emissivity of clear skies. *Solar Energy 32*(5), 663 – 664.

Bijma, S., A. Koelemij, H. Oversloot, P. van Staalduinen, and H. Visser (1997, November). Assessment and recomendations for application of the solarnor energy roof/facade. Technical report, TNO Building and Construction Reasearch.

Bliss, R. W. (1961). Atmospheric radiation near the surface of the ground: A summary for engineers. *Solar Energy 5*(3), 103 – 120.

Brunt, D. (1932). Notes on radiation in the atmosphere. *Quarterly Journal of the Royal Meteorological society 58*, 389–420.

Duffie, J. A. and W. A. Beckman (2006). *Solar engineering of thermal processes* (3rd ed.). John Wiley & Sons, Inc.

Fernandes da Silva, L. C. (2008). New generation of solar thermal collectors. Master's thesis, University of Oslo.

Frank, T. and T. Püntener (1986). Oberfløchentemperaturen von besonnten fensterglasscheiben und ihre auswirkungen auf raumklima und komfort. NEFF-Projekt Nr. 266.

Holter, Ø., F. Ingebretsen, and H. Parr (1998). *Fysikk og energiressurser* (2 ed.). Universitetsforlaget AS, Postboks 2959 Tøyen, 0608 Oslo: Universitetsforlaget.

Idso, S. and R. Jackson (1969). Thermal radiation from atmosphere. *Journal of geophysical research 74*(23), 5397–5403.

Idso, S. B. (1974). On the use of equations to estimate atmospheric thermal radiation. *Arch. Met. Geoph. Biokl. 22*, 287–299. Ser. B.

Iziomon, M. G., H. Mayer, and A. Matzarakis (2003). Downward atmospheric longwave irradiance under clear and cloudy skies: Measurement and parameterization. *Journal of Atmospheric and Solar-Terrestrial Physics 65*(10), 1107 – 1116.

Khedari, J., W. Mansirisub, S. Chaima, N. Pratinthong, and J. Hirunlabh (2000, 04). Field measurements of performance of roof solar collector. *Energy and Buildings 31*(3), 171–178.

Khedari, J., J. Waewsak, S. Thepa, and J. Hirunlabh (2000). Field investigation of night radiation cooling under tropical climate. *Renewable Energy 20*(2), 183 – 193.

Kipp & Zonen (2009). *Instruction manual, CG1 Pyrgeometer & CG2 Net pyrgeometer* (0204 ed.). Kipp & Zonen B.V. Rontgenweg 1, 2624 BD Delft: Kipp & Zonen.

Martin, M. and P. Berdahl (1984). Characteristics of infrared sky radiation in the united states. *Solar Energy 33*(3-4), 321 – 336.

MathWorks (2009, 10). Matlab 7.9 product description. Internet: `http://www.mathworks.com/products/matlab/description1.html`.

Meir, M. G., J. B. Rekstad, and O. M. Løvvik (2002, 01). A study of a polymer-based radiative cooling system. *Solar Energy 73*(6), 403–417.

National Instruments (2009, 10). Product and services. Internet: `http://www.ni.com/labview/`.

Norwegian Meteorological Institute (2009, 07). Kvaliteten på observasjonene. Internet: http://met.no/Meteorologi/A_male_varet/Observasjoner_fra_land/Dette_blir_malt/Kvaliteten_pa_observasjonene/.

Skartveit, A., J. A. Olseth, G. Czeplak, and M. Rommel (1996). On the estimation of atmospheric radiation from surface meteorological data. *Solar Energy 56*(4), 349 – 359.

Spectral Sciences (2009, 10). Modtran. Internet: www.modtran.org.

Storås, H. (1997, 02). Om kjøling av bygninger ved utnyttelse av infrarød stråling mot nattehimmelen. Master's thesis, University of Oslo.

Swinbank, W. C. (1963). Long-wave radiation from clear skies. *Quarterly Journal of the Royal Meteorological Society 89*(381), 339 – 348.

Tappel, T. (2007). Temperaturkontroll av solfangere ved tvungen konveksjon. Master's thesis, Universitetet for miljø- og biovitenskap.

Taylor, J. (1997). *An introduction to Error Analysis* (Second ed.). 55D Gate Five Road, Sausalito, CA 94965: University Science Books.

Van Wely, L. (2009, 10). Email communication with senior engineer in radiometry at Kipp & Zonen B.V.

Nomenclature

A_{hem} Area of hemisphere $[m^2]$

A_{Pb} Relative area of Physics building $[m^2]$

A_{rad} Area of radiator $[m^2]$

A_{rel} Relative area of a hemisphere

α Absorptance of radiation on a surface

α_{cs} Absorptance of cover sheet

α_{rad} Absorptance of radiator

C_1 $= (C_2 \cdot T_{\text{dry}})/(C_3 + T_{\text{dry}})$

C_2 $= 17.08085$

C_3 $= 234.175$

CDD Cooling degree days $[^\circ\text{C} \cdot \text{days}]$

CDH_{m} Cooling degree hours for one month [Kh]

CDH_{n} Cooling degree hours for one night [Kh]

$\delta R_{\text{rad,offset}}$ The offset error in radiation caused by the surrounding buildings [%]

$\Delta T_{\text{PB-sky}}$ The difference between the temperature of the Physics building and the sky temperature [K]

$\Delta T_{\text{rad-sky}}$ The difference between the radiator and the sky temperature [K]

ε Emittance

ε_0 Sky emittance for clear sky

ε_{c}	Hemispherical cloud emittance
$\varepsilon_{\mathrm{sky}}$	Sky emittance from model
$\varepsilon_{\mathrm{rad}}$	Emittance of radiator
$\varepsilon_{\mathrm{sys}}$	Total emittance of system
HDD	Heating degree days [°C · days]
λ	Wavelength [m]
λ_{m}	Wavelength where the blackbody radiation has its peak [m]
L_{loc}	Local meridian [°]
L_{st}	Standard meridian [°]
n	Fraction of the sky covered by clouds ($0 \leq n \leq 1$)
NH	Lower cloud cover, downloaded from the Norwegian Meteorological Institute$0 \leq NH \leq 8$
n_{i}	Refractive index of material i
N_{m}	Number of nights in month m, with measurements
n_{m}	Number of nights in month m
NN	Cloud cover, downloaded from the Norwegian Meteorological Institute in integers $0 \leq NN \leq 8$
NX	Mean cloud cover, $(NN + NH/2)$
ϕ_{h}	Azimuth angle used in calculation of the area of a hemisphere [rad]
P_{net}	Net power radiated out of a surface [W]
$R_{\uparrow}$	Radiation emitted from a surface toward the sky [W/m^2]
R_{actual}	Blackbody radiation absorbed in the pyrgeometer [W/m^2]
R	Radiated energy from blackbody radiation [W/m^2]
r_{h}	Radius used in calculation of the area of a hemisphere, $r = 1$ when only relative areas are found [m]
$R_{\downarrow}$	Radiation from the sky absorbed at a surface [W/m^2]
R_{atm}	Downward atmospheric infrared radiation [W/m^2]

ρ	Reflectance of radiation on a surface
ρ_{cs}	Reflectance of cover sheet
ρ_{rad}	Reflectance of radiator
R_{net}	Net atmospheric infrared radiation [W/m^2]
$r_{\parallel}$	Reflectance for radiation with polarization parallel to the surface plane
$r_{\perp}$	Reflectance for radiation with polarization perpendicular to the surface plane
R_{sky}	Downward atmospheric infrared radiation from sky without building [W/m^2]
R_{surf}	Blackbody radiation from surface [W/m^2]
r_{tot}	Total reflectance of radiation on a surface
S	Sensitivity/Calibration constant for pyrgeometer $\left[\frac{\mu\text{V}}{\text{W/m}^2}\right]$
σ	Stefan-Boltzmann constant $\left(5.67 \cdot 10^{-8} \frac{W}{m^2 \cdot K^4}\right)$
T_{A}	Ambient temperature [K]
τ	Transmittance of radiation through a surface
T_{dp}	Dew point temperature [°C]
T_{dry}	Dry bulb temperature [°C]
θ_{h}	Elevation angle used in calculation of the area of a hemisphere [rad]
θ_{i}	Angle of incidence [°]
θ_{t}	Angle of transmittance [°]
t_{m}	Hours from midnight in solar time
t_{loc}	Local time
t_{solar}	Solar time
t_{st}	Standard time
T_{Pb}	Temperature of Physics building [K]
T_{p}	Pyrgeometer temperature [K]

T_{rad} Temperature of radiator [K]

τ_{cs} Transmittance of cover sheet

T_{sky} Sky temperature [K]

$T_{\mathrm{sky,pyr}}$ Sky temperature calculated from measurements of atmospheric radiation [K]

$T_{\mathrm{sky,met}}$ Sky temperature calculated from meteorological data [K]

T Temperature of a body [K]

U_{emf} Output voltage from pyrgeometer [μV]

z_{c} Cloud base height [km]

z_* Constant for normalization of the cloud base height, ($z_* = 8.2\mathrm{km}$)

Appendix A

Appendix

A.1 Computer programs

A.1.1 Labview program

Figure A.1 shows the block diagram of the LabVIEW program made to collect measurements from the pyrgeometer and the ambient temperature. Figure A.2 shows a screenshot of the same program in action.

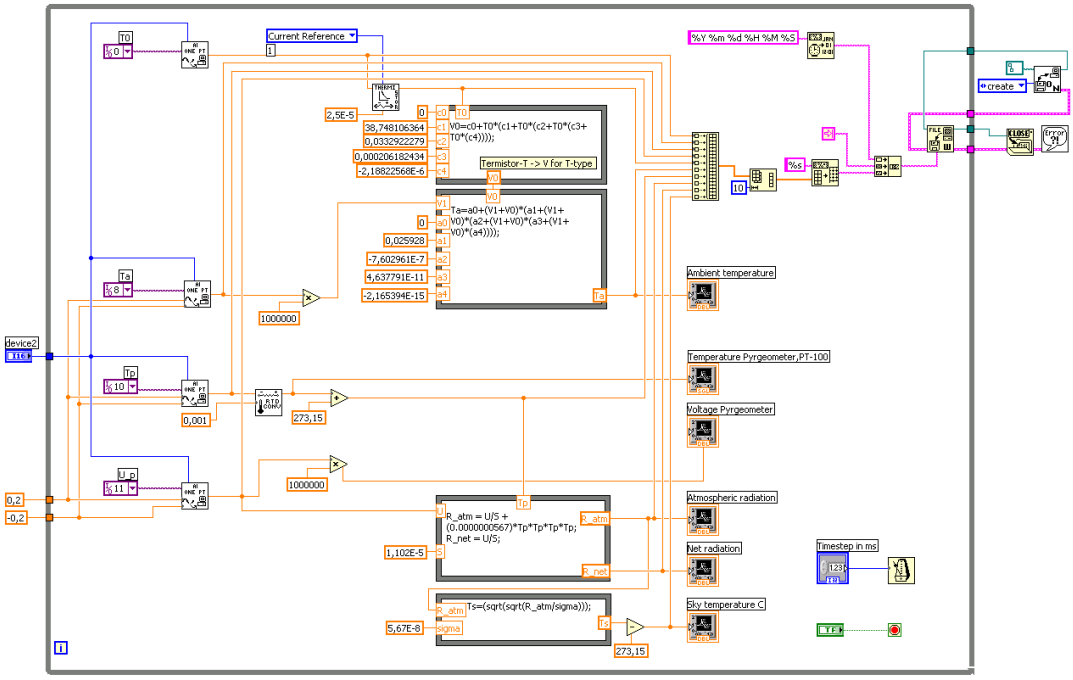

Figure A.1: Screen shot of the block diagram for the LabVIEW program, made for acquiring the pyrgeometer data.

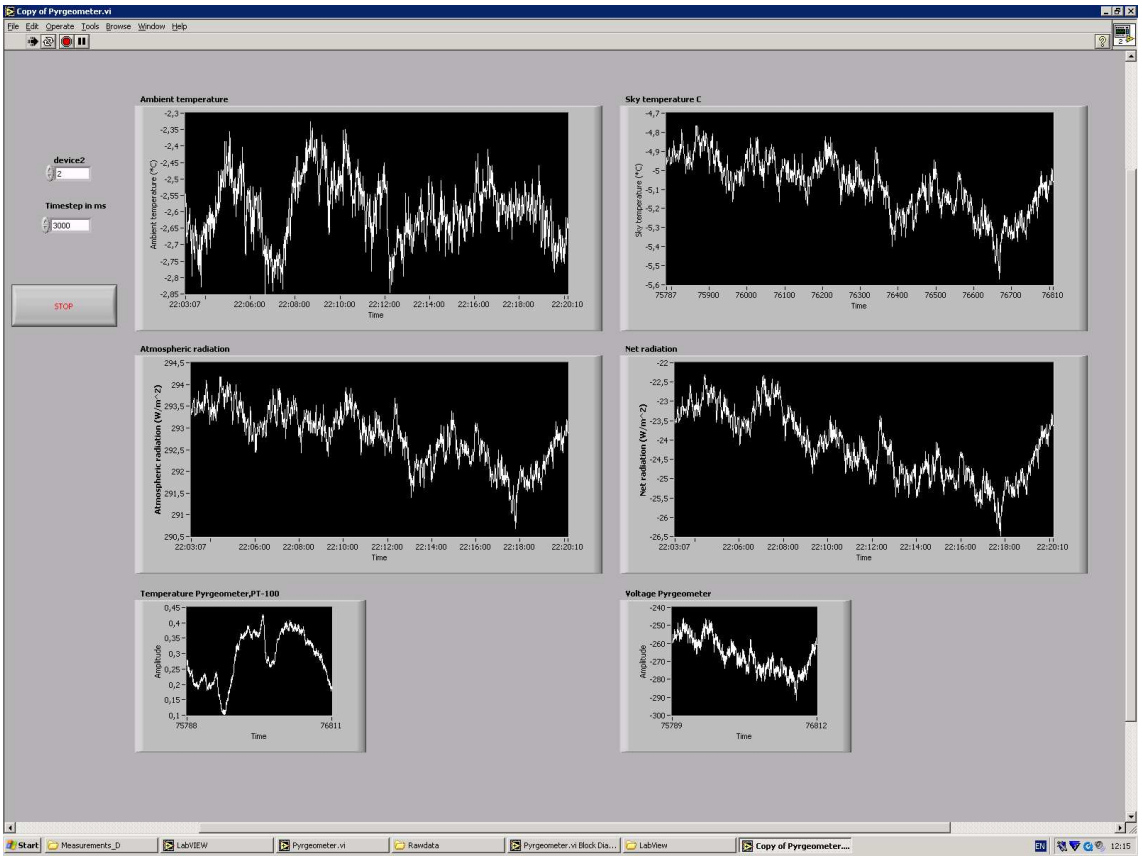

Figure A.2: Screen shot of the LabVIEW program, made for acquiring the pyrgeometer data.

A.1.2 Java programs

This program was written to import files downloaded from `www.eklima.no`, combine them into one file, in CSV fileformat.

```
/**
Program som leser inn alle filnavnene i mappa Metdata,
sorterer de etter dato/alfabet,
leser inn filene linje for linje, og bytter ut
’,’  med ’.’
’ ’  med ’;’
’tab’ med ’;’.
Skriver til en ny fil.

Henning Degnes-Ødemark
16.03.2009
*/


import easyIO.*;
import java.io.File;
import java.util.Arrays;

class CombineMet
{
    public static void main(String args[])
    {
      Out wrFile = new Out("../Combined/MetData.csv");
File dir = new File("../Metdata/");
File [] fList = dir.listFiles();
Arrays.sort(fList);
for(File files:fList)
    {
if(files.isFile())
    {
In infile = new In(files.getAbsolutePath());

while(!infile.endOfFile())
    {
String Line = infile.inLine();
Line = Line.replace(’,’, ’.’);
Line = Line.replace(’ ’, ’;’);
Line = Line.replace(’\t’, ’;’);

wrFile.outln(Line);
    }

infile.close();
    }
    }//end for
wrFile.close();
// Some meteorological data downloaded comes with ’.’ values insetead of ’NaN’
System.out.println("Remember to check for . values");
    }//end main
}//end CombineFile
```

This program was written to make the raw data files from the pyrgeometer measurements into one combined CSV file.

```
/**
Program som leser inn alle filnavnene i mappa rawdata,
sorterer de etter dato/alfabet,
leser inn filene linje for linje, og bytter ut
’,’  med ’.’
’ ’  med ’;’
’\t’ med ’;’.
Skriver til en ny fil.

Henning Degnes-Ødemark
16.03.2009
*/


import easyIO.*;
import java.io.File;
import java.util.Arrays;

class CombineMet
{
    public static void main(String args[])
    {
      Out wrFile = new Out("../Combined/MetData.csv");
File dir = new File("../Metdata/");
File [] fList = dir.listFiles();
Arrays.sort(fList);
for(File files:fList)
    {
if(files.isFile())
    {
In infile = new In(files.getAbsolutePath());

while(!infile.endOfFile())
    {
String Line = infile.inLine();
Line = Line.replace(’,’, ’.’);
Line = Line.replace(’ ’, ’;’);
Line = Line.replace(’\t’, ’;’);

wrFile.outln(Line);
    }

infile.close();
    }
    }//end for
wrFile.close();
// Some meteorological data downloaded comes with ’.’ values insetead of ’NaN’
System.out.println("Remember to check for . values");
    }//end main
}//end CombineFile
```

A.1.3 Matlab program

```
%% Executable part of NSR
function NSR(Option)
%% Information
% Combined program for all data analysis of the NSR master project
% Henning Degnes-Ødemark 2009

format long;
set(0,'DefaultFigureWindowStyle','docked');

if nargin ==1 && strcmp(Option,'Calc')
    T0 = clock;
    [Met Sun Comb] = ReadInData;
    Calculation(Comb,Sun,1);
end

if nargin==0
    All_Option = input('Do it all(y/n)?','s');
    NoGraphics = input('Run in no graphics mode(y/n)? ','s');
    if All_Option =='y'
        A0(NoGraphics)
    else
        Option = input('Convert files to h5 (y/n)? ','s');
        if Option=='y'
            ConvertToH5;
        end
        Option = input('Combine data (y/n)? ','s');
        if Option=='y'
            CombinePyrMet;
        end
        Option = input('Calculate data (y/n)? ','s');
        if Option=='y'
            [Met Sun Comb] = ReadInData;
            Calculation(Comb,Sun);
        end
        Option = input('Classification of nights (y/n)? ','s');
        if Option=='y'
            [Met Sun] = ReadInData;
            Classificate(Met,Sun,NoGraphics);
        end
        Option = input('Get info(y/n)? ','s');
        if Option=='y'
            H5info();
        end
        T0 = clock;
    end
elseif strcmp(Option,'ANG')
    T0 = A0('y');
end

format short;
Elapsed_Time = etime(clock,T0);
disp(['Total Calculation time: ' num2str(Elapsed_Time) ' sec']);
end
%% Do it all in no grapic mode
function T0 = A0(NoGraphics)
  T0 = clock;
  disp('Does it all:');
  disp(' Deleting NSR.h5');
  delete H5/NSR.h5;
  ConvertToH5;
  CombinePyrMet;
  [Met Sun PyrMet] = ReadInData;
  Calculation(PyrMet,Sun);
  Classificate(Met,Sun,NoGraphics);
  DHN(1,'NG');
  DHN(2)
end

%% Converting the input file (Combined_raw.csv) to Hdf5 format
function ConvertToH5()
  tic
  format long;
  disp(' Converting data to H5:');
  disp('  Importing data...');
  A = importdata('../Combined/PyrgData.csv');
  B = importdata('../Combined/MetData.csv');
  C = importdata('../Combined/SunData.csv');
  [A B] = Calibrate(A,B);
size(B)
```

```
% Fix time in pyrgeometer measurements
  disp('  Fixing time vectors for daylight savings...');
  DatoVector = A(:,1:6);
  DatoNumb = datenum(DatoVector);

  D1 = datenum([2008 03 30 02 00 00]);
  D2 = datenum([2008 10 26 02 00 00]);
  D3 = datenum([2008 10 26 03 00 00]);
  D4 = datenum([2009 03 29 02 00 00]);
  D5 = datenum([2009 10 25 02 00 00]);
  D6 = datenum([2009 10 25 03 00 00]);
  T1 = find(DatoNumb > D1,1);
  F1 = find(DatoNumb > D2 & DatoNumb < D3);
  S_F1 = size(F1);

for i=F1(1):F1(S_F1)
  if DatoNumb(i)<DatoNumb(i-1)
      T2 = i-1;
  end
end

  T3 = find(DatoNumb > D4,1);
  F2 = find(DatoNumb > D5 & DatoNumb < D6);

if ~isempty(F2)
    for j=F2(1):F2(S_F1)
        if DatoNumb(j)<DatoNumb(j-1)
            T4 = j-1;
        end
    end
else
    T4=length(DatoNumb);
end
NyDatoVector = DatoVector;
NyDatoVector(T1:T2,1:6) = [DatoVector(T1:T2,1:3) DatoVector(T1:T2,4)-1 DatoVector(T1:T2,5:6)];
NyDatoVector(T3:T4,1:6) = [DatoVector(T3:T4,1:3) DatoVector(T3:T4,4)-1 DatoVector(T3:T4,5:6)];
NyDatoNumb = datenum(NyDatoVector);
NyDatoVector = datevec(NyDatoNumb);
A(:,1:6) = NyDatoVector(:,1:6);

% Fix time in Sunset/Sunrise
% Find date where summer time begins and ends
F1 = find(C(:,1)==2008 & C(:,2)>3,1);
F2 = find(C(:,1)==2008 & C(:,2)==10 & C(:,3)==26);
F3 = find(C(:,1)==2009 & C(:,2)==3 & C(:,3)==29);
F4 = length(C);%find(C(:,1)==2009 & C(:,2)<10,'last')  % As long as we are into summer-time

C(F1:F2-1,4) = C(F1:F2-1,4)-1;
C(F1:F2-1,6) = C(F1:F2-1,6)-1;
C(F3:F4-1,4) = C(F3:F4-1,4)-1;
C(F3:F4-1,6) = C(F3:F4-1,6)-1;

% Write to h5 file
disp('  Writes /G1/Pyrg to file...');
A_details.Location = '/G1';
A_details.Name = 'Pyrg';
disp('  Writes /G2/Met to file...');
B_details.Location = '/G2';
B_details.Name = 'Met';
disp('  Writes /G2/Sun to file...');
C_details.Location = '/G2';
C_details.Name = 'Sun';

attrG1 = 'Measured data';
attrG1_details.Name = 'Description';
attrG1_details.AttachedTo = '/G1';
attrG1_details.AttachType = 'group';

attrG2 = 'Data from external sources';
attrG2_details.Name = 'Description';
attrG2_details.AttachedTo = '/G2';
attrG2_details.AttachType = 'group';

hdf5write('H5/NSR.h5',A_details,A);
hdf5write('H5/NSR.h5',B_details,B,'WriteMode','append');
hdf5write('H5/NSR.h5',C_details,C,'WriteMode','append');
hdf5write('H5/NSR.h5',attrG1_details,attrG1,attrG2_details,attrG2,'WriteMode','append');

Pyrg_Head = {'YYYY', 'MM', 'DD', 'hh' ,'mm', 'ss' ,'V_TO', 'V_TA', 'V_TP' ,'V_P' ,'T_O' ,'T_A', 'T_P' ,'R_atm', 'R_net' ,'T_sky'};
hdf5write('H5/NSR.h5','/G1/Pyrghead',Pyrg_Head,'WriteMode','append');
Met_Head = {'St.No','YYYY','MM','DD','hh','HL','NH','NN','UU','TA','TD'};
hdf5write('H5/NSR.h5','/G2/Methead',Met_Head,'WriteMode','append');
Sun_Head = {'YYYY','MM','DD','SRhh','SRmm','SShh','SSmm'};
```

```
hdf5write('H5/NSR.h5','/G2/Sunhead',Sun_Head,'WriteMode','append');

toc
end

%% Read in data
function [Met,Sun,Comb] = ReadInData()
disp('  Reads in data...');
Met  = hdf5read('H5/NSR.h5','/G2/Met');
Sun  = hdf5read('H5/NSR.h5','/G2/Sun');
Comb = hdf5read('H5/NSR.h5','/G3/Comb');
end

%% Calibrating the ambient temperature measurements
function  [A B] = Calibrate(A,B)
disp('  Calibrates Pyrgeometer data...');
TA_m_uncal = A(:,12);                                    % Makes vector of all uncalibrated ambient temperature measurements
a = -0.000244307015156;                                  % Calibration constants
b = 1.017211728561162;
c = -0.148726832250834;

TA_m_cal = a*TA_m_uncal.^2 + b.*TA_m_uncal + c;          % Calibrates the vector

A(:,12) = TA_m_cal(:);                                   % Write the calibrated vector over the uncalibrated one in the matrix

disp('  Remove bad datapoints...');                       % Removes bad datapoints
disp('   TA < -40');
F40 = find(TA_m_cal(:)<-40);
plot(A(F40,1),TA_m_cal(F40),'.')
datetick('x')
A(F40,12) = NaN;

disp('   NX < 0');
FNH = find(B(:,7)<0);
B(FNH,7) = NaN; %#ok<*FNDSB>
FNN = find(B(:,8)<0);
B(FNN,8) = NaN;

end

%% Combining the pyrgeometer measurement and the meteorological values
function CombinePyrMet(A,B)
tic
disp(' Combining Pyrgeometer data and Meteorological data:');
if nargin<2
    A = hdf5read('H5/NSR.h5','G1/Pyrg');
    B = hdf5read('H5/NSR.h5','G2/Met');
end

S_A = size(A);
S_B = size(B);
C = NaN(S_A(1),14);
C(:,1:6) = A(:,1:6);    % Date and time from pyrgeomether file
C(:,7)   = A(:,12);     % TA_m from pyrgeomether file
C(:,8)   = A(:,14);     % R_atm_m from pyrgeomether file

DateVecB = B(:,2:5);
DateVecB(:,5:6) = 0;
DNumA = datenum(A(:,1:6));
DNumB = datenum(DateVecB);

disp('  Combining...');
for i=1:S_B(1)
    I = find(DNumA<=DNumB(i),1,'last');
    if numel(I)
        C(I,9:14) = B(i,6:11);                  % Col 12-17(C) => D 5-10 = B 6-11
    end
end

attrG3 = 'Calculated data';
attrG3_details.Name = 'Description';
attrG3_details.AttachedTo = '/G3/';
attrG3_details.AttachType = 'group';
disp('  Writes /G3/Comb to file...');
CombHead = {'YYYY','MM','DD','hh','mm','ss','TA_m','R_atm','HL','NH','NN','UU','TA_met','TD_met'};
hdf5write('H5/NSR.h5','/G3/Comb',C,'WriteMode','append');
hdf5write('H5/NSR.h5',attrG3_details,attrG3,'WriteMode','append');
hdf5write('H5/NSR.h5','/G3/Combhead',CombHead,'WriteMode','append');

toc
end

%% Calculates different data
```

```
function Calculation(A,S,NoWrite)
disp(' Calculates data:');

%% Defining constants
S_A = size(A);
S_S = size(S);
sigma  = 5.670400e-8;                                                    % Stefan-Bolzmanns constant
e_c = 1;                                                                 % Hemisfærisk cloud-emittance
z_s = 8.2;                                                               % Constant in km
T_rad = 25+273.15;                                                       % Radiator temperature in [K]

C_2    = 17.08085;                                                       % Constant for calculation of the dew point temperature
C_3    = 234.175;                                                        % Constant for calculation of the dew point temperature
TA_m   = A(:,7);                                                         % Ambient temperature in Celcius
R_atm  = A(:,8);                                                         % Atmospheric radiation in W/m^2
HL     = A(:,9)/1000;                                                    % Cloud altitude in [km]
NH     = A(:,10)/8;                                                      % Cloud cover, lower cloud [0,1]
NN     = A(:,11)/8;                                                      % Cloud cover [0,1]
UU     = A(:,12)/100;                                                    % Relative humidity [0,100]
TD_met = A(:,14);                                                        % The meteorological dew point temperature
T_abs  = TA_m+273.15;                                                    % Ambient temperature in Kelvin

%% Solar time correction

d = 1:365;
B = ((d-1)*(365/360))*(pi/180);
E = 229.2*(0.000075 + 0.001868*cos(B) - 0.032077*sin(B) - 0.014615*cos(2*B) - 0.04089*sin(2*B));
t_loc = datenum(A(:,1:6));
t_add =4*(345-349.59)+E;
t_add(366) = mean([t_add(1) t_add(365)]);
tm = round(t_add);
ts = round((t_add-tm)*60);
t_s = zeros(S_A(1),1);

tic
for i=1:S_A(1)
    n = daynumber(t_loc(i));
    t_s(i) = addtodate(t_loc(i),tm(n),'min');
    t_s(i) = addtodate(t_s(i),ts(n),'sec');
end
toc
DV = datevec(t_s);
hh = DV(:,4);        % Hour [0,23] corrected to solar time

 %% Cloud cover definitions

a = 0.5;
b = 0.5;
N=(a*NH+b*NN);                % Uses the mean of cloud cover if a=b=0.5, otherwise the weight of a and b
I_NH = isnan(NH);
I_NN = isnan(NN);

F_NX = find(I_NH-I_NN~=0);       % Finds the entries where one of the NX is not NaN and the other is NaN
N_F_NX = length(F_NX);
for i=1:N_F_NX
    if I_NH(F_NX(i))==1
        N(F_NX(i)) = NN(F_NX(i));       % Sets N=NN when NH = NaN
    elseif I_NN(F_NX(i))==1
        N(F_NX(i)) = NH(F_NX(i));       % Sets N=NH when NN = NaN
    end
end

%% Finding mean value of measured TA
n=5;
TA_mean = NaN(S_A(1),1);
F_UU = find(~isnan(UU));
N_F_UU = length(F_UU);
for i=1:N_F_UU
    j = F_UU(i);
    if j<n
        TA_mean(j) = mean(TA_m(j:j+n));
    elseif j>N_F_UU-n
        TA_mean(j) = mean(TA_m(j-n:j));
    else
        TA_mean(j) = mean(TA_m(j-n:j+n));
    end
end

%% Test for HL_max>4000m and change e_c
if max(HL)>4
    F4km = find(HL>4 & HL<11);
    e_c(F4km) = 0.74-0.084*(HL-4);
    F11km = find(HL>11);
```

```
    e_c(F11km) = 0.15;
end
%% Calculates
C_1    = (TA_mean*C_2)./(TA_mean+C_3);                                    % Constant for calculation of the dew point temperature
TD_c   = C_3*((log(UU)+C_1))./(C_2 -(log(UU)+C_1));                       % Calculated dew point temperature (C)
Eps_ex = R_atm./((T_abs.^4)*sigma);                                       % Experimentally determined epsilon
T_skya  = (R_atm/sigma).^(1/4);                                           % T_sky from radiated energy [K]
T_sky = T_skya-273.15;                                                    % T_sky [C]
Eps_0  = 0.711 + 0.0056*TD_c + 0.000073*TD_c.^2 + 0.013*cos((2*pi*hh)/24); % Calculate Epsilon_0
Eps_met= Eps_0 + (1-Eps_0)*e_c.*N.*exp(-(HL)/z_s);                        % Calculate Epsilon, from meteorological values
R_atm_met = (sigma*Eps_met).*((TA_mean+273.15).^4);                       % Calculate atmospheric radiation from met. values
T_sky_met = (R_atm_met/sigma).^(1/4)-273.15;                              % Calculate T_sky from meteorological values[C]
P_inst = sigma*(T_rad.^4-T_skya.^4);                                      % Calculate net power a radiator with a const T_rad [W]
Delta_T = T_rad - T_skya;                                                 % Difference between the T_rad (25 degree C) and T_sky
D_TD = TD_met - TD_c;                                                     % Calculates the difference between dew point temp.


%% Interpolates values of T_sky_met:
disp('  Interpolates T_sky_met...');

F_Tsky = find(~isnan(T_sky_met));                                         % Finds rows with values for T_sky_met
N_F = length(F_Tsky);                                                     % Number of rows in T_sky_met with values
T_s_met_int = NaN(S_A(1),1);                                              % Preallocation of vector for interpolated T_sky

for i =1:N_F-1
    T1 = T_sky_met(F_Tsky(i));                                            % First value for T_sky_met
    T2 = T_sky_met(F_Tsky(i+1));                                          % Second value for T_sky_met
    ra = F_Tsky(i);                                                       % First row number
    rb = F_Tsky(i+1);                                                     % Second row number
    Nr = rb-ra-1;                                                         % Number of rows between ra and rb
    DT = T2-T1;                                                           % Difference in temperature
    T_int = T1:(DT/Nr):T2;                                                % Interpolated values calculated
    N_T_int = length(T_int);                                              % Length of vector with interpolated values
    T_s_met_int(ra:rb-1,1) = T_int(1:N_T_int);                            % Interpolated values put into vector of T_sky_met
end

Delta_T_met = T_rad - (T_s_met_int +273.15);

%% Puts values into new array C
disp('Put values into array');

C = NaN(S_A(1),19);                                                       % Makes array C

C(:,1) = datenum(A(:,1:6));                                               % Datenumber for date
C(:,2) = TA_m;                                                            % Ambient temperature in Celcius [C]
C(:,3) = R_atm;                                                           % Atmospheric radiation
C(:,4) = Eps_ex;                                                          % Experimental epsilon
C(:,5) = T_sky;                                                           % Sky temperature from measured values [C]
C(:,6) = TD_c;                                                            % Calculated dew point temperature
C(:,7:8) = A(:,13:14);                                                    % TA_met and TD_met
C(:,9:12) = A(:,9:12);                                                    % HL,NH,NN,UU
C(:,13) = Eps_met;                                                        % Epsilon from Berdahls formula, based on meteorological data
C(:,14) = T_sky_met;                                                      % Sky temperature from Berdahls formula
C(:,15) = P_inst;                                                         % Effect of radiator with T_rad = 25 *C, and epsilon=1
C(:,16) = D_TD;                                                           % TD_met - TD_c [C]
C(:,17) = Delta_T;                                                        % T_rad - T_skya [K]
C(:,18) = Delta_T_met;                                                    % T_rad - (T_s_met_int +273.15) [K]
C(:,19) = T_s_met_int;                                                    % Interpolated sky temperature from meteorological values


%% Find night values
disp('  Finding night values...')
q=1;
for i=1:S_S(1)-1
    sunset_d1  = datenum([S(i,1:3) S(i,6:7) 00]);              % Make datenum for sunset day 1
    sunrise_d2 = datenum([S(i+1,1:5) 00]);                     % Make datenum for sunrise day 2
    F_Night = find(C(:,1) > sunset_d1 & C(:,1) < sunrise_d2);  % Find the rows in C at night
    N_F_Night = length(F_Night);                               % Length of night in rows
    NightArray(q:q+N_F_Night-1,:) = C(F_Night,:);              % Make NightArray, with only night time values from C
    q=q+N_F_Night;                                             % Update counter q
end

%% Display
DT1 = NightArray(:,14)-NightArray(:,5);
DT2 = NightArray(:,19)-NightArray(:,5);
CloudTest(x+1,1:12) =[a b mmm(DT1,'s') mmm(DT2,'s')];


%end
format bank;
CloudTest

figure;
```

```
plot(CloudTest(:,1),CloudTest(:,4))


% Writes to file

if NoWrite
    disp('No new files where written')
else
tic
disp('  Writes /G3/Calc to file...');
C_Head = {'DateNum','TA_m','R_atm','Eps_ex','T_sky','TD_c','TA_met','TD_met','HL','NH','NN','UU','Eps_met','T_sky_met','P_inst',...
  'D_TD','DeltaT','Delta_T_met','T_s_met_int'};
hdf5write('H5/NSR.h5','/G3/Calc',C,'WriteMode','append');                              % Write C to h5 file
disp('  Writes /G3/CalcNight to file...');
hdf5write('H5/NSR.h5','/G3/CalcNight',NightArray,'WriteMode','append');                % Write NightArray to h5 file
disp('  Writes /G3/CalcHead to file...');
hdf5write('H5/NSR.h5','/G3/CalcHead',C_Head,'WriteMode','append');                     % Write Header to h5 file
toc
% end
end

%% function Classification
function Classificate(A,S,NoGraphics)
%% Define vectors
disp(' Classification started:');
tic
LS = length(S);

NH = A(:,7);
NN = A(:,8);
DayVec = A(:,2:5);
DayVec(:,5:6)=0;

Date = datenum(DayVec);

%Day1 = datenum([Day1_v(1,1:3) 15 00 00]);
%Day2 = addtodate(Day1,1,'Day');

%Day2_v = datevec(Day2);
%LastDay = datenum(Day1_v(N_D));

F1 = find(isnan(NH)==0);
N_F1 = length(F1);
F2 = find(isnan(NN)==0);
N_F2 = length(F2);
F_neg = find(NH<0);
NH(F_neg) = NaN;

%% Loop to linear interpolate cloud cover
disp('  Linear interpolation of cloud cover...');

for i=1:N_F1-1
    NH1 = NH(F1(i));
    NH2 = NH(F1(i+1));
    r1 = F1(i);
    r2 = F1(i+1);
    Nr = r2-r1;
    DeltaNH = NH2-NH1;

    if Nr<5
        if  DeltaNH == 0
            NH(r1:r2)=NH1;
        else
            NH_int = NH1:(DeltaNH/Nr):NH2;
            N_NH_int = length(NH_int);
            NH(r1:r2)=NH_int(1:N_NH_int);
        end
    end
end
for i=1:N_F2-1
    NN1 = NN(F2(i));
    NN2 = NN(F2(i+1));
    r1 = F2(i);
    r2 = F2(i+1);
    Nr = r2-r1;
    DeltaNN = NN2-NN1;
    if Nr<5
        if DeltaNN == 0
            NN(r1:r2)=NN1;
        else
            NN_int = NN1:(DeltaNN/Nr):NN2;
            N_NN_int = length(NN_int);
            NN(r1:r2)=NN_int(1:N_NN_int);
```

```
        end
    end
end
%A(:,7) = NH;
%A(:,8) = NN;
%% Calculates the mean cloud cover
disp('  Calculates mean cloud cover for nights...');
Night_N_mean = NaN(LS,8);

for i=1:LS-1
    sunset_d1  = datenum([S(i,1:3) S(i,6:7) 00]);                       % Make datenum for sunset day 1
    sunrise_d2 = datenum([S(i+1,1:5) 00]);                              % Make datenum for sunrise day 2
    NightLength = etime(datevec(sunrise_d2),datevec(sunset_d1));
    F_Night = find(Date(:,1) > sunset_d1 & Date(:,1) < sunrise_d2);     % Find the rows in Metdata at nighttime
    N_F_Night = length(F_Night);                                        % Length of night in rows
    Night_N_mean(i,1:3) = S(i,1:3);
    if N_F_Night >1
        Night_N_mean(i,4) = mean(NH(F_Night));
        Night_N_mean(i,5) = mean(NN(F_Night));
        Night_N_mean(i,8) = NightLength;
    end
end

NH_mean = Night_N_mean(:,4);
NN_mean = Night_N_mean(:,5);

%% Finds and classifies the nights
disp('  Finds and classifies the nights...');
NoGraphics ='n';

NX = mean([NH_mean NN_mean],2);
size(NX)

F1  = find(NH_mean<=1 & NN_mean<=4);
F2  = find(NH_mean<=1 & NN_mean>4);
F3  = find(NH_mean>1  & NH_mean<=3 & NN_mean<=4);
F4  = find(NH_mean>1  & NH_mean<=3 & NN_mean>4);
F5  = find(NH_mean>3  & NH_mean<=5 & NN_mean<=4);
F6  = find(NH_mean>3  & NH_mean<=5 & NN_mean>4);
F7  = find(NH_mean>5  & NH_mean<=7 & NN_mean<=4);
F8  = find(NH_mean>5  & NH_mean<=7 & NN_mean>4);
F9  = find(NH_mean>7  & NN_mean<=4);
F10 = find(NH_mean>7  & NN_mean>4);

% Makes first classification list (Class1)
for i=1:10
    eval(['Night_N_mean(F' num2str(i) ',6)=' num2str(i) ';'])   % Put the classification (i:[0,10]) to column 6 in the Night_N_mean array
    eval(['N1(' num2str(i) ') = length(F' num2str(i) ');'])     % Makes N1 with the number of nights in each classification
end

Night_N_mean(F1,7) = 1;
Night_N_mean(F2,7) = 1;
Night_N_mean(F3,7) = 2;
Night_N_mean(F4,7) = 3;
Night_N_mean(F5,7) = 4;
Night_N_mean(F6,7) = 4;
Night_N_mean(F7,7) = 5;
Night_N_mean(F8,7) = 5;
Night_N_mean(F9,7) = 6;
Night_N_mean(F10,7) = 6;

if NoGraphics ~='y'
    figure;
    bar(N1)
end
% Makes second classification list (Class2)
N2(1) = N1(1) + N1(2);
N2(2) = N1(3);
N2(3) = N1(4);
N2(4) = N1(5) + N1(6);
N2(5) = N1(7) + N1(8);
N2(6) = N1(9) + N1(10);

if NoGraphics ~='y'
    figure;
    bar(N2)
end

% Makes third classificaiton list (Class3)
N3(1) = N1(1) + N1(2);
N3(2) = N1(3) + N1(4);
N3(3) = N1(5) + N1(6);
N3(4) = N1(7) + N1(8);
```

```
N3(5) = N1(9) + N1(10);

if NoGraphics ~='y'
    figure;
    bar(N3)
end
D = NaN(LS,1);
for i=1:LS-1
    D(i) = Night_N_mean(i+1,7)-Night_N_mean(i,7);
end
if NoGraphics ~='y'
    figure;
    bar(D)
end

for i=-6:6
    eval(['FD' int2str(i+7) ' = find(D==' int2str(i) ');']);
    eval(['ND(' int2str(i+7) ')=length(FD' int2str(i+7) ');']);
end

if NoGraphics ~='y'
    bar(ND);
    set(gca,'XTickLabel',{'-6','-5','-4','-3','-2','-1','0','1','2','3','4','5','6'},...
        'XTick',[1 2 3 4 5 6 7 8 9 10 11 12 13]);
    title('The difference between classification of day i and i-1');
    xlabel('Difference in classification');
    ylabel('Number of nights in each category');
end
ClassHead = {'Year','Month','Day','NH_mean','NN_mean','Class1','Class2','Night_length'};
disp('  Writes /G3/Classification to file...');
hdf5write('H5/NSR.h5','/G3/Classification',Night_N_mean,'WriteMode','append');
disp('  Writes /G3/ClassHead to file...');
hdf5write('H5/NSR.h5','/G3/Classhead',ClassHead,'WriteMode','append');

% fid = fopen('Liste.txt', 'wt');
% W(:,2:9) = Night_N_mean;
% W(:,1) = 1:length(Night_N_mean);
% for i=1:length(W)
%     fprintf(fid, '%3d & %4d & %2d & %2d & %6.3f & %6.3f & %2d & %d & %6.0f \\\\\n', W(i,:));
% end
% fclose('all');
toc
end

%% H5 info
function H5info()
File = ('H5/NSR.h5');
Fileinfo = hdf5info(File);
GroupH = Fileinfo.GroupHierarchy;
Groups = GroupH.Groups;
Groups.Name
%    Groups.Attributes
SG = size(Groups);
%Names = cell(SG(2),3);
for i=1:SG(2)
    Names{i,1} = Groups(i).Name; %#ok<AGROW>

    %    Names{i,2} = Dims(i);
    %    Names{i,3} = Dims(i,2);
end
for j=1:9
    DName = Groups(3).Datasets(j).Name;
end
disp(Names);
disp(DName);
LG = length(Groups);
LGD = length(Groups.Datasets);
DsNames = cell{LG,LGD};
for i=1:length(Groups)
    for j=1:length(Groups(i).Datasets)
        DsNames{i,j} = Groups(i).Datasets(j).Name;
    end;
end
disp(DsNames)

end
```

A.1.4 HDF5

Figure A.3 shows the hiearchy in the .h5 file.

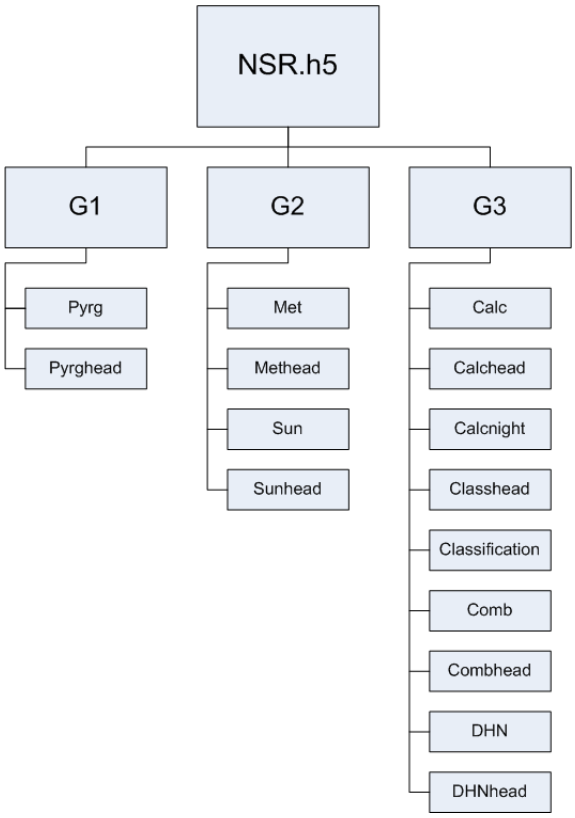

Figure A.3: Structure for the .H5 file.

A.2 Results

A.2.1 List of measurements

Table A.1: List of all days within the period from June 2008 to July 2009. Measurement start-time and date and end-time and date are shown, and missing data is indicated.

Day #	Date	Start date	Start time	Stop date	Stop time	Missing data
Day number	Date	Start date	Start time	Stop date	Stop time	Missing data
1	2008.06.01	-	-	-	-	Yes
2	2008.06.02	2008.06.02	16.18	2008.06.03	15.00	Yes
3	2008.06.03	2008.06.03	15.00	2008.06.04	14.51	-
4	2008.06.04	2008.06.04	15.19	2008.06.05	15.00	-
5	2008.06.05	2008.06.05	15.00	2008.06.06	15.00	-
6	2008.06.06	2008.06.06	15.00	2008.06.07	15.00	-
7	2008.06.07	2008.06.07	15.00	2008.06.08	15.00	-
8	2008.06.08	2008.06.08	15.00	2008.06.09	15.00	-
9	2008.06.09	2008.06.09	15.00	2008.06.10	12.42	-
10	2008.06.10	-	-	-	-	Yes
11	2008.06.11	2008.06.11	16.56	2008.06.12	15.00	-
12	2008.06.12	2008.06.12	15.00	2008.06.13	15.00	-
13	2008.06.13	2008.06.13	15.00	2008.06.14	15.00	-
14	2008.06.14	2008.06.14	15.00	2008.06.14	15.55	Yes
15	2008.06.15	-	-	-	-	Yes
16	2008.06.16	2008.06.16	15.47	2008.06.17	15.00	-
17	2008.06.17	2008.06.17	15.00	2008.06.18	15.00	-
18	2008.06.18	2008.06.18	15.00	2008.06.19	15.00	-
19	2008.06.19	2008.06.19	15.00	2008.06.20	15.00	-
20	2008.06.20	2008.06.20	15.00	2008.06.21	15.00	-
21	2008.06.21	2008.06.21	15.00	2008.06.22	15.00	-
22	2008.06.22	2008.06.22	15.00	2008.06.23	15.00	-
23	2008.06.23	2008.06.23	15.00	2008.06.24	15.00	-
24	2008.06.24	2008.06.24	15.00	2008.06.25	15.00	-
25	2008.06.25	2008.06.25	15.00	2008.06.26	15.00	Yes
26	2008.06.26	2008.06.26	15.00	2008.06.27	15.00	-
27	2008.06.27	2008.06.27	15.00	2008.06.28	14.58	-
28	2008.06.28	2008.06.29	13.33	2008.06.29	15.00	Yes
29	2008.06.29	2008.06.29	15.00	2008.06.30	15.00	-
30	2008.06.30	2008.06.30	15.00	2008.07.01	15.00	-
31	2008.07.01	2008.07.01	15.00	2008.07.02	15.00	-
32	2008.07.02	2008.07.02	15.00	2008.07.03	15.00	-
33	2008.07.03	2008.07.03	15.00	2008.07.04	15.00	-
34	2008.07.04	2008.07.04	15.00	2008.07.05	15.00	-
35	2008.07.05	2008.07.05	15.00	2008.07.05	15.21	Yes
36	2008.07.06	-	-	-	-	Yes
37	2008.07.07	-	-	-	-	Yes
38	2008.07.08	-	-	-	-	Yes
39	2008.07.09	-	-	-	-	Yes
40	2008.07.10	-	-	-	-	Yes
41	2008.07.11	-	-	-	-	Yes
42	2008.07.12	-	-	-	-	Yes
43	2008.07.13	2008.07.14	14.16	2008.07.14	15.00	Yes
44	2008.07.14	2008.07.14	15.00	2008.07.15	15.00	Yes
45	2008.07.15	2008.07.15	15.00	2008.07.16	15.00	-
46	2008.07.16	2008.07.16	15.00	2008.07.17	15.00	-
47	2008.07.17	2008.07.17	15.00	2008.07.18	15.00	-
48	2008.07.18	2008.07.18	15.00	2008.07.19	15.00	-
49	2008.07.19	2008.07.19	15.00	2008.07.20	15.00	-
50	2008.07.20	2008.07.20	15.00	2008.07.21	15.00	-
51	2008.07.21	2008.07.21	15.00	2008.07.22	15.00	-
52	2008.07.22	2008.07.22	15.00	2008.07.23	15.00	-
53	2008.07.23	2008.07.23	15.00	2008.07.24	15.00	-
54	2008.07.24	2008.07.24	15.00	2008.07.25	15.00	-
55	2008.07.25	2008.07.25	15.00	2008.07.26	15.00	-
56	2008.07.26	2008.07.26	15.00	2008.07.27	15.00	-
57	2008.07.27	2008.07.27	15.00	2008.07.28	15.00	-
58	2008.07.28	2008.07.28	15.00	2008.07.29	15.00	-
59	2008.07.29	2008.07.29	15.00	2008.07.30	15.00	-
60	2008.07.30	2008.07.30	15.00	2008.07.31	15.00	-
61	2008.07.31	2008.07.31	15.00	2008.08.01	15.00	-
62	2008.08.01	2008.08.01	15.00	2008.08.02	15.00	-
63	2008.08.02	2008.08.02	15.00	2008.08.03	15.00	-
64	2008.08.03	2008.08.03	15.00	2008.08.04	15.00	-
65	2008.08.04	2008.08.04	15.00	2008.08.05	15.00	-
66	2008.08.05	2008.08.05	15.00	2008.08.06	15.00	-
67	2008.08.06	2008.08.06	15.00	2008.08.07	15.00	-
68	2008.08.07	2008.08.07	15.00	2008.08.08	15.00	-

Continued on Next Page...

Table A.1 – Continued

Day #	Date	Start date	Start time	Stop date	Stop time	Missing data
69	2008.08.08	2008.08.08	15.00	2008.08.09	15.00	-
70	2008.08.09	2008.08.09	15.00	2008.08.10	15.00	-
71	2008.08.10	2008.08.10	15.00	2008.08.11	15.00	-
72	2008.08.11	2008.08.11	15.00	2008.08.12	15.00	-
73	2008.08.12	2008.08.12	15.00	2008.08.13	15.00	-
74	2008.08.13	2008.08.13	15.00	2008.08.14	15.00	-
75	2008.08.14	2008.08.14	15.00	2008.08.15	15.00	-
76	2008.08.15	2008.08.15	15.00	2008.08.16	01.19	Yes
77	2008.08.16	-	-	-	-	Yes
78	2008.08.17	2008.08.18	12.46	2008.08.18	15.00	Yes
79	2008.08.18	2008.08.18	15.00	2008.08.19	15.00	-
80	2008.08.19	2008.08.19	15.00	2008.08.20	15.00	-
81	2008.08.20	2008.08.20	15.00	2008.08.21	15.00	-
82	2008.08.21	2008.08.21	15.00	2008.08.22	15.00	-
83	2008.08.22	2008.08.22	15.00	2008.08.23	15.00	-
84	2008.08.23	2008.08.23	15.00	2008.08.24	15.00	-
85	2008.08.24	2008.08.24	15.00	2008.08.25	15.00	-
86	2008.08.25	2008.08.25	15.00	2008.08.26	15.00	-
87	2008.08.26	2008.08.26	15.00	2008.08.27	15.00	-
88	2008.08.27	2008.08.27	15.00	2008.08.28	15.00	-
89	2008.08.28	2008.08.28	15.00	2008.08.29	15.00	-
90	2008.08.29	2008.08.29	15.00	2008.08.30	15.00	-
91	2008.08.30	2008.08.30	15.00	2008.08.31	15.00	-
92	2008.08.31	2008.08.31	15.00	2008.09.01	15.00	Yes
93	2008.09.01	2008.09.01	15.00	2008.09.02	15.00	Yes
94	2008.09.02	2008.09.02	15.00	2008.09.03	15.00	Yes
95	2008.09.03	2008.09.03	15.00	2008.09.04	15.00	Yes
96	2008.09.04	2008.09.04	15.00	2008.09.05	15.00	Yes
97	2008.09.05	2008.09.05	15.00	2008.09.06	15.00	-
98	2008.09.06	2008.09.06	15.00	2008.09.07	15.00	-
99	2008.09.07	2008.09.07	15.00	2008.09.08	15.00	-
100	2008.09.08	2008.09.08	15.00	2008.09.09	15.00	-
101	2008.09.09	2008.09.09	15.00	2008.09.10	15.00	-
102	2008.09.10	2008.09.10	15.00	2008.09.11	15.00	-
103	2008.09.11	2008.09.11	15.00	2008.09.12	15.00	-
104	2008.09.12	2008.09.12	15.00	2008.09.13	15.00	-
105	2008.09.13	2008.09.13	15.00	2008.09.14	15.00	-
106	2008.09.14	2008.09.14	15.00	2008.09.15	15.00	-
107	2008.09.15	2008.09.15	15.00	2008.09.16	01.15	Yes
108	2008.09.16	2008.09.17	12.36	2008.09.17	15.00	Yes
109	2008.09.17	2008.09.17	15.00	2008.09.18	15.00	-
110	2008.09.18	2008.09.18	15.00	2008.09.19	15.00	-
111	2008.09.19	2008.09.19	15.00	2008.09.20	15.00	-
112	2008.09.20	2008.09.20	15.00	2008.09.21	15.00	-
113	2008.09.21	2008.09.21	15.00	2008.09.22	15.00	-
114	2008.09.22	2008.09.22	15.00	2008.09.23	15.00	-
115	2008.09.23	2008.09.23	15.00	2008.09.24	15.00	-
116	2008.09.24	2008.09.24	15.00	2008.09.25	15.00	-
117	2008.09.25	2008.09.25	15.00	2008.09.26	15.00	-
118	2008.09.26	2008.09.26	15.00	2008.09.27	15.00	-
119	2008.09.27	2008.09.27	15.00	2008.09.28	15.00	-
120	2008.09.28	2008.09.28	15.00	2008.09.29	15.00	-
121	2008.09.29	2008.09.29	15.00	2008.09.30	15.00	-
122	2008.09.30	2008.09.30	15.00	2008.10.01	15.00	-
123	2008.10.01	2008.10.01	15.00	2008.10.02	15.00	-
124	2008.10.02	2008.10.02	15.00	2008.10.03	15.00	-
125	2008.10.03	2008.10.03	15.00	2008.10.04	15.00	-
126	2008.10.04	2008.10.04	15.00	2008.10.05	15.00	-
127	2008.10.05	2008.10.05	15.00	2008.10.06	15.00	-
128	2008.10.06	2008.10.06	15.00	2008.10.07	15.00	-
129	2008.10.07	2008.10.07	15.00	2008.10.08	15.00	-
130	2008.10.08	2008.10.08	15.00	2008.10.09	15.00	-
131	2008.10.09	2008.10.09	15.00	2008.10.10	15.00	-
132	2008.10.10	2008.10.10	15.00	2008.10.11	15.00	-
133	2008.10.11	2008.10.11	15.00	2008.10.12	15.00	-
134	2008.10.12	2008.10.12	15.00	2008.10.13	15.00	-
135	2008.10.13	2008.10.13	15.00	2008.10.14	15.00	-
136	2008.10.14	2008.10.14	15.00	2008.10.15	15.00	-
137	2008.10.15	2008.10.15	15.00	2008.10.16	15.00	-
138	2008.10.16	2008.10.16	15.00	2008.10.17	15.00	-
139	2008.10.17	2008.10.17	15.00	2008.10.18	15.00	-
140	2008.10.18	2008.10.18	15.00	2008.10.19	15.00	-
141	2008.10.19	2008.10.19	15.00	2008.10.20	15.00	-
142	2008.10.20	2008.10.20	15.00	2008.10.21	15.00	Yes
143	2008.10.21	2008.10.21	15.00	2008.10.22	15.00	-
144	2008.10.22	2008.10.22	15.00	2008.10.23	15.00	-
145	2008.10.23	2008.10.23	15.00	2008.10.24	15.00	-
146	2008.10.24	2008.10.24	15.00	2008.10.25	15.00	Yes
147	2008.10.25	2008.10.25	15.00	2008.10.26	15.00	-
148	2008.10.26	2008.10.26	15.00	2008.10.27	15.00	-

Continued on Next Page...

Table A.1 – Continued

Day #	Date	Start date	Start time	Stop date	Stop time	Missing data
149	2008.10.27	2008.10.27	15.00	2008.10.28	15.00	-
150	2008.10.28	2008.10.28	15.00	2008.10.29	15.00	-
151	2008.10.29	2008.10.29	15.00	2008.10.30	15.00	-
152	2008.10.30	2008.10.30	15.00	2008.10.31	15.00	-
153	2008.10.31	2008.10.31	15.00	2008.11.01	15.00	-
154	2008.11.01	2008.11.01	15.00	2008.11.02	15.00	-
155	2008.11.02	2008.11.02	15.00	2008.11.03	15.00	-
156	2008.11.03	2008.11.03	15.00	2008.11.04	13.48	-
157	2008.11.04	2008.11.05	15.00	2008.11.05	15.00	Yes
158	2008.11.05	2008.11.05	15.00	2008.11.06	15.00	-
159	2008.11.06	2008.11.06	15.00	2008.11.07	15.00	-
160	2008.11.07	2008.11.07	15.00	2008.11.08	15.00	-
161	2008.11.08	2008.11.08	15.00	2008.11.09	15.00	-
162	2008.11.09	2008.11.09	15.00	2008.11.10	15.00	-
163	2008.11.10	2008.11.10	15.00	2008.11.11	15.00	-
164	2008.11.11	2008.11.11	15.00	2008.11.12	15.00	-
165	2008.11.12	2008.11.12	15.00	2008.11.13	15.00	-
166	2008.11.13	2008.11.13	15.00	2008.11.14	15.00	-
167	2008.11.14	2008.11.14	15.00	2008.11.15	15.00	-
168	2008.11.15	2008.11.15	15.00	2008.11.16	15.00	-
169	2008.11.16	2008.11.16	15.00	2008.11.17	15.00	-
170	2008.11.17	2008.11.17	15.00	2008.11.18	15.00	-
171	2008.11.18	2008.11.18	15.00	2008.11.19	15.00	-
172	2008.11.19	2008.11.19	15.00	2008.11.20	15.00	-
173	2008.11.20	2008.11.20	15.00	2008.11.21	15.00	-
174	2008.11.21	2008.11.21	15.00	2008.11.22	15.00	-
175	2008.11.22	2008.11.22	15.00	2008.11.23	15.00	-
176	2008.11.23	2008.11.23	15.00	2008.11.24	15.00	-
177	2008.11.24	2008.11.24	15.00	2008.11.25	15.00	-
178	2008.11.25	2008.11.25	15.00	2008.11.26	15.00	-
179	2008.11.26	2008.11.26	15.00	2008.11.27	15.00	-
180	2008.11.27	2008.11.27	15.00	2008.11.28	15.00	-
181	2008.11.28	2008.11.28	15.00	2008.11.29	15.00	-
182	2008.11.29	2008.11.29	15.00	2008.11.30	15.00	-
183	2008.11.30	2008.11.30	15.00	2008.12.01	15.00	-
184	2008.12.01	2008.12.01	15.00	2008.12.02	15.00	-
185	2008.12.02	2008.12.02	15.00	2008.12.03	15.00	-
186	2008.12.03	2008.12.03	15.00	2008.12.04	15.00	-
187	2008.12.04	2008.12.04	15.00	2008.12.05	15.00	-
188	2008.12.05	2008.12.05	15.00	2008.12.06	15.00	-
189	2008.12.06	2008.12.06	15.00	2008.12.07	15.00	-
190	2008.12.07	2008.12.07	15.00	2008.12.08	15.00	-
191	2008.12.08	2008.12.08	15.00	2008.12.09	15.00	-
192	2008.12.09	2008.12.09	15.00	2008.12.10	15.00	-
193	2008.12.10	2008.12.10	15.00	2008.12.11	15.00	-
194	2008.12.11	2008.12.11	15.00	2008.12.12	15.00	-
195	2008.12.12	2008.12.12	15.00	2008.12.13	15.00	Yes
196	2008.12.13	2008.12.13	15.00	2008.12.14	12.38	-
197	2008.12.14	-	-	-	-	Yes
198	2008.12.15	-	-	-	-	Yes
199	2008.12.16	-	-	-	-	Yes
200	2008.12.17	-	-	-	-	Yes
201	2008.12.18	-	-	-	-	Yes
202	2008.12.19	-	-	-	-	Yes
203	2008.12.20	-	-	-	-	Yes
204	2008.12.21	-	-	-	-	Yes
205	2008.12.22	-	-	-	-	Yes
206	2008.12.23	-	-	-	-	Yes
207	2008.12.24	-	-	-	-	Yes
208	2008.12.25	-	-	-	-	Yes
209	2008.12.26	-	-	-	-	Yes
210	2008.12.27	-	-	-	-	Yes
211	2008.12.28	-	-	-	-	Yes
212	2008.12.29	2008.12.30	07.58	2008.12.30	15.00	Yes
213	2008.12.30	2008.12.30	15.00	2008.12.31	15.00	-
214	2008.12.31	2008.12.31	15.00	2009.01.01	15.00	-
215	2009.01.01	2009.01.01	15.00	2009.01.02	15.00	-
216	2009.01.02	2009.01.02	15.00	2009.01.03	15.00	-
217	2009.01.03	2009.01.03	15.00	2009.01.04	15.00	-
218	2009.01.04	2009.01.04	15.00	2009.01.05	15.00	-
219	2009.01.05	2009.01.05	15.00	2009.01.06	15.00	-
220	2009.01.06	2009.01.06	15.00	2009.01.07	15.00	-
221	2009.01.07	2009.01.07	15.00	2009.01.08	15.00	-
222	2009.01.08	2009.01.08	15.00	2009.01.09	15.00	-
223	2009.01.09	2009.01.09	15.00	2009.01.10	15.00	-
224	2009.01.10	2009.01.10	15.00	2009.01.11	15.00	-
225	2009.01.11	2009.01.11	15.00	2009.01.12	15.00	-
226	2009.01.12	2009.01.12	15.00	2009.01.13	15.00	-
227	2009.01.13	2009.01.13	15.00	2009.01.14	15.00	-
228	2009.01.14	2009.01.14	15.00	2009.01.15	15.00	Yes

Continued on Next Page...

Table A.1 – Continued

Day #	Date	Start date	Start time	Stop date	Stop time	Missing data
229	2009.01.15	2009.01.15	15.00	2009.01.16	15.00	-
230	2009.01.16	2009.01.16	15.00	2009.01.17	15.00	-
231	2009.01.17	2009.01.17	15.00	2009.01.18	15.00	-
232	2009.01.18	2009.01.18	15.00	2009.01.19	15.00	-
233	2009.01.19	2009.01.19	15.00	2009.01.20	15.00	-
234	2009.01.20	2009.01.20	15.00	2009.01.21	15.00	-
235	2009.01.21	2009.01.21	15.00	2009.01.22	15.00	-
236	2009.01.22	2009.01.22	15.00	2009.01.23	15.00	-
237	2009.01.23	2009.01.23	15.00	2009.01.24	15.00	-
238	2009.01.24	2009.01.24	15.00	2009.01.25	15.00	-
239	2009.01.25	2009.01.25	15.00	2009.01.26	15.00	-
240	2009.01.26	2009.01.26	15.00	2009.01.27	15.00	-
241	2009.01.27	2009.01.27	15.00	2009.01.28	15.00	-
242	2009.01.28	2009.01.28	15.00	2009.01.29	15.00	-
243	2009.01.29	2009.01.29	15.00	2009.01.30	15.00	-
244	2009.01.30	2009.01.30	15.00	2009.01.31	15.00	-
245	2009.01.31	2009.01.31	15.00	2009.02.01	15.00	-
246	2009.02.01	2009.02.01	15.00	2009.02.02	15.00	-
247	2009.02.02	2009.02.02	15.00	2009.02.03	15.00	-
248	2009.02.03	2009.02.03	15.00	2009.02.04	15.00	-
249	2009.02.04	2009.02.04	15.00	2009.02.05	15.00	-
250	2009.02.05	2009.02.05	15.00	2009.02.06	15.00	-
251	2009.02.06	2009.02.06	15.00	2009.02.07	15.00	-
252	2009.02.07	2009.02.07	15.00	2009.02.08	15.00	-
253	2009.02.08	2009.02.08	15.00	2009.02.09	15.00	-
254	2009.02.09	2009.02.09	15.00	2009.02.10	15.00	-
255	2009.02.10	2009.02.10	15.00	2009.02.11	15.00	-
256	2009.02.11	2009.02.11	15.00	2009.02.12	15.00	-
257	2009.02.12	2009.02.12	15.00	2009.02.13	15.00	-
258	2009.02.13	2009.02.13	15.00	2009.02.14	15.00	-
259	2009.02.14	2009.02.14	15.00	2009.02.15	15.00	-
260	2009.02.15	2009.02.15	15.00	2009.02.16	15.00	-
261	2009.02.16	2009.02.16	15.00	2009.02.17	15.00	-
262	2009.02.17	2009.02.17	15.00	2009.02.18	15.00	-
263	2009.02.18	2009.02.18	15.00	2009.02.19	15.00	-
264	2009.02.19	2009.02.19	15.00	2009.02.20	15.00	-
265	2009.02.20	2009.02.20	15.00	2009.02.21	15.00	-
266	2009.02.21	2009.02.21	15.00	2009.02.22	15.00	-
267	2009.02.22	2009.02.22	15.00	2009.02.23	15.00	-
268	2009.02.23	2009.02.23	15.00	2009.02.24	15.00	-
269	2009.02.24	2009.02.24	15.00	2009.02.25	15.00	-
270	2009.02.25	2009.02.25	15.00	2009.02.26	15.00	-
271	2009.02.26	2009.02.26	15.00	2009.02.27	15.00	-
272	2009.02.27	2009.02.27	15.00	2009.02.28	15.00	-
273	2009.02.28	2009.02.28	15.00	2009.03.01	15.00	-
274	2009.03.01	2009.03.01	15.00	2009.03.02	15.00	-
275	2009.03.02	2009.03.02	15.00	2009.03.03	15.00	-
276	2009.03.03	2009.03.03	15.00	2009.03.04	15.00	-
277	2009.03.04	2009.03.04	15.00	2009.03.05	15.00	-
278	2009.03.05	2009.03.05	15.00	2009.03.06	15.00	-
279	2009.03.06	2009.03.06	15.00	2009.03.07	15.00	-
280	2009.03.07	2009.03.07	15.00	2009.03.08	15.00	-
281	2009.03.08	2009.03.08	15.00	2009.03.09	15.00	Yes
282	2009.03.09	2009.03.09	15.00	2009.03.10	15.00	-
283	2009.03.10	2009.03.10	15.00	2009.03.11	15.00	-
284	2009.03.11	2009.03.11	15.00	2009.03.12	15.00	-
285	2009.03.12	2009.03.12	15.00	2009.03.13	02.14	Yes
286	2009.03.13	-	-	-	-	Yes
287	2009.03.14	-	-	-	-	Yes
288	2009.03.15	2009.03.16	08.45	2009.03.16	15.00	Yes
289	2009.03.16	2009.03.16	15.00	2009.03.17	15.00	Yes
290	2009.03.17	2009.03.17	15.00	2009.03.18	15.00	-
291	2009.03.18	2009.03.18	15.00	2009.03.19	15.00	-
292	2009.03.19	2009.03.19	15.00	2009.03.20	15.00	-
293	2009.03.20	2009.03.20	15.00	2009.03.21	15.00	-
294	2009.03.21	2009.03.21	15.00	2009.03.22	15.00	-
295	2009.03.22	2009.03.22	15.00	2009.03.23	15.00	-
296	2009.03.23	2009.03.23	15.00	2009.03.24	15.00	-
297	2009.03.24	2009.03.24	15.00	2009.03.25	15.00	-
298	2009.03.25	2009.03.25	15.00	2009.03.26	15.00	-
299	2009.03.26	2009.03.26	15.00	2009.03.27	15.00	-
300	2009.03.27	2009.03.27	15.00	2009.03.28	15.00	-
301	2009.03.28	2009.03.28	15.00	2009.03.29	15.00	-
302	2009.03.29	2009.03.29	15.00	2009.03.30	15.00	-
303	2009.03.30	2009.03.30	15.00	2009.03.31	15.00	-
304	2009.03.31	2009.03.31	15.00	2009.04.01	15.00	-
305	2009.04.01	2009.04.01	15.00	2009.04.02	15.00	-
306	2009.04.02	2009.04.02	15.00	2009.04.03	15.00	-
307	2009.04.03	2009.04.03	15.00	2009.04.04	15.00	-
308	2009.04.04	2009.04.04	15.00	2009.04.05	15.00	-

Continued on Next Page...

Table A.1 – Continued

Day #	Date	Start date	Start time	Stop date	Stop time	Missing data
309	2009.04.05	2009.04.05	15.00	2009.04.06	15.00	-
310	2009.04.06	2009.04.06	15.00	2009.04.07	15.00	-
311	2009.04.07	2009.04.07	15.00	2009.04.08	15.00	-
312	2009.04.08	2009.04.08	15.00	2009.04.09	15.00	-
313	2009.04.09	2009.04.09	15.00	2009.04.10	15.00	-
314	2009.04.10	2009.04.10	15.00	2009.04.11	15.00	-
315	2009.04.11	2009.04.11	15.00	2009.04.12	15.00	-
316	2009.04.12	2009.04.12	15.00	2009.04.13	15.00	-
317	2009.04.13	2009.04.13	15.00	2009.04.14	15.00	-
318	2009.04.14	2009.04.14	15.00	2009.04.15	15.00	-
319	2009.04.15	2009.04.15	15.00	2009.04.16	15.00	-
320	2009.04.16	2009.04.16	15.00	2009.04.17	15.00	-
321	2009.04.17	2009.04.17	15.00	2009.04.18	15.00	-
322	2009.04.18	2009.04.18	15.00	2009.04.19	15.00	-
323	2009.04.19	2009.04.19	15.00	2009.04.20	01.17	Yes
324	2009.04.20	-	-	-	-	Yes
325	2009.04.21	2009.04.21	16.29	2009.04.22	15.00	Yes
326	2009.04.22	2009.04.22	15.00	2009.04.23	15.00	-
327	2009.04.23	2009.04.23	15.00	2009.04.24	15.00	-
328	2009.04.24	2009.04.24	15.00	2009.04.25	15.00	Yes
329	2009.04.25	2009.04.25	15.00	2009.04.26	15.00	-
330	2009.04.26	2009.04.26	15.00	2009.04.27	15.00	-
331	2009.04.27	2009.04.27	15.00	2009.04.28	15.00	-
332	2009.04.28	2009.04.28	15.00	2009.04.29	15.00	-
333	2009.04.29	2009.04.29	15.00	2009.04.30	15.00	-
334	2009.04.30	2009.04.30	15.00	2009.05.01	15.00	-
335	2009.05.01	2009.05.01	15.00	2009.05.02	15.00	-
336	2009.05.02	2009.05.02	15.00	2009.05.03	15.00	-
337	2009.05.03	2009.05.03	15.00	2009.05.04	15.00	-
338	2009.05.04	2009.05.04	15.00	2009.05.05	15.00	-
339	2009.05.05	2009.05.05	15.00	2009.05.06	15.00	-
340	2009.05.06	2009.05.06	15.00	2009.05.07	15.00	-
341	2009.05.07	2009.05.07	15.00	2009.05.08	15.00	-
342	2009.05.08	2009.05.08	15.00	2009.05.09	15.00	-
343	2009.05.09	2009.05.09	15.00	2009.05.10	15.00	-
344	2009.05.10	2009.05.10	15.00	2009.05.11	15.00	-
345	2009.05.11	2009.05.11	15.00	2009.05.12	15.00	-
346	2009.05.12	2009.05.12	15.00	2009.05.13	15.00	-
347	2009.05.13	2009.05.13	15.00	2009.05.14	15.00	-
348	2009.05.14	2009.05.14	15.00	2009.05.15	15.00	-
349	2009.05.15	2009.05.15	15.00	2009.05.16	15.00	-
350	2009.05.16	2009.05.16	15.00	2009.05.17	15.00	-
351	2009.05.17	2009.05.17	15.00	2009.05.18	15.00	-
352	2009.05.18	2009.05.18	15.00	2009.05.19	15.00	-
353	2009.05.19	2009.05.19	15.00	2009.05.20	15.00	-
354	2009.05.20	2009.05.20	15.00	2009.05.21	15.00	-
355	2009.05.21	2009.05.21	15.00	2009.05.22	15.00	-
356	2009.05.22	2009.05.22	15.00	2009.05.23	15.00	-
357	2009.05.23	2009.05.23	15.00	2009.05.24	15.00	-
358	2009.05.24	2009.05.24	15.00	2009.05.25	15.00	-
359	2009.05.25	2009.05.25	15.00	2009.05.26	15.00	-
360	2009.05.26	2009.05.26	15.00	2009.05.27	15.00	-
361	2009.05.27	2009.05.27	15.00	2009.05.28	15.00	-
362	2009.05.28	2009.05.28	15.00	2009.05.29	15.00	-
363	2009.05.29	2009.05.29	15.00	2009.05.30	15.00	-
364	2009.05.30	2009.05.30	15.00	2009.05.31	15.00	-
365	2009.05.31	2009.05.31	15.00	2009.06.01	15.00	-
366	2009.06.01	2009.06.01	15.00	2009.06.02	15.00	-
367	2009.06.02	2009.06.02	15.00	2009.06.03	15.00	-
368	2009.06.03	2009.06.03	15.00	2009.06.04	15.00	-
369	2009.06.04	2009.06.04	15.00	2009.06.05	15.00	-
370	2009.06.05	2009.06.05	15.00	2009.06.06	15.00	-
371	2009.06.06	2009.06.06	15.00	2009.06.07	15.00	-
372	2009.06.07	2009.06.07	15.00	2009.06.08	15.00	-
373	2009.06.08	2009.06.08	15.00	2009.06.09	15.00	-
374	2009.06.09	2009.06.09	15.00	2009.06.10	15.00	-
375	2009.06.10	2009.06.10	15.00	2009.06.11	15.00	-
376	2009.06.11	2009.06.11	15.00	2009.06.12	01.16	Yes
377	2009.06.12	-	-	-	-	Yes
378	2009.06.13	-	-	-	-	Yes
379	2009.06.14	2009.06.15	08.17	2009.06.15	15.00	Yes
380	2009.06.15	2009.06.15	15.00	2009.06.16	15.00	-
381	2009.06.16	2009.06.16	15.00	2009.06.17	15.00	-
382	2009.06.17	2009.06.17	15.00	2009.06.18	15.00	-
383	2009.06.18	2009.06.18	15.00	2009.06.19	15.00	-
384	2009.06.19	2009.06.19	15.00	2009.06.20	15.00	-
385	2009.06.20	2009.06.20	15.00	2009.06.21	15.00	-
386	2009.06.21	2009.06.21	15.00	2009.06.22	15.00	-
387	2009.06.22	2009.06.22	15.00	2009.06.23	15.00	-
388	2009.06.23	2009.06.23	15.00	2009.06.24	15.00	-

Continued on Next Page...

Table A.1 – Continued

Day #	Date	Start date	Start time	Stop date	Stop time	Missing data
389	2009.06.24	2009.06.24	15.00	2009.06.25	15.00	-
390	2009.06.25	2009.06.25	15.00	2009.06.26	15.00	-
391	2009.06.26	2009.06.26	15.00	2009.06.27	15.00	-
392	2009.06.27	2009.06.27	15.00	2009.06.28	15.00	-
393	2009.06.28	2009.06.28	15.00	2009.06.29	15.00	-
394	2009.06.29	2009.06.29	15.00	2009.06.30	01.59	Yes
395	2009.06.30	-	-	-	-	Yes
396	2009.07.01	2009.07.02	08.24	2009.07.02	15.00	Yes
397	2009.07.02	2009.07.02	15.00	2009.07.03	15.00	-
398	2009.07.03	2009.07.03	15.00	2009.07.04	15.00	-
399	2009.07.04	2009.07.04	15.00	2009.07.05	15.00	-
400	2009.07.05	2009.07.05	15.00	2009.07.06	15.00	-
401	2009.07.06	2009.07.06	15.00	2009.07.07	15.00	-
402	2009.07.07	2009.07.07	15.00	2009.07.08	12.31	-
403	2009.07.08	-	-	-	-	Yes

A.2.2 Raw data graphs

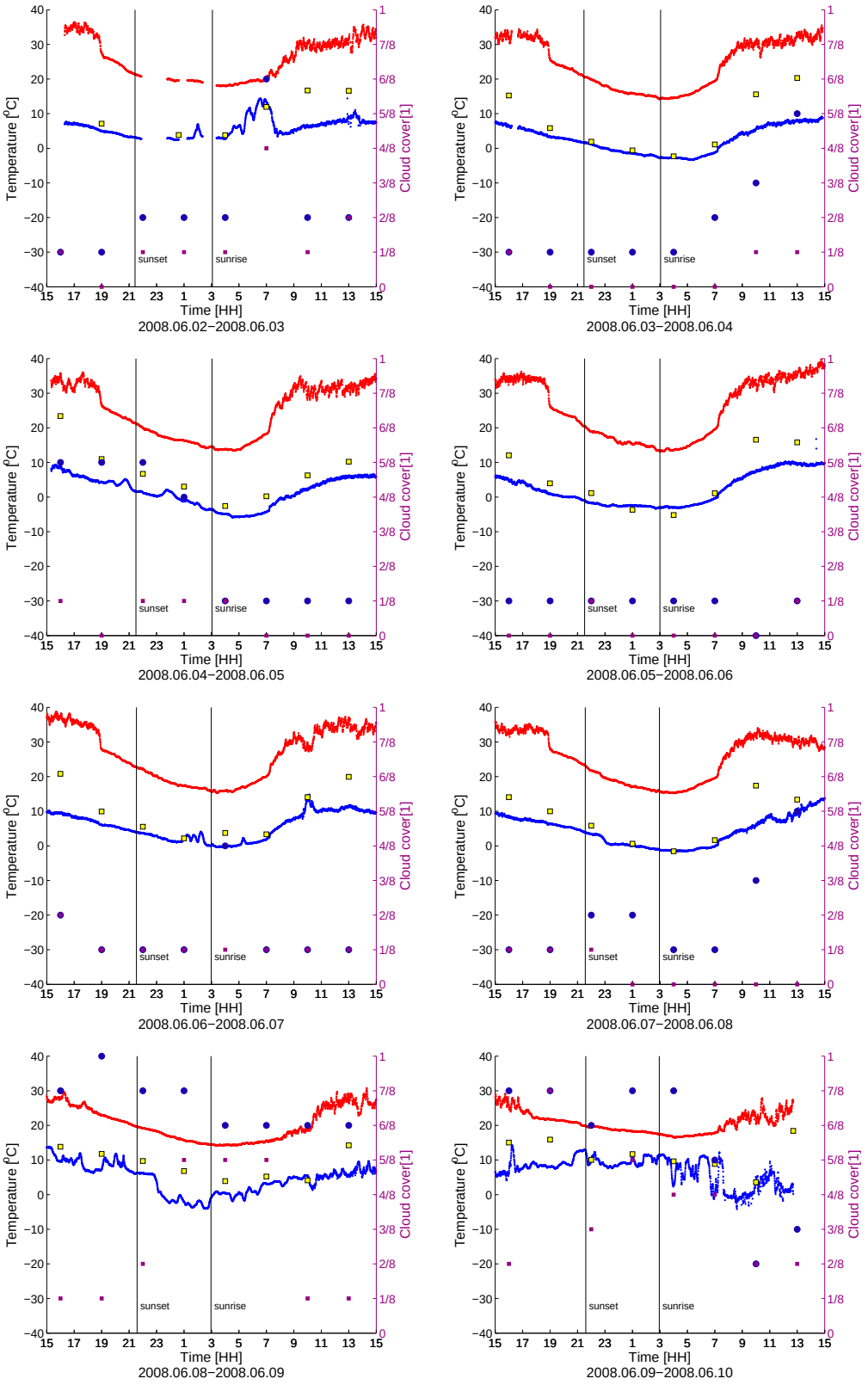

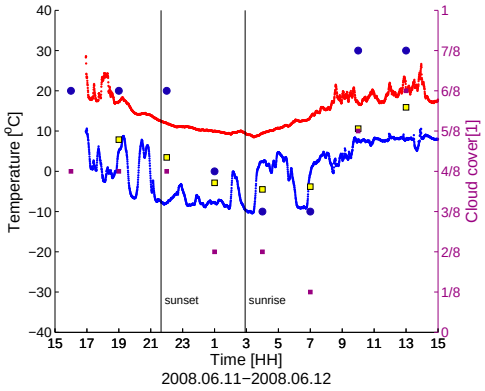

2008.06.11–2008.06.12

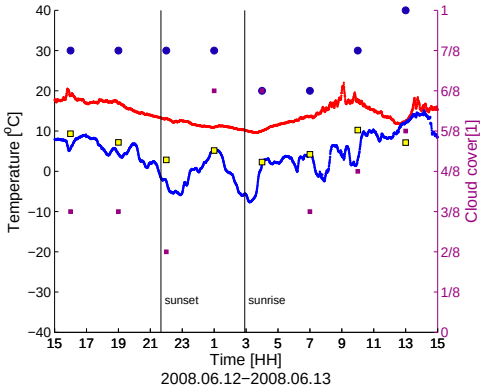

2008.06.12–2008.06.13

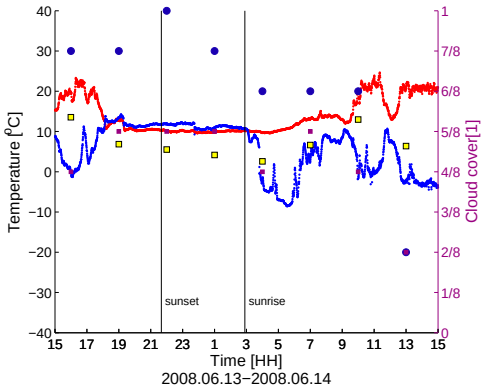

2008.06.13–2008.06.14

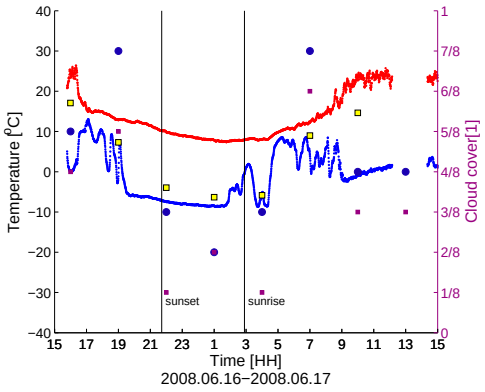

2008.06.16–2008.06.17

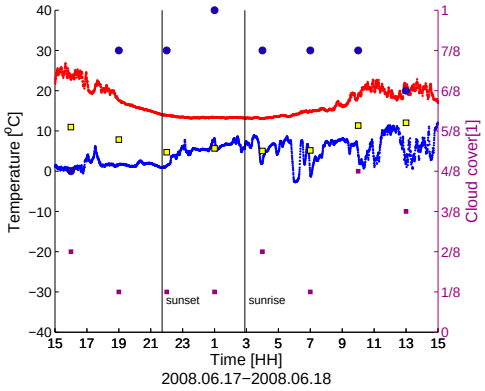

2008.06.17–2008.06.18

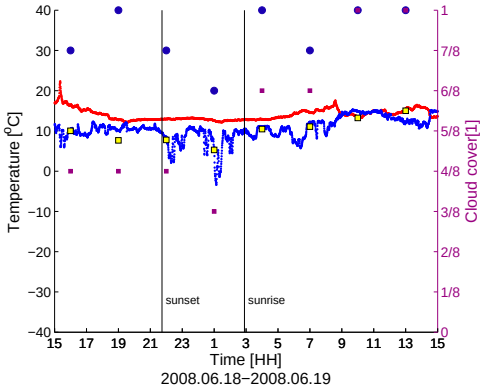

2008.06.18–2008.06.19

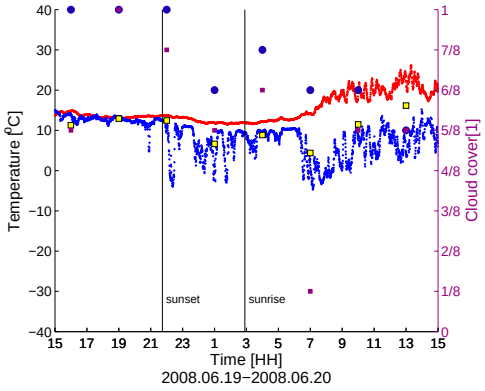

2008.06.19–2008.06.20

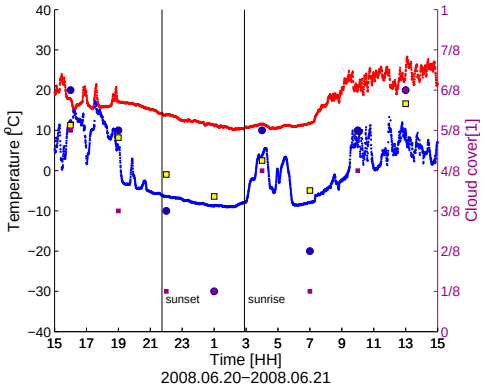

2008.06.20–2008.06.21

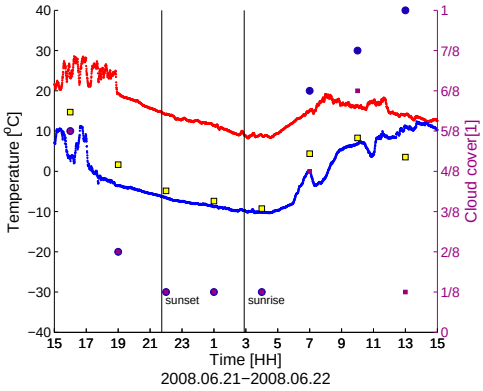
Temperature [°C]
Cloud cover[1]
Time [HH]
sunset
sunrise
2008.06.21−2008.06.22

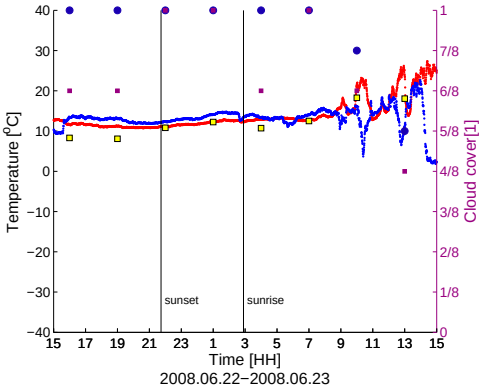
Temperature [°C]
Cloud cover[1]
Time [HH]
sunset
sunrise
2008.06.22−2008.06.23

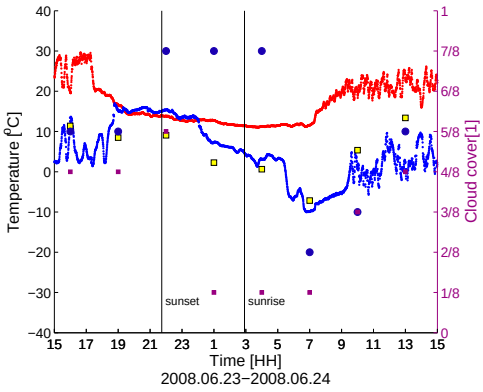
Temperature [°C]
Cloud cover[1]
Time [HH]
sunset
sunrise
2008.06.23−2008.06.24

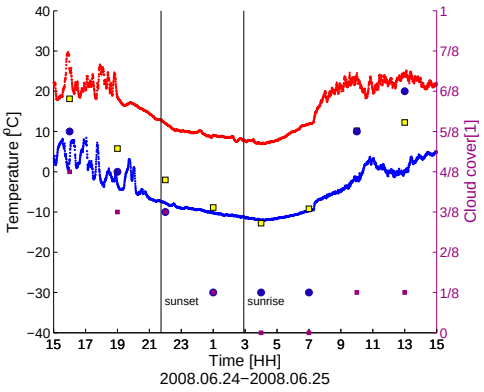
Temperature [°C]
Cloud cover[1]
Time [HH]
sunset
sunrise
2008.06.24−2008.06.25

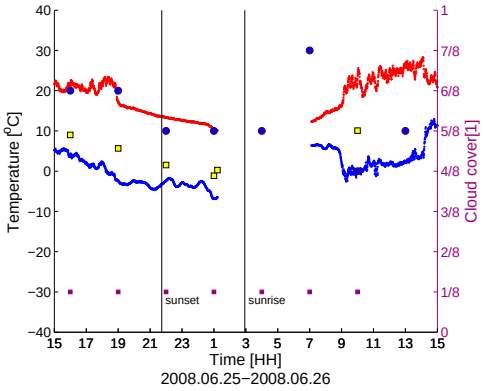
Temperature [°C]
Cloud cover[1]
Time [HH]
sunset
sunrise
2008.06.25−2008.06.26

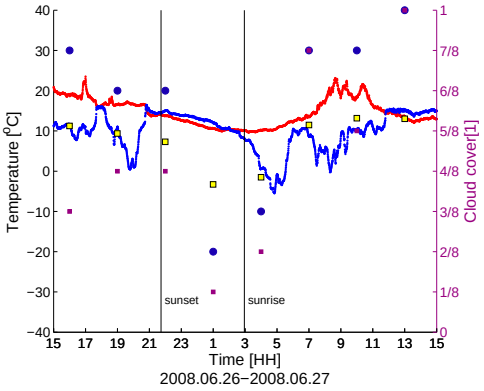
Temperature [°C]
Cloud cover[1]
Time [HH]
sunset
sunrise
2008.06.26−2008.06.27

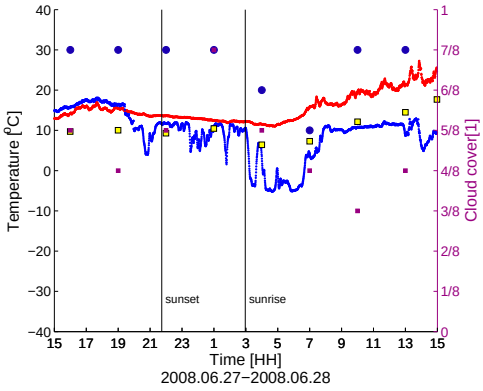
Temperature [°C]
Cloud cover[1]
Time [HH]
sunset
sunrise
2008.06.27−2008.06.28

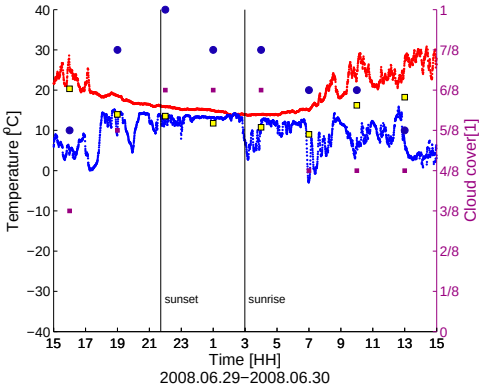
Temperature [°C]
Cloud cover[1]
Time [HH]
sunset
sunrise
2008.06.29−2008.06.30

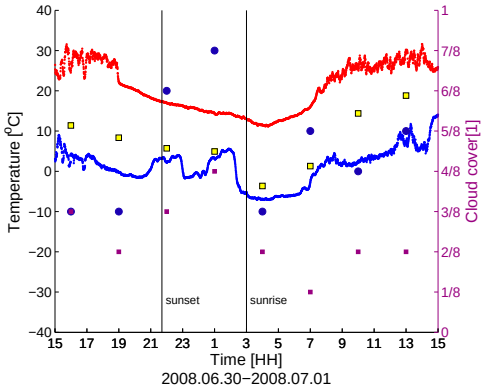

2008.06.30−2008.07.01

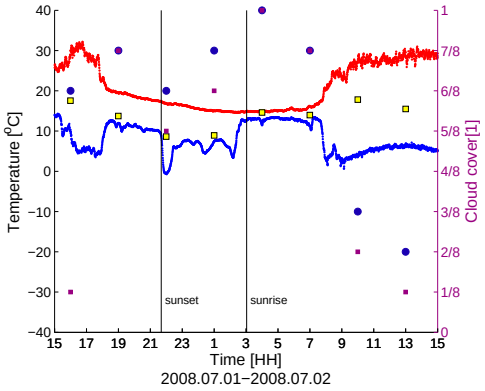

2008.07.01−2008.07.02

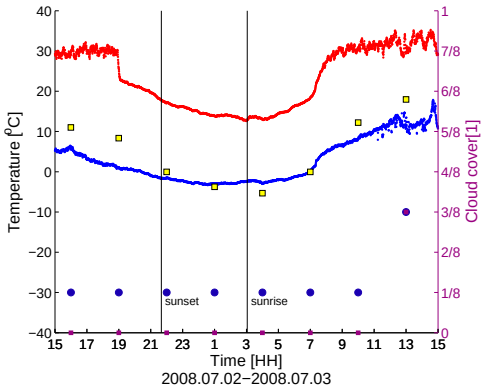

2008.07.02−2008.07.03

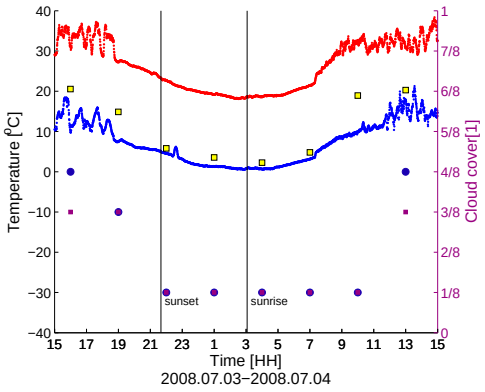

2008.07.03−2008.07.04

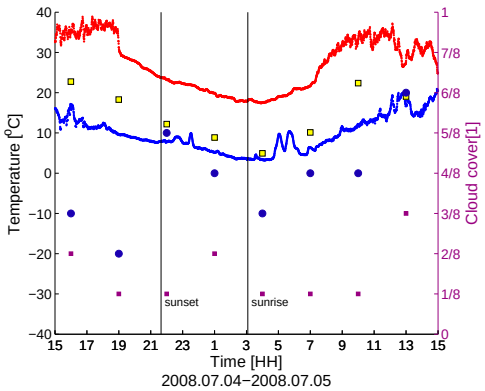

2008.07.04−2008.07.05

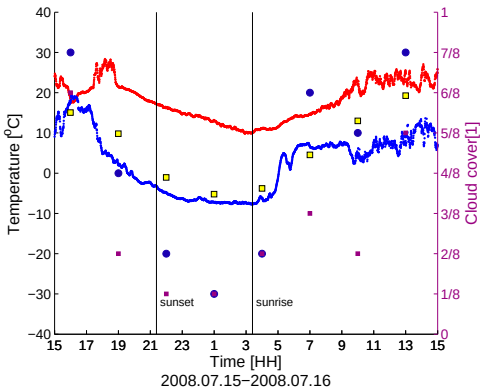

2008.07.15−2008.07.16

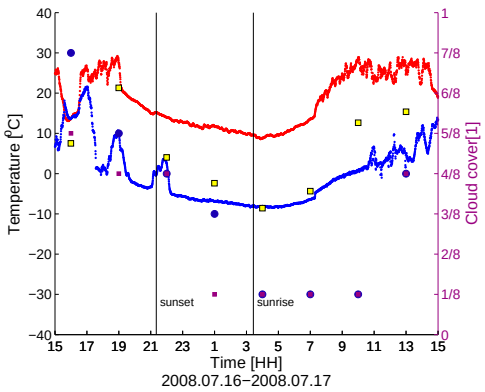

2008.07.16−2008.07.17

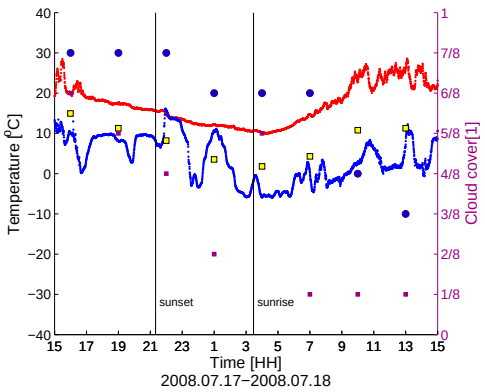

2008.07.17−2008.07.18

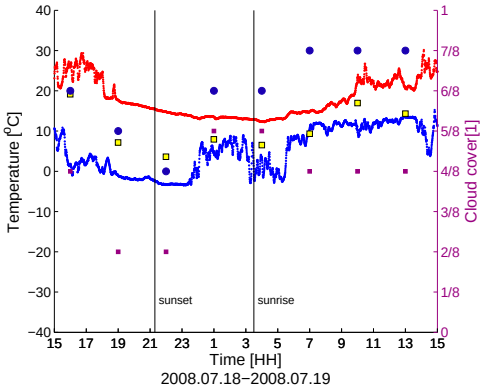

2008.07.18–2008.07.19

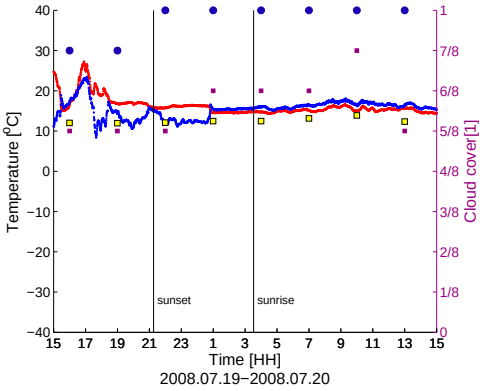

2008.07.19–2008.07.20

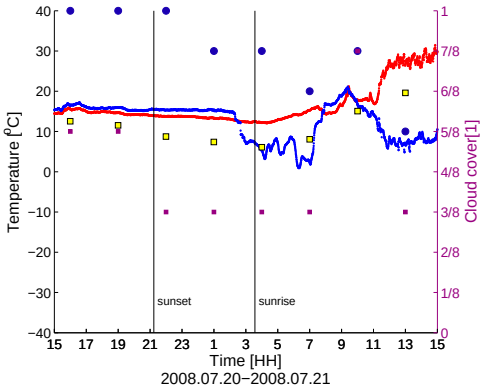

2008.07.20–2008.07.21

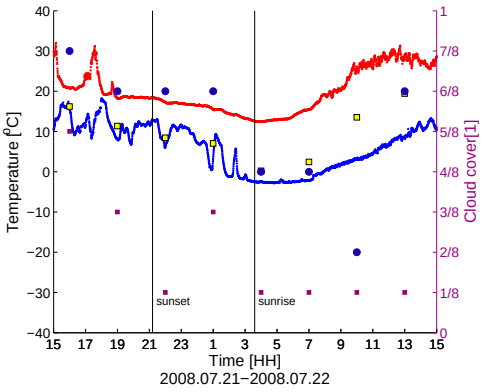

2008.07.21–2008.07.22

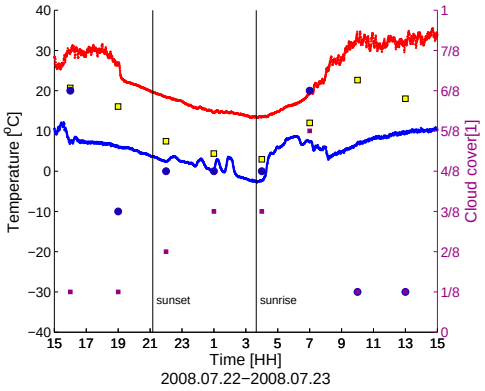

2008.07.22–2008.07.23

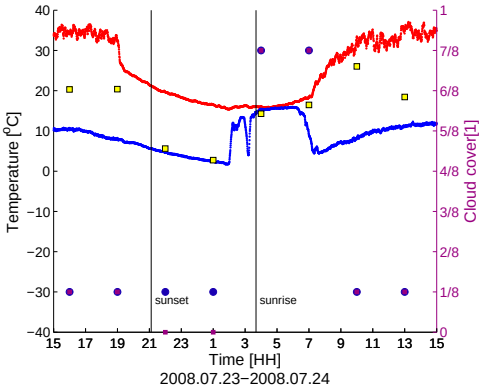

2008.07.23–2008.07.24

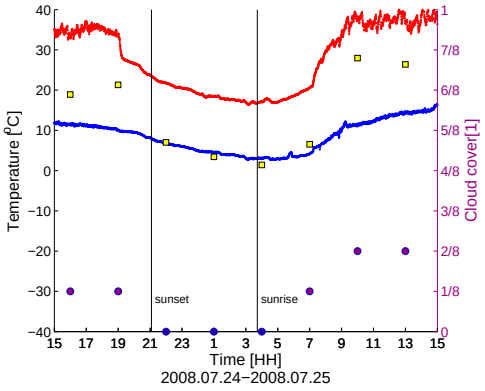

2008.07.24–2008.07.25

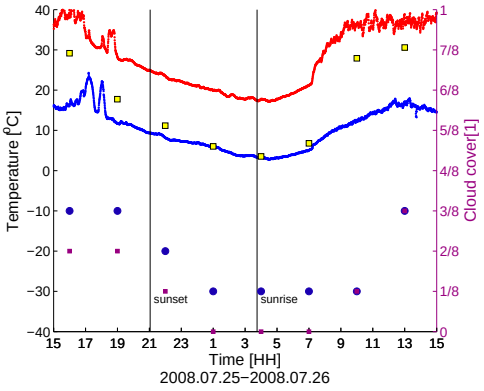

2008.07.25–2008.07.26

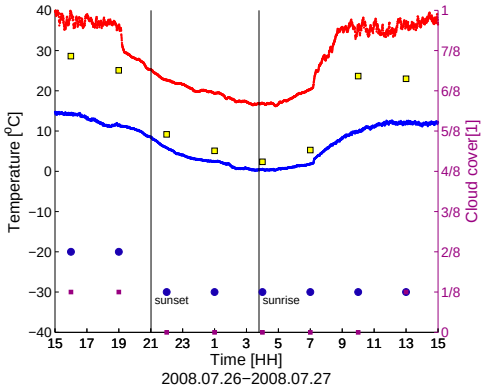
Temperature [°C]
Cloud cover[1]
Time [HH]
sunset
sunrise
2008.07.26−2008.07.27

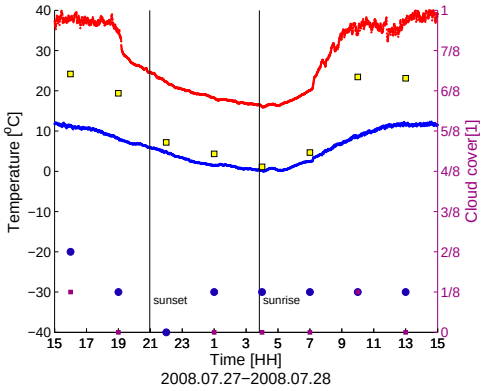
Temperature [°C]
Cloud cover[1]
Time [HH]
sunset
sunrise
2008.07.27−2008.07.28

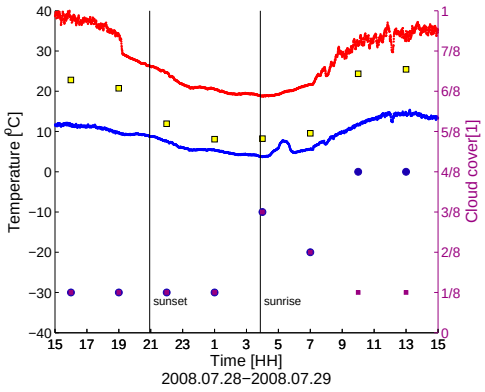
Temperature [°C]
Cloud cover[1]
Time [HH]
sunset
sunrise
2008.07.28−2008.07.29

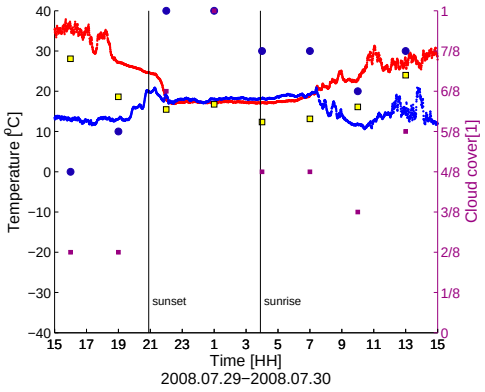
Temperature [°C]
Cloud cover[1]
Time [HH]
sunset
sunrise
2008.07.29−2008.07.30

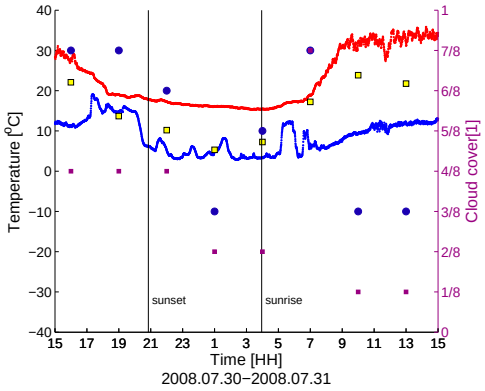
Temperature [°C]
Cloud cover[1]
Time [HH]
sunset
sunrise
2008.07.30−2008.07.31

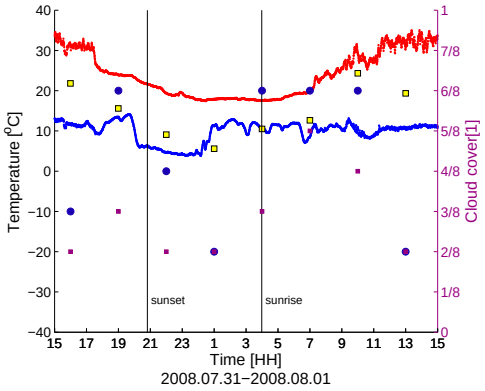
Temperature [°C]
Cloud cover[1]
Time [HH]
sunset
sunrise
2008.07.31−2008.08.01

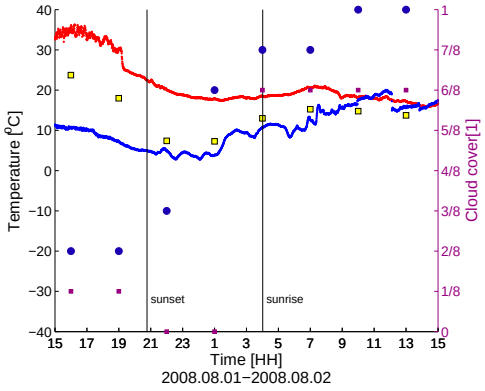
Temperature [°C]
Cloud cover[1]
Time [HH]
sunset
sunrise
2008.08.01−2008.08.02

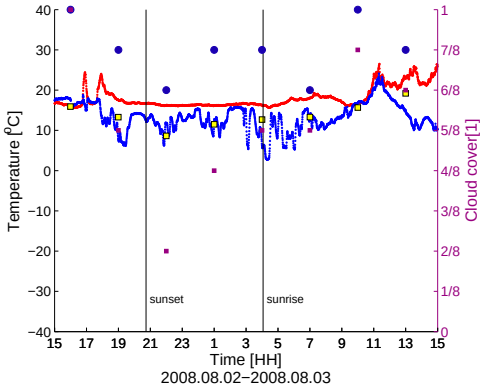
Temperature [°C]
Cloud cover[1]
Time [HH]
sunset
sunrise
2008.08.02−2008.08.03

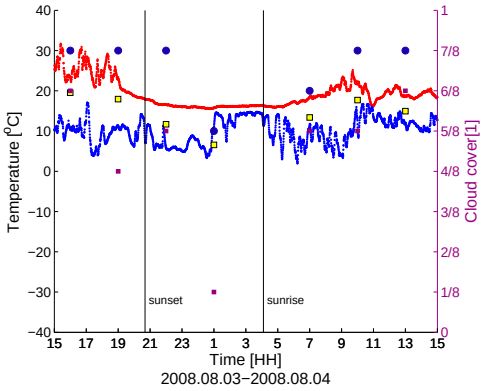
Temperature [°C]
Cloud cover[1]
Time [HH]
sunset
sunrise
2008.08.03−2008.08.04

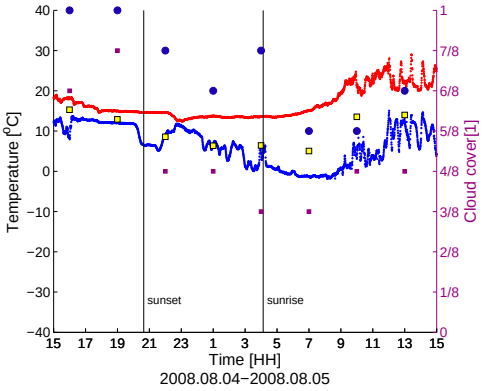
Temperature [°C]
Cloud cover[1]
Time [HH]
sunset
sunrise
2008.08.04−2008.08.05

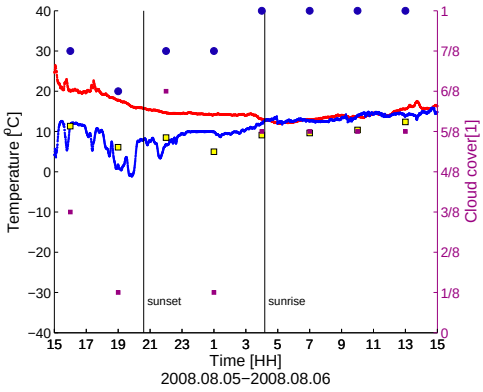
Temperature [°C]
Cloud cover[1]
Time [HH]
sunset
sunrise
2008.08.05−2008.08.06

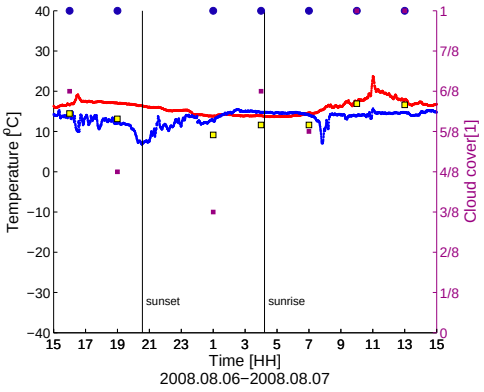
Temperature [°C]
Cloud cover[1]
Time [HH]
sunset
sunrise
2008.08.06−2008.08.07

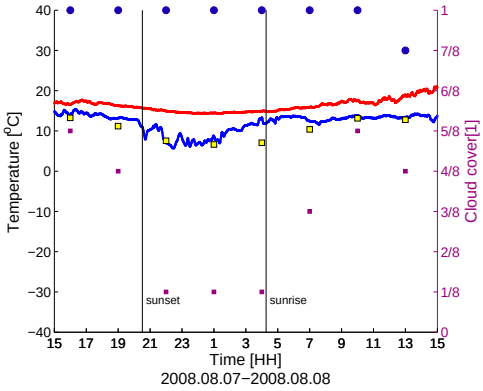
Temperature [°C]
Cloud cover[1]
Time [HH]
sunset
sunrise
2008.08.07−2008.08.08

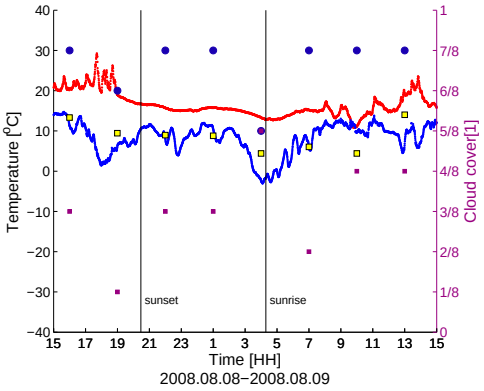
Temperature [°C]
Cloud cover[1]
Time [HH]
sunset
sunrise
2008.08.08−2008.08.09

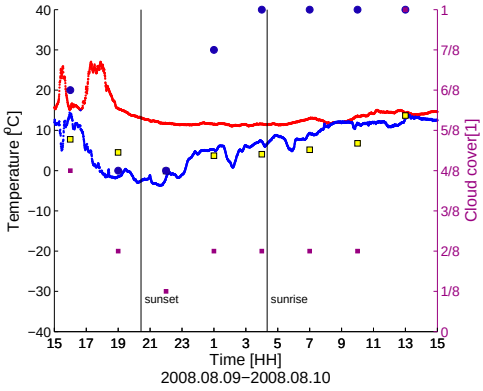
Temperature [°C]
Cloud cover[1]
Time [HH]
sunset
sunrise
2008.08.09−2008.08.10

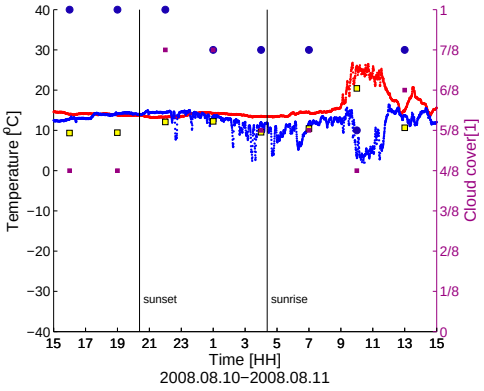
Temperature [°C]
Cloud cover[1]
Time [HH]
sunset
sunrise
2008.08.10−2008.08.11

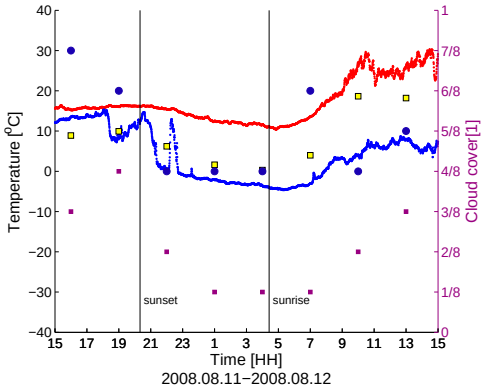

2008.08.11–2008.08.12

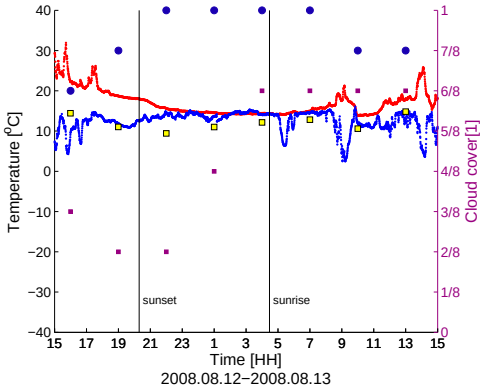

2008.08.12–2008.08.13

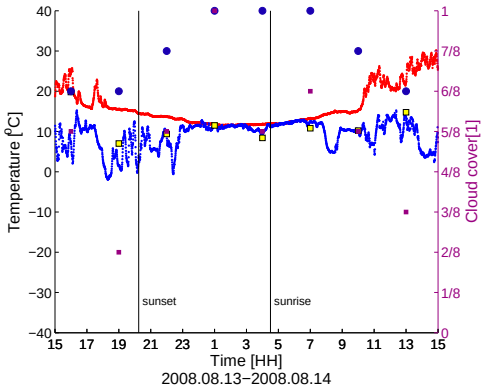

2008.08.13–2008.08.14

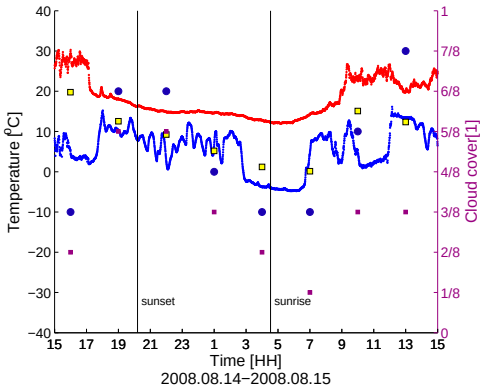

2008.08.14–2008.08.15

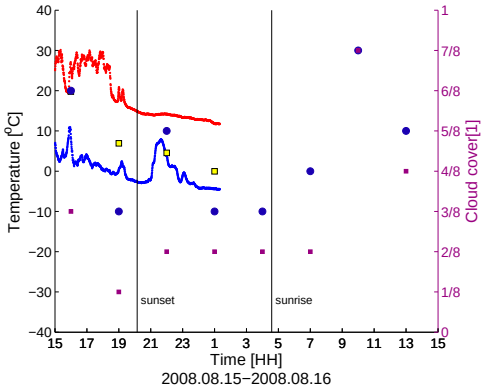

2008.08.15–2008.08.16

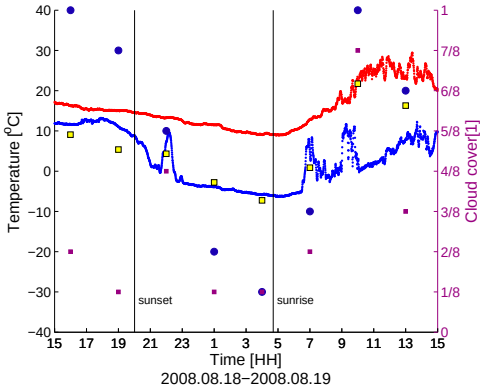

2008.08.18–2008.08.19

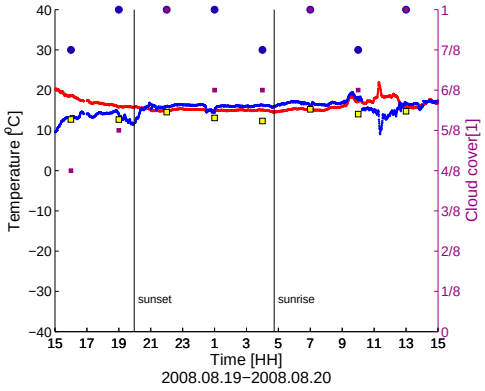

2008.08.19–2008.08.20

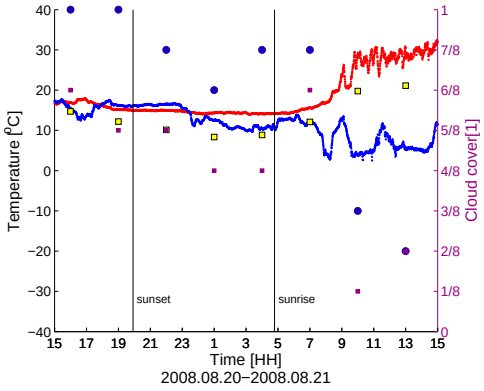

2008.08.20–2008.08.21

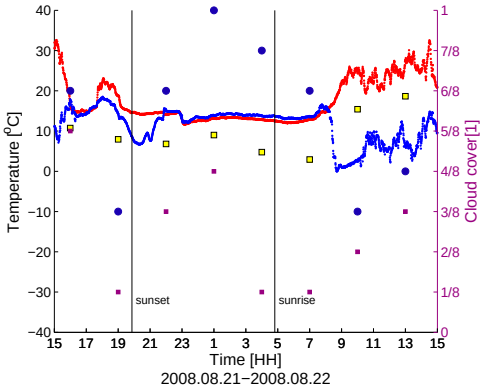

2008.08.21–2008.08.22

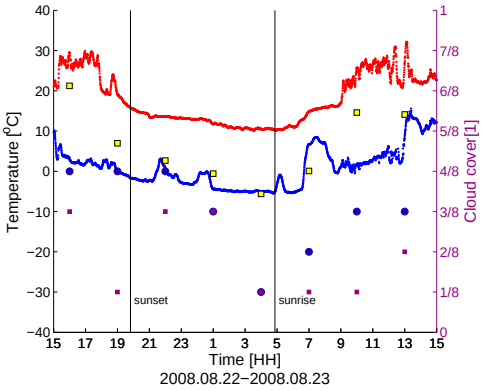

2008.08.22–2008.08.23

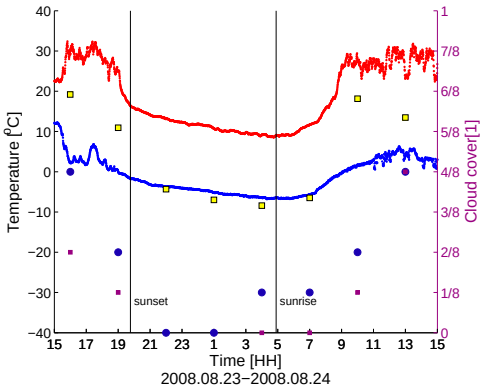

2008.08.23–2008.08.24

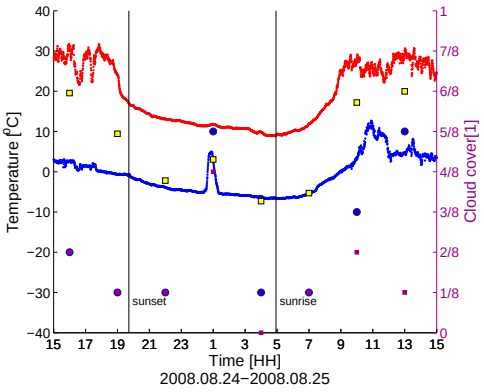

2008.08.24–2008.08.25

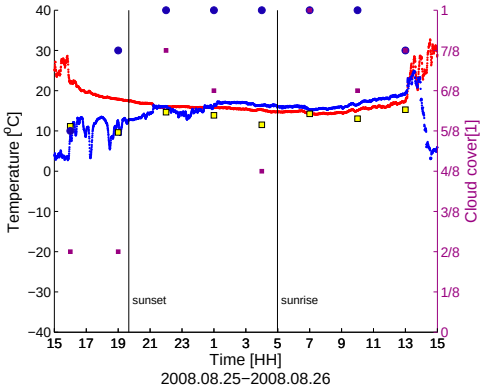

2008.08.25–2008.08.26

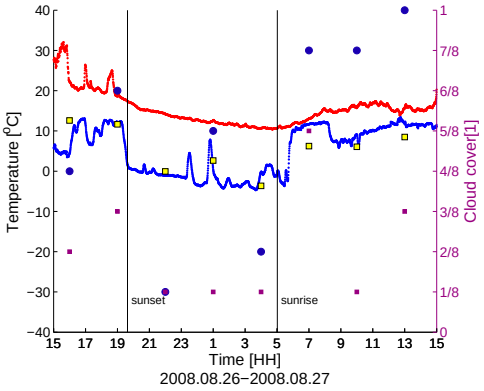

2008.08.26–2008.08.27

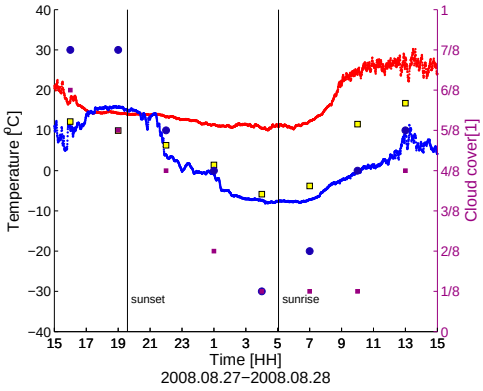

2008.08.27–2008.08.28

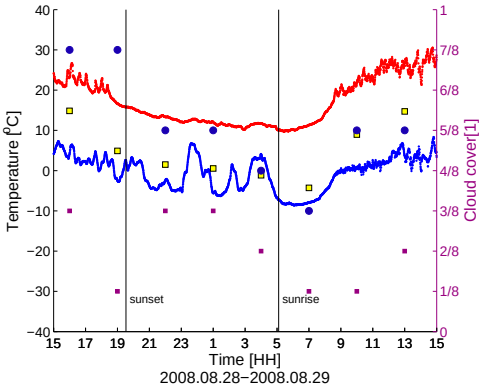

2008.08.28–2008.08.29

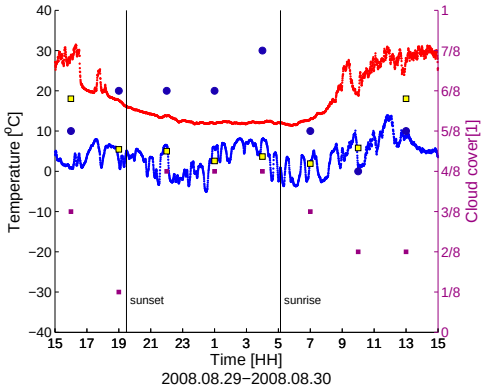

2008.08.29–2008.08.30

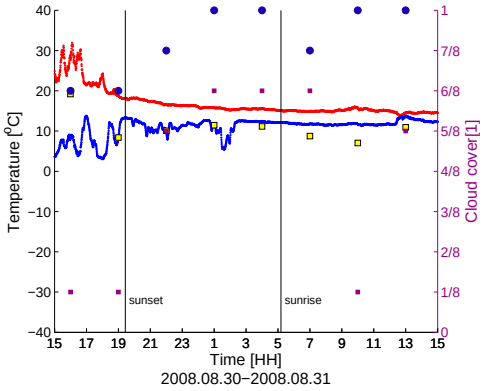

2008.08.30–2008.08.31

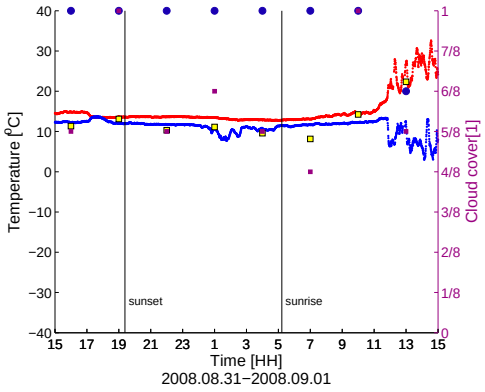

2008.08.31–2008.09.01

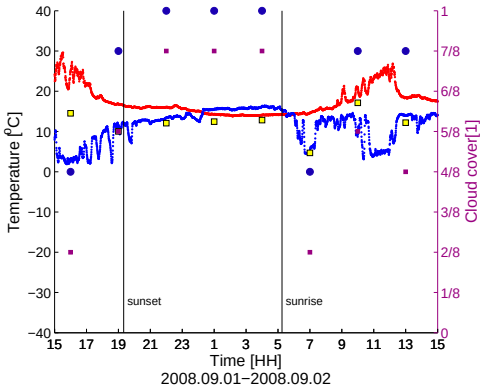

2008.09.01–2008.09.02

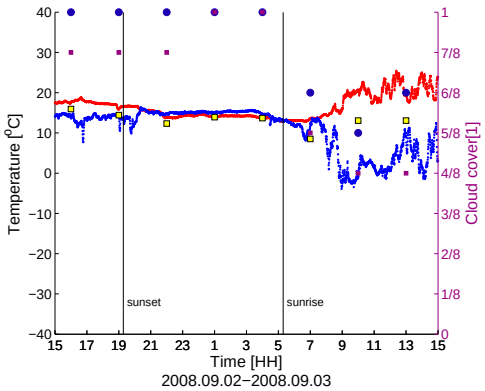

2008.09.02–2008.09.03

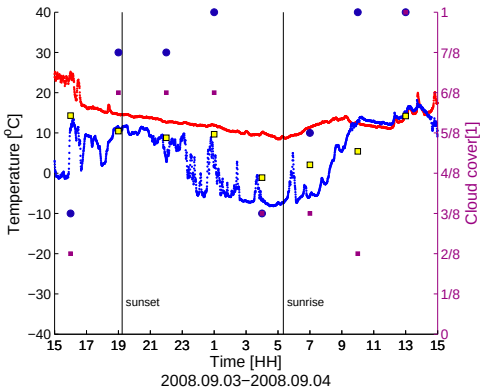

2008.09.03–2008.09.04

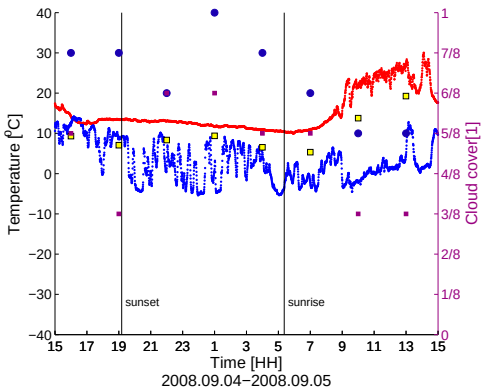

2008.09.04–2008.09.05

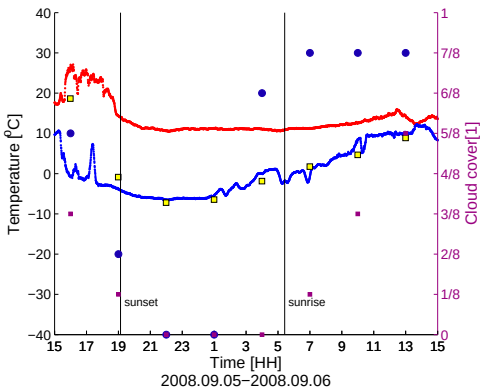

2008.09.05–2008.09.06

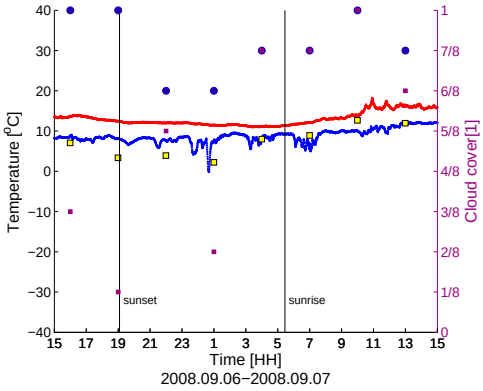

2008.09.06–2008.09.07

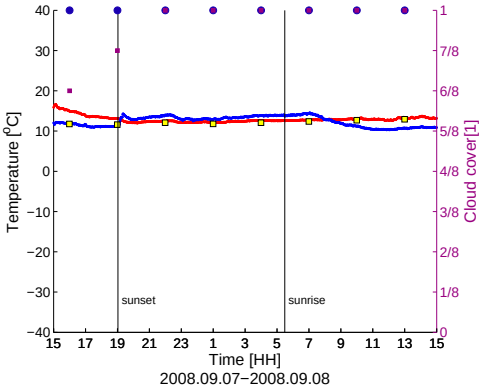

2008.09.07–2008.09.08

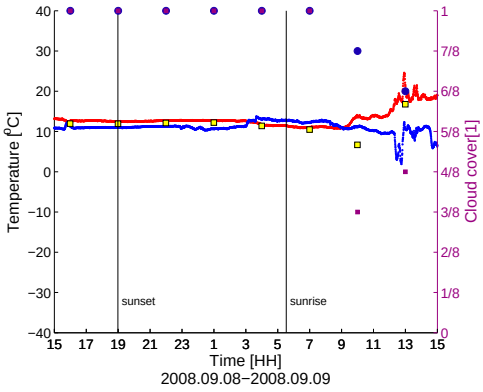

2008.09.08–2008.09.09

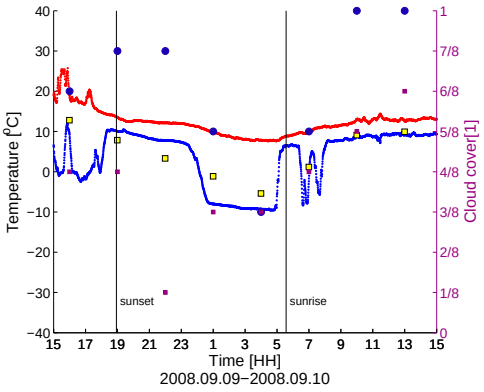

2008.09.09–2008.09.10

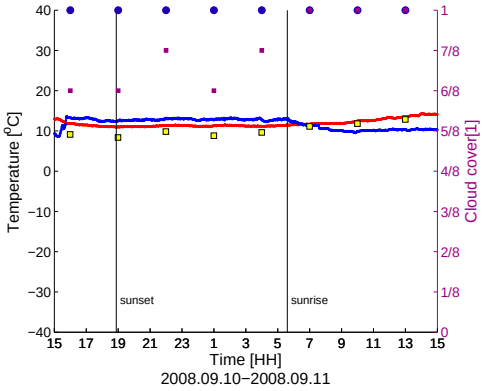

2008.09.10–2008.09.11

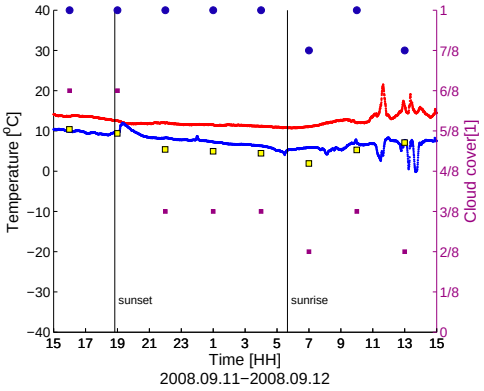

2008.09.11–2008.09.12

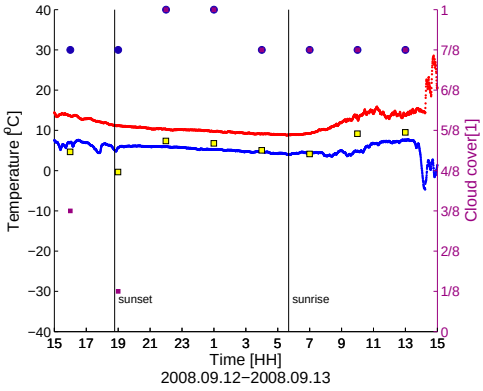

2008.09.12–2008.09.13

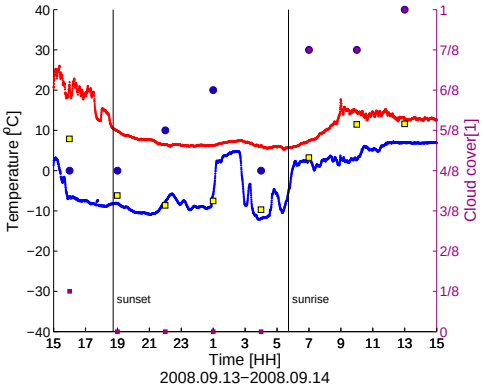

2008.09.13–2008.09.14

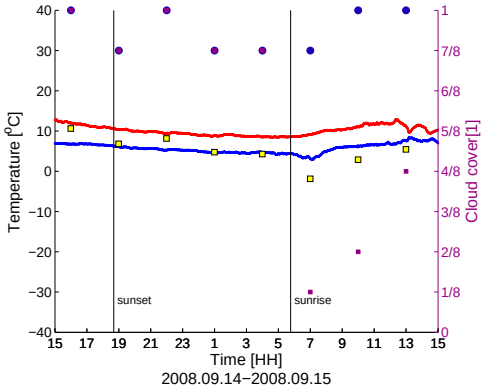

2008.09.14–2008.09.15

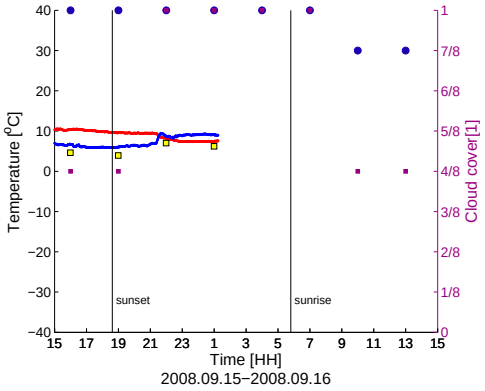

2008.09.15–2008.09.16

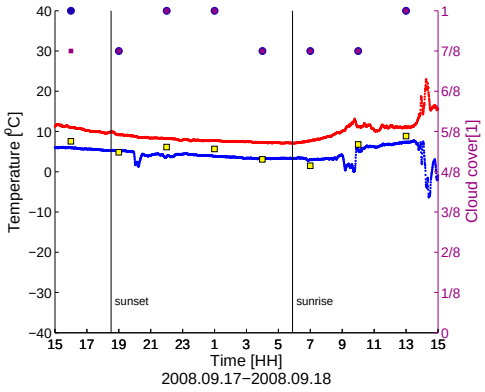

2008.09.17–2008.09.18

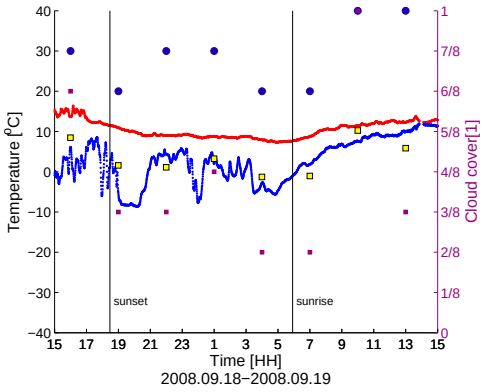

2008.09.18–2008.09.19

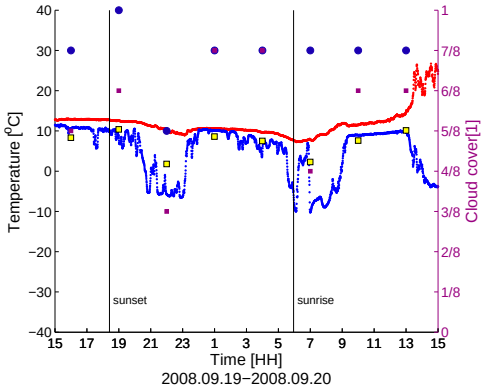

2008.09.19–2008.09.20

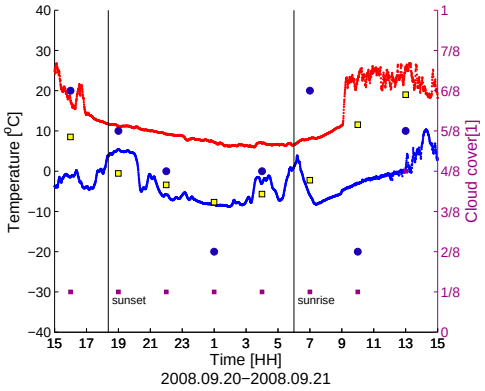

2008.09.20–2008.09.21

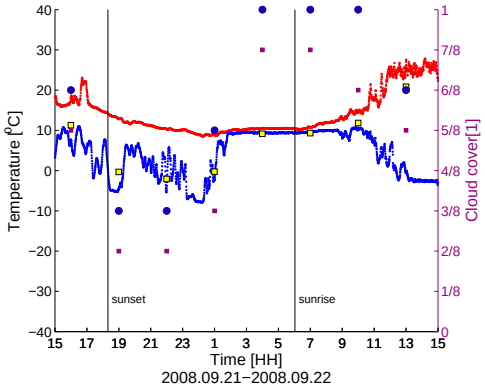

2008.09.21–2008.09.22

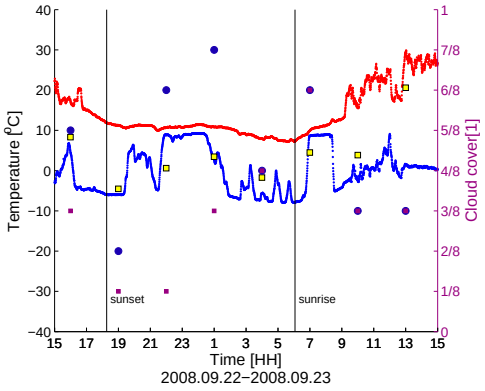

2008.09.22–2008.09.23

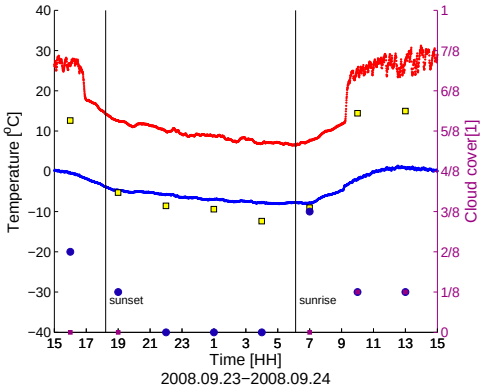
Temperature [°C]
Cloud cover[1]
Time [HH]
sunset
sunrise
2008.09.23–2008.09.24

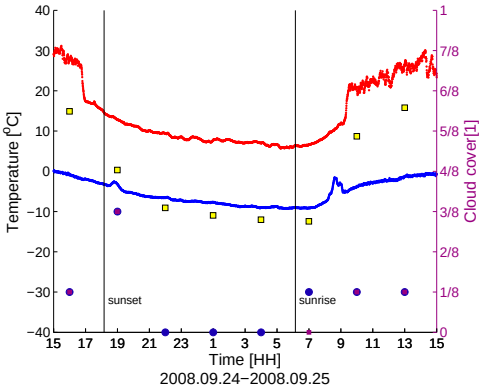
Temperature [°C]
Cloud cover[1]
Time [HH]
sunset
sunrise
2008.09.24–2008.09.25

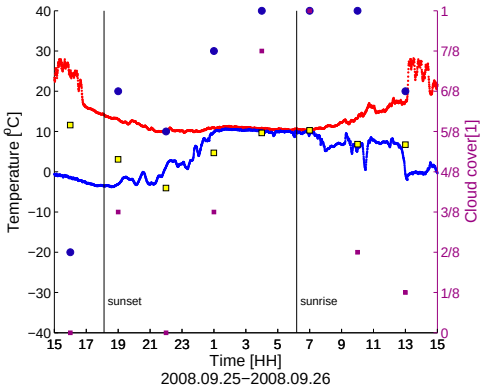
Temperature [°C]
Cloud cover[1]
Time [HH]
sunset
sunrise
2008.09.25–2008.09.26

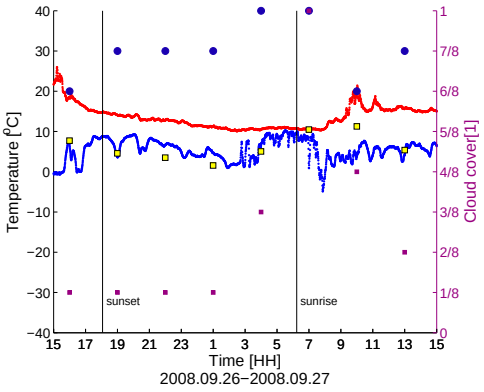
Temperature [°C]
Cloud cover[1]
Time [HH]
sunset
sunrise
2008.09.26–2008.09.27

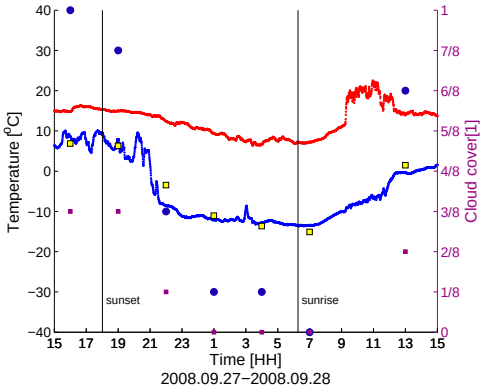
Temperature [°C]
Cloud cover[1]
Time [HH]
sunset
sunrise
2008.09.27–2008.09.28

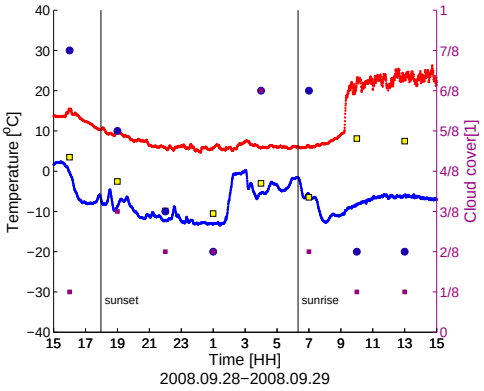
Temperature [°C]
Cloud cover[1]
Time [HH]
sunset
sunrise
2008.09.28–2008.09.29

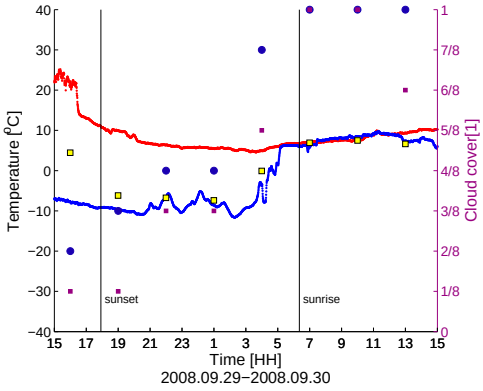
Temperature [°C]
Cloud cover[1]
Time [HH]
sunset
sunrise
2008.09.29–2008.09.30

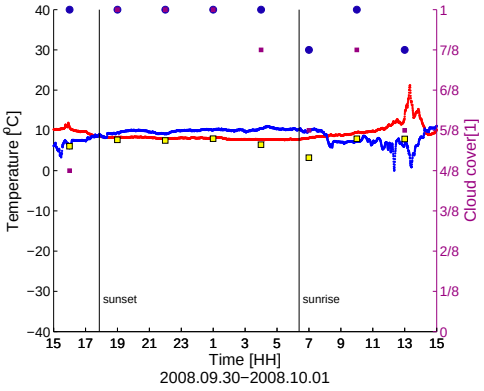
Temperature [°C]
Cloud cover[1]
Time [HH]
sunset
sunrise
2008.09.30–2008.10.01

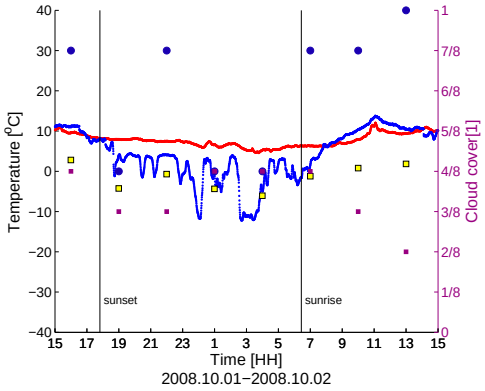

2008.10.01–2008.10.02

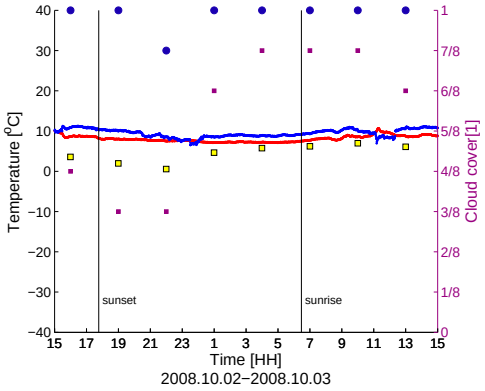

2008.10.02–2008.10.03

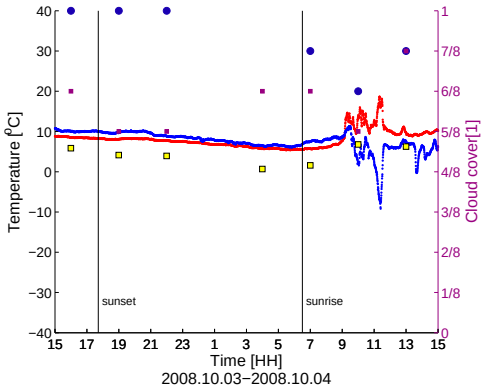

2008.10.03–2008.10.04

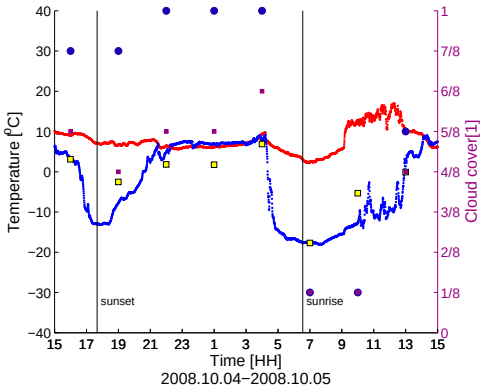

2008.10.04–2008.10.05

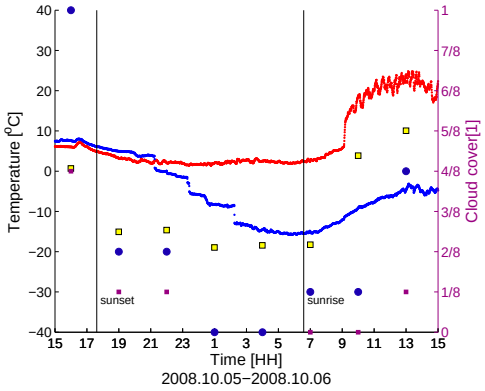

2008.10.05–2008.10.06

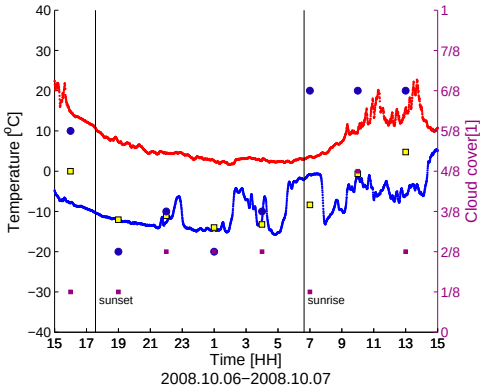

2008.10.06–2008.10.07

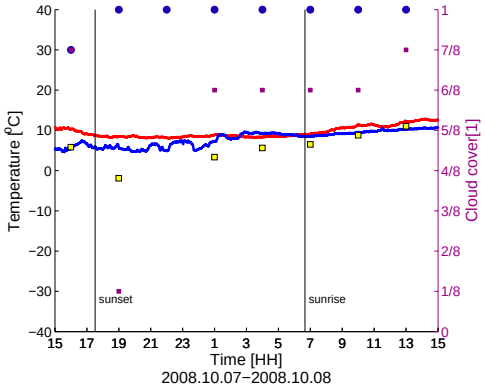

2008.10.07–2008.10.08

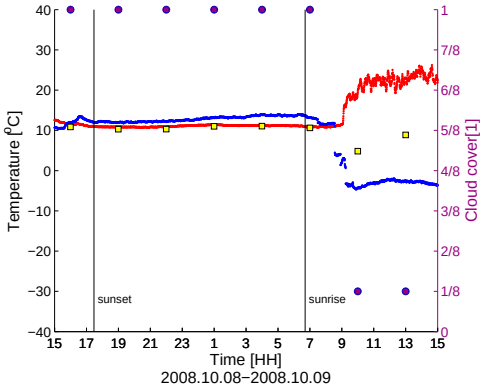

2008.10.08–2008.10.09

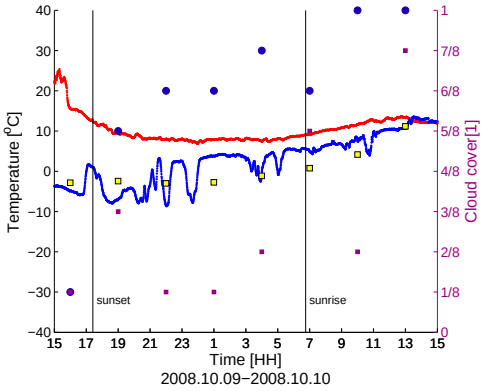

2008.10.09–2008.10.10

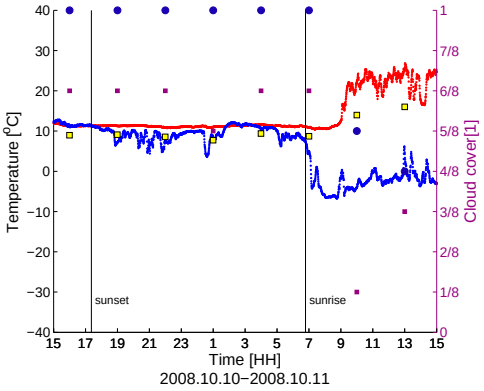

2008.10.10–2008.10.11

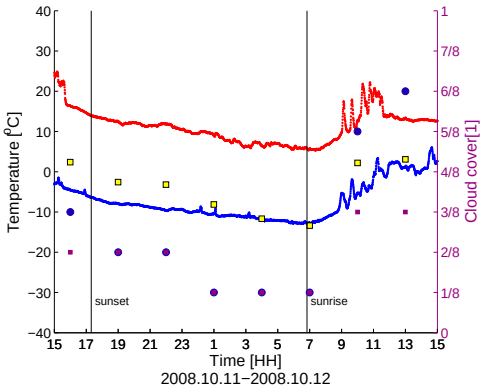

2008.10.11–2008.10.12

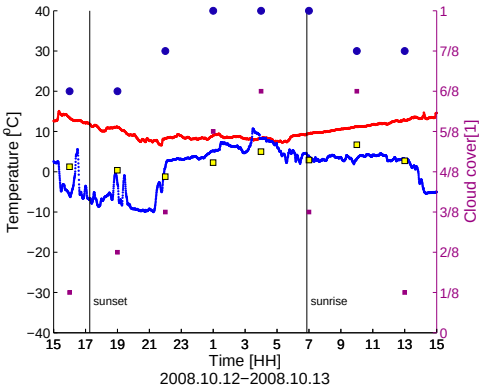

2008.10.12–2008.10.13

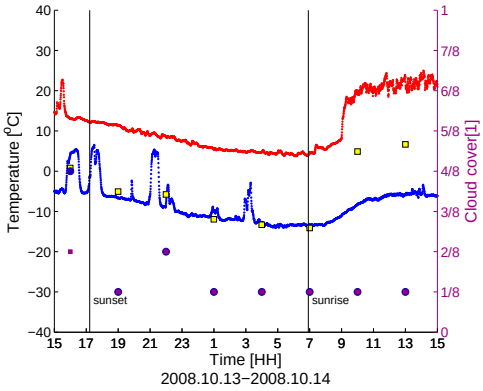

2008.10.13–2008.10.14

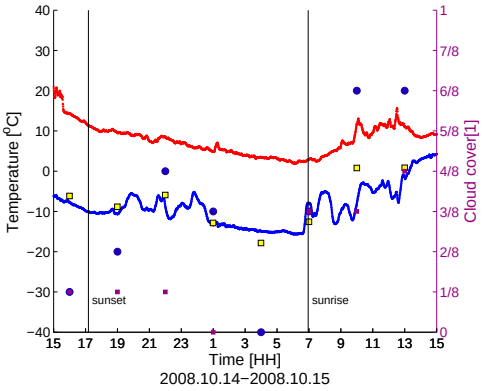

2008.10.14–2008.10.15

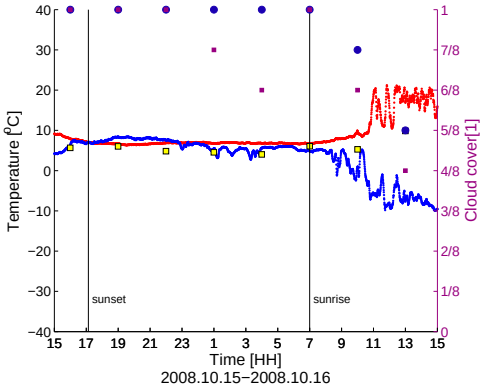

2008.10.15–2008.10.16

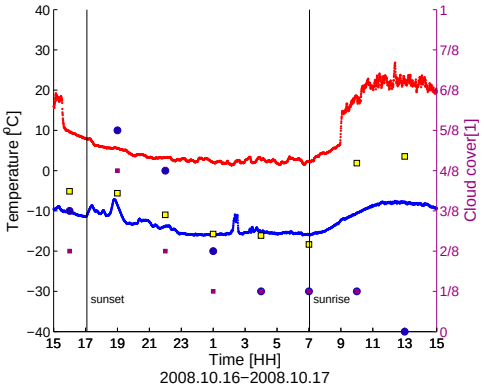

2008.10.16–2008.10.17

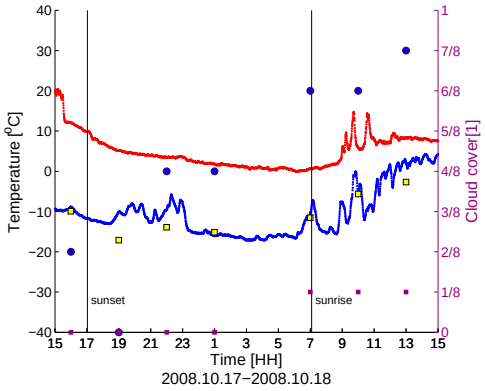

2008.10.17–2008.10.18

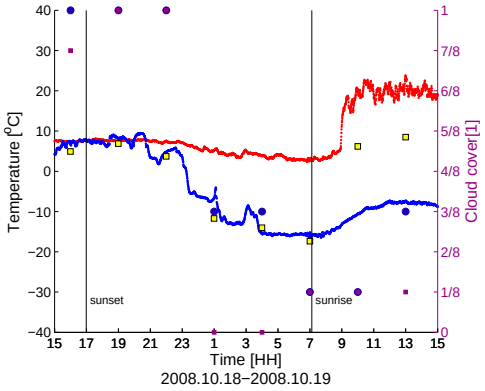

2008.10.18–2008.10.19

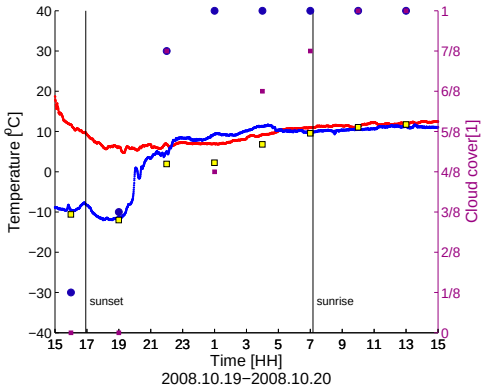

2008.10.19–2008.10.20

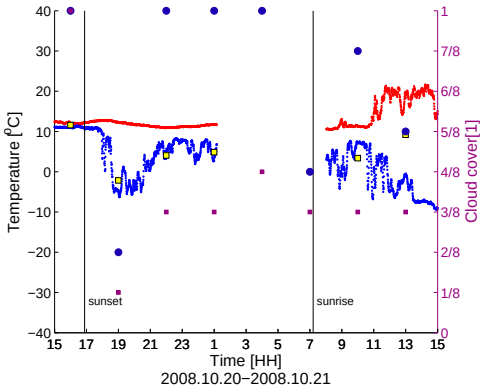

2008.10.20–2008.10.21

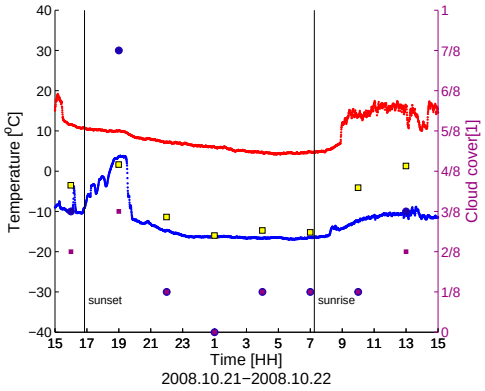

2008.10.21–2008.10.22

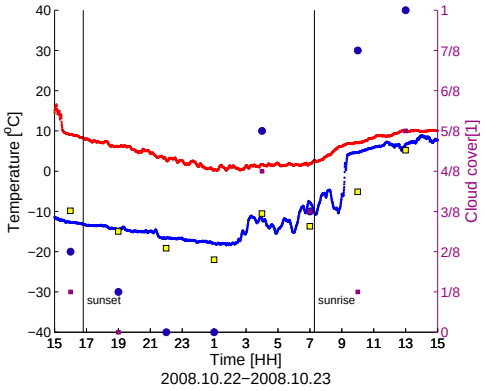

2008.10.22–2008.10.23

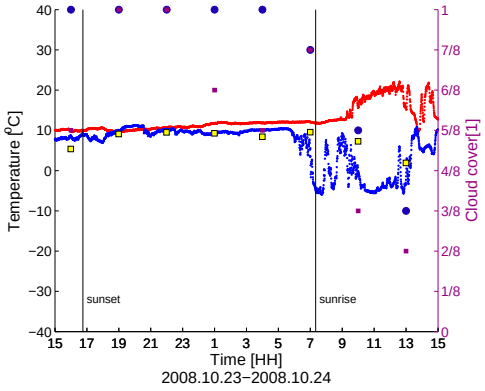

2008.10.23–2008.10.24

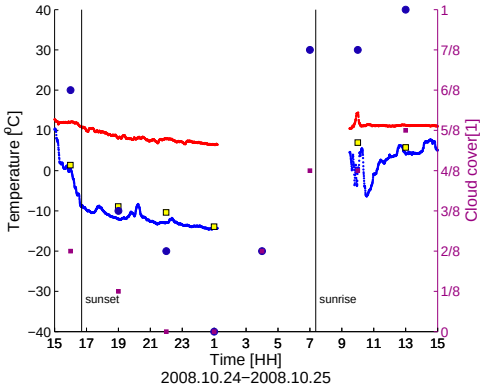

2008.10.24–2008.10.25

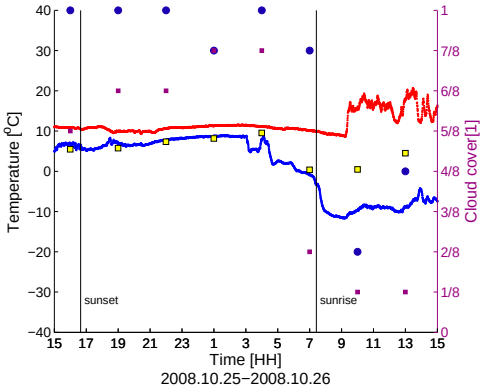

2008.10.25–2008.10.26

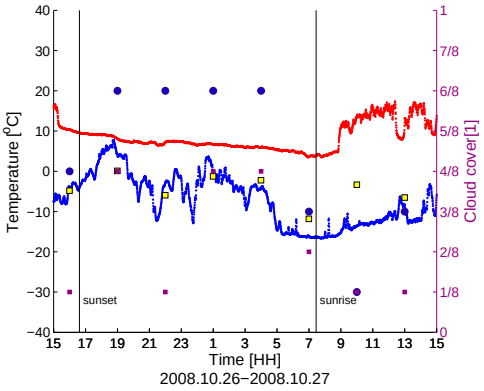

2008.10.26–2008.10.27

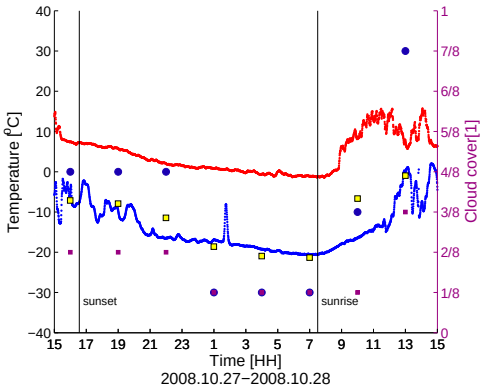

2008.10.27–2008.10.28

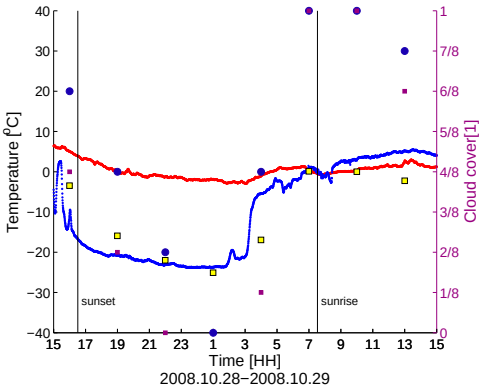

2008.10.28–2008.10.29

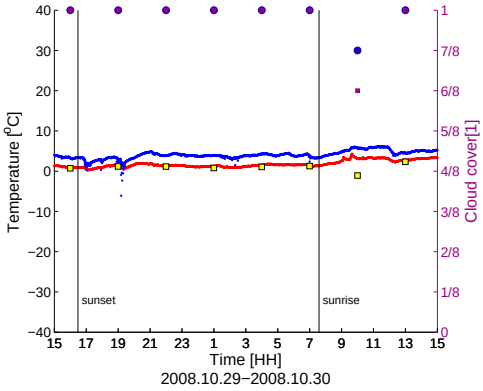

2008.10.29–2008.10.30

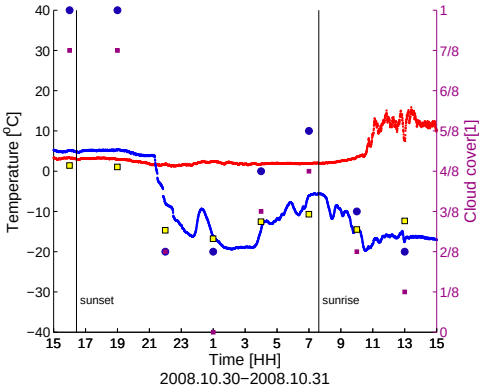

2008.10.30–2008.10.31

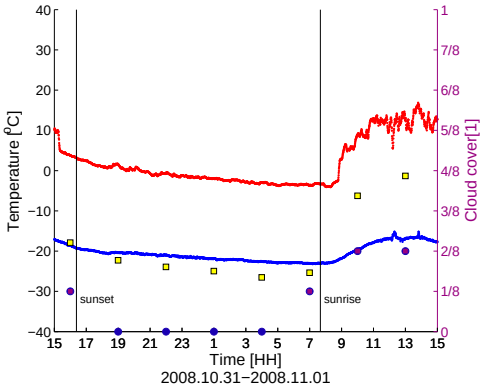

2008.10.31–2008.11.01

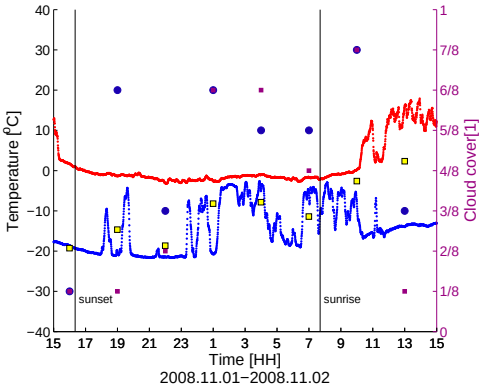

2008.11.01–2008.11.02

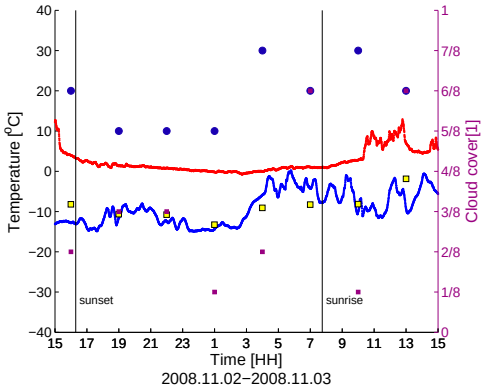

2008.11.02–2008.11.03

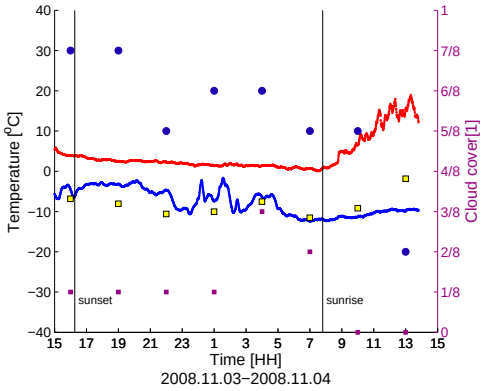

2008.11.03–2008.11.04

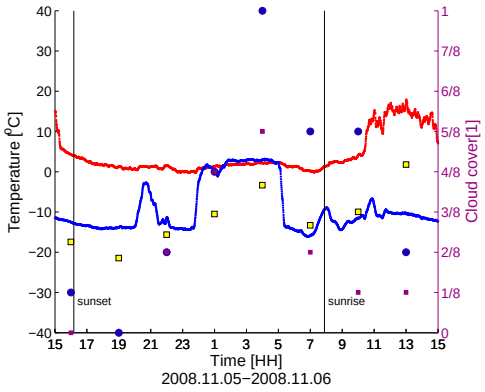

2008.11.05–2008.11.06

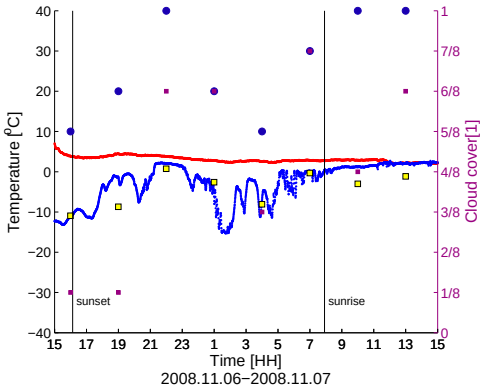

2008.11.06–2008.11.07

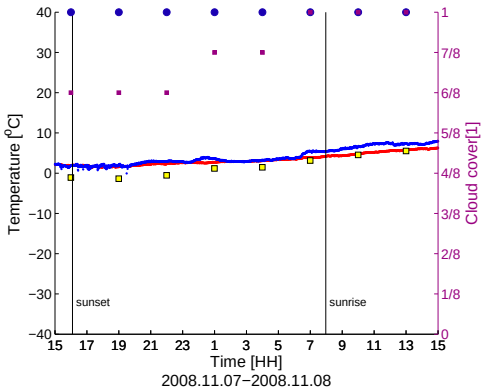

2008.11.07–2008.11.08

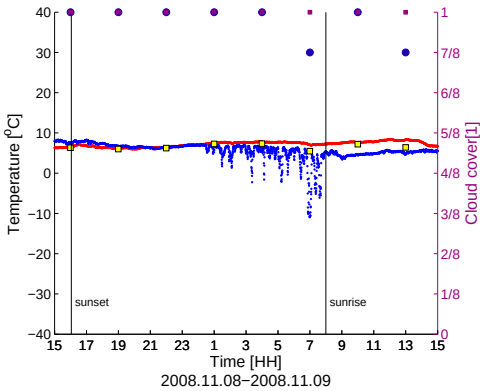

2008.11.08–2008.11.09

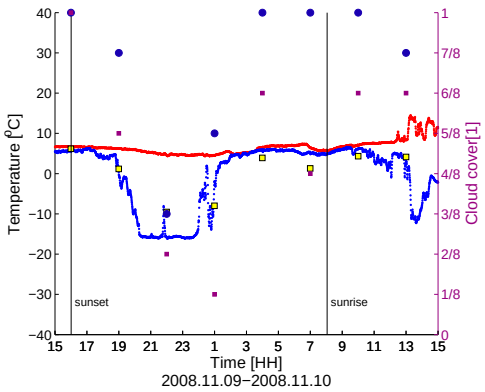

2008.11.09–2008.11.10

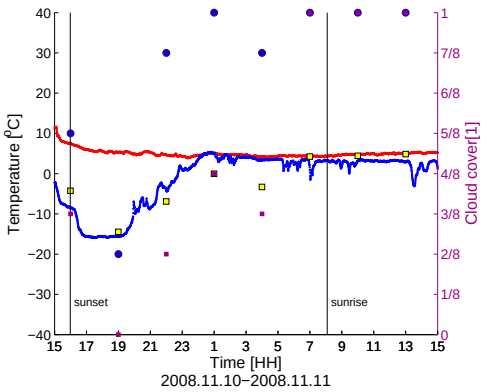

2008.11.10–2008.11.11

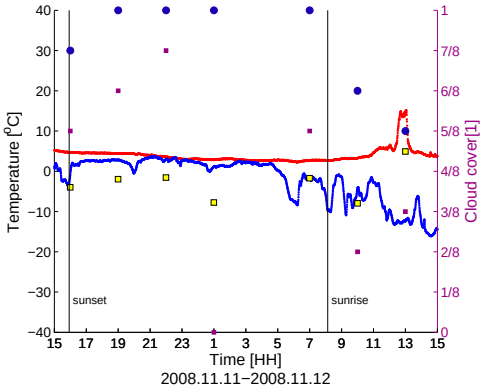

2008.11.11–2008.11.12

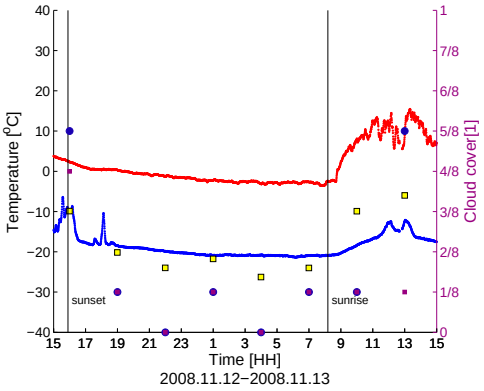

2008.11.12–2008.11.13

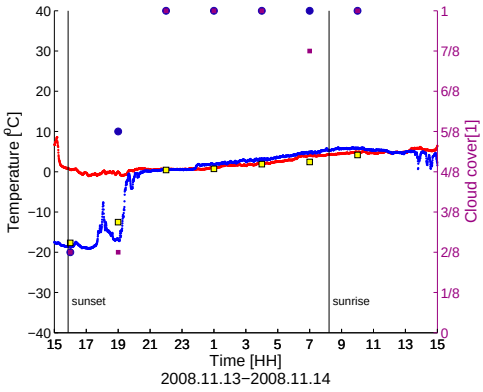

2008.11.13–2008.11.14

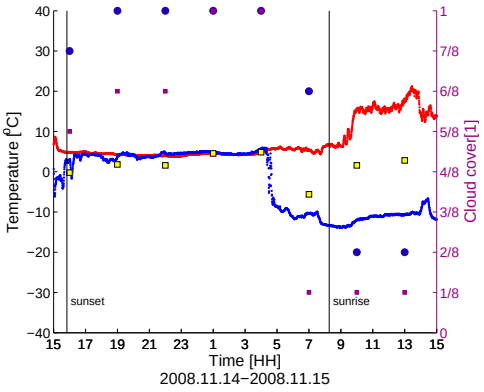

2008.11.14–2008.11.15

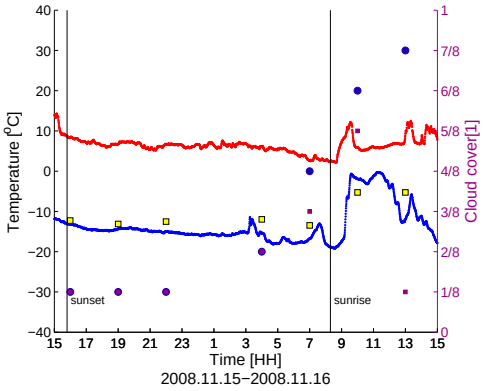

2008.11.15–2008.11.16

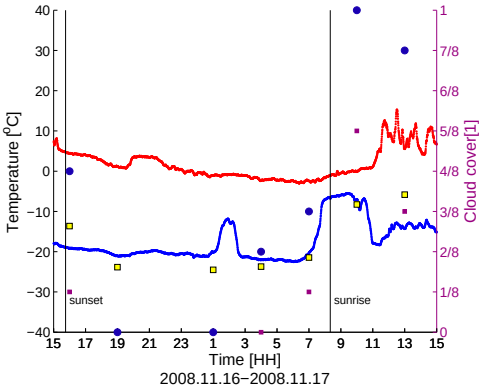

2008.11.16–2008.11.17

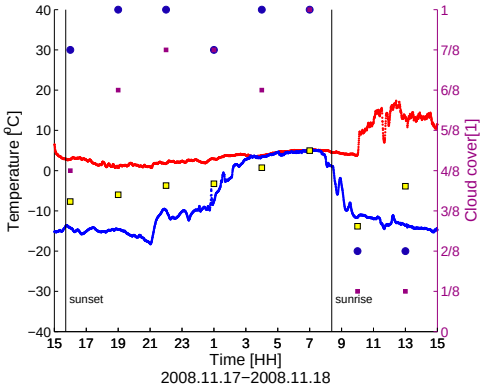

2008.11.17–2008.11.18

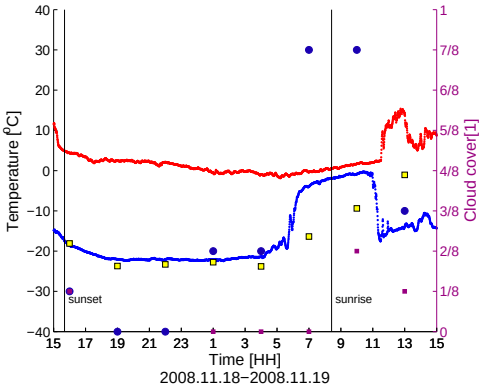

2008.11.18–2008.11.19

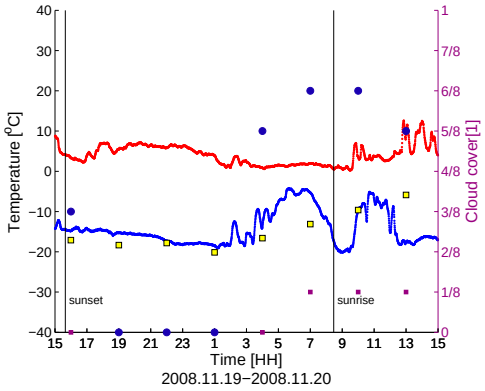

2008.11.19–2008.11.20

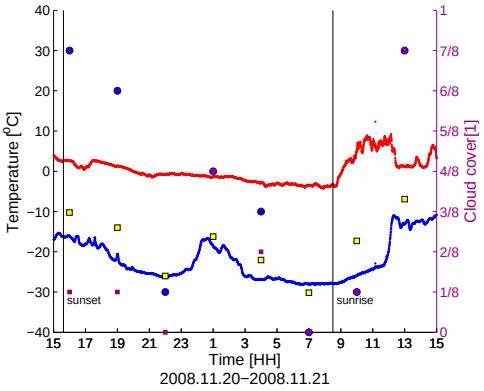

2008.11.20–2008.11.21

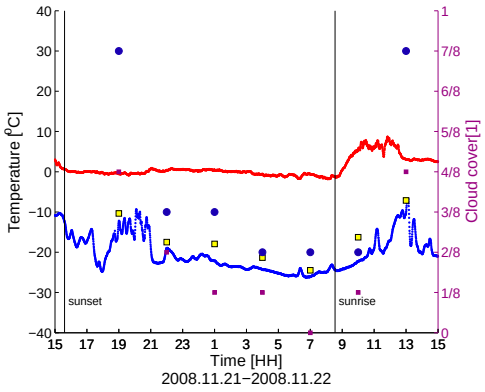

2008.11.21–2008.11.22

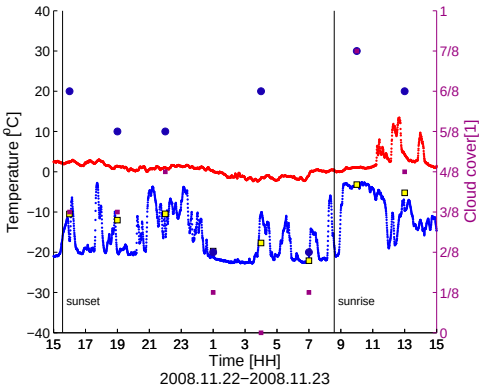

2008.11.22–2008.11.23

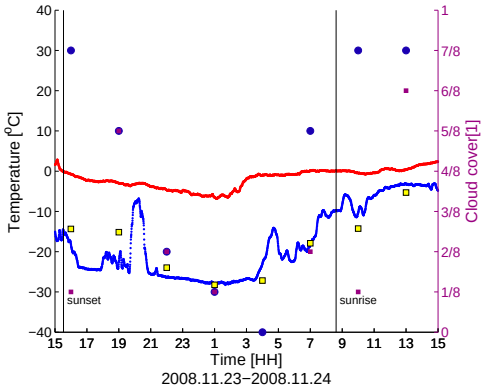

2008.11.23–2008.11.24

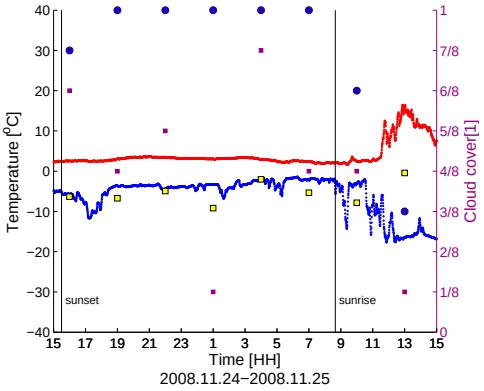

2008.11.24–2008.11.25

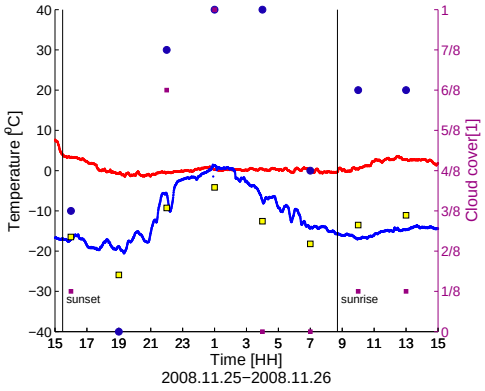

2008.11.25–2008.11.26

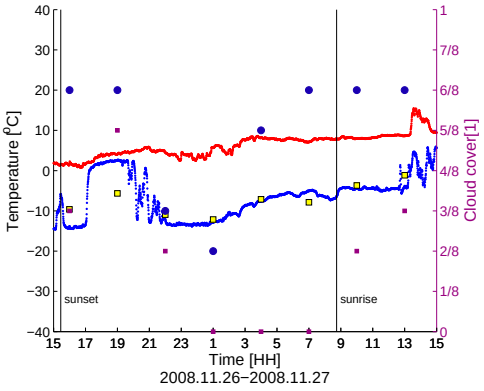

2008.11.26–2008.11.27

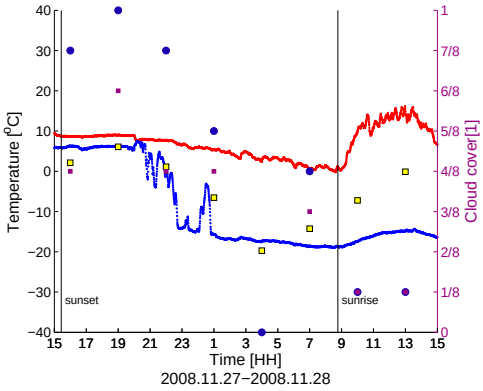
Temperature [°C]
Cloud cover[1]
sunset
sunrise
Time [HH]
2008.11.27–2008.11.28

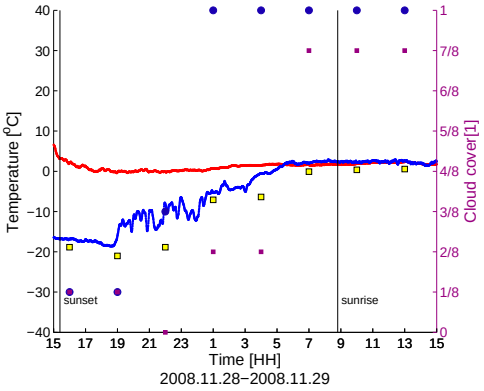
Temperature [°C]
Cloud cover[1]
sunset
sunrise
Time [HH]
2008.11.28–2008.11.29

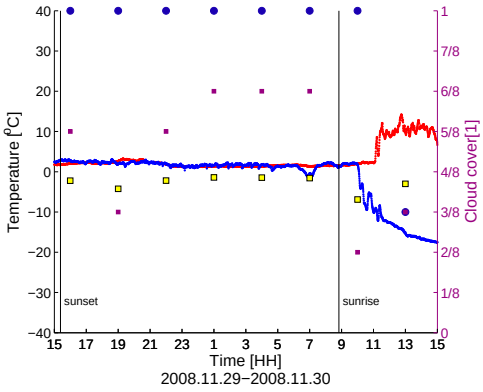
Temperature [°C]
Cloud cover[1]
sunset
sunrise
Time [HH]
2008.11.29–2008.11.30

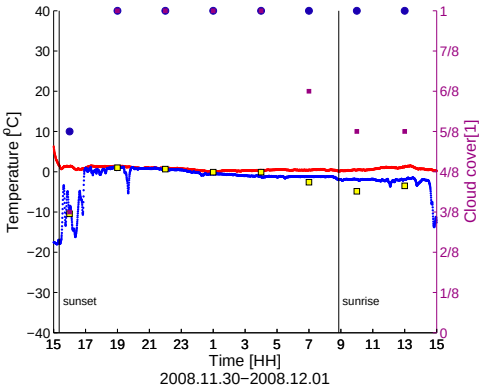
Temperature [°C]
Cloud cover[1]
sunset
sunrise
Time [HH]
2008.11.30–2008.12.01

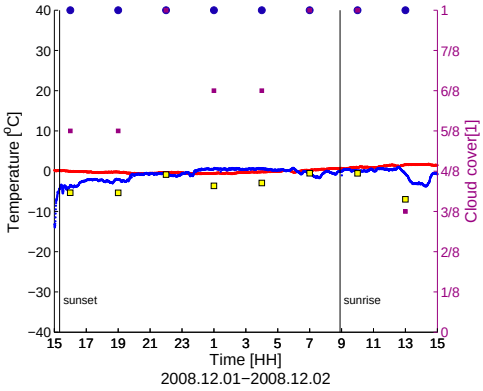
Temperature [°C]
Cloud cover[1]
sunset
sunrise
Time [HH]
2008.12.01–2008.12.02

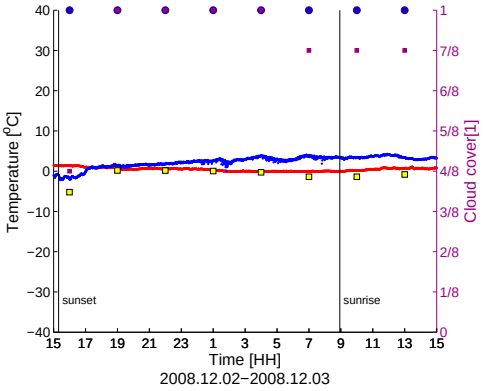
Temperature [°C]
Cloud cover[1]
sunset
sunrise
Time [HH]
2008.12.02–2008.12.03

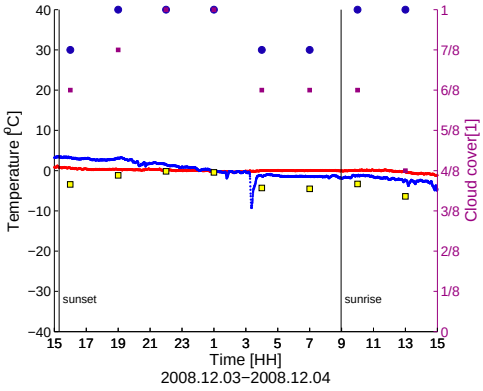
Temperature [°C]
Cloud cover[1]
sunset
sunrise
Time [HH]
2008.12.03–2008.12.04

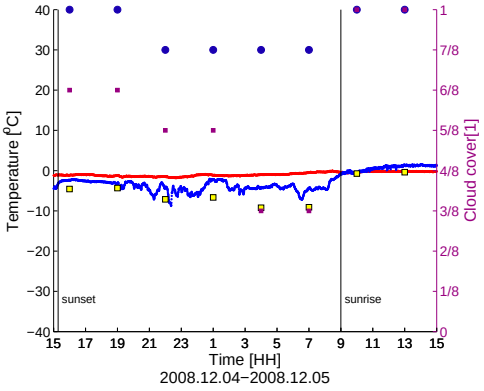
Temperature [°C]
Cloud cover[1]
sunset
sunrise
Time [HH]
2008.12.04–2008.12.05

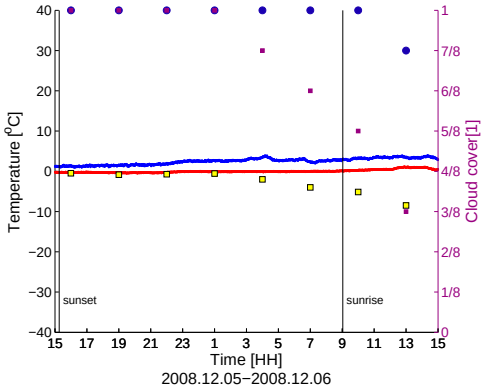

2008.12.05–2008.12.06

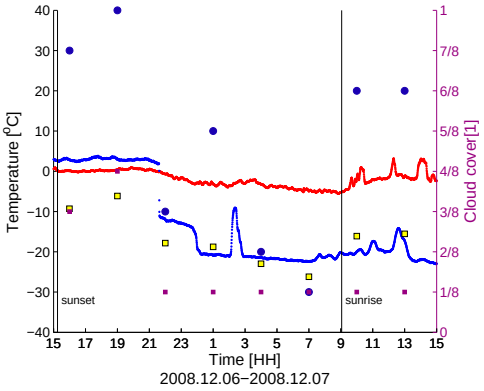

2008.12.06–2008.12.07

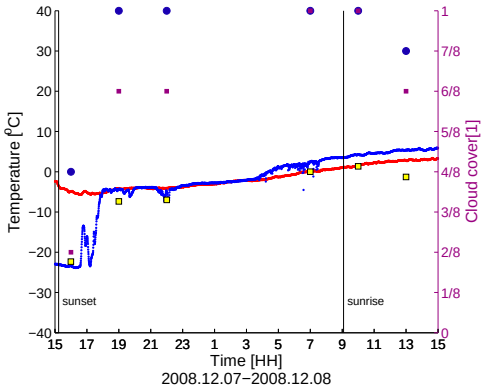

2008.12.07–2008.12.08

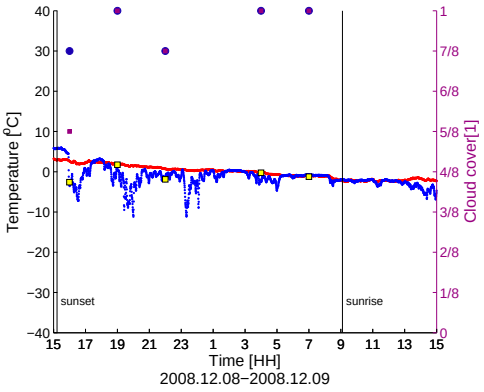

2008.12.08–2008.12.09

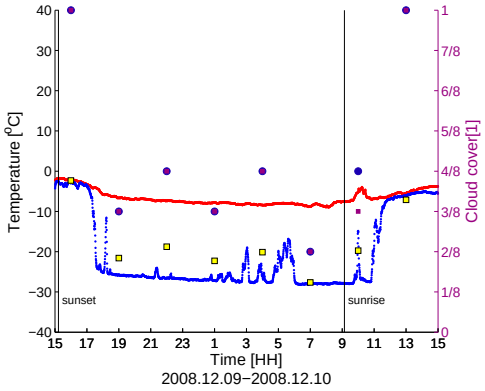

2008.12.09–2008.12.10

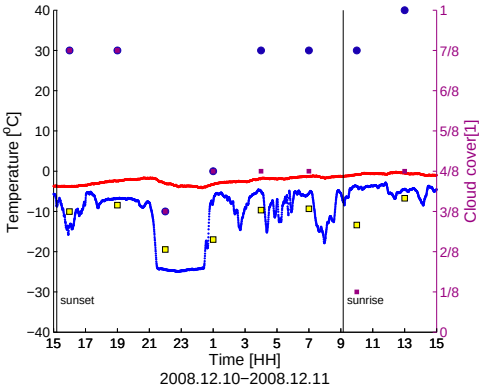

2008.12.10–2008.12.11

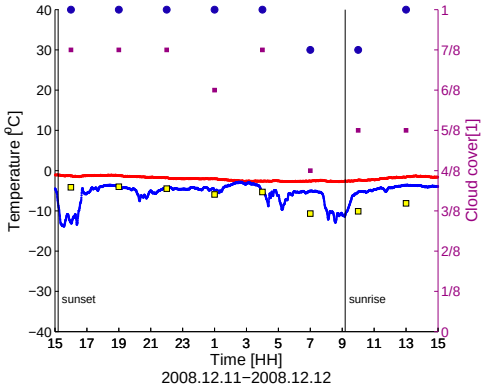

2008.12.11–2008.12.12

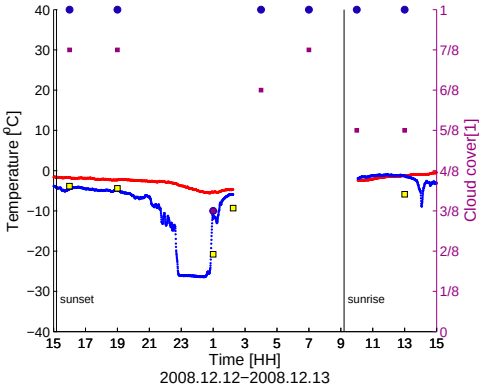

2008.12.12–2008.12.13

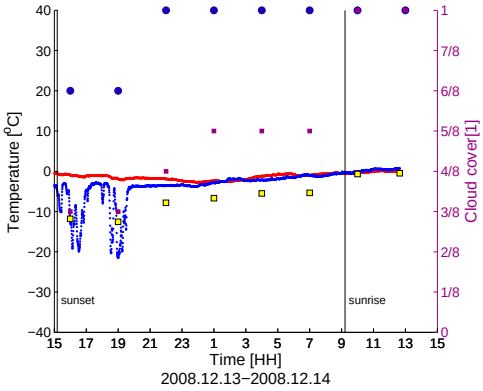
Temperature [°C]
Cloud cover[1]
Time [HH]
sunset
sunrise
2008.12.13−2008.12.14

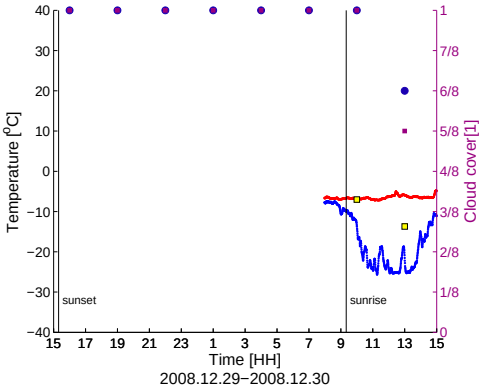
Temperature [°C]
Cloud cover[1]
Time [HH]
sunset
sunrise
2008.12.29−2008.12.30

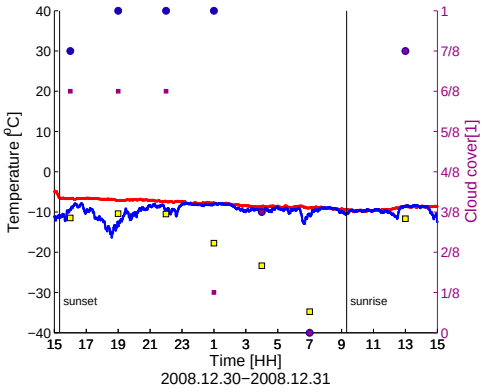
Temperature [°C]
Cloud cover[1]
Time [HH]
sunset
sunrise
2008.12.30−2008.12.31

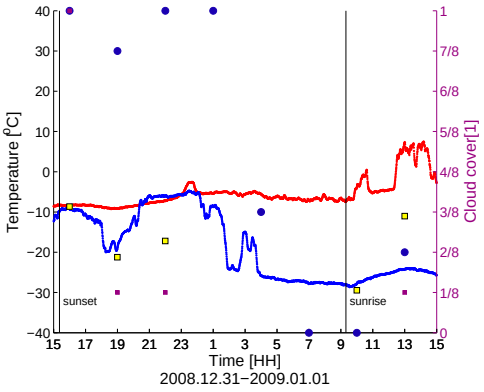
Temperature [°C]
Cloud cover[1]
Time [HH]
sunset
sunrise
2008.12.31−2009.01.01

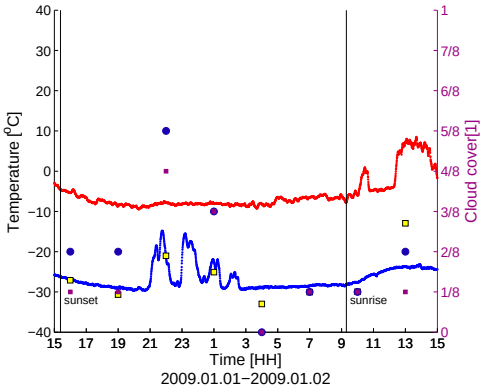
Temperature [°C]
Cloud cover[1]
Time [HH]
sunset
sunrise
2009.01.01−2009.01.02

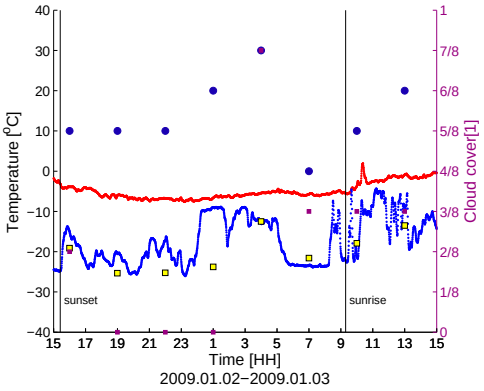
Temperature [°C]
Cloud cover[1]
Time [HH]
sunset
sunrise
2009.01.02−2009.01.03

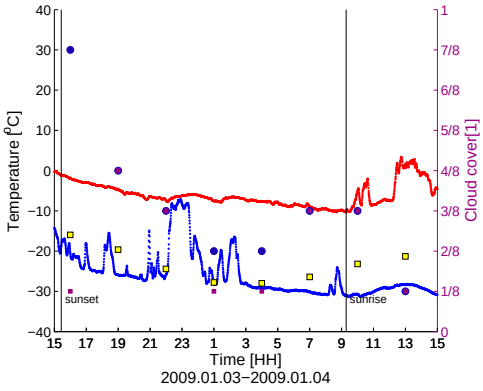
Temperature [°C]
Cloud cover[1]
Time [HH]
sunset
sunrise
2009.01.03−2009.01.04

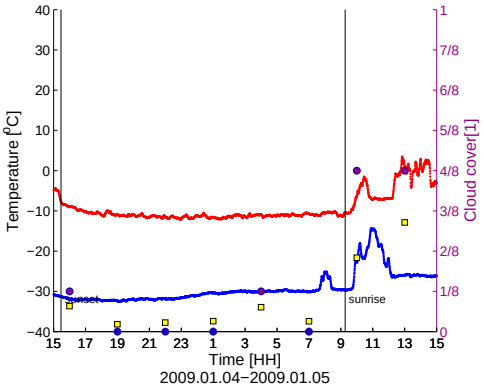
Temperature [°C]
Cloud cover[1]
Time [HH]
sunset
sunrise
2009.01.04−2009.01.05

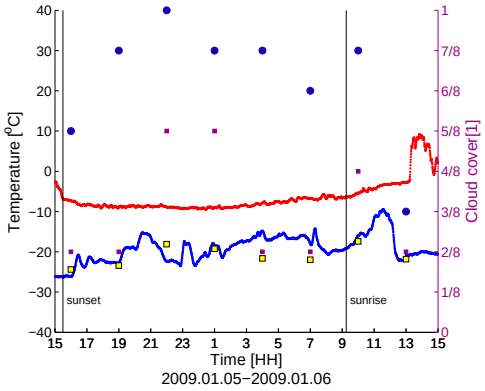

2009.01.05–2009.01.06

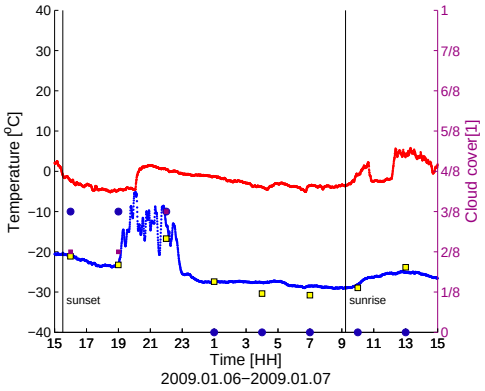

2009.01.06–2009.01.07

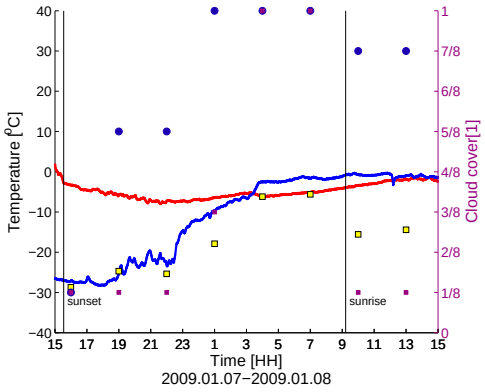

2009.01.07–2009.01.08

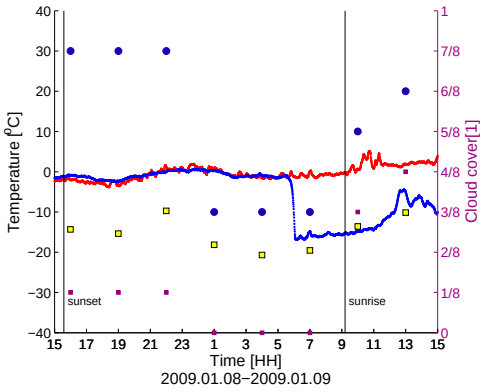

2009.01.08–2009.01.09

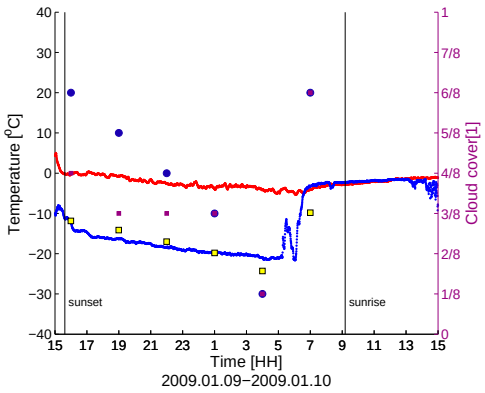

2009.01.09–2009.01.10

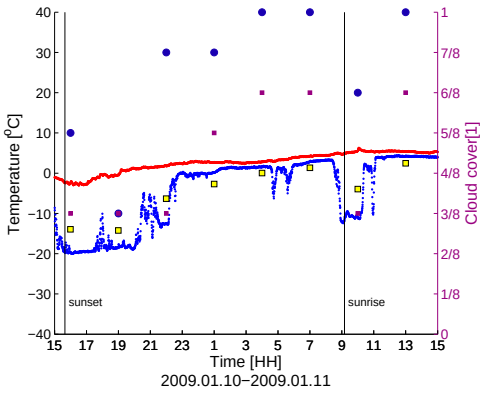

2009.01.10–2009.01.11

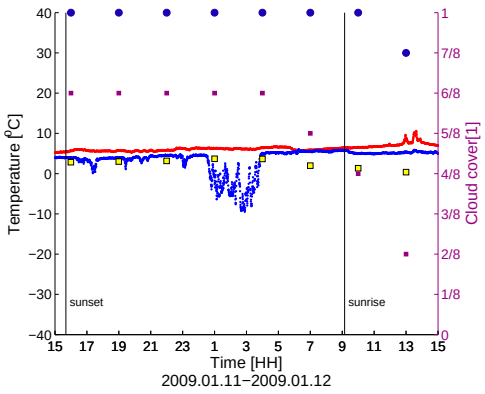

2009.01.11–2009.01.12

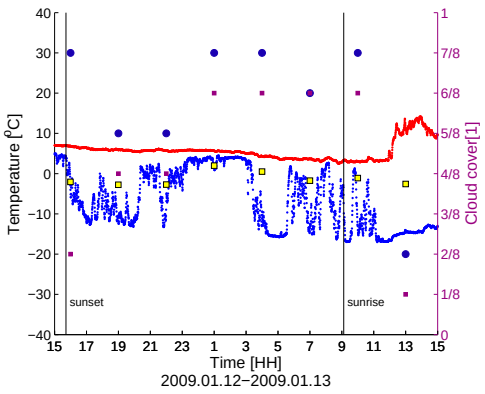

2009.01.12–2009.01.13

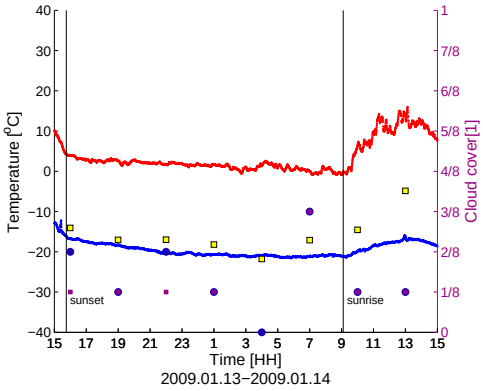
Temperature [°C]
Cloud cover[1]
sunset
sunrise
Time [HH]
2009.01.13−2009.01.14

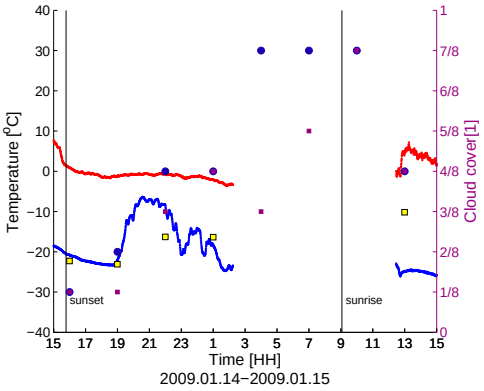
Temperature [°C]
Cloud cover[1]
sunset
sunrise
Time [HH]
2009.01.14−2009.01.15

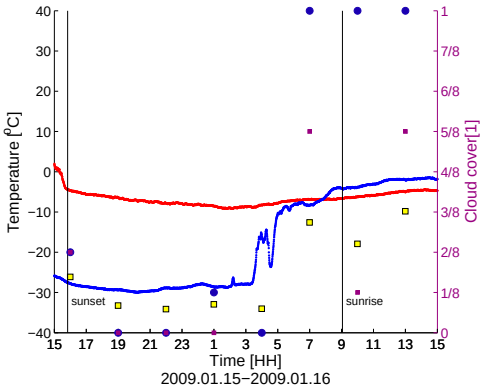
Temperature [°C]
Cloud cover[1]
sunset
sunrise
Time [HH]
2009.01.15−2009.01.16

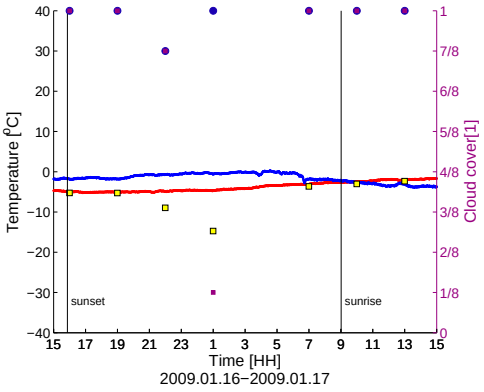
Temperature [°C]
Cloud cover[1]
sunset
sunrise
Time [HH]
2009.01.16−2009.01.17

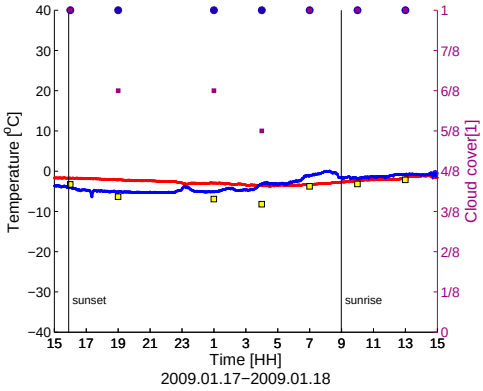
Temperature [°C]
Cloud cover[1]
sunset
sunrise
Time [HH]
2009.01.17−2009.01.18

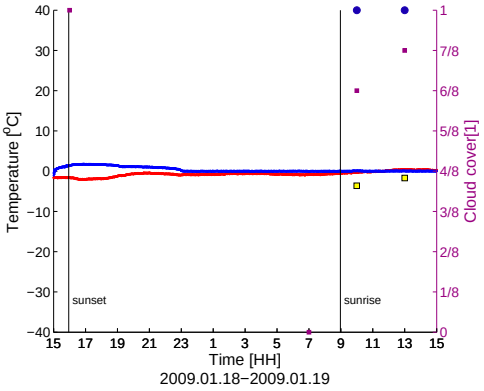
Temperature [°C]
Cloud cover[1]
sunset
sunrise
Time [HH]
2009.01.18−2009.01.19

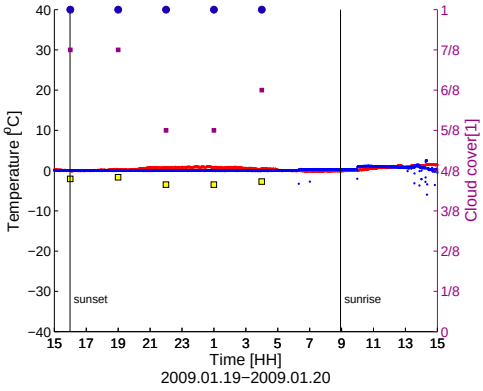
Temperature [°C]
Cloud cover[1]
sunset
sunrise
Time [HH]
2009.01.19−2009.01.20

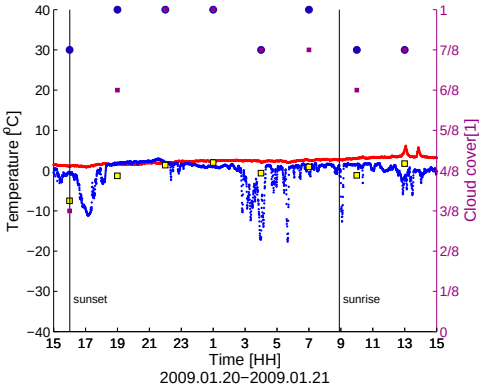
Temperature [°C]
Cloud cover[1]
sunset
sunrise
Time [HH]
2009.01.20−2009.01.21

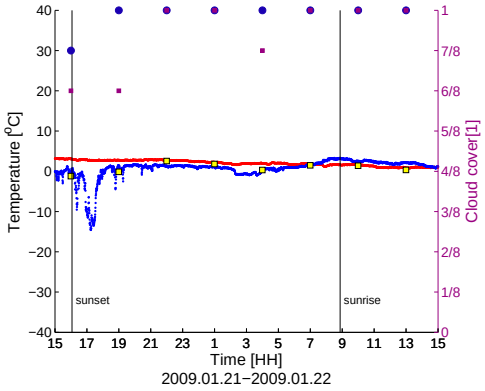

2009.01.21−2009.01.22

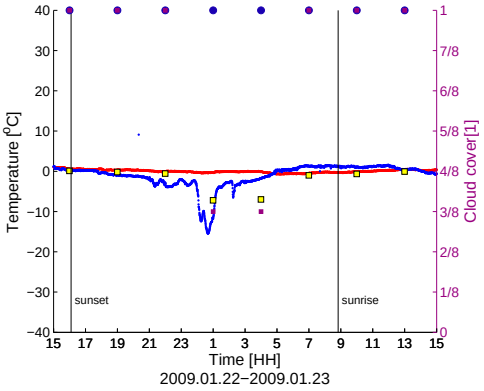

2009.01.22−2009.01.23

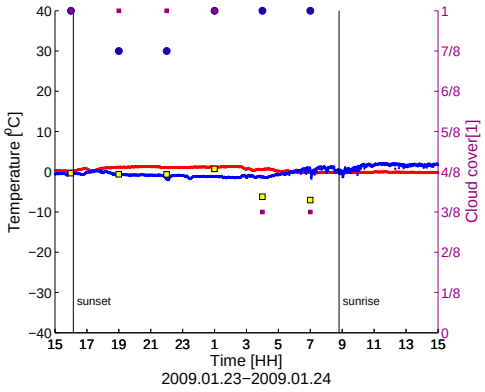

2009.01.23−2009.01.24

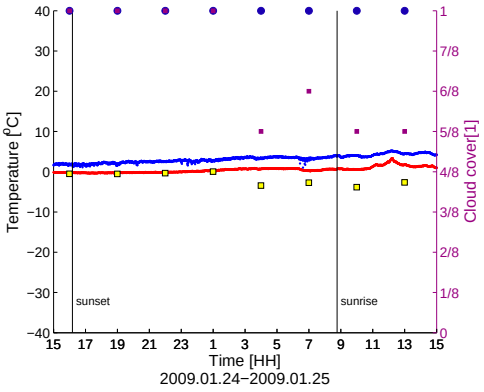

2009.01.24−2009.01.25

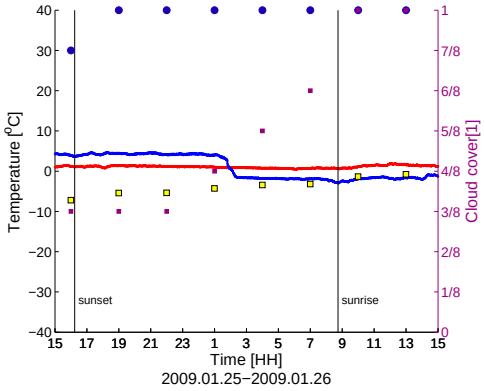

2009.01.25−2009.01.26

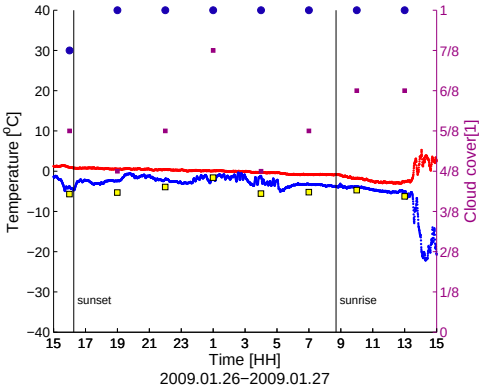

2009.01.26−2009.01.27

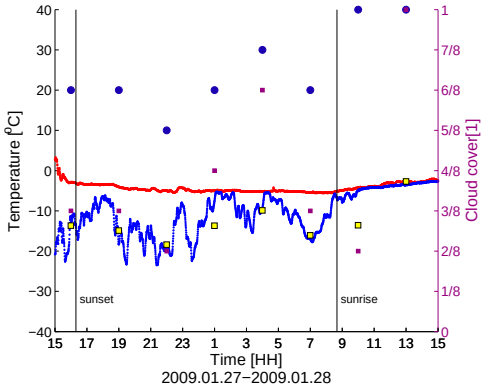

2009.01.27−2009.01.28

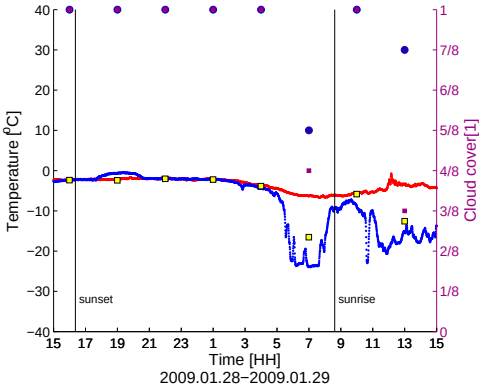

2009.01.28−2009.01.29

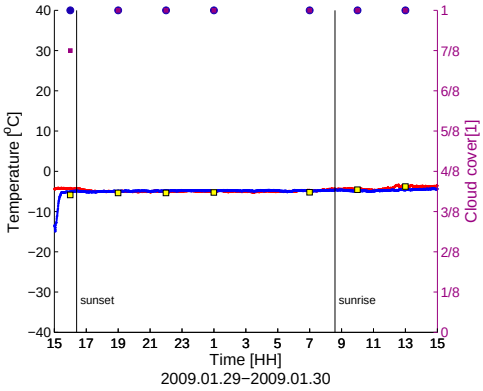
Temperature [°C]
Cloud cover[1]
sunset
sunrise
Time [HH]
2009.01.29−2009.01.30

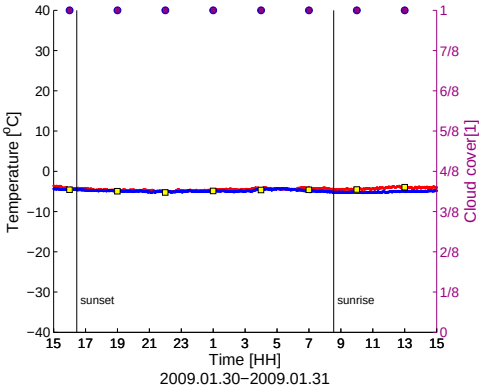
Temperature [°C]
Cloud cover[1]
sunset
sunrise
Time [HH]
2009.01.30−2009.01.31

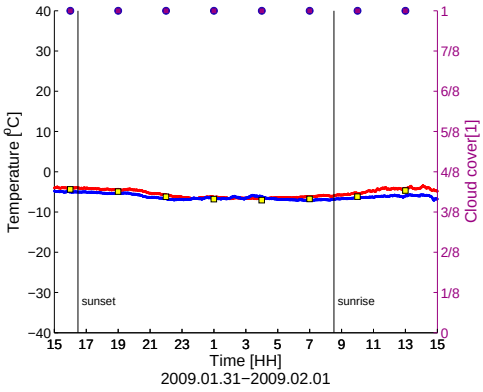
Temperature [°C]
Cloud cover[1]
sunset
sunrise
Time [HH]
2009.01.31−2009.02.01

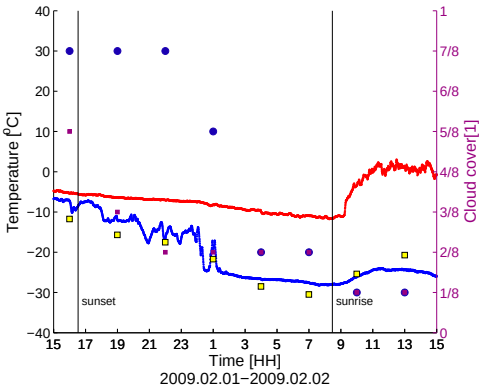
Temperature [°C]
Cloud cover[1]
sunset
sunrise
Time [HH]
2009.02.01−2009.02.02

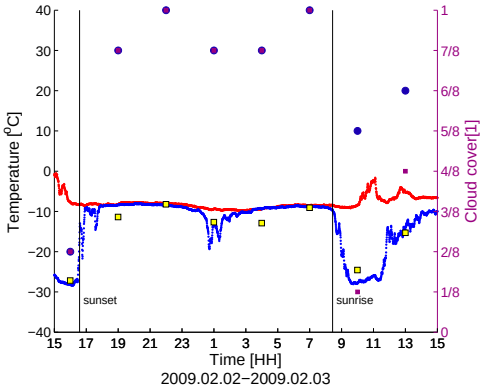
Temperature [°C]
Cloud cover[1]
sunset
sunrise
Time [HH]
2009.02.02−2009.02.03

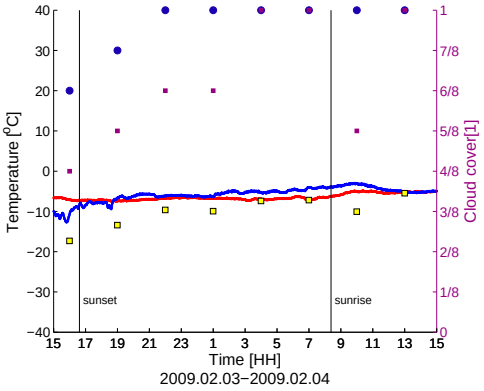
Temperature [°C]
Cloud cover[1]
sunset
sunrise
Time [HH]
2009.02.03−2009.02.04

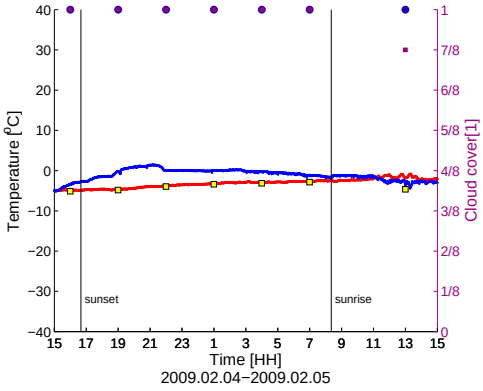
Temperature [°C]
Cloud cover[1]
sunset
sunrise
Time [HH]
2009.02.04−2009.02.05

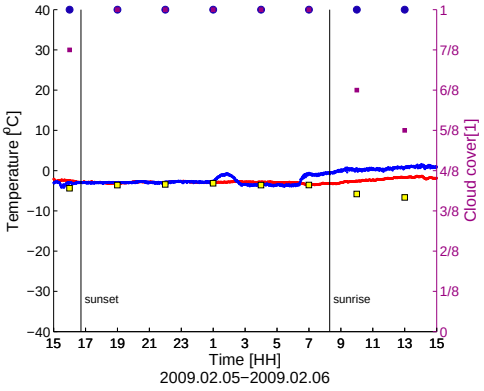
Temperature [°C]
Cloud cover[1]
sunset
sunrise
Time [HH]
2009.02.05−2009.02.06

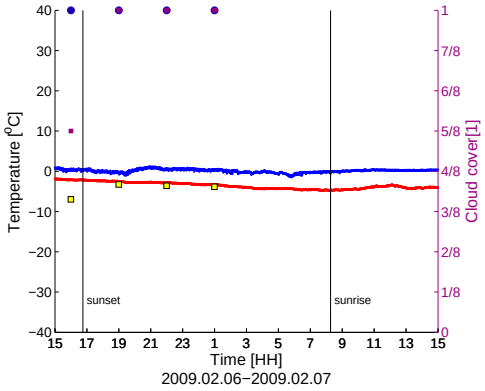

2009.02.06–2009.02.07

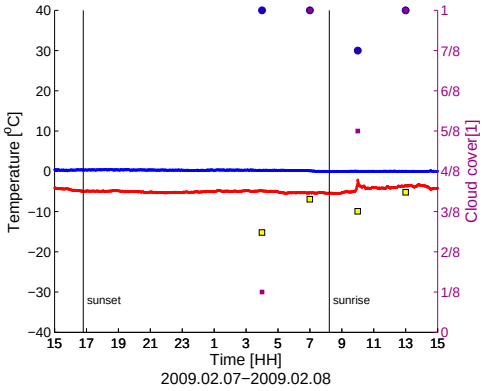

2009.02.07–2009.02.08

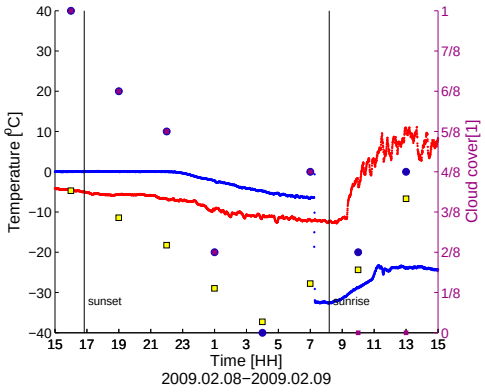

2009.02.08–2009.02.09

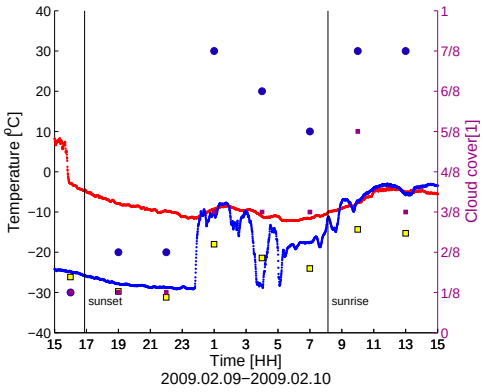

2009.02.09–2009.02.10

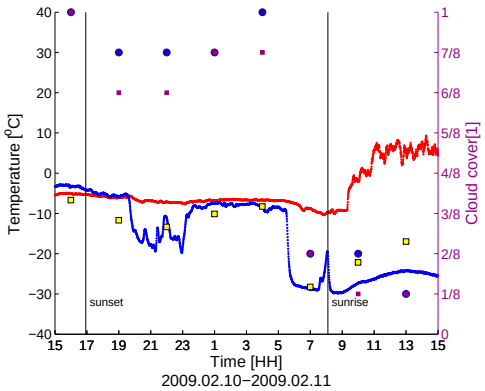

2009.02.10–2009.02.11

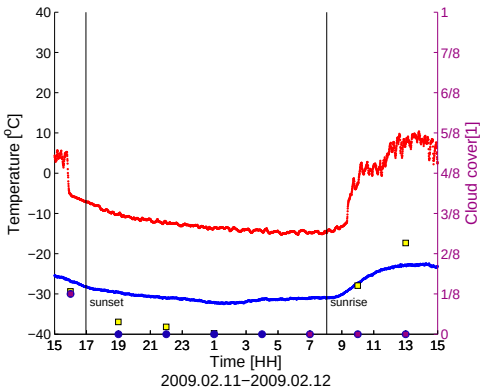

2009.02.11–2009.02.12

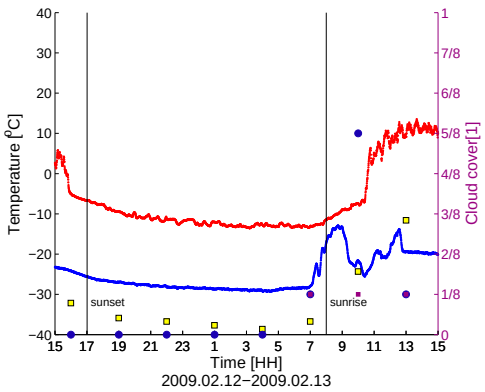

2009.02.12–2009.02.13

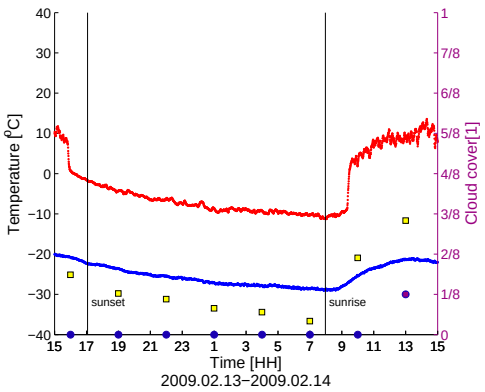

2009.02.13–2009.02.14

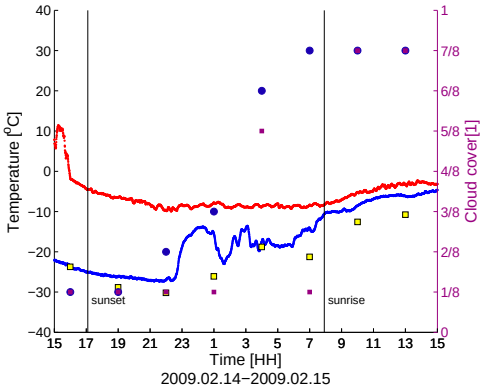
Temperature [°C]
Cloud cover[1]
sunset
sunrise
Time [HH]
2009.02.14−2009.02.15

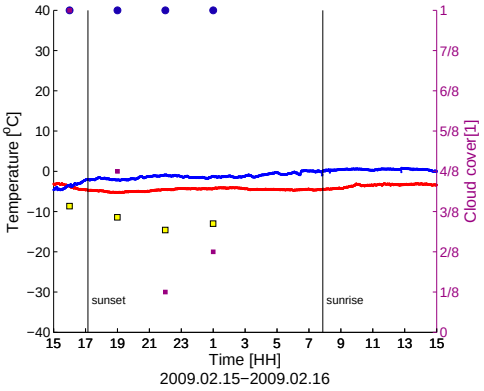
Temperature [°C]
Cloud cover[1]
sunset
sunrise
Time [HH]
2009.02.15−2009.02.16

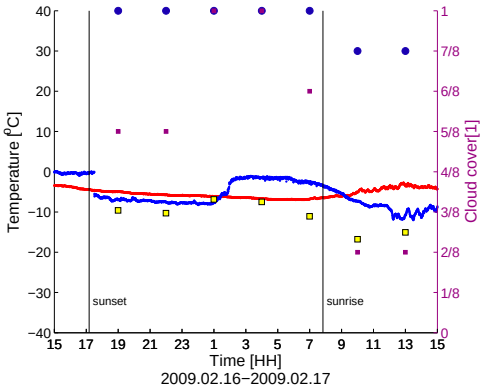
Temperature [°C]
Cloud cover[1]
sunset
sunrise
Time [HH]
2009.02.16−2009.02.17

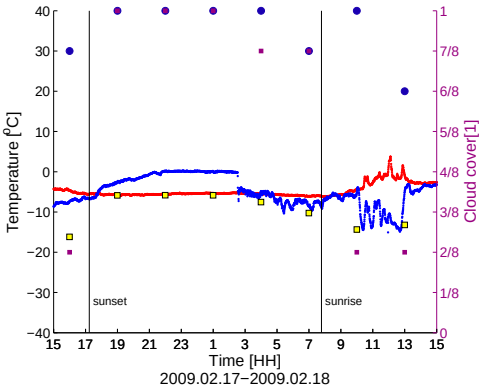
Temperature [°C]
Cloud cover[1]
sunset
sunrise
Time [HH]
2009.02.17−2009.02.18

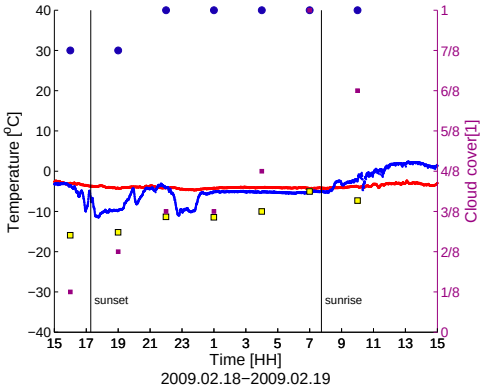
Temperature [°C]
Cloud cover[1]
sunset
sunrise
Time [HH]
2009.02.18−2009.02.19

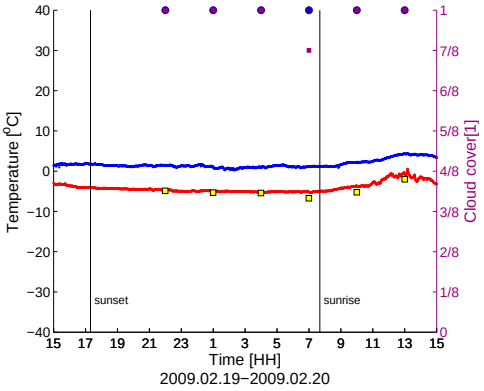
Temperature [°C]
Cloud cover[1]
sunset
sunrise
Time [HH]
2009.02.19−2009.02.20

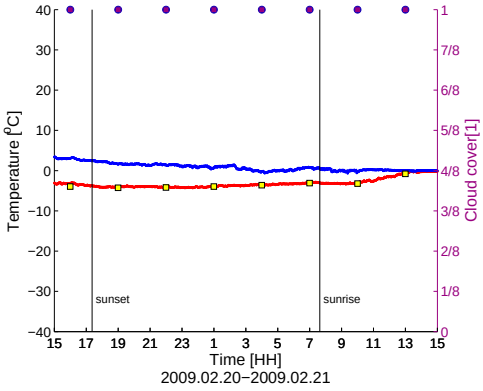
Temperature [°C]
Cloud cover[1]
sunset
sunrise
Time [HH]
2009.02.20−2009.02.21

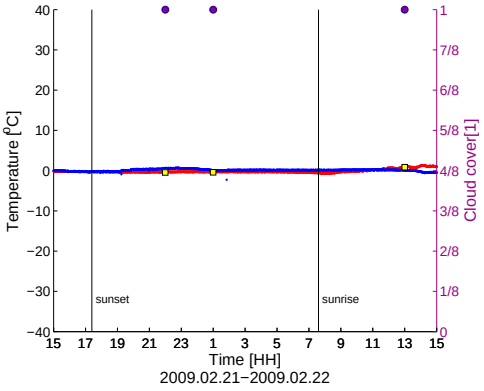
Temperature [°C]
Cloud cover[1]
sunset
sunrise
Time [HH]
2009.02.21−2009.02.22

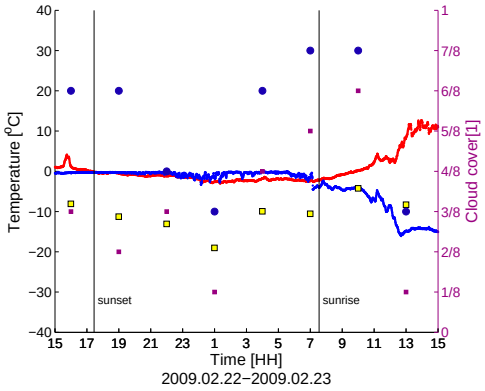

2009.02.22–2009.02.23

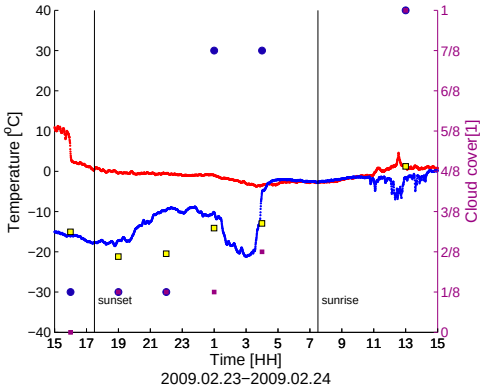

2009.02.23–2009.02.24

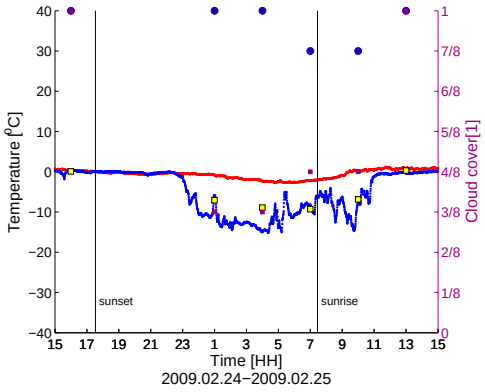

2009.02.24–2009.02.25

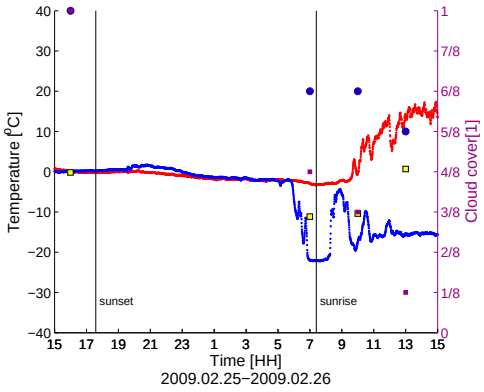

2009.02.25–2009.02.26

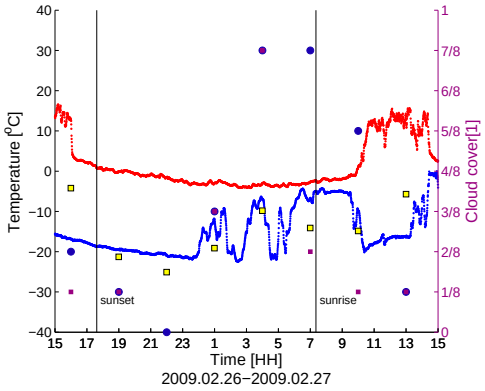

2009.02.26–2009.02.27

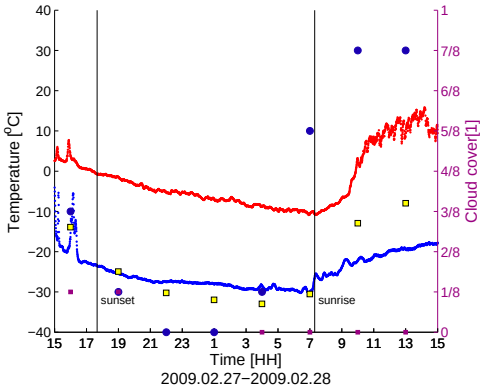

2009.02.27–2009.02.28

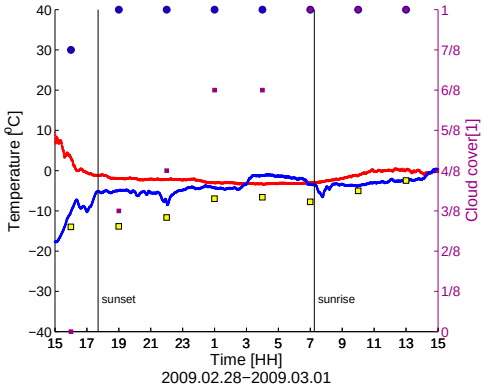

2009.02.28–2009.03.01

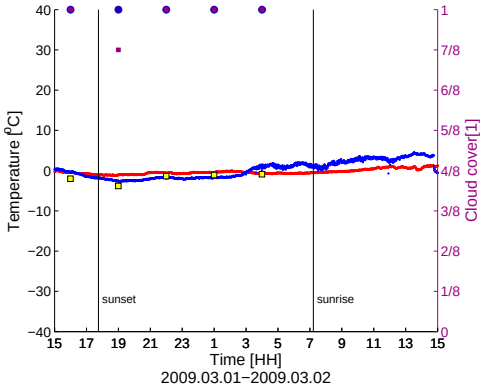

2009.03.01–2009.03.02

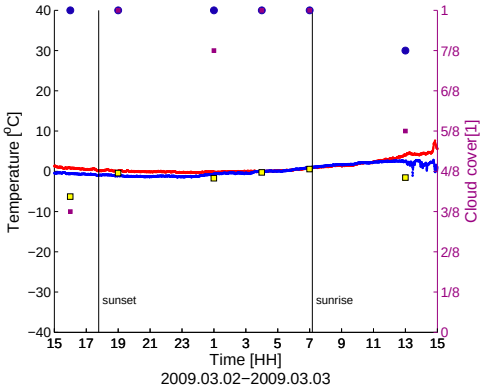

2009.03.02−2009.03.03

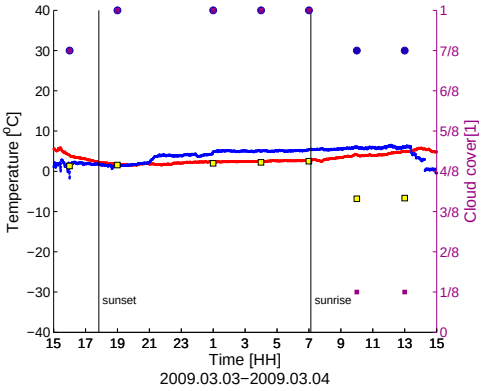

2009.03.03−2009.03.04

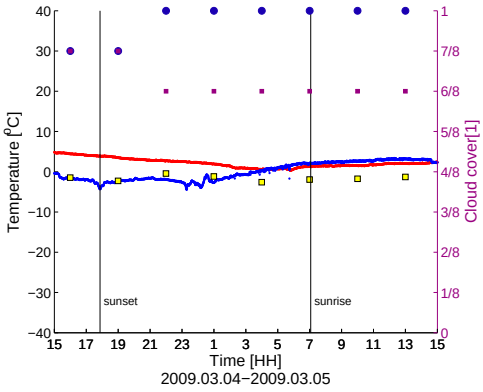

2009.03.04−2009.03.05

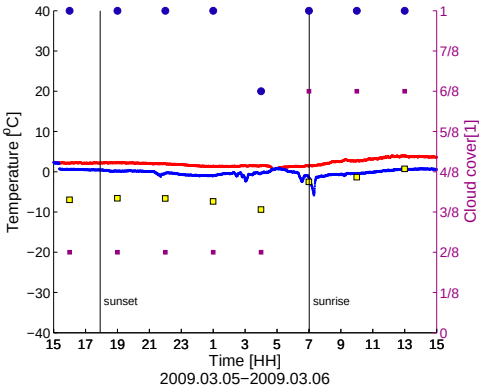

2009.03.05−2009.03.06

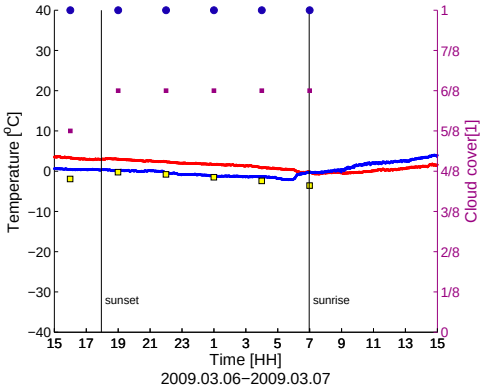

2009.03.06−2009.03.07

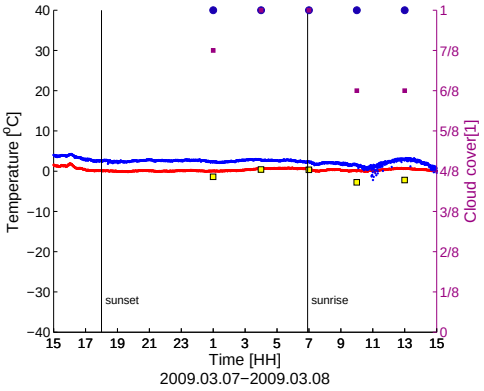

2009.03.07−2009.03.08

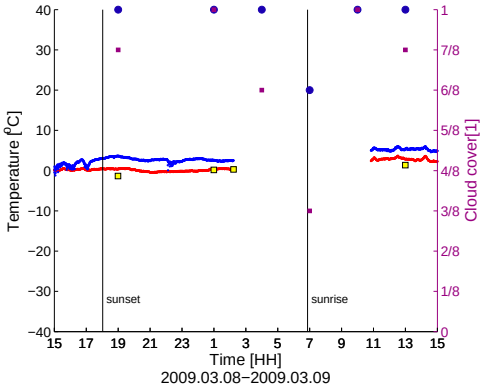

2009.03.08−2009.03.09

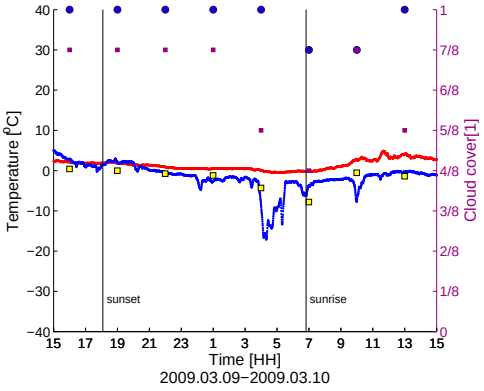

2009.03.09−2009.03.10

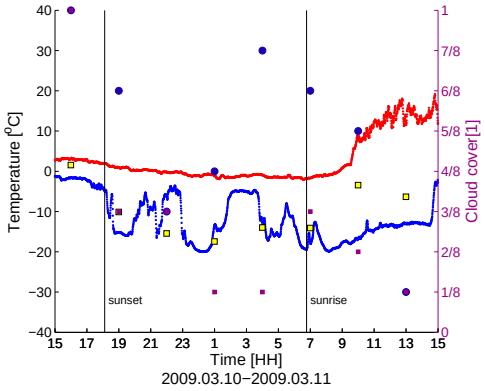

2009.03.10–2009.03.11

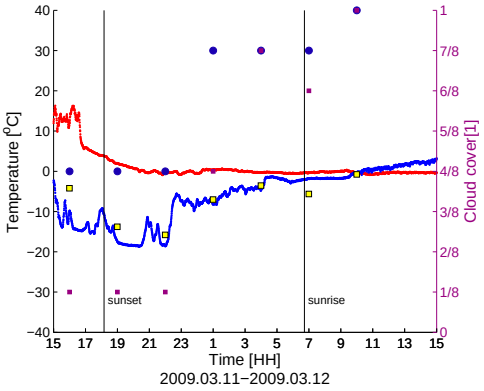

2009.03.11–2009.03.12

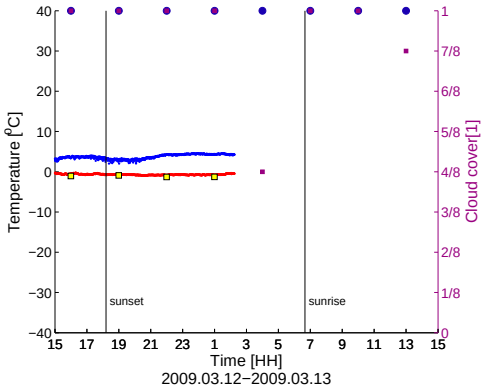

2009.03.12–2009.03.13

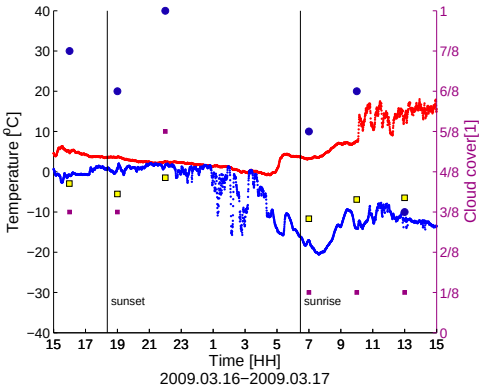

2009.03.16–2009.03.17

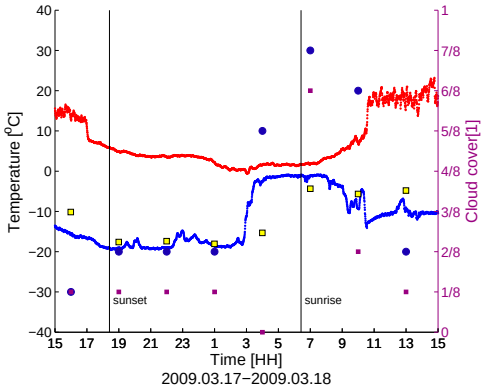

2009.03.17–2009.03.18

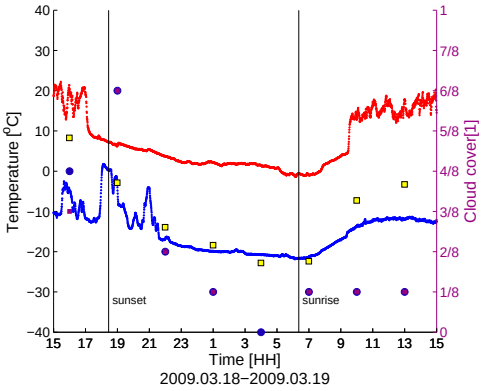

2009.03.18–2009.03.19

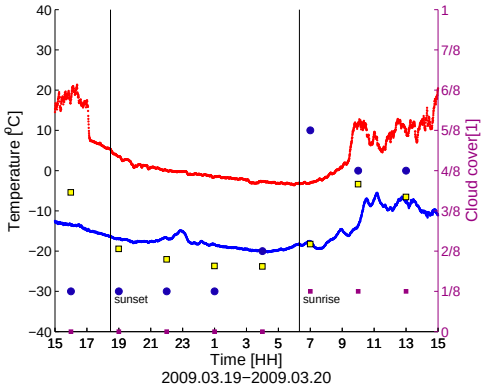

2009.03.19–2009.03.20

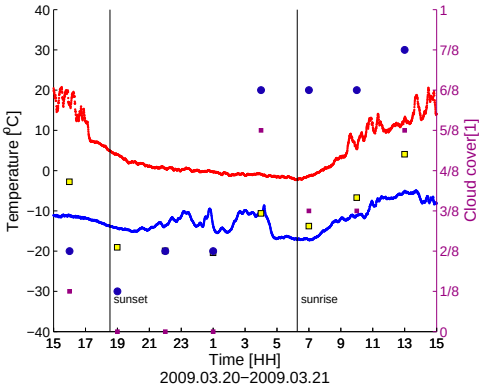

2009.03.20–2009.03.21

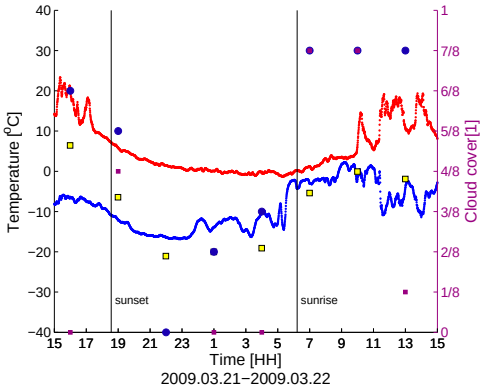
Temperature [°C]
Cloud cover[1]
Time [HH]
sunset
sunrise
2009.03.21−2009.03.22

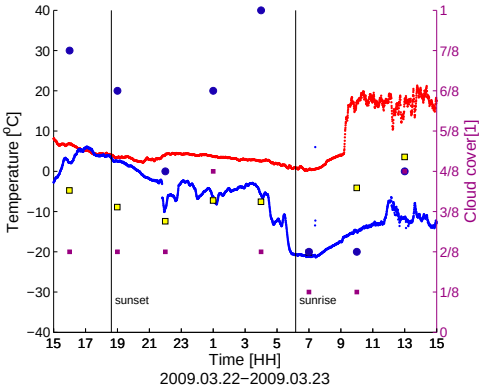
Temperature [°C]
Cloud cover[1]
Time [HH]
sunset
sunrise
2009.03.22−2009.03.23

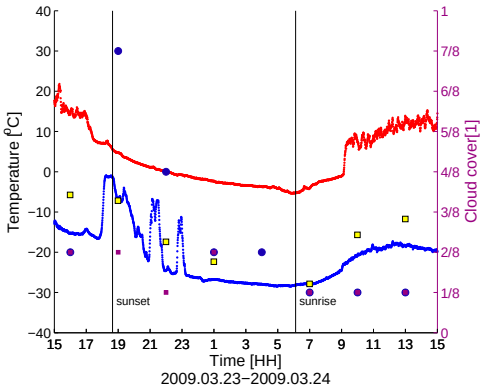
Temperature [°C]
Cloud cover[1]
Time [HH]
sunset
sunrise
2009.03.23−2009.03.24

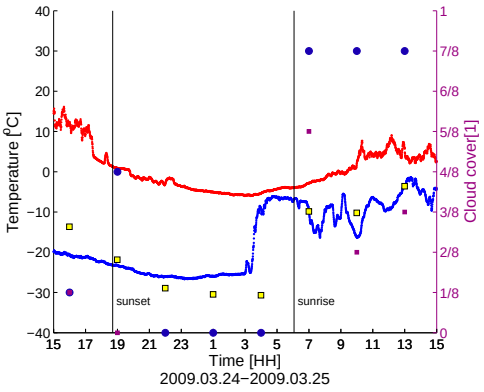
Temperature [°C]
Cloud cover[1]
Time [HH]
sunset
sunrise
2009.03.24−2009.03.25

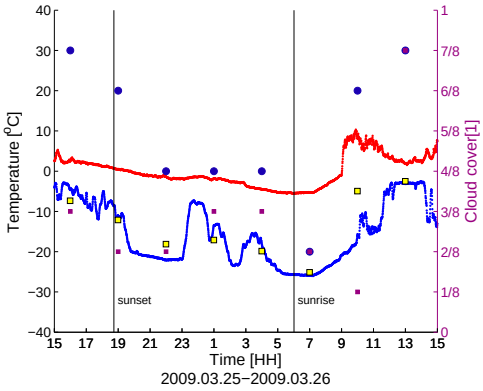
Temperature [°C]
Cloud cover[1]
Time [HH]
sunset
sunrise
2009.03.25−2009.03.26

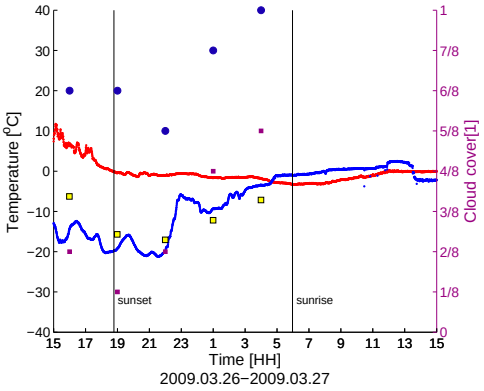
Temperature [°C]
Cloud cover[1]
Time [HH]
sunset
sunrise
2009.03.26−2009.03.27

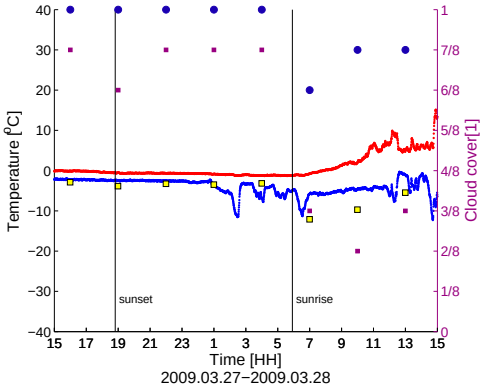
Temperature [°C]
Cloud cover[1]
Time [HH]
sunset
sunrise
2009.03.27−2009.03.28

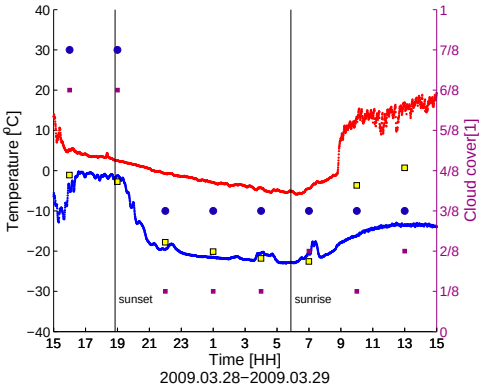
Temperature [°C]
Cloud cover[1]
Time [HH]
sunset
sunrise
2009.03.28−2009.03.29

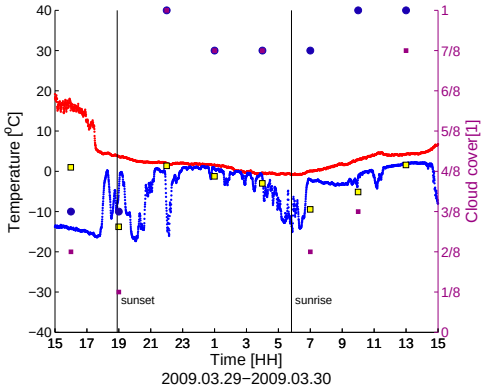
Temperature [°C]
Cloud cover[1]
Time [HH]
sunset
sunrise
2009.03.29–2009.03.30

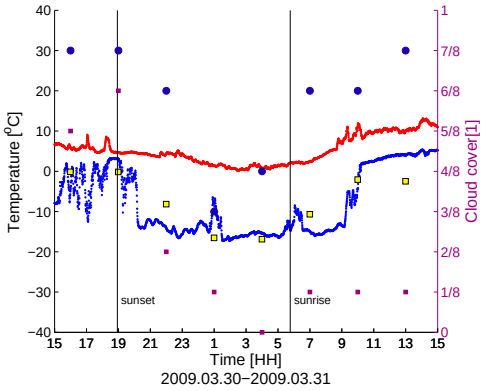
Temperature [°C]
Cloud cover[1]
Time [HH]
sunset
sunrise
2009.03.30–2009.03.31

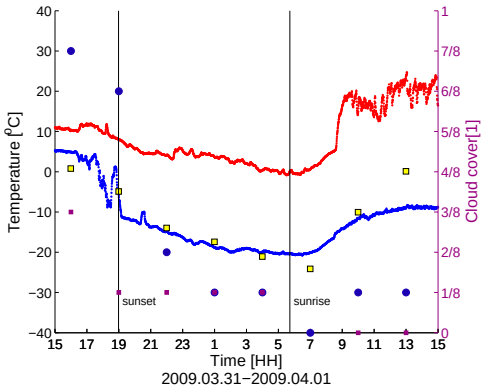
Temperature [°C]
Cloud cover[1]
Time [HH]
sunset
sunrise
2009.03.31–2009.04.01

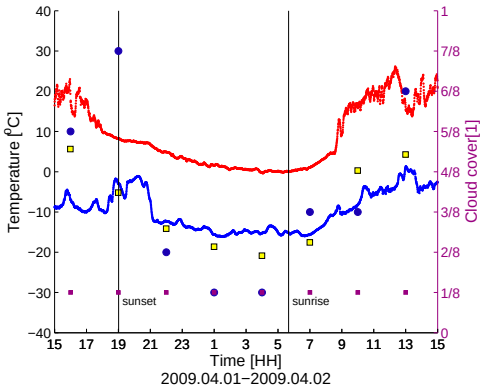
Temperature [°C]
Cloud cover[1]
Time [HH]
sunset
sunrise
2009.04.01–2009.04.02

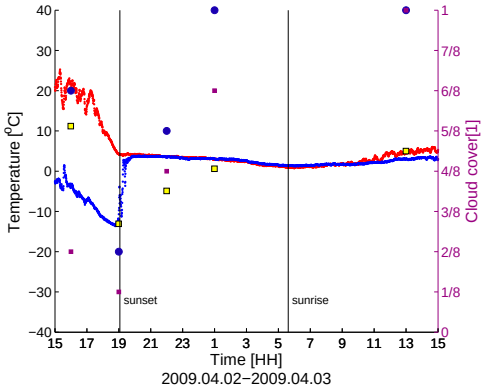
Temperature [°C]
Cloud cover[1]
Time [HH]
sunset
sunrise
2009.04.02–2009.04.03

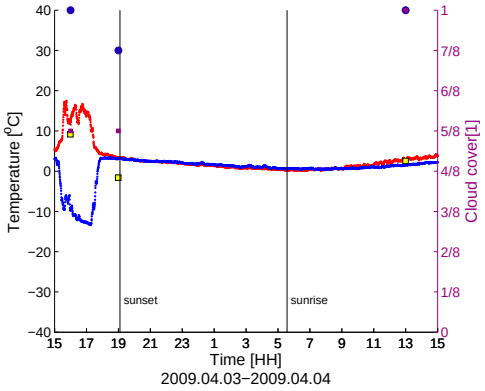
Temperature [°C]
Cloud cover[1]
Time [HH]
sunset
sunrise
2009.04.03–2009.04.04

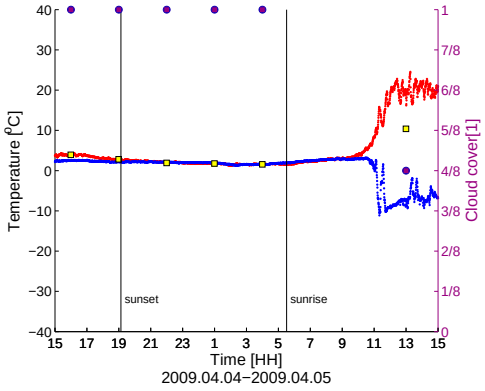
Temperature [°C]
Cloud cover[1]
Time [HH]
sunset
sunrise
2009.04.04–2009.04.05

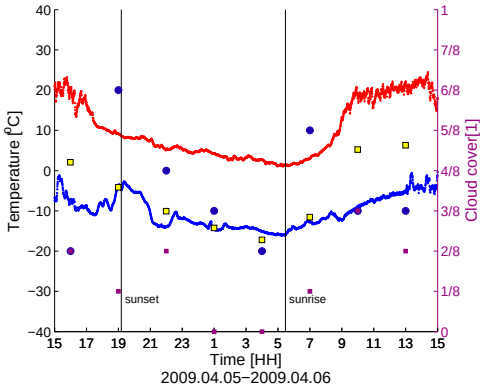
Temperature [°C]
Cloud cover[1]
Time [HH]
sunset
sunrise
2009.04.05–2009.04.06

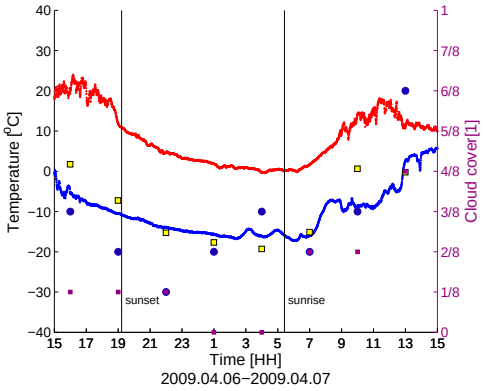
Temperature [°C]
Cloud cover[1]
sunset
sunrise
Time [HH]
2009.04.06−2009.04.07

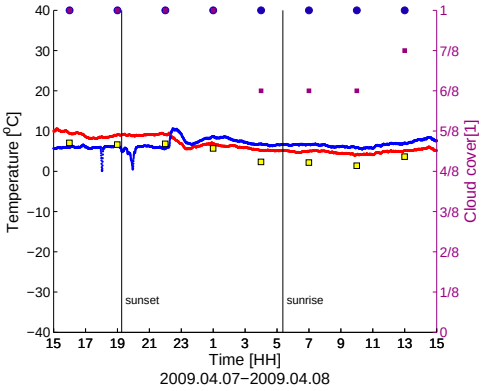
Temperature [°C]
Cloud cover[1]
sunset
sunrise
Time [HH]
2009.04.07−2009.04.08

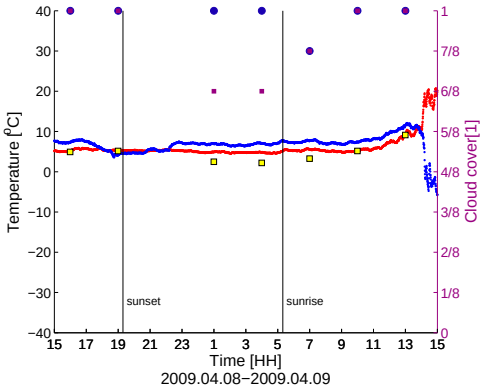
Temperature [°C]
Cloud cover[1]
sunset
sunrise
Time [HH]
2009.04.08−2009.04.09

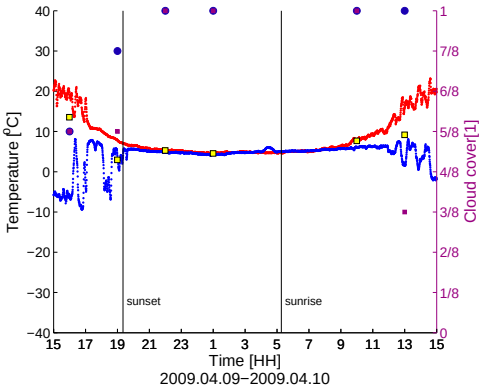
Temperature [°C]
Cloud cover[1]
sunset
sunrise
Time [HH]
2009.04.09−2009.04.10

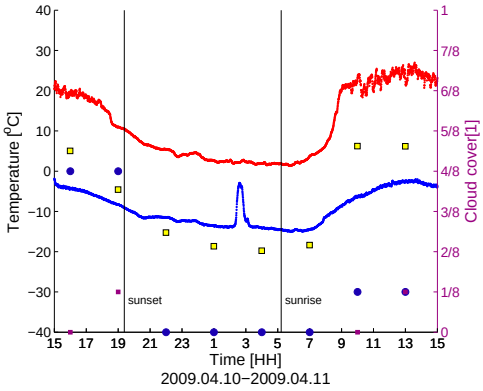
Temperature [°C]
Cloud cover[1]
sunset
sunrise
Time [HH]
2009.04.10−2009.04.11

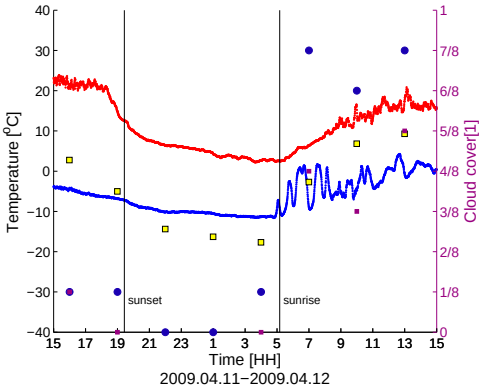
Temperature [°C]
Cloud cover[1]
sunset
sunrise
Time [HH]
2009.04.11−2009.04.12

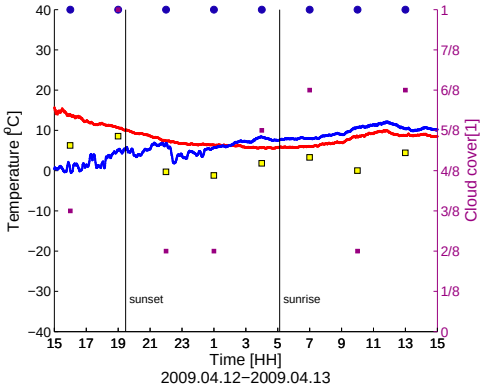
Temperature [°C]
Cloud cover[1]
sunset
sunrise
Time [HH]
2009.04.12−2009.04.13

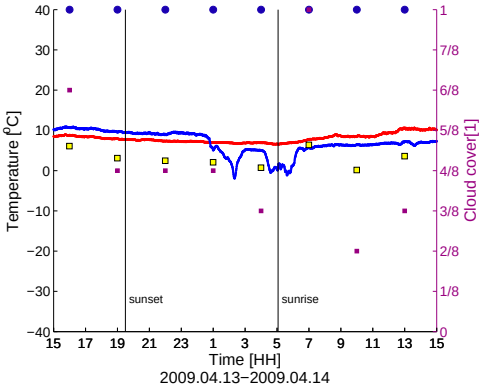
Temperature [°C]
Cloud cover[1]
sunset
sunrise
Time [HH]
2009.04.13−2009.04.14

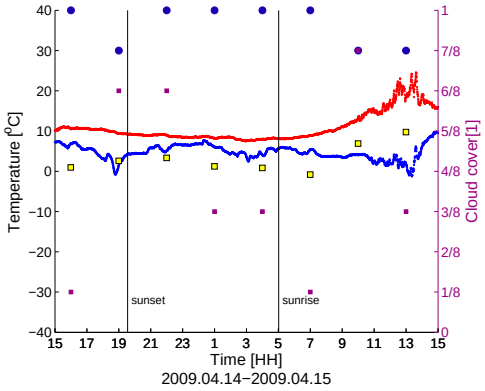

2009.04.14−2009.04.15

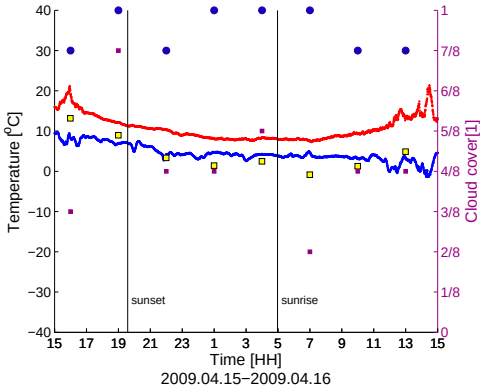

2009.04.15−2009.04.16

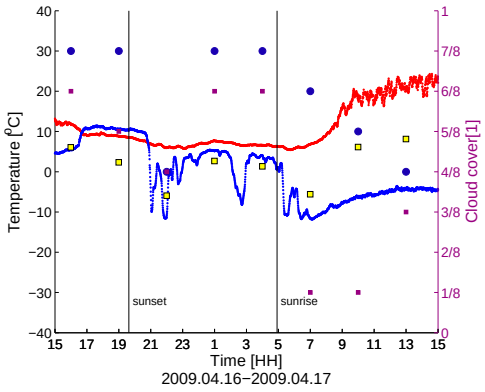

2009.04.16−2009.04.17

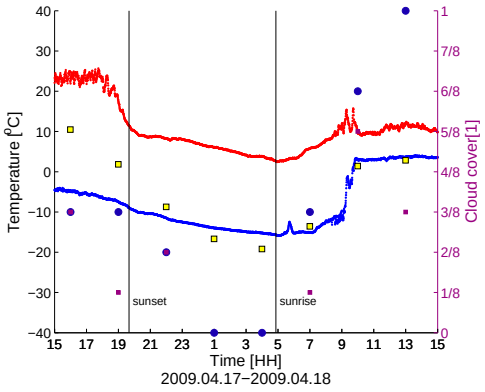

2009.04.17−2009.04.18

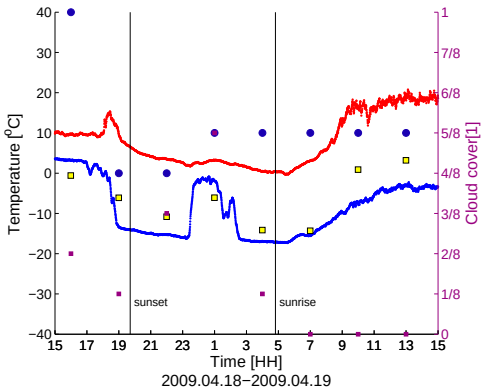

2009.04.18−2009.04.19

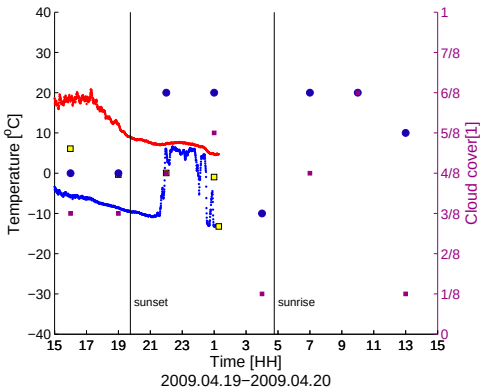

2009.04.19−2009.04.20

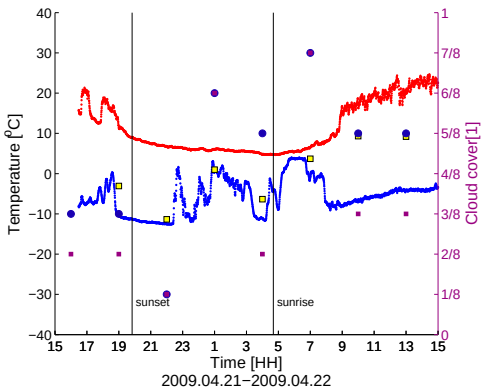

2009.04.21−2009.04.22

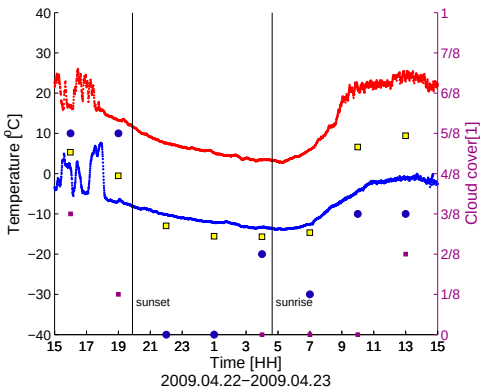

2009.04.22−2009.04.23

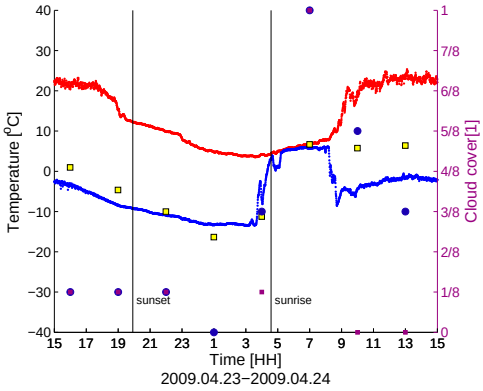

2009.04.23–2009.04.24

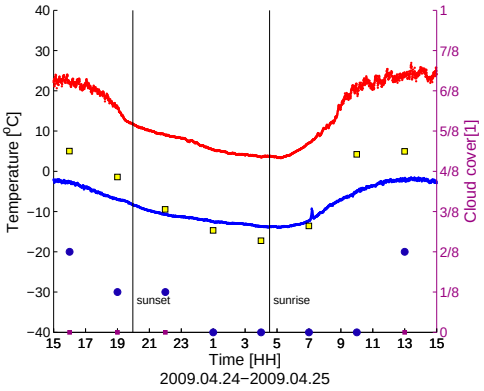

2009.04.24–2009.04.25

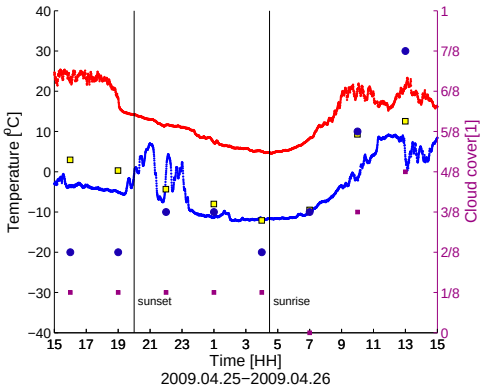

2009.04.25–2009.04.26

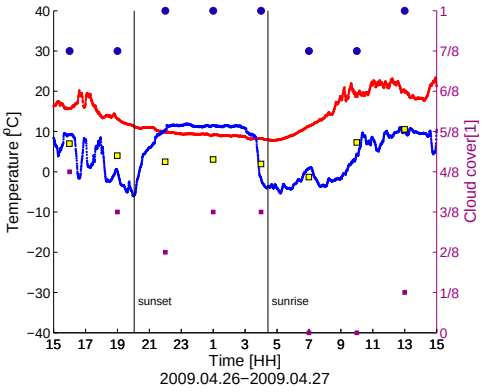

2009.04.26–2009.04.27

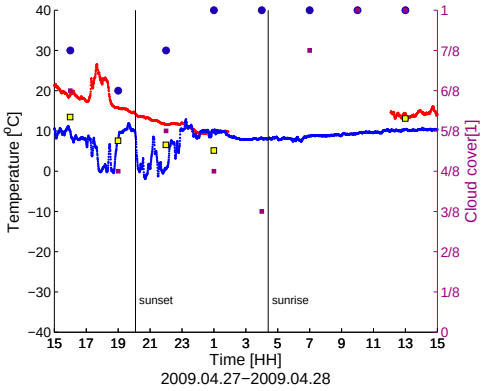

2009.04.27–2009.04.28

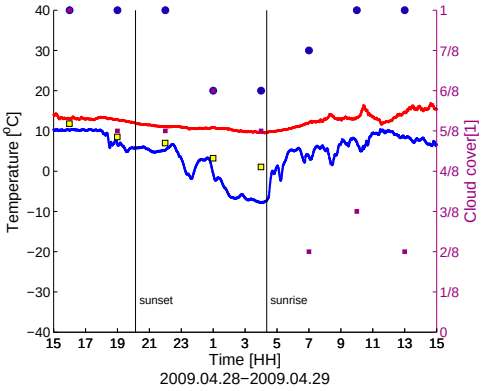

2009.04.28–2009.04.29

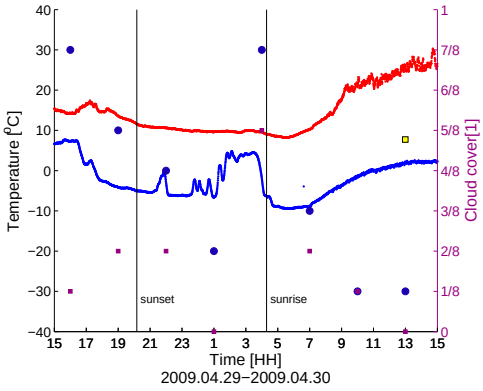

2009.04.29–2009.04.30

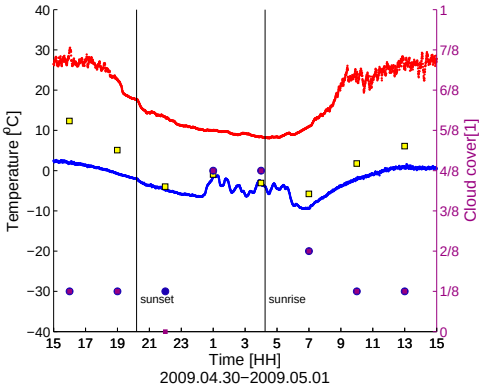

2009.04.30–2009.05.01

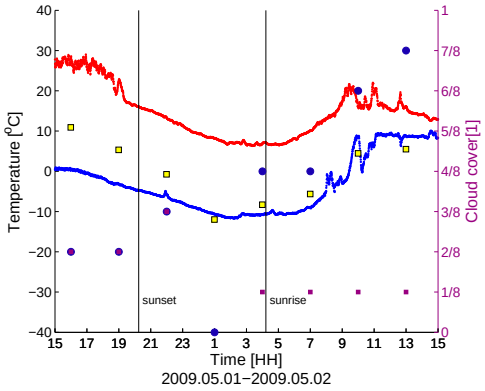
Temperature [°C]
Cloud cover[1]
sunset
sunrise
Time [HH]
2009.05.01−2009.05.02

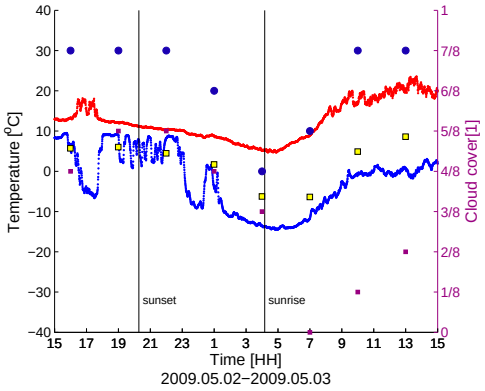
Temperature [°C]
Cloud cover[1]
sunset
sunrise
Time [HH]
2009.05.02−2009.05.03

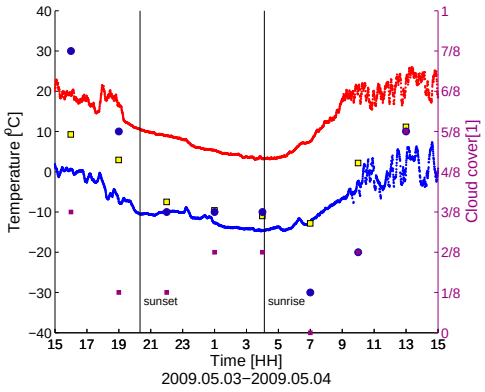
Temperature [°C]
Cloud cover[1]
sunset
sunrise
Time [HH]
2009.05.03−2009.05.04

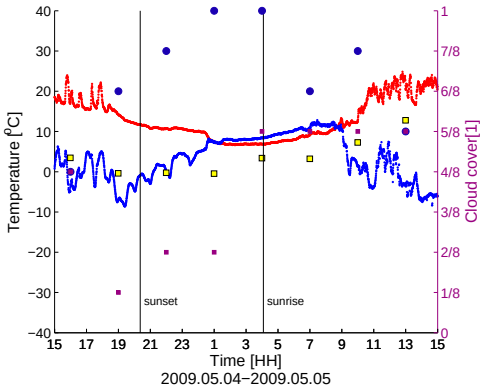
Temperature [°C]
Cloud cover[1]
sunset
sunrise
Time [HH]
2009.05.04−2009.05.05

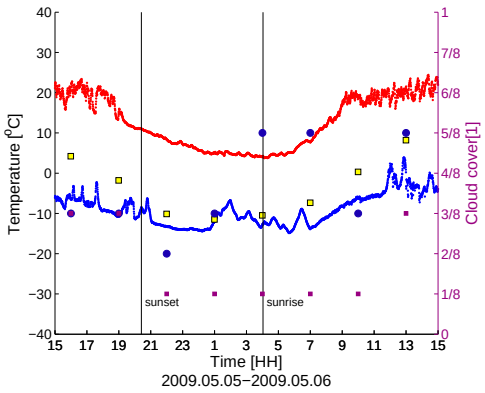
Temperature [°C]
Cloud cover[1]
sunset
sunrise
Time [HH]
2009.05.05−2009.05.06

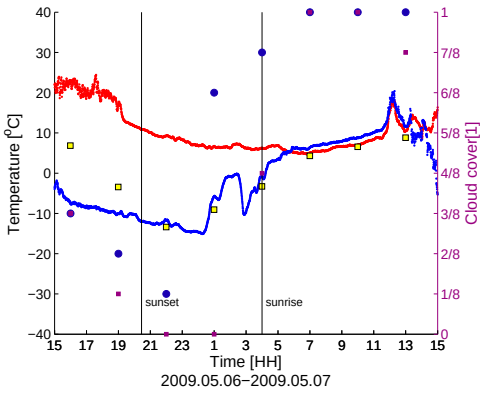
Temperature [°C]
Cloud cover[1]
sunset
sunrise
Time [HH]
2009.05.06−2009.05.07

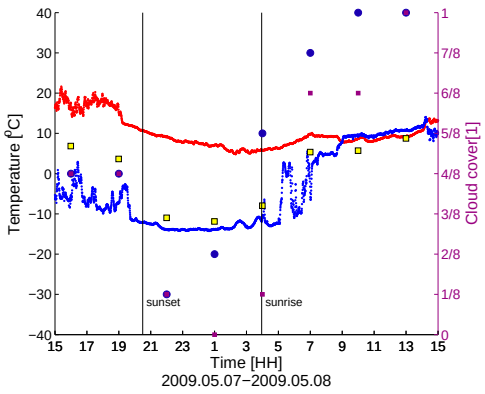
Temperature [°C]
Cloud cover[1]
sunset
sunrise
Time [HH]
2009.05.07−2009.05.08

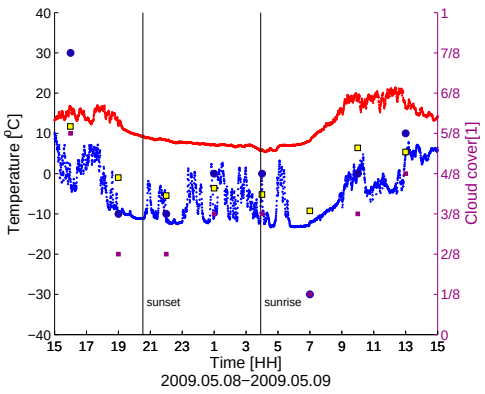
Temperature [°C]
Cloud cover[1]
sunset
sunrise
Time [HH]
2009.05.08−2009.05.09

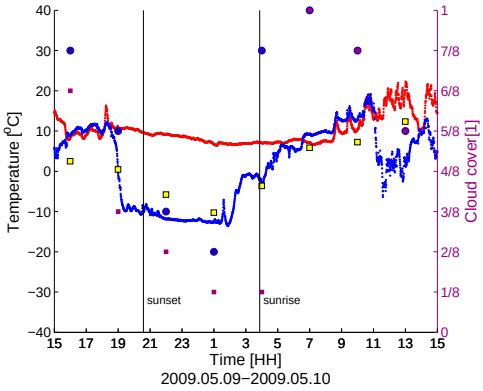

2009.05.09–2009.05.10

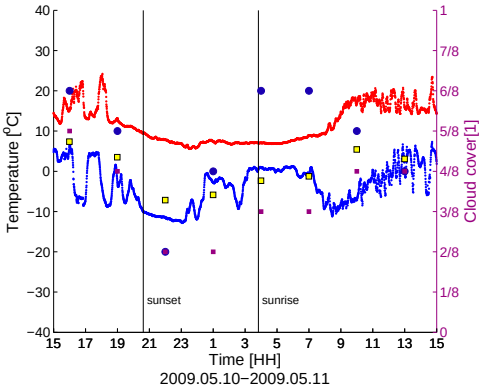

2009.05.10–2009.05.11

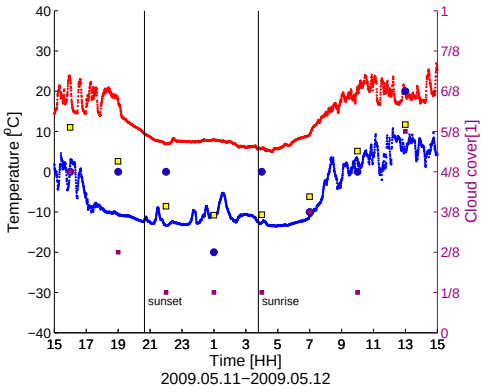

2009.05.11–2009.05.12

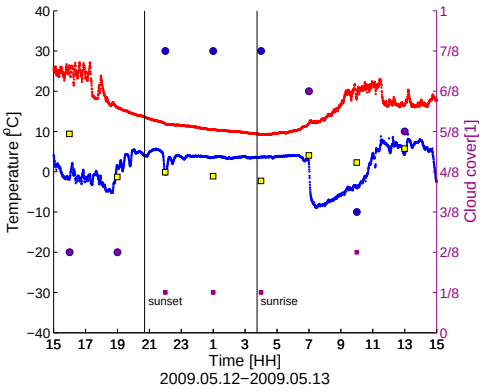

2009.05.12–2009.05.13

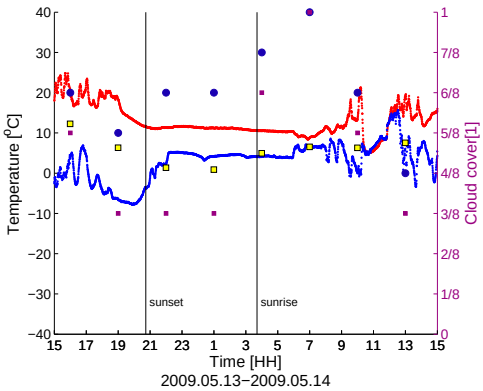

2009.05.13–2009.05.14

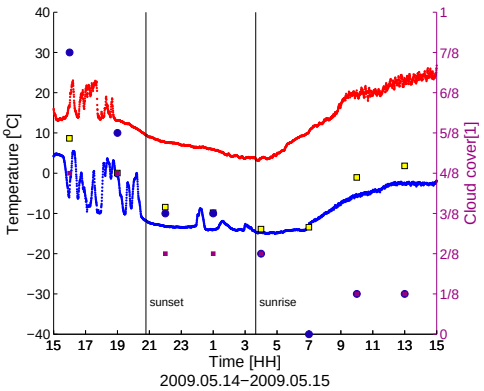

2009.05.14–2009.05.15

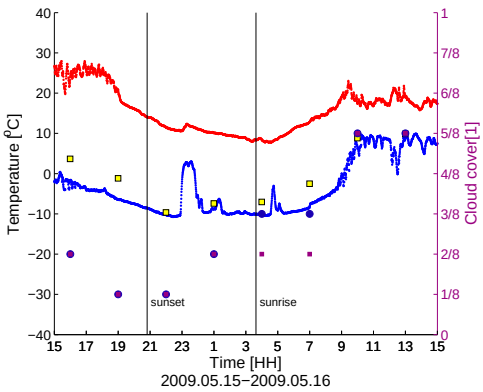

2009.05.15–2009.05.16

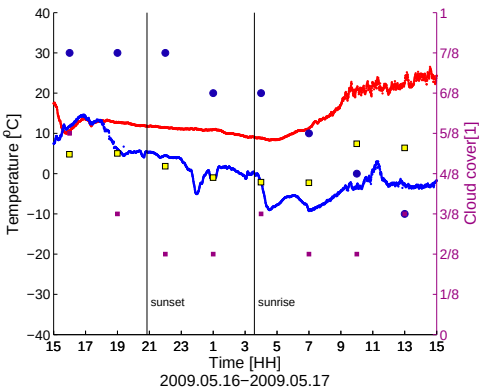

2009.05.16–2009.05.17

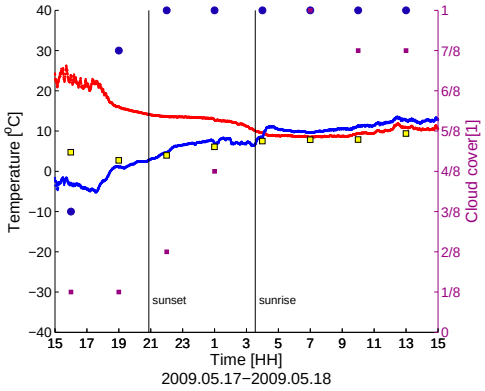

2009.05.17−2009.05.18

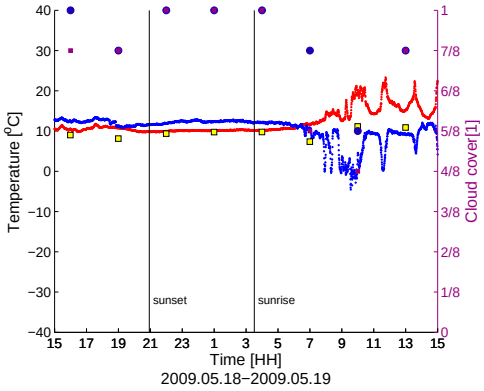

2009.05.18−2009.05.19

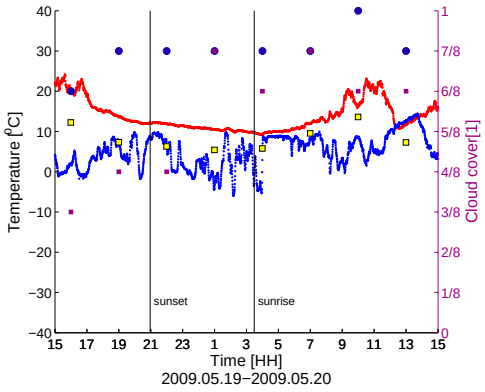

2009.05.19−2009.05.20

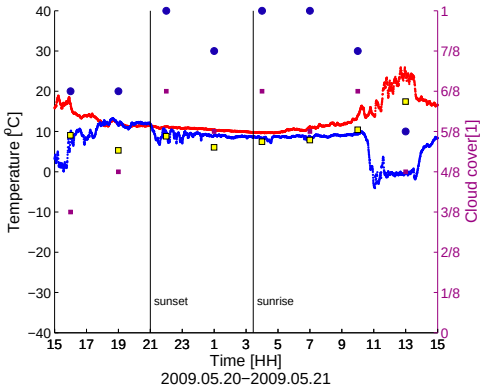

2009.05.20−2009.05.21

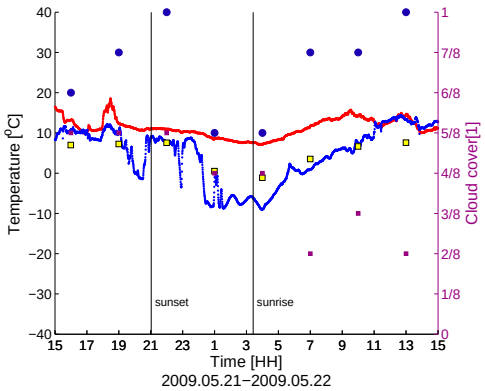

2009.05.21−2009.05.22

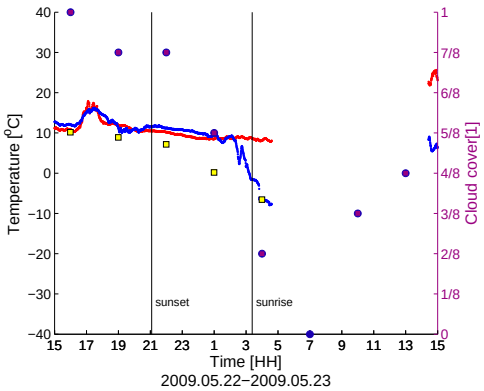

2009.05.22−2009.05.23

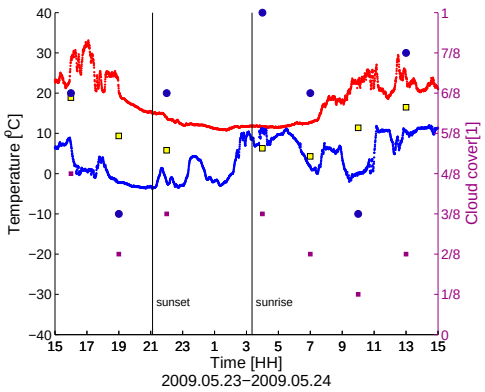

2009.05.23−2009.05.24

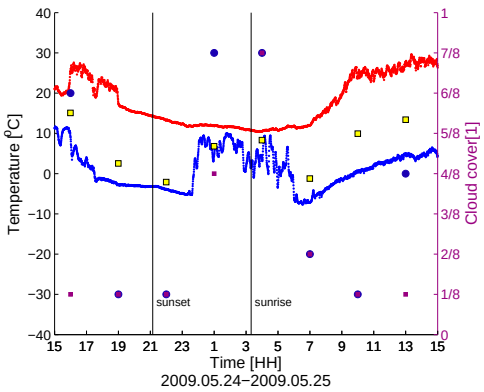

2009.05.24−2009.05.25

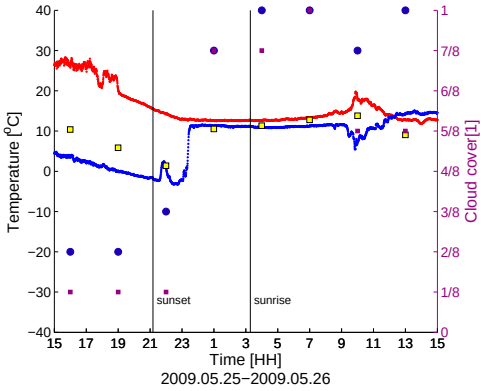
Temperature [°C]
Cloud cover[1]
Time [HH]
sunset
sunrise
2009.05.25−2009.05.26

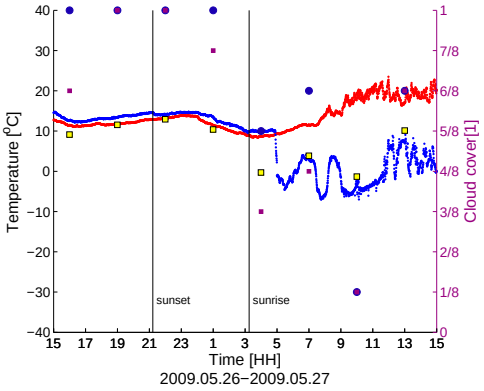
Temperature [°C]
Cloud cover[1]
Time [HH]
sunset
sunrise
2009.05.26−2009.05.27

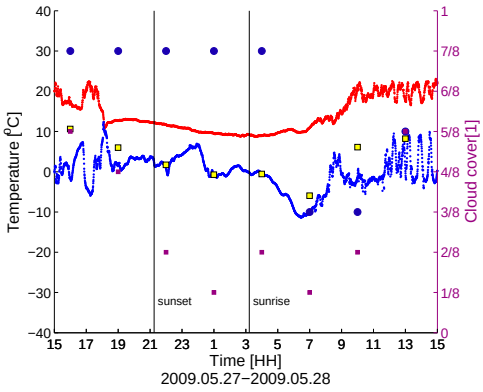
Temperature [°C]
Cloud cover[1]
Time [HH]
sunset
sunrise
2009.05.27−2009.05.28

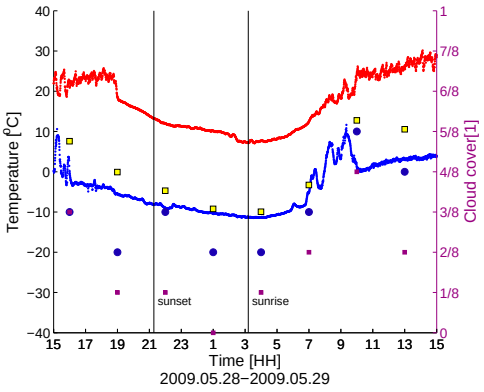
Temperature [°C]
Cloud cover[1]
Time [HH]
sunset
sunrise
2009.05.28−2009.05.29

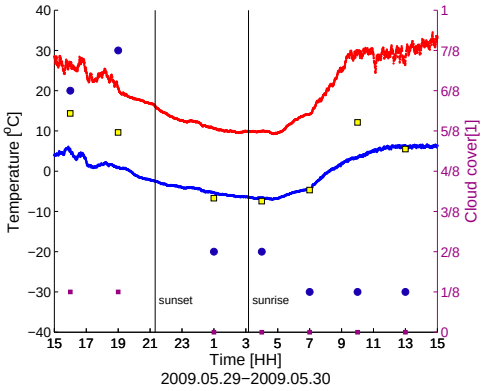
Temperature [°C]
Cloud cover[1]
Time [HH]
sunset
sunrise
2009.05.29−2009.05.30

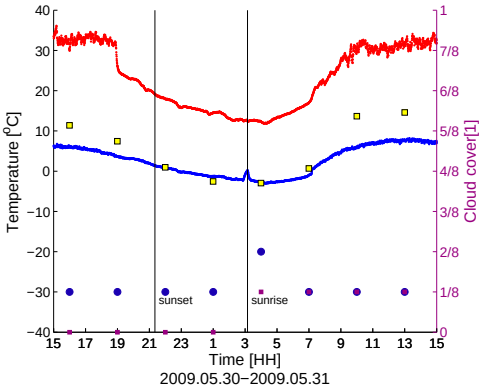
Temperature [°C]
Cloud cover[1]
Time [HH]
sunset
sunrise
2009.05.30−2009.05.31

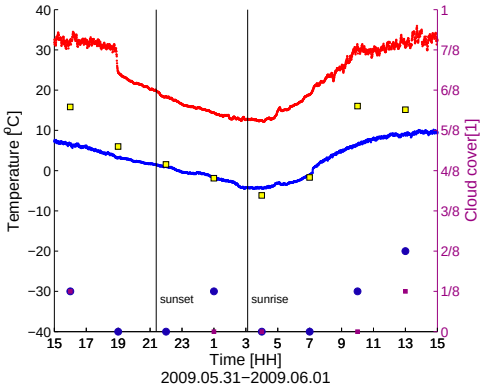
Temperature [°C]
Cloud cover[1]
Time [HH]
sunset
sunrise
2009.05.31−2009.06.01

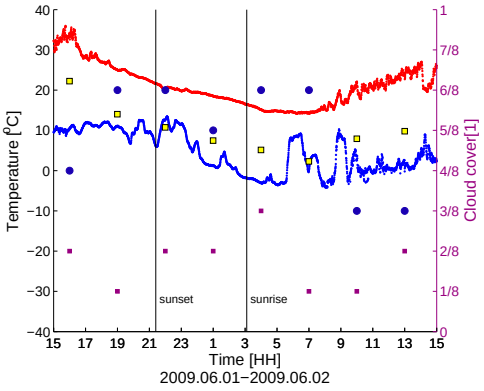
Temperature [°C]
Cloud cover[1]
Time [HH]
sunset
sunrise
2009.06.01−2009.06.02

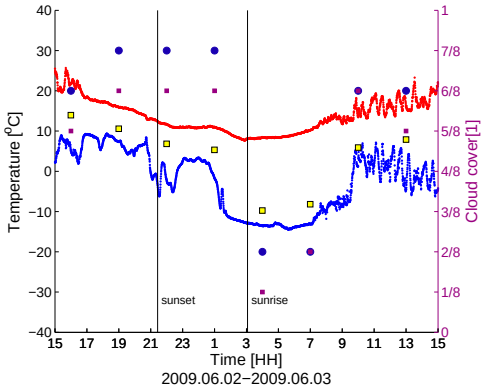

2009.06.02−2009.06.03

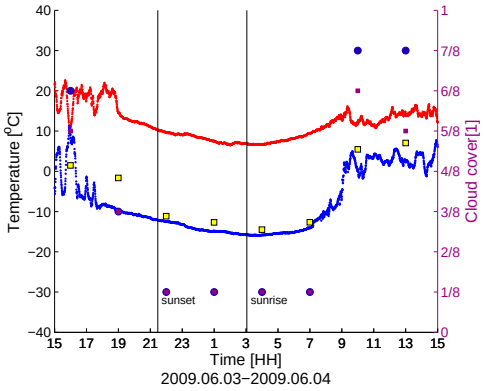

2009.06.03−2009.06.04

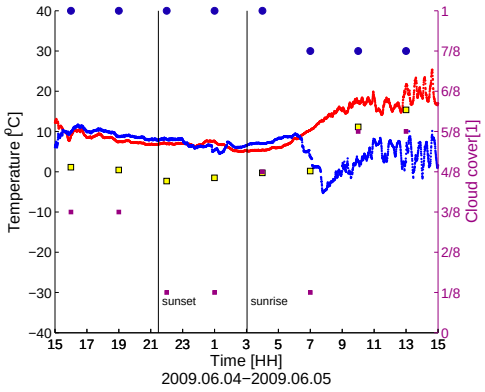

2009.06.04−2009.06.05

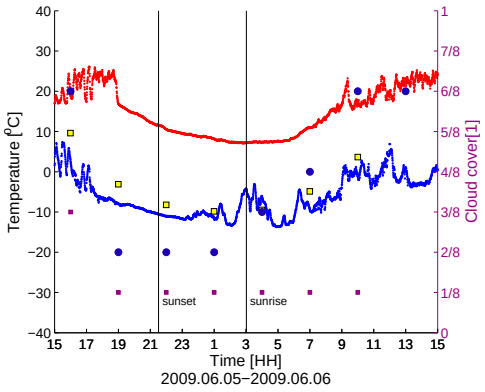

2009.06.05−2009.06.06

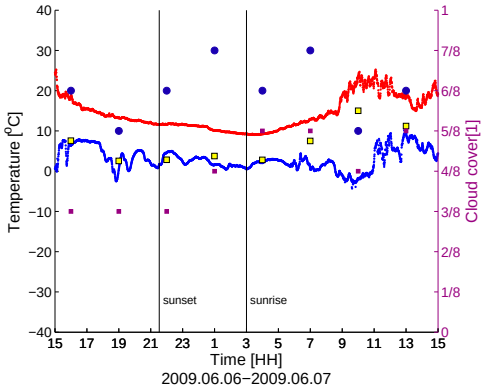

2009.06.06−2009.06.07

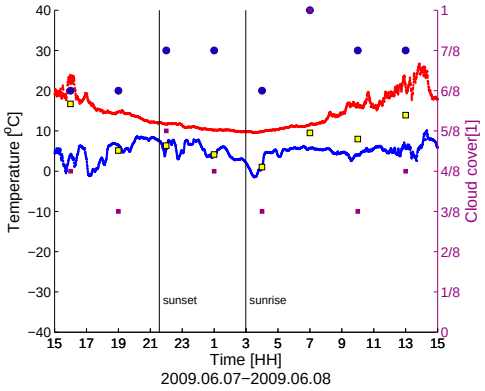

2009.06.07−2009.06.08

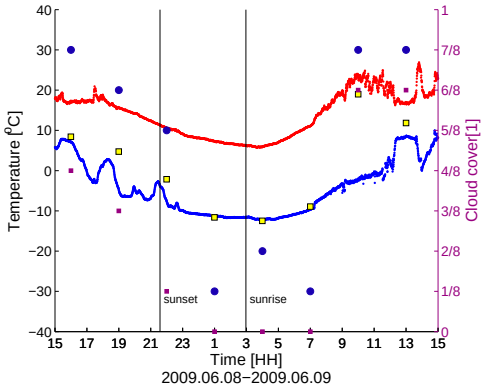

2009.06.08−2009.06.09

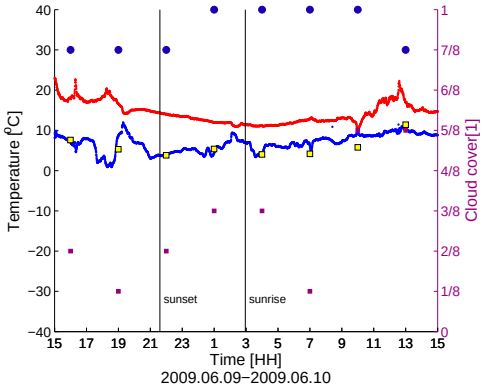

2009.06.09−2009.06.10

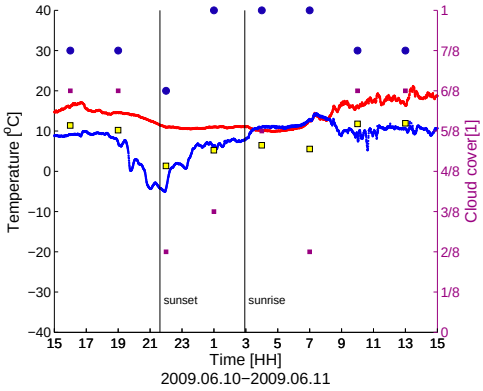

2009.06.10−2009.06.11

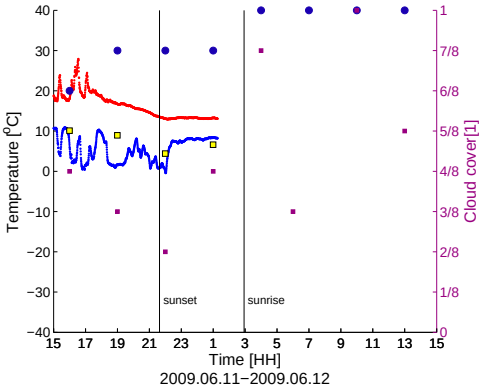

2009.06.11−2009.06.12

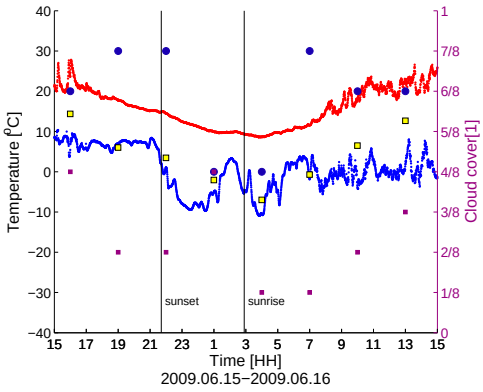

2009.06.15−2009.06.16

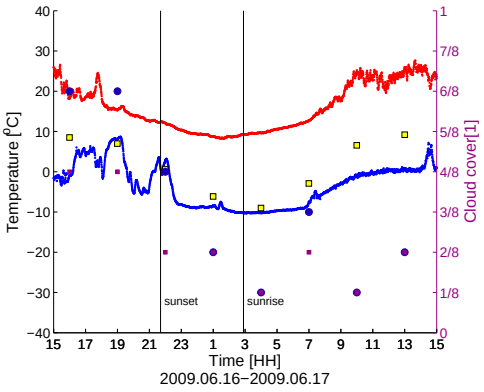

2009.06.16−2009.06.17

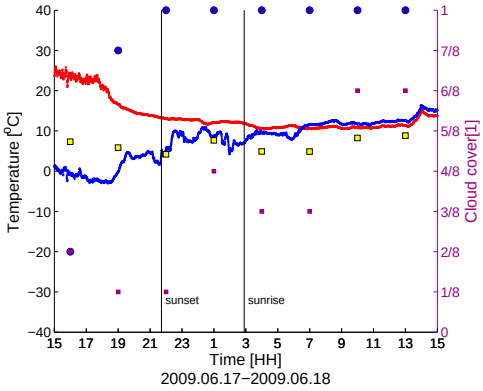

2009.06.17−2009.06.18

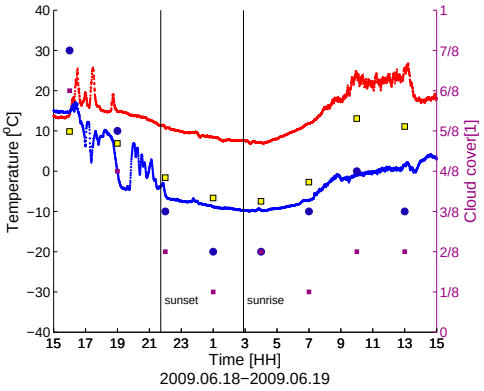

2009.06.18−2009.06.19

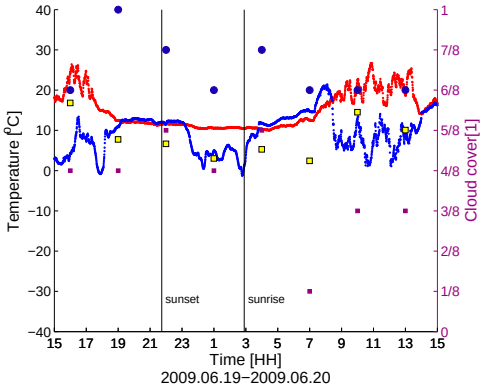

2009.06.19−2009.06.20

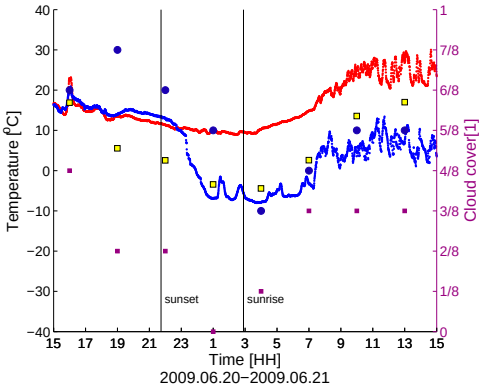

2009.06.20−2009.06.21

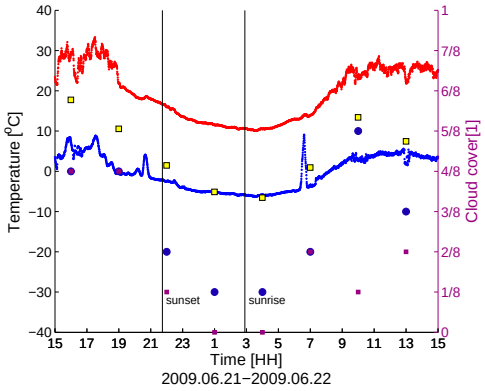
Temperature [°C]
Cloud cover[1]
Time [HH]
sunset
sunrise
2009.06.21−2009.06.22

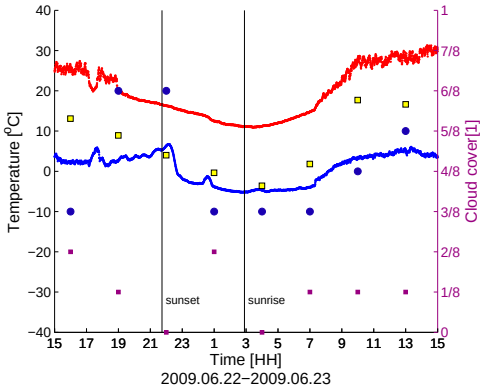
Temperature [°C]
Cloud cover[1]
Time [HH]
sunset
sunrise
2009.06.22−2009.06.23

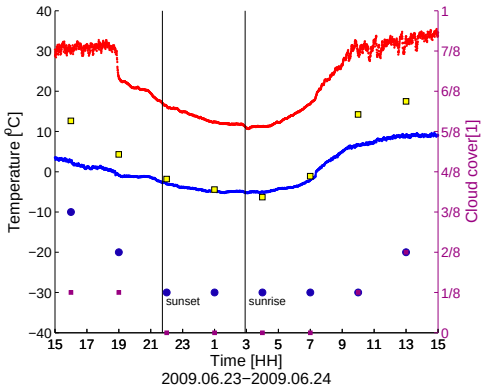
Temperature [°C]
Cloud cover[1]
Time [HH]
sunset
sunrise
2009.06.23−2009.06.24

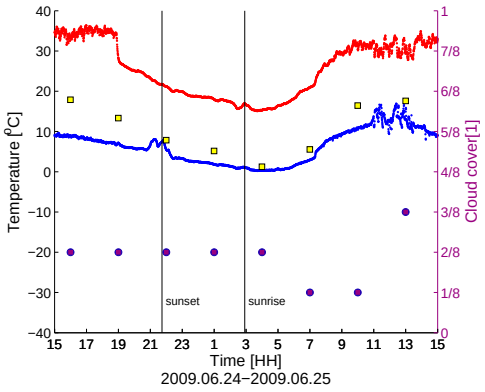
Temperature [°C]
Cloud cover[1]
Time [HH]
sunset
sunrise
2009.06.24−2009.06.25

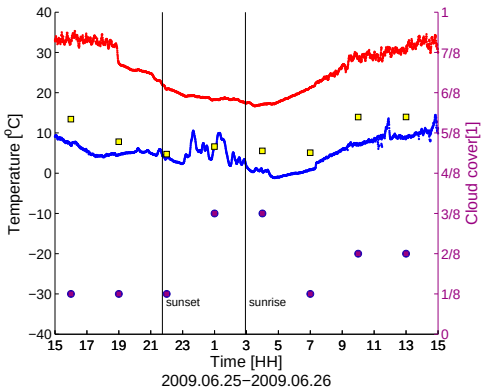
Temperature [°C]
Cloud cover[1]
Time [HH]
sunset
sunrise
2009.06.25−2009.06.26

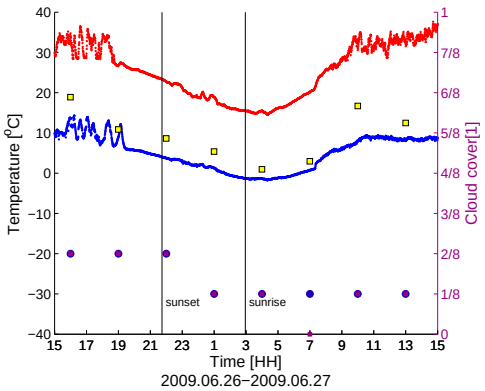
Temperature [°C]
Cloud cover[1]
Time [HH]
sunset
sunrise
2009.06.26−2009.06.27

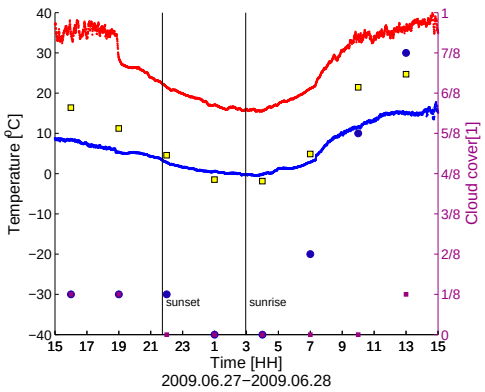
Temperature [°C]
Cloud cover[1]
Time [HH]
sunset
sunrise
2009.06.27−2009.06.28

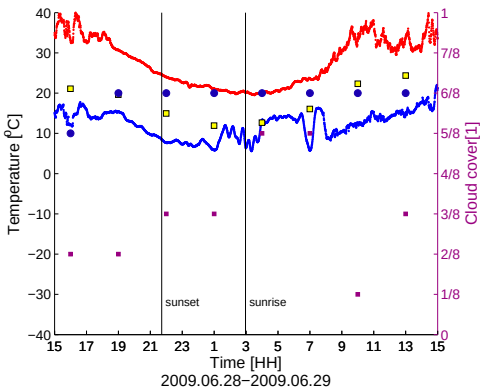
Temperature [°C]
Cloud cover[1]
Time [HH]
sunset
sunrise
2009.06.28−2009.06.29

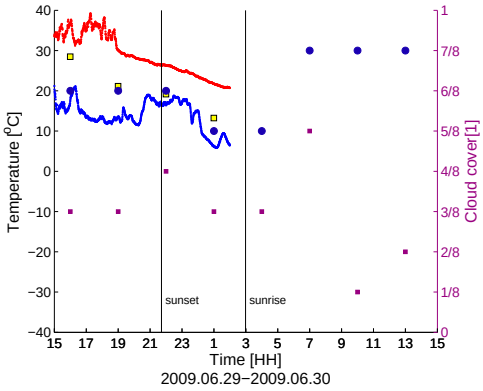
Temperature [°C]
Cloud cover[1]
Time [HH]
sunset
sunrise
2009.06.29−2009.06.30

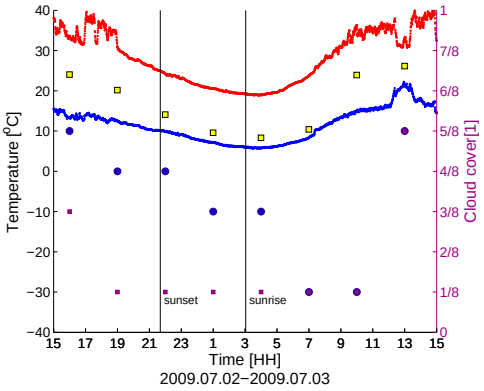
Temperature [°C]
Cloud cover[1]
Time [HH]
sunset
sunrise
2009.07.02−2009.07.03

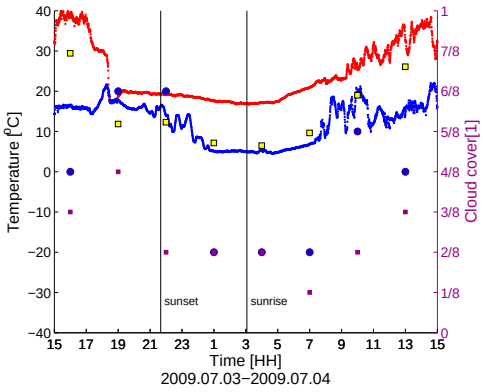
Temperature [°C]
Cloud cover[1]
Time [HH]
sunset
sunrise
2009.07.03−2009.07.04

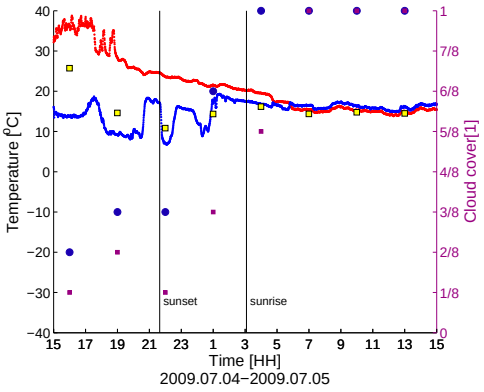
Temperature [°C]
Cloud cover[1]
Time [HH]
sunset
sunrise
2009.07.04−2009.07.05

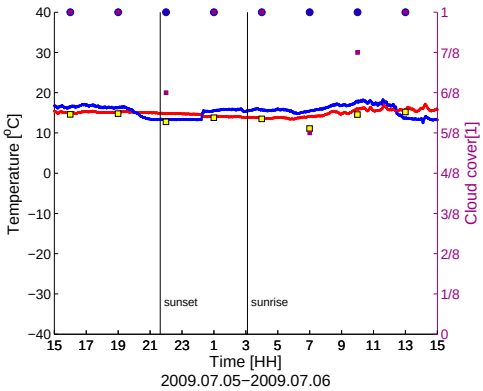
Temperature [°C]
Cloud cover[1]
Time [HH]
sunset
sunrise
2009.07.05−2009.07.06

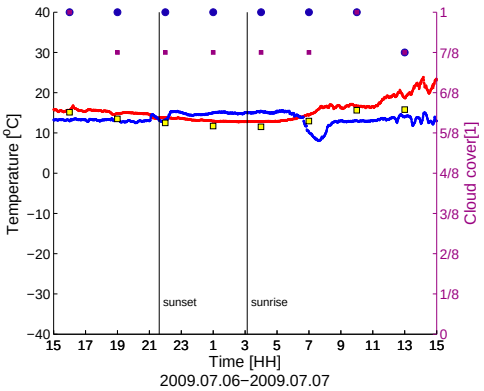
Temperature [°C]
Cloud cover[1]
Time [HH]
sunset
sunrise
2009.07.06−2009.07.07